

Combination of Solutions for Geodetic and Geodynamic Applications of the Global Positioning System (GPS)

Inauguraldissertation
der Philosophisch-naturwissenschaftlichen Fakultät
der Universität Bern

vorgelegt von

Elmar Brockmann

aus Deutschland

Leiter der Arbeit: Prof. Dr. G. Beutler,
Astronomisches Institut Universität Bern
Prof. Dr. I. Baueršima,
Astronomisches Institut Universität Bern

Combination of Solutions for Geodetic and Geodynamic Applications of the Global Positioning System (GPS)

Inauguraldissertation
der Philosophisch-naturwissenschaftlichen Fakultät
der Universität Bern

vorgelegt von

Elmar Brockmann

aus Deutschland

Leiter der Arbeit: Prof. Dr. G. Beutler,
Astronomisches Institut Universität Bern
Prof. Dr. I. Baueršima,
Astronomisches Institut Universität Bern

Von der Philosophisch-naturwissenschaftlichen Fakultät angenommen.

Der Dekan:

Bern, den 26. Juni 1996

Prof. Dr. H. Pfander

Acknowledgements

I thank Gerhard Beutler for employing me, for introducing me in the secrets of the GPS processing, for leaving enough freedom for various studies, and for giving me the time to finish this thesis. Thanks also for the personal support during the last four years.

I gratefully acknowledge the guidance received from all members of the GPS group, Markus Rothacher, Werner Gurtner, Tim Springer, Robert Weber, Stefan Schaer, and Simon Fankhauser.

In particular I would like to thank Tim Springer and Robert Weber. They did the hard work of analyzing GPS data of the IGS on each day. This is the essential basis of the presented results.

I thank also the reviewers Ivo Bauersima, Gerhard Beutler, and Markus Rothacher for their great work and the patience necessary for reading the manuscript written in my interpretation of english grammar. Thanks in particular to Ivo Bauersima, who found the last but one typing error in the formulas.

Contents

Acknowledgements	i
1. Introduction	1
1.1 Subject of the Thesis	1
1.2 Introduction to the GPS System	2
1.2.1 The Global Positioning System (GPS)	3
1.2.2 The International GPS Service for Geodynamics (IGS)	5
I Theory	9
2. Least-Squares Adjustment	11
2.1 Linear Statistical Models	11
2.1.1 Gauss-Markoff Model	11
2.1.2 Gauss-Markoff Model with Constraints on Parameters	15
2.1.3 Other Statistical Models	16
2.2 Parameter Pre-elimination	17
2.3 Sequential Adjustment Methods	19
2.3.1 Common Adjustment	20
2.3.2 Sequential Least-Squares Adjustment	21
2.3.3 Summary of Sequential LSE Formulae	23
2.3.4 Computation of the RMS in the Sequential LSE	24
2.4 Applications Related to Sequential LSE	26
2.4.1 Special Cases of Sequential LSE	26
2.4.2 Recursive Parameter Estimation	27
2.5 Parameter Transformations	32
2.5.1 Principles	33
2.5.2 Applications	34
2.5.3 Estimation of Fourier Coefficients	43
2.5.4 Blocking Frequencies	48
2.6 Constraints for Normal Equations	50
2.6.1 Apriori Constraints as Fictitious Observations	50

2.6.2	Constraints as Fictitious Observations with Large Weights . . .	53
2.6.3	Applications for Apriori Constraints	54
2.6.4	Free Network Adjustment	57
2.7	Equivalence of Combining Normal Equations and Covariances	63
2.8	Estimation of Group RMS Values	65
2.8.1	General Estimation Formulae	65
2.8.2	Applications of the Group RMS	66
3.	Orbit Determination	73
3.1	Modeling the GPS Satellite Orbits	73
3.1.1	Equation of Motion for GPS Satellites	73
3.1.2	Perturbing Forces	75
3.1.3	Eclipsing Satellites	79
3.1.4	Stochastic Orbit Modeling	80
3.2	Estimation of Satellite Orbits	82
4.	Combination of Consecutive Daily Arcs	85
4.1	Introduction	85
4.2	Problem Definition	85
4.3	Combination of Osculating Elements and Dynamical Parameters . .	87
4.3.1	One Set of Dynamical Parameters for the Combined Arc . . .	87
4.3.2	n Sets of Dynamical Parameters for the Combined Arc	90
4.4	Combination of Stochastic Parameters	91
4.5	Combination of Osculating Elements, Dynamical Parameters and Stochastic Parameters	93
4.6	Implementation Aspects	93
4.7	Partial Derivatives: Computation and Accuracy	95
4.8	Equivalence of the Orbit Combination with the Conventional Orbit Determination	96
5.	Processing Strategies using Normal Equations	99
5.1	Multi-Session Solutions	99
5.2	Processing in the Baseline Mode	102
5.2.1	Differences to a Network Solution	102
5.2.2	Baseline Processing Concept	108
5.3	Network Solutions based on Subnetwork Results	109
5.3.1	Processing Scheme	109
5.3.2	Impact of Subnetworks on Network Solutions	110
5.4	Processing in Sequences of Sub-Diurnal Intervals	112
5.5	Long-Arc Computation	113
5.6	Modularity of Combination Strategies	115

II	Results	119
6.	Estimation of Coordinates and Velocities	121
6.1	Introduction	121
6.2	Accuracy of the Coordinate and Velocity Estimation	121
6.3	Accuracy for Different Processing Strategies	123
6.4	Error Propagation for the Coordinate Precision	127
6.5	Expected Precision of Long Time Series of Continuous Observations	128
7.	Combination of GPS solutions of Different Analysis Centers	133
7.1	Combination of Regional Solutions with Global Network Solutions .	133
7.1.1	Introduction	133
7.1.2	Existing Global and Regional Networks	133
7.1.3	Distributed Processing in Europe: A Case Study	135
7.1.4	Applications	146
7.1.5	Problem Areas	147
7.2	Combination of Global Solutions of the IGS Analysis Centers	149
7.2.1	Analyzed Data	149
7.2.2	Processing Methods	149
7.2.3	Results	151
8.	Selected Results from Multi-Annual GPS Solutions	157
8.1	Multi-Annual Combined Solutions: A Description	157
8.2	Coordinates	158
8.2.1	Coordinate Repeatabilities	158
8.2.2	Accuracy of Global Site Coordinates	168
8.3	Velocities	172
8.3.1	GPS-Derived Horizontal Velocities for the IGS Network	172
8.3.2	Vertical Velocities	176
8.4	Earth Rotation	178
8.4.1	Quality of Different ERP Models	178
8.4.2	ERPs Derived from Long-Arcs	180
8.4.3	ERPs and the Definition of the Geodetic Datum	182
8.5	Center of Mass	188
8.6	Satellite Antenna Offsets	192
	Bibliography	194
III	Appendix	203
A.	Program Structure of ADDNEQ	205

A.1 Flowchart of Program ADDNEQ	206
List of Figures	207
List of Tables	210

1. Introduction

1.1 Subject of the Thesis

The increasing number of permanent GPS stations all over the world was the motivation to develop a new program, called `ADDNEQ`, under the *Bernese Software 3.5* to be able to derive from sequentially processed session solutions a statistically correct combined parameter estimate. Originally coordinate- and velocity parameters were considered, only.

The theory of combining sequential solutions is well known in geodesy since HELMERT [1872]. Limited computational resources in the first half of this century were the reason why these methods were applied to almost every network adjustment derived from classical geodetic measurements.

Computing power is no problem nowadays, but the increased number of observations collected e.g. from permanent GPS arrays (see e.g. Figure 5.1) asks for sequential methods, again.

Sequential adjustment techniques are in general independent of the observation types of the individual solutions. This implies that results of different techniques (classical geodetic techniques or space techniques GPS, SLR, VLBI, DORIS) may be combined. In this thesis we focus on the combination of results achieved by GPS, only. A short introduction to GPS is given in the next section.

It can be said without exaggeration that the program `ADDNEQ` (a flowchart is shown in Figure A.1) was developed and steadily improved over the last four years to meet the growing requirements of the CODE (Center for Orbit Determination in Europe) Analysis Center of the IGS (International GPS Service for Geodynamics). An overview of the IGS may be found at the end of this chapter.

Normal equations may be stored for a sequence of solutions including all possible types of unknown parameters (coordinates, troposphere, orbit parameters, earth rotation parameters, nutation parameters, center of mass, satellite antenna offsets, etc.).

`ADDNEQ` is today a central feature of the CODE processing, allowing it to produce not only the official CODE products but also a big variety of *different solutions series* for special studies. It is a rather rapid and efficient process to produce a "new" series covering several months or even several years based on the stored normal equations.

The theoretical background for possible "model changes" based on normal equations is given in Chapter 2.

The computation of long-arc orbits is also a powerful application of combining solutions. At CODE 3-days-solutions (and arcs) are created based on the normal equations (and the a priori orbit information) of sequential daily solutions. Longer arcs (e.g. 5- or 7-days-arcs) are extremely useful for near-real time applications of orbit determination. Important information concerning the orbit parameterization is given in Chapter 3. The theory of the combining consecutive daily arcs, which is published in [BEUTLER ET AL. 1996], is topic of Chapter 4.

A summary of processing strategies using normal equations concludes the theoretical part of this thesis. The modularity of the combination is the main reason for the diverse application possibilities.

In Chapter 6 we study the quality of site coordinates and velocities achievable by the analysis of long time series of network solutions. These results are useful to assess the quality of the coordinate and velocity estimates of the combined solutions derived from more than 2 years of IGS processing at CODE.

The combination of GPS solutions of different Analysis Centers is the subject of Chapter 7. For the maintenance and densification of terrestrial reference systems such applications are extremely important, in particular in view of the growing number of regional permanent GPS sites all over the world. Due to the availability of the Software Independent EXchange format (SINEX) it is possible to combine results of different Analysis Centers using the full covariance information. A well-defined reference frame is only guaranteed, if networks and subnetworks are processed in a consistent way. A case study shows the impact of inconsistencies of different processing strategies. As an example we show combinations of the SINEX submissions of the IGS Analysis Centers.

As mentioned before, a big variety of solution types may be created using ADDNEQ. In the final Chapter 8 we show results derived from more than 2 years of processing IGS data at CODE. We focus on some parameter types like coordinates, velocities, Earth rotation, center of mass, and satellite antenna offsets. We mentioned also that ADDNEQ was originally designed to produce the annual CODE station coordinate- and velocity solutions for the ITRF. As an example we discuss the preparation of the CODE contribution for 1995. Coordinate residuals of individual sequential solutions with respect to the combined solution show periodical variations. In part, such variations may be explained by imperfect tide models.

1.2 Introduction to the GPS System

Because all results shown in this thesis are derived from processing GPS data of the IGS, a short introduction to the *Global Positioning System* GPS as well as to the *International GPS Service for Geodynamics* IGS is included below.

1.2.1 The Global Positioning System (GPS)

The NAVSTAR GPS (NAVigation by Timing and Ranging Global Positioning System) is a satellite-based radio navigation system developed by the U.S. Department of Defense (DoD) and the Defense Mapping Agency (DMA) since 1973 for real time navigation. A first test configuration consisting of 7 satellites became available in 1983. The "final" configuration of 24 satellites (21 operational and 3 spares) was reached in 1994. The satellites are distributed in 6 different orbital planes with inclinations of 55° with respect to the Earth's equatorial plane. The orbits are almost circular with a height of about 20200 km above the Earth's surface and an orbital period of exactly 12 sidereal hours. This means that identical satellite constellations occur in the earth-fixed system always after approximately $23^h 56^m$ universal time (UT).

The full constellation guarantees that for any time and for any location at the Earth's surface 4-8 satellites (above 15° elevation) are simultaneously visible.

So far three different types of GPS satellites have to be distinguished: *Block I* satellites (development satellites), *Block II* satellites (production satellites), and *Block IIR* satellites (replenishment satellites). At present (April 1996) 25 satellites are available. Only one satellite (Space Vehicle Number (SVN) 12) of the Block I generation (of totally 11 launched) is still alive. The higher inclination of 63° can clearly be seen in Figure 1.1. No Block IIR satellites are in orbit, yet.

Each satellite is equipped with high performance frequency standards. Two L-band frequencies are derived from the *fundamental frequency* of 10.23 MHz: the frequencies $L_1 = 154 \cdot 10.23$ Mhz and $L_2 = 120 \cdot 10.23$ Mhz are equivalent to wavelengths of 19.05 cm and 24.45 cm, respectively.

A pseudo random noise (PRN) code, also called C/A (clear acquisition) code, is modulated on the L_1 frequency. The code, consisting of randomly distributed sequences of binary values, is emitted with a frequency of 1.023 MHz and is repeated every millisecond. A more precise P-(precision or protected) code is modulated on both fundamental carriers L_1 and L_2 with a frequency of 10.23 MHz. The extremely long P-code repeats itself after 266 days.

The wavelength corresponding to one chip is 300 m for the C/A-code, 30 m for the P-code.

Information about the satellite (orbit information, clock information), the so-called *navigation message*, is also available on both fundamental carriers.

The orbital information is regularly uploaded to the satellite. Updated data are achieved by analyzing the data of several monitor stations located around the world. The remarkable quality of the broadcast orbits is at present (1996) better than 3-5 m.

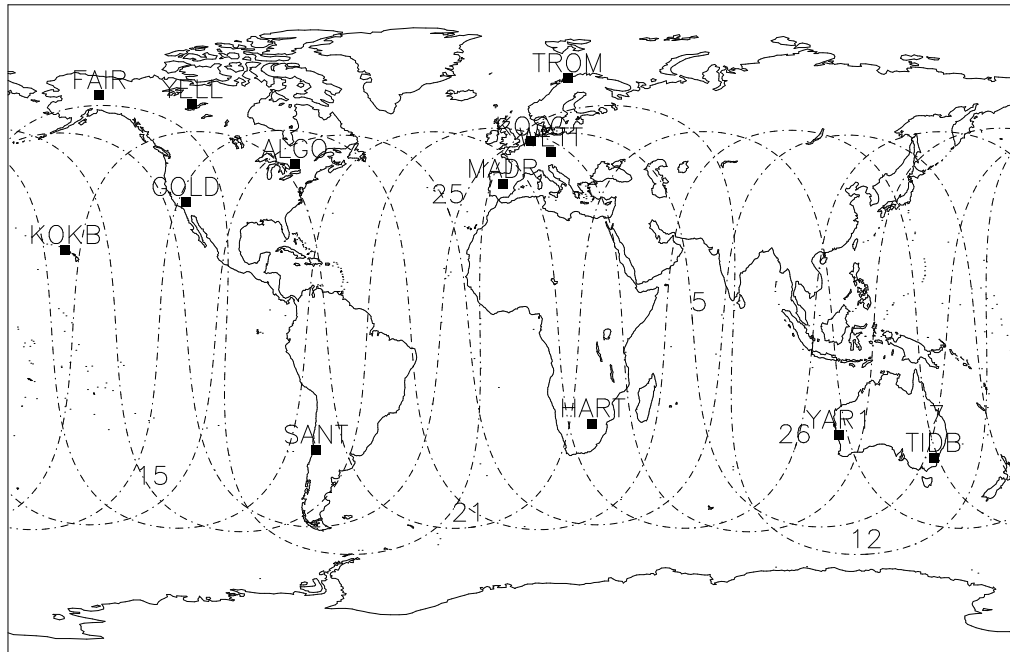


Figure 1.1: 13 IGS core sites defining the reference frame of the satellite orbits. The ground tracks of 6 Block II satellites (all of different orbital planes) and one Block I satellite (SVN 12) is plotted for Nov. 12, 1995.

GPS is a *one-way ranging system*: a signal is transmitted by the satellite and is observed by a receiver. The observable is in essence the signal travel time between satellite and receiver.

Due to clock synchronization errors we cannot directly obtain ranges from the code observations. These observations are therefore called *pseudoranges*.

Assuming that the receiver can determine the pseudoranges with about 1% relative error (with respect to the chip length) we obtain a precision for the pseudoranges of 3 m and 30 cm, respectively.

The *carrier beat phase* is the important observable for high precision applications. It is derived from the comparison between the received (Doppler-shifted) signal and the reference signal generated in the receiver. Assuming that the differences are measured with a relative accuracy of 1% we obtain a precision for the phase observations of about 2 mm.

Pseudorange observations are unambiguous. This is not true for the phase observables. An initially unknown ambiguity parameter (integer number of cycles) has to be included in the corresponding observation equations. For a variety of reasons it may happen that the receiver loses the phase-lock to a particular satellite. An additional pre-processing step is therefore necessary to repair so-called *cycle slips* or to introduce new ambiguity parameters when a cycle slip was detected.

More details about the GPS system can be found in [HOFMANN-WELLENHOF ET AL. 1994; LEICK 1995; SEEGER 1993; WELLS ET AL. 1987].

The highest precision is achieved in the *relative static* observation mode when two (or more) GPS receivers are observing continuously. Differencing the observations of two receivers eliminates the unknown satellite clock and reduces (dependent on the distance) common error sources (ionospheric and tropospheric errors, multipath, and satellite orbit errors). We should emphasize that GPS is an *interferometric* technique.

1.2.2 The International GPS Service for Geodynamics (IGS)

At the 20th General Assembly of the International Union of Geodesy and Geophysics (IUGG) in Vienna in August 1991 Resolution No 5 recommended that the concept of the IGS be explored over the next four years. Meanwhile an IAG (International Association of Geodesy) *Service* is established (since 1994). An overview of the history and the structure of IGS is given e.g. by BEUTLER ET AL. [1994].

The primary objectives of the IGS is to provide a service to support, through GPS data products, geodetic and geophysical research activities. According to the *Terms of References* of IGS [NEILAN 1995]

IGS collects, archives, and distributes GPS observation data sets of sufficient accuracy to satisfy the objectives of a wide range of applications and experimentations. These data sets are used by the IGS to generate the following data products:

- high accuracy GPS ephemerides,
- earth rotation parameters,
- coordinates and velocities of the IGS tracking stations,
- GPS satellite and tracking station clock information,
- ionospheric information.

IGS is a collaboration of more than 60 international agencies [NEILAN 1995]. Most of them are contributing observations to the IGS. The structure of IGS is given by the components *Network of tracking stations* (more than 80 permanent operational receivers are available through the IGS), *Data Centers* (3 global Data Centers and 7

Regional Data Centers), *Analysis and Associate Analysis Centers*, *Analysis Center Coordinator*, *Central Bureau* and *Governing Board*. Table 1.1 lists the 7 Analysis Centers, which perform every day the estimates of the GPS satellite orbits, Earth rotation parameters, etc.

Table 1.1: The seven Analysis Centers of the IGS.

CODE	Center for Orbit Determination in Europe	Switzerland
ESA	European Space Agency	Germany
GFZ	GeoForschungsZentrum	Germany
JPL	Jet Propulsion Laboratory	USA
NOOA ^a	National Oceanic and Atmospheric Administration	USA
NRCan	Natural Resources Canada (formerly EMR)	Canada
SIO	Scripps Institution of Oceanography	USA

Since the IGS service was established, combined IGS orbits/clocks are produced by the IGS Analysis Center Coordinator (J. Kouba, NRC) [BEUTLER ET AL. 1995]. This precise and highly reliable product is available with a delay of approximately 2 weeks. For 1994 the typical quality of the IGS orbits was about 10-20 *cm* [KOUBA 1995B]. The Earth rotation estimates are showing an RMS of less than 0.6 *mas* with respect to the IERS pole combination. The satellite clocks are consistent on a 1 *ns* level even for periods with SA (Selective Availability).

The mentioned products refer to the ITRS (International Terrestrial Reference System). This system is realized by constraining the coordinates of 13 IGS core sites (see Figure 1.1) to the ITRF (International Terrestrial Reference Frame) values (at present ITRF93).

The steadily increasing number of tracking sites, much better distribution of these sites (see Table 1.2), and improved processing techniques of the IGS Analysis Centers led to a steady improvement of IGS products. Recent orbit comparisons show an improvement factor of about 2 with respect to the 1994 values.

Table 1.2: Workload of the daily 3-days CODE solutions.

<i>Datum</i>	<i># Sat.</i>	<i># Stat.</i>	<i># Obs.</i>	<i># Par.</i>
June 92	19	25	50,000	2,000
Jan. 93	21	28	60,000	2,300
Jan. 94	26	38	180,000	6,200
Jan. 95	25	49	250,000	9,000
Jan. 96	25	63	280,000	12,000

^a 3-character abbreviation used for this center also: NGS (National Geodetic Survey)

So-called *super-rapid* IGS orbits, available since January 1996 with a delay of about 36 hours, are another example for the rapid development within the IGS. Also available are weekly combined coordinate solutions in the SINEX format (see Section 7.2) and a combined GPS pole.

Comparisons of ionospheric and tropospheric results are planned.

Part I
Theory

2. Least-Squares Adjustment

In this chapter a synopsis of least-squares adjustment is given. We introduce the notation and the basic models used in later sections. We start with the frequently used *Gauss-Markoff Model* of full rank. Important aspects such as *pre-elimination*, *introduction of a priori constraints*, and *sequential least-squares estimation* are explained. Sequential least-squares adjustment allows a post processing without going back to the original observations. The chapter concludes with applications to demonstrate the flexibility and the power of these methods.

2.1 Linear Statistical Models

2.1.1 Gauss-Markoff Model

2.1.1.1 Observation Equations

The *Gauss-Markoff Model* (GMM) of full rank is given by e.g. KOCH [1988]:

$$\mathbf{E}(\mathbf{y}) = \mathbf{X}\boldsymbol{\beta} \quad ; \quad \mathbf{D}(\mathbf{y}) = \sigma^2 \mathbf{P}^{-1} \quad (2.1-1)$$

\mathbf{X} $n \times u$ matrix of given coefficients with full rank $rg\mathbf{X} = u$; \mathbf{X} is also called *design matrix*.

$\boldsymbol{\beta}$ $u \times 1$ vector of unknowns

\mathbf{y} $n \times 1$ vector of observations

\mathbf{P} $n \times n$ positive definite weight matrix

n, u number of observations, number of unknowns

$\mathbf{E}(\cdot)$ operator of expectation

$\mathbf{D}(\cdot)$ operator of dispersion

σ^2 variance of unit weight (variance factor).

For $n > u$ the equation system $\mathbf{X}\boldsymbol{\beta} = \mathbf{y}$ is not consistent. The rank space of \mathbf{X} is \mathcal{R}^u but the rank space of the observations \mathbf{y} is \mathcal{R}^n . With the addition of the residual vector \mathbf{e} to the observation vector \mathbf{y} one obtain a consistent but ambiguous system of equations, also called system of *observation equations*:

$$\mathbf{y} + \mathbf{e} = \mathbf{X}\boldsymbol{\beta} \quad \text{with} \quad \mathbf{E}(\mathbf{e}) = \mathbf{0} \quad \text{and} \quad \mathbf{D}(\mathbf{e}) = \mathbf{D}(\mathbf{y}) = \sigma^2 \mathbf{P}^{-1} \quad (2.1-2)$$

(2.1-1) and (2.1-2) are formally identical. $\mathbf{E}(\mathbf{e}) = \mathbf{0}$ is valid because $\mathbf{E}(\mathbf{y}) = \mathbf{X}\boldsymbol{\beta}$ and $\mathbf{D}(\mathbf{e}) = \mathbf{D}(\mathbf{y})$ follows from the law of error propagation.

2.1.1.2 Method of Least-Squares

The method of least-squares asks for restrictions for the observation equations (2.1-1) or (2.1-2). The parameter estimation of $\boldsymbol{\beta}$ minimizes the quadratic form

$$\Omega(\boldsymbol{\beta}) = \frac{1}{\sigma^2} (\mathbf{y} - \mathbf{X}\boldsymbol{\beta})' \mathbf{P} (\mathbf{y} - \mathbf{X}\boldsymbol{\beta}). \quad (2.1-3)$$

The introduction of the condition $\Omega(\boldsymbol{\beta}) \rightarrow \min.$ is necessary to lead us from the ambiguous observations (2.1-1) or (2.1-2) to an unambiguous normal equation system (NEQ system) for the determination of $\boldsymbol{\beta}$.

The estimation of the minimum values for $\Omega(\boldsymbol{\beta})$ requires to solve the u equations $d\Omega(\boldsymbol{\beta})/d\boldsymbol{\beta} = \mathbf{0}$, also called *normal equations*.

The following formulae summarize the *Least-Squares Estimation* (LSE) results in the Gauss-Markoff Model:

Normal equations:

$$\mathbf{X}' \mathbf{P} \mathbf{X} \hat{\boldsymbol{\beta}} = \mathbf{X}' \mathbf{P} \mathbf{y} \quad (2.1-4)$$

Estimates:

$$\text{of } \boldsymbol{\beta}: \quad \hat{\boldsymbol{\beta}} = (\mathbf{X}' \mathbf{P} \mathbf{X})^{-1} \mathbf{X}' \mathbf{P} \mathbf{y} \quad (2.1-5)$$

$$\text{of the (variance-)covariance matrix: } \mathbf{D}(\hat{\boldsymbol{\beta}}) = \hat{\sigma}^2 (\mathbf{X}' \mathbf{P} \mathbf{X})^{-1} \quad (2.1-6)$$

$$\text{of the observations: } \hat{\mathbf{y}} = \mathbf{X} \hat{\boldsymbol{\beta}} = \mathbf{R} \mathbf{y} \quad (2.1-7)$$

$$\text{of the residuals: } \hat{\mathbf{e}} = \hat{\mathbf{y}} - \mathbf{y} = -\mathbf{R}^\perp \mathbf{y} \quad (2.1-8)$$

$$\begin{array}{l} 1. \\ 2. \end{array} \text{ of the quadratic form: } \Omega = \hat{\mathbf{e}}' \mathbf{P} \hat{\mathbf{e}} = \mathbf{y}' \mathbf{P} \mathbf{y} - \mathbf{y}' \mathbf{P} \mathbf{X} \hat{\boldsymbol{\beta}} \quad (2.1-9)$$

$$\text{of the variance of unit weight (variance factor): } \hat{\sigma}^2 = \Omega / (n - u) \quad (2.1-10)$$

Degree of freedom / Redundancy:

$$f = n - u = \text{Sp}(\mathbf{F}) \quad (2.1-11)$$

$$\mathbf{F} = \mathbf{P} \mathbf{Q}_{\hat{\mathbf{e}}\hat{\mathbf{e}}} = \mathbf{I} - \mathbf{P} \mathbf{X} \mathbf{Q}_{\hat{\boldsymbol{\beta}}\hat{\boldsymbol{\beta}}} \mathbf{X}' \quad (2.1-12)$$

Normal equation matrices:

$$\mathbf{X}'\mathbf{P}\mathbf{X}, \quad \mathbf{X}'\mathbf{P}\mathbf{y}, \quad (\mathbf{y}'\mathbf{P}\mathbf{y}) \quad (2.1-13)$$

Cofactor Matrices:

$$\mathbf{Q}_{\hat{\beta}\hat{\beta}} = \Sigma_{\hat{\beta}\hat{\beta}} = (\mathbf{X}'\mathbf{P}\mathbf{X})^{-1} \quad (2.1-14)$$

$$\mathbf{Q}_{\hat{y}\hat{y}} = \mathbf{X}\mathbf{Q}_{\hat{\beta}\hat{\beta}}\mathbf{X}' = \mathbf{R}\mathbf{P}^{-1}\mathbf{R}' = \mathbf{R}\mathbf{P}^{-1} = \mathbf{P}^{-1}\mathbf{R}' \quad (2.1-15)$$

$$\mathbf{Q}_{\hat{e}\hat{e}} = \mathbf{P}^{-1} - \mathbf{X}\mathbf{Q}_{\hat{\beta}\hat{\beta}}\mathbf{X}' = \mathbf{R}^\perp\mathbf{P}^{-1}\mathbf{R}^{\perp'} = \mathbf{R}^\perp\mathbf{P}^{-1} = \mathbf{P}^{-1}\mathbf{R}^{\perp'} \quad (2.1-16)$$

Orthogonal Projectors:

$$\mathbf{R} = \mathbf{X}(\mathbf{X}'\mathbf{P}\mathbf{X})^{-1}\mathbf{X}'\mathbf{P}^{-1} \quad (2.1-17)$$

$$\mathbf{R}^\perp = (\mathbf{I} - \mathbf{R}) \quad (2.1-18)$$

Properties:

$$\mathbf{X}'\mathbf{P}\hat{\mathbf{e}} = \emptyset \quad (2.1-19)$$

$$\mathbf{R}\mathbf{X} = \mathbf{X} \quad (2.1-20)$$

$$\mathbf{R}^\perp\mathbf{X} = \emptyset \quad (2.1-21)$$

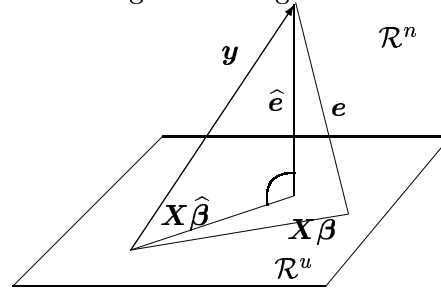
$$\Omega \rightarrow \min. \quad (2.1-22)$$

The estimation (2.1-5) is also a best linear unbiased estimation in approximation theory.

The same estimate is achieved according to the method of least-squares and in case of normally distributed observations with the *Maximum-Likelihood Method*.

In spite of these agreements the adjustment of the variance of unit weight $\hat{\sigma}^2$ is unbiased ($\mathbf{E}(\sigma^2) = \sigma^2$) only for the LSE method.

A geometrical interpretation of the LSE procedure is given in Figure 2.1. With rank $\mathbf{X} = u$ the column vectors of \mathbf{X} defines a u - dimensional sub-space \mathcal{R}^u of \mathcal{R}^n in which $\mathbf{X}\boldsymbol{\beta}$ can be estimated. This is given by the plane in Figure 2.1. $\hat{\boldsymbol{\beta}}$ is determined so that $\mathbf{X}\hat{\boldsymbol{\beta}}$ is the orthogonal projection of the observation vector $\mathbf{y} \in \mathcal{R}^n$ in the sub-space \mathcal{R}^u



$$\mathbf{R}\mathbf{y} = \mathbf{X}\hat{\boldsymbol{\beta}}. \quad (2.1-23)$$

Figure 2.1: Geometrical Interpretation of the least-squares estimation (LSE).

(2.1-17) easily verifies this relationship.

The projection divides \mathbf{y} in two parts:

$\mathbf{y} = \mathbf{R}\mathbf{y} + (\mathbf{I} - \mathbf{R})\mathbf{y}$ or with eqns. (2.1-23), (2.1-8), and (2.1-18) $\mathbf{y} = \mathbf{X}\hat{\boldsymbol{\beta}} - \hat{\mathbf{e}}$. A consequence of this fact is the property (2.1-19) $\mathbf{X}'\mathbf{P}\hat{\mathbf{e}} = \mathbf{0}$.

Linearization

In satellite geodesy the observation equations usually are nonlinear. Instead of the linear GMM (2.1-1) or (2.1-2) we define the following model:

$$\mathbf{y} + \mathbf{e} = \mathbf{f}(\boldsymbol{\beta}) \quad \text{with} \quad \mathbf{E}(\mathbf{e}) = \mathbf{0} \quad \text{and} \quad \mathbf{D}(\mathbf{e}) = \mathbf{D}(\mathbf{y}) = \sigma^2 \mathbf{P}^{-1} \quad (2.1-24)$$

where $\mathbf{f}(\cdot)$ denotes a real differentiable function with of the unknown parameters $\boldsymbol{\beta}$. If apriori (i.e. approximate) values $\boldsymbol{\beta}|_0$ for the unknown parameters $\boldsymbol{\beta}$ are known a Taylor series expansion for the observation equation is performed to transform the nonlinear problem to a linear one:

$$\mathbf{f}(\boldsymbol{\beta}) = \mathbf{f}(\boldsymbol{\beta})|_{\boldsymbol{\beta}=\boldsymbol{\beta}|_0} + \partial_{\boldsymbol{\beta}}\mathbf{f}(\boldsymbol{\beta})|_{\boldsymbol{\beta}=\boldsymbol{\beta}|_0}\Delta\boldsymbol{\beta} \quad (2.1-25)$$

with $\Delta\boldsymbol{\beta} = \boldsymbol{\beta} - \boldsymbol{\beta}|_0$ and $\partial_{\boldsymbol{\beta}}\mathbf{f}(\boldsymbol{\beta})|_{\boldsymbol{\beta}=\boldsymbol{\beta}|_0}$ as the *Jacobian* matrix evaluated at $\boldsymbol{\beta}|_0$. Introduction of eqn. (2.1-25) in eqn. (2.1-24) gives

$$(\mathbf{y} - \mathbf{f}(\boldsymbol{\beta})|_{\boldsymbol{\beta}=\boldsymbol{\beta}|_0}) + \mathbf{e} = \partial_{\boldsymbol{\beta}}\mathbf{f}(\boldsymbol{\beta})|_{\boldsymbol{\beta}=\boldsymbol{\beta}|_0}\Delta\boldsymbol{\beta} \quad (2.1-26)$$

which still has the form $\Delta\mathbf{y} + \mathbf{e} = \mathbf{X}\Delta\boldsymbol{\beta}$ but with

$$\begin{aligned} \Delta\mathbf{y} &= \mathbf{y} - \mathbf{f}(\boldsymbol{\beta})|_{\boldsymbol{\beta}=\boldsymbol{\beta}|_0} \quad \text{and} \\ \mathbf{X} &= \partial_{\boldsymbol{\beta}}\mathbf{f}(\boldsymbol{\beta})|_{\boldsymbol{\beta}=\boldsymbol{\beta}|_0} \quad \text{and} \\ \Delta\boldsymbol{\beta} &= \boldsymbol{\beta} - \boldsymbol{\beta}|_0. \end{aligned}$$

The meaning of the residual vector \mathbf{e} remains unchanged.

The corresponding normal equations have the the same form as eqn. (2.1-4):

$$\mathbf{X}'\mathbf{P}\mathbf{X}\Delta\hat{\boldsymbol{\beta}} = \mathbf{X}'\mathbf{P}\Delta\mathbf{y}. \quad (2.1-27)$$

The estimates of \mathbf{y} and $\boldsymbol{\beta}$ results in:

$$\hat{\mathbf{y}} = \Delta\hat{\mathbf{y}} + \mathbf{f}(\boldsymbol{\beta})|_{\boldsymbol{\beta}=\boldsymbol{\beta}|_0} \quad \text{and} \quad \hat{\boldsymbol{\beta}} = \Delta\hat{\boldsymbol{\beta}} + \boldsymbol{\beta}|_0. \quad (2.1-28)$$

It is necessary that the apriori values $\boldsymbol{\beta}|_0$ are good enough to approximate the nonlinear function with a first order Taylor series expansion. If this is not true, additional iterations are necessary using the latest estimated parameter as the new approximate value. If this procedure does not converge the partial derivatives in the design matrix \mathbf{X} have to be recomputed using the improved parameter estimation. Criteria for stopping the iterations are mostly based on the values of the parameter increments $\Delta\hat{\boldsymbol{\beta}}$ and the corresponding rms error.

The linearization quality and the validity of the Taylor series expansion (and the associated partial derivatives) may be proved by the test

$$\Delta \hat{\mathbf{y}} + \mathbf{X}(\boldsymbol{\beta})|_{\boldsymbol{\beta}=\boldsymbol{\beta}_0} \Delta \hat{\boldsymbol{\beta}} + \hat{\mathbf{e}} = \mathbf{X}(\hat{\boldsymbol{\beta}}). \quad (2.1-29)$$

2.1.2 Gauss-Markoff Model with Constraints on Parameters

The *Gauss-Markoff model with constraints on parameters* (other authors also use the expression "with restrictions" or "with conditions") can be used to include apriori information in addition to the observation equations. In the following we include a very short summary of the necessary formulae.

2.1.2.1 Observation Equations

The Gauss-Markoff Model (GMM) of full rank and with constraints on parameters is given by KOCH [1988] or RAO [1973]:

$$\mathbf{E}(\mathbf{y}) = \mathbf{X}\boldsymbol{\beta} \quad \text{with} \quad \mathbf{H}\boldsymbol{\beta} = \mathbf{w} \quad \text{and} \quad \mathbf{D}(\mathbf{y}) = \sigma^2 \mathbf{P}^{-1} \quad (2.1-30)$$

\mathbf{H} $r \times u$ constraint matrix of given coefficients with $\text{rg } \mathbf{H} = r$

\mathbf{w} $r \times 1$ vector of known constants

r number of constraints with $r < u$.

2.1.2.2 Summary of Least-Squares Estimation Formulae

The method of least-squares in the GMM with constraints minimizes the quadratic form Ω of eqn. (2.1-9) and meets the equation $\mathbf{H}\boldsymbol{\beta} = \mathbf{w}$.

Lets us summarize the *Least-Squares Estimation* (LSE) of the GMM with constraints:

Normal equations:

$$\begin{bmatrix} \mathbf{X}'\mathbf{P}\mathbf{X} & \mathbf{H}' \\ \mathbf{H} & \mathbf{0} \end{bmatrix} \begin{bmatrix} \tilde{\boldsymbol{\beta}} \\ \mathbf{k} \end{bmatrix} = \begin{bmatrix} \mathbf{X}'\mathbf{P}\mathbf{y} \\ \mathbf{w} \end{bmatrix} \quad (2.1-31)$$

Estimates:

$$\begin{aligned} \tilde{\boldsymbol{\beta}} &= (\mathbf{X}'\mathbf{P}\mathbf{X})^{-1}(\mathbf{X}'\mathbf{P}\mathbf{y} - \mathbf{H}'\mathbf{k}) = (\mathbf{X}'\mathbf{P}\mathbf{X})^{-1}(\mathbf{X}'\mathbf{P}\mathbf{y} \\ &\quad + \mathbf{H}'(\mathbf{H}(\mathbf{X}'\mathbf{P}\mathbf{X})^{-1}\mathbf{H}')^{-1}(\mathbf{w} - \mathbf{H}'(\mathbf{X}'\mathbf{P}\mathbf{X})^{-1}\mathbf{X}'\mathbf{P}\mathbf{y})) \end{aligned} \quad (2.1-32)$$

$$= \hat{\boldsymbol{\beta}} - (\mathbf{X}'\mathbf{P}\mathbf{X})^{-1}\mathbf{H}'(\mathbf{H}(\mathbf{X}'\mathbf{P}\mathbf{X})^{-1}\mathbf{H}')^{-1}(\mathbf{H}\hat{\boldsymbol{\beta}} - \mathbf{w}) \quad (2.1-33)$$

$$\begin{aligned} D(\tilde{\beta}) &= \sigma^2((\mathbf{X}'\mathbf{P}\mathbf{X})^{-1} \\ &\quad - (\mathbf{X}'\mathbf{P}\mathbf{X})^{-1}\mathbf{H}'(\mathbf{H}(\mathbf{X}'\mathbf{P}\mathbf{X})^{-1}\mathbf{H}')^{-1}\mathbf{H}(\mathbf{X}'\mathbf{P}\mathbf{X})^{-1}) \end{aligned} \quad (2.1-34)$$

$$\begin{aligned} \tilde{\Omega} &\stackrel{1.}{=} \Omega + (\mathbf{H}\hat{\beta} - \mathbf{w})'(\mathbf{H}(\mathbf{X}'\mathbf{P}\mathbf{X})^{-1}\mathbf{H}')^{-1}(\mathbf{H}\hat{\beta} - \mathbf{w}) \\ &= \Omega + (\tilde{\beta} - \hat{\beta})'(\mathbf{X}'\mathbf{P}\mathbf{X})^{-1}(\tilde{\beta} - \hat{\beta}) \end{aligned} \quad (2.1-35)$$

$$\begin{aligned} \tilde{\Omega} &\stackrel{2.}{=} \mathbf{y}'\mathbf{P}\mathbf{y} - \mathbf{y}'\mathbf{P}\mathbf{X}\tilde{\beta} - \mathbf{w}'\mathbf{k} \end{aligned} \quad (2.1-36)$$

$$\tilde{\sigma}^2 = \tilde{\Omega}/(n - u + r) \quad (2.1-37)$$

Properties:

$$\tilde{\Omega} \geq \Omega \quad (2.1-38)$$

$$\mathbf{X}'\mathbf{P}\hat{\mathbf{e}} + \mathbf{H}'\mathbf{k} = \mathbf{0} \quad (2.1-39)$$

The difference $\tilde{\Omega} - \Omega$ is an important quantity indicating whether an additional constraint is useful or not. This value is therefore frequently used for hypothesis tests [KOCH 1988].

2.1.3 Other Statistical Models

The method of least-squares adjustment is a special case in the theory of the linear statistical models. In this section we give an overview of the relations of the GMM to more general models.

The formulae of the GMM discussed above may also be derived from the more general *Bayesian inference* [KOCH 1990] and as a special case from the *mixed adjustment model* in standard statistical techniques.

The *Bayesian inference* are based on the Bayes' theorem only. The theorem allows to derive the aposteriori distribution for the unknown parameters as a function of the density distribution of the observation and the apriori density function of the unknown parameters. Based on the aposteriori distribution the estimates of the unknown parameters and their confidence regions are computed. Introducing no additional apriori information for the unknown parameters leads us directly to the formulae of the standard statistical techniques.

In the *mixed adjustment model* of the standard statistical techniques the vector \mathbf{e} of the observation equation of the GMM (2.1-2) is replaced by a linear combination $-\mathbf{Z}\boldsymbol{\gamma}$ of the unknown parameters $\boldsymbol{\gamma}$:

$$\mathbf{y} = \mathbf{X}\boldsymbol{\beta} + \mathbf{Z}\boldsymbol{\gamma} \quad \text{with} \quad \mathbf{E}(\boldsymbol{\gamma}) = \boldsymbol{\emptyset} \quad \text{and} \quad \mathbf{D}(\boldsymbol{\gamma}) = \sigma^2 \mathbf{P}^{-1}. \quad (2.1-40)$$

This model is the general case of classical statistical techniques [HELMERT 1872] and is also called *Gauss-Helmert Model* [WOLF 1978]. $\mathbf{X}\boldsymbol{\beta}$ may be interpreted as a systematic trend whereas $\mathbf{Z}\boldsymbol{\gamma}$ is the random part of the model. The latter part is also called *signal*. These formulae allow for a prediction of the parameter $\boldsymbol{\beta}$.

Let us replace the vector \mathbf{y} by $\mathbf{Z}\bar{\mathbf{y}} + \mathbf{c}$ in eqn. (2.1-40) where $\bar{\mathbf{y}}$ is as a $r \times 1$ vector of observations and \mathbf{c} an $n \times 1$ vector of constants. The resulting observation equation proves the statement that $\boldsymbol{\gamma}$ is the error vector of $\bar{\mathbf{y}}$.

The well known *model for prediction and filtering* may be derived by replacing \mathbf{y} in eqn. (2.1-40) by $\mathbf{y} + \mathbf{e}$. This allows to take into account observation noise in addition to the signal $\mathbf{Z}\boldsymbol{\gamma}$.

The model based on r *Condition Equations* only results from the mixed model with $\mathbf{X} = \boldsymbol{\emptyset}$.

The formulae of the *linear Bucy-Kalman filter* [GELB 1974] which are often used in modern geodesy are under special conditions also a member of this family. In Section 2.4.2 we derive the filter equations which are identical to the formulae of the sequential LSE in Section 2.3.

2.2 Parameter Pre-elimination

The method of *pre-elimination* of parameters is a basic tool to reduce the dimension of the NEQ system without losing information (apart from the parameters pre-eliminated).

With a separation of the parameter vector $\hat{\boldsymbol{\beta}}$ into the vectors $\hat{\boldsymbol{\beta}}_1$ and $\hat{\boldsymbol{\beta}}_2$ we may write the NEQ system (2.1-4) in the form:

$$\begin{bmatrix} \mathbf{N}_{11} & \mathbf{N}_{12} \\ \mathbf{N}_{21} & \mathbf{N}_{22} \end{bmatrix} \begin{bmatrix} \hat{\boldsymbol{\beta}}_1 \\ \hat{\boldsymbol{\beta}}_2 \end{bmatrix} = \begin{bmatrix} \mathbf{b}_1 \\ \mathbf{b}_2 \end{bmatrix}. \quad (2.2-1)$$

The quadratic form $\mathbf{y}'\mathbf{P}\mathbf{y}$ is also given and remains for the time being unchanged.

In order to eliminate the parameter vector $\hat{\boldsymbol{\beta}}_2$ from the NEQ system the second line of eqn. (2.2-1) is multiplied by $-\mathbf{N}_{12}\mathbf{N}_{22}^{-1}$:

$$\begin{bmatrix} \mathbf{N}_{11} & \mathbf{N}_{12} \\ -\mathbf{N}_{12}\mathbf{N}_{22}^{-1}\mathbf{N}_{21} & -\mathbf{N}_{12} \end{bmatrix} \begin{bmatrix} \hat{\boldsymbol{\beta}}_1 \\ \hat{\boldsymbol{\beta}}_2 \end{bmatrix} = \begin{bmatrix} \mathbf{b}_1 \\ -\mathbf{N}_{12}\mathbf{N}_{22}^{-1}\mathbf{b}_2 \end{bmatrix}. \quad (2.2-2)$$

Evaluating the matrix multiplication and adding the resulting two equations leaves us with

$$\left(\mathbf{N}_{11} - \underbrace{\mathbf{N}_{12} \mathbf{N}_{22}^{-1} \mathbf{N}_{12}}_a \right) \hat{\boldsymbol{\beta}}_1 = \mathbf{b}_1 - \underbrace{\mathbf{N}_{12} \mathbf{N}_{22}^{-1} \mathbf{b}_2}_b \quad (2.2-3)$$

or in abbreviated form

$$\tilde{\mathbf{N}}_{11} \hat{\boldsymbol{\beta}}_1 = \tilde{\mathbf{b}}_1. \quad (2.2-4)$$

This new NEQ is reduced by the parameter vector $\hat{\boldsymbol{\beta}}_2$. Due to the correction terms a and b in eqn. (2.2-3) the resulting NEQ still contains the full information coming from this pre-eliminated parameter $\hat{\boldsymbol{\beta}}_2$.

The quadratic form $\tilde{\Omega}$ in (2.1-9) can be derived with (2.2-2) and (2.2-3) in the following way:

$$\begin{aligned} \tilde{\Omega} &= \mathbf{y}' \mathbf{P} \mathbf{y} - \mathbf{y}' \mathbf{P} \mathbf{X} \hat{\boldsymbol{\beta}} \\ &= \mathbf{y}' \mathbf{P} \mathbf{y} - [\mathbf{b}'_1 \mathbf{b}'_2] \begin{bmatrix} \hat{\boldsymbol{\beta}}_1 \\ \hat{\boldsymbol{\beta}}_2 \end{bmatrix} \\ &= \mathbf{y}' \mathbf{P} \mathbf{y} - \mathbf{b}'_1 \hat{\boldsymbol{\beta}}_1 - \mathbf{b}'_2 \mathbf{N}_{22}^{-1} (\mathbf{b}_2 - \mathbf{N}_{21} \hat{\boldsymbol{\beta}}_1) \\ &= \mathbf{y}' \mathbf{P} \mathbf{y} - \mathbf{b}'_1 \hat{\boldsymbol{\beta}}_1 - \mathbf{b}'_2 \mathbf{N}_{22}^{-1} \mathbf{b}_2 - \mathbf{b}'_2 \mathbf{N}_{22}^{-1} \mathbf{N}_{21} \hat{\boldsymbol{\beta}}_1 \\ &= \underbrace{\mathbf{y}' \mathbf{P} \mathbf{y} - \hat{\boldsymbol{\beta}}'_1 (\mathbf{b}_1 - \mathbf{N}_{12} \mathbf{N}_{22}^{-1} \mathbf{b}_2)}_{\Omega} - \underbrace{\mathbf{b}'_2 \mathbf{N}_{22}^{-1} \mathbf{b}_2}_c. \end{aligned} \quad (2.2-5)$$

The quadratic form Ω (respectively $\mathbf{y}' \mathbf{P} \mathbf{y}$) corresponding to the reduced NEQ system (2.2-4) has to be corrected by the term $c = -\mathbf{b}'_2 \mathbf{N}_{22}^{-1} \mathbf{b}_2$.

If required the parameter $\hat{\boldsymbol{\beta}}_2$ may be recomputed using the result for $\hat{\boldsymbol{\beta}}_1$:

$$\hat{\boldsymbol{\beta}}_2 = \mathbf{N}_{22}^{-1} (\mathbf{b}_2 - \mathbf{N}_{21} \hat{\boldsymbol{\beta}}_1) \quad (2.2-6)$$

and with the law of error propagation we find for $\mathbf{Q}_{\hat{\boldsymbol{\beta}}_2 \hat{\boldsymbol{\beta}}_2}$:

$$\mathbf{Q}_{\hat{\boldsymbol{\beta}}_2 \hat{\boldsymbol{\beta}}_2} = \mathbf{N}_{22}^{-1} + \mathbf{N}_{22}^{-1} \mathbf{N}_{21} (\mathbf{N}_{11} - \mathbf{N}_{12} \mathbf{N}_{22}^{-1} \mathbf{N}_{12})^{-1} \mathbf{N}_{12} \mathbf{N}_{22}^{-1}. \quad (2.2-7)$$

The matrix of cofactors $\mathbf{Q}_{\hat{\boldsymbol{\beta}}_1 \hat{\boldsymbol{\beta}}_1}$ results from eqn. (2.2-3) and eqn. (2.1-14) in

$$\mathbf{Q}_{\hat{\boldsymbol{\beta}}_1 \hat{\boldsymbol{\beta}}_1} = (\mathbf{N}_{11} - \mathbf{N}_{12} \mathbf{N}_{22}^{-1} \mathbf{N}_{12})^{-1} \quad (2.2-8)$$

and may be written using the matrix identity [KOCH 1988]

$$(\mathbf{A}^{-1} - \mathbf{B}\mathbf{D}^{-1}\mathbf{C})^{-1} = \mathbf{A} + \mathbf{A}\mathbf{B}(\mathbf{D} - \mathbf{C}\mathbf{A}\mathbf{B})^{-1}\mathbf{C}\mathbf{A} \quad (2.2-9)$$

in a similar way as eqn. (2.2-7):

$$\mathbf{Q}_{\hat{\beta}_1\hat{\beta}_1} = \mathbf{N}_{11}^{-1} + \mathbf{N}_{11}^{-1}\mathbf{N}_{21} \left(\mathbf{N}_{22} - \mathbf{N}_{12}\mathbf{N}_{11}^{-1}\mathbf{N}_{12} \right)^{-1} \mathbf{N}_{12}\mathbf{N}_{11}^{-1}. \quad (2.2-10)$$

The similarity of the formulae for $\mathbf{Q}_{\hat{\beta}_1\hat{\beta}_1}$ and $\mathbf{Q}_{\hat{\beta}_2\hat{\beta}_2}$ are clearly due to the fact that the selection of the indices is arbitrary.

The determination of partial covariance matrices (i.e. elimination of parameters from the covariance matrix) from the (inverse) normal equation matrix is trivial. The inverse normal equation matrix on the left hand side of eqn. (2.2-1) according to [KOCH 1988] is given by

$$\begin{bmatrix} \mathbf{N}_{11} & \mathbf{N}_{12} \\ \mathbf{N}_{21} & \mathbf{N}_{22} \end{bmatrix}^{-1} = \begin{bmatrix} \mathbf{N}_{11}^{-1} + \mathbf{N}_{11}^{-1}\mathbf{N}_{21} \left(\mathbf{N}_{22} - \mathbf{N}_{12}\mathbf{N}_{11}^{-1}\mathbf{N}_{12} \right)^{-1} \mathbf{N}_{12}\mathbf{N}_{11}^{-1} & - \left(\mathbf{N}_{22} - \mathbf{N}_{12}\mathbf{N}_{11}^{-1}\mathbf{N}_{12} \right)^{-1} \mathbf{N}_{12}\mathbf{N}_{11}^{-1} \\ -\mathbf{N}_{11}^{-1}\mathbf{N}_{12} \left(\mathbf{N}_{22} - \mathbf{N}_{12}\mathbf{N}_{11}^{-1}\mathbf{N}_{12} \right)^{-1} & \left(\mathbf{N}_{22} - \mathbf{N}_{12}\mathbf{N}_{11}^{-1}\mathbf{N}_{12} \right)^{-1} \end{bmatrix}. \quad (2.2-11)$$

Comparison with eqn. (2.2-10) shows that we may skip the corresponding rows and columns to eliminate parameters from the resulting cofactor matrix resp. from the covariance matrix. From the parameter estimation vector we have to cut the rows. The quadratic form remains unchanged because the influence of all parameters was already taken into account.

2.3 Sequential Adjustment Methods

In this section we review the concept of sequential least-squares estimation techniques. The results for the LSE using all observations in one step are the same as splitting up the LSE in different parts and combining the results in a latter step. The two estimation procedures are general knowledge in the geodetic world since HELMERT [1872]. Many geodetic applications based on this concept are known as so-called *Helmert blocking*. In "old" times the methods of sequential LSE were important because of the missing computer power. In "modern" times the same methods are applied (in particular for GPS) in order to handle the big number of observations. Figure 5.1 gives an impression of the number of observations and solve-for parameters when analysing the global GPS network of the IGS.

To prove the identity of both methods we first solve for the parameters according the common adjustment in one step. Thereafter we verify that the same results are obtained using sequential adjustment. We first consider the estimation of the

unknown parameters and then the estimation of the variance of unit weight later on.

Let us start with the observation equations (see eqn. (2.1-1)):

$$\begin{aligned} \mathbf{y}_1 + \mathbf{e}_1 &= \mathbf{X}_1 \boldsymbol{\beta}_c + \mathbf{O}_1 \boldsymbol{\gamma}_1 & \text{with} & \quad \mathbf{D}(\mathbf{y}_1) = \sigma_1^2 \mathbf{P}_1^{-1} \\ \mathbf{y}_2 + \mathbf{e}_2 &= \mathbf{X}_2 \boldsymbol{\beta}_c + \mathbf{O}_2 \boldsymbol{\gamma}_2 & \text{with} & \quad \mathbf{D}(\mathbf{y}_2) = \sigma_2^2 \mathbf{P}_2^{-1}. \end{aligned} \quad (2.3-1)$$

In this case we divided the observation array \mathbf{y} into two independent observation series \mathbf{y}_1 and \mathbf{y}_2 . We would like to estimate the parameters $\boldsymbol{\beta}_c$ common to both parts with the help of both observation parts \mathbf{y}_1 and \mathbf{y}_2 . The parameter types $\boldsymbol{\gamma}_1$ and $\boldsymbol{\gamma}_2$ are only relevant for the individual observation series.

The proof of the equivalence of both methods is based on the important assumption that both observation series are independent.

The division into two parts is general enough. If both methods are leading to the same results we can derive formulae for additional sub-divisions by assuming one observation series to be already the result of an accumulation of different observation series.

In the case of nonlinear problems it is assumed that the Taylor series expansion (2.1-25) is evaluated at the same apriori value $\boldsymbol{\beta}|_0$. This is not a general requirement, as we will see in Section 2.5.2, but it makes the derivation easier.

2.3.1 Common Adjustment

In matrix notation we may write the observation equation (2.3-1) in the form:

$$\begin{aligned} \begin{bmatrix} \mathbf{y}_1 \\ \mathbf{y}_2 \end{bmatrix} + \begin{bmatrix} \mathbf{e}_1 \\ \mathbf{e}_2 \end{bmatrix} &= \begin{bmatrix} \mathbf{X}_1 & \mathbf{O}_1 & \emptyset \\ \mathbf{X}_2 & \emptyset & \mathbf{O}_2 \end{bmatrix} \begin{bmatrix} \boldsymbol{\beta}_c \\ \boldsymbol{\gamma}_1 \\ \boldsymbol{\gamma}_2 \end{bmatrix} \\ \text{with} \quad \mathbf{D} \left(\begin{bmatrix} \mathbf{y}_1 \\ \mathbf{y}_2 \end{bmatrix} \right) &= \sigma_c^2 \begin{bmatrix} \mathbf{P}_1^{-1} & \emptyset \\ \emptyset & \mathbf{P}_2^{-1} \end{bmatrix} \end{aligned} \quad (2.3-2)$$

which has the form

$$\mathbf{y}_c + \mathbf{e}_c = \mathbf{X}_c \boldsymbol{\beta}_c^* \quad \text{with} \quad \mathbf{D}(\mathbf{y}_c) = \sigma_c^2 \mathbf{P}_c^{-1}. \quad (2.3-3)$$

The independence of both observation series is expressed by the zero values of the off diagonal elements in the dispersion matrix.

Substituting the corresponding values for \mathbf{y}_c , \mathbf{X}_c and $\boldsymbol{\beta}_c$ in eqn. (2.1-4) leads to the normal equation system of the LSE:

$$\begin{bmatrix} (\mathbf{X}'_1 \mathbf{P}_1 \mathbf{X}_1 + \mathbf{X}'_2 \mathbf{P}_2 \mathbf{X}_2) & \mathbf{X}'_1 \mathbf{P}_1 \mathbf{O}_1 & \mathbf{X}'_2 \mathbf{P}_2 \mathbf{O}_2 \\ \mathbf{O}'_1 \mathbf{P}_1 \mathbf{X}_1 & \mathbf{O}'_1 \mathbf{P}_1 \mathbf{O}_1 & \emptyset \\ \mathbf{O}'_2 \mathbf{P}_2 \mathbf{X}_2 & \emptyset & \mathbf{O}'_2 \mathbf{P}_2 \mathbf{O}_2 \end{bmatrix} \begin{bmatrix} \hat{\boldsymbol{\beta}}_c \\ \hat{\boldsymbol{\gamma}}_1 \\ \hat{\boldsymbol{\gamma}}_2 \end{bmatrix}$$

$$= \begin{bmatrix} (\mathbf{X}'_1 \mathbf{P}_1 \mathbf{y}_1 + \mathbf{X}'_2 \mathbf{P}_2 \mathbf{y}_2) \\ \mathbf{O}'_1 \mathbf{P}_1 \mathbf{y}_1 \\ \mathbf{O}'_2 \mathbf{P}_2 \mathbf{y}_2 \end{bmatrix}. \quad (2.3-4)$$

In order to derive the parameter estimates $\hat{\beta}_c$ we pre-eliminate the parameters $\hat{\gamma}_1$ and $\hat{\gamma}_2$.

Pre-elimination of $\hat{\gamma}_1$ gives according to eqns. (2.2-1) and (2.2-3):

$$\begin{aligned} & \begin{bmatrix} (\mathbf{X}'_1 \mathbf{P}_1 \mathbf{X}_1 + \mathbf{X}'_2 \mathbf{P}_2 \mathbf{X}_2) - \mathbf{X}'_1 \mathbf{P}_1 \mathbf{O}_1 (\mathbf{O}'_1 \mathbf{P}_1 \mathbf{O}_1)^{-1} \mathbf{O}'_1 \mathbf{P}_1 \mathbf{X}_1 & \mathbf{X}'_2 \mathbf{P}_2 \mathbf{O}_2 \\ \mathbf{O}'_2 \mathbf{P}_2 \mathbf{X}_2 & \mathbf{O}'_2 \mathbf{P}_2 \mathbf{O}_2 \end{bmatrix} \begin{bmatrix} \hat{\beta}_c \\ \hat{\gamma}_2 \end{bmatrix} \\ &= \begin{bmatrix} (\mathbf{X}'_1 \mathbf{P}_1 \mathbf{y}_1 + \mathbf{X}'_2 \mathbf{P}_2 \mathbf{y}_2) - \mathbf{X}'_1 \mathbf{P}_1 \mathbf{O}_1 (\mathbf{O}'_1 \mathbf{P}_1 \mathbf{O}_1)^{-1} \mathbf{O}'_1 \mathbf{P}_1 \mathbf{y}_1 \\ \mathbf{O}'_2 \mathbf{P}_2 \mathbf{y}_2 \end{bmatrix}. \end{aligned} \quad (2.3-5)$$

And pre-eliminating additionally $\hat{\gamma}_2$ results in:

$$\begin{aligned} & \begin{bmatrix} (\mathbf{X}'_1 \mathbf{P}_1 \mathbf{X}_1 + \mathbf{X}'_2 \mathbf{P}_2 \mathbf{X}_2) - \mathbf{X}'_1 \mathbf{P}_1 \mathbf{O}_1 (\mathbf{O}'_1 \mathbf{P}_1 \mathbf{O}_1)^{-1} \mathbf{O}'_1 \mathbf{P}_1 \mathbf{X}_1 \cdots \\ \cdots - \mathbf{X}'_2 \mathbf{P}_2 \mathbf{O}_2 (\mathbf{O}'_2 \mathbf{P}_2 \mathbf{O}_2)^{-1} \mathbf{O}'_2 \mathbf{P}_2 \mathbf{X}_2 \end{bmatrix} \hat{\beta}_c \\ &= \begin{bmatrix} (\mathbf{X}'_1 \mathbf{P}_1 \mathbf{y}_1 + \mathbf{X}'_2 \mathbf{P}_2 \mathbf{y}_2) - \mathbf{X}'_1 \mathbf{P}_1 \mathbf{O}_1 (\mathbf{O}'_1 \mathbf{P}_1 \mathbf{O}_1)^{-1} \mathbf{O}'_1 \mathbf{P}_1 \mathbf{y}_1 \cdots \\ \cdots - \mathbf{X}'_2 \mathbf{P}_2 \mathbf{O}_2 (\mathbf{O}'_2 \mathbf{P}_2 \mathbf{O}_2)^{-1} \mathbf{O}'_2 \mathbf{P}_2 \mathbf{y}_2 \end{bmatrix}. \end{aligned} \quad (2.3-6)$$

Concerning the common parameter β_c the NEQ system is equivalent to the original NEQ system (2.3-4). The impact of $\hat{\gamma}_1$ and $\hat{\gamma}_2$ on the parameters β_c is taken into account.

2.3.2 Sequential Least-Squares Adjustment

The sequential LSE treats in the first step each observation series independently. An estimation is performed for the unknown parameters using only the observations of a particular observation series. In a second step the contribution of each sequential parameter estimation to the common estimation is computed.

Starting with the same observation equations as in the previous section, eqns. (2.3-1), we may write

$$\begin{aligned} \mathbf{y}_1 + \mathbf{e}_1 &= \mathbf{X}_1 \beta_1 + \mathbf{O}_1 \gamma_1 & \text{with} & \quad \mathbf{D}(\mathbf{y}_1) = \sigma_1^2 \mathbf{P}_1^{-1} \\ \mathbf{y}_2 + \mathbf{e}_2 &= \mathbf{X}_2 \beta_2 + \mathbf{O}_2 \gamma_2 & \text{with} & \quad \mathbf{D}(\mathbf{y}_2) = \sigma_2^2 \mathbf{P}_2^{-1} \end{aligned} \quad (2.3-7)$$

or, in more general notation:

$$\mathbf{y}_i + \mathbf{e}_i = \mathbf{X}_i \beta_i + \mathbf{O}_i \gamma_i \quad \text{with} \quad \mathbf{D}(\mathbf{y}_i) = \sigma_i^2 \mathbf{P}_i^{-1}, \quad i = 1, 2 \quad (2.3-8)$$

where the vector $\hat{\beta}_i$ denotes the values of the common parameter vector β_c satisfying observation series y_i only.

First step: Solving each individual NEQ

The normal equations for the observation equation systems $i = 1, 2$ may be written according to eqn. (2.1-4) as

$$\begin{bmatrix} X_i' P_i X_i & X_i' P_i O_i \\ O_i' P_i X_i & O_i' P_i O_i \end{bmatrix} \begin{bmatrix} \hat{\beta}_i \\ \hat{\gamma}_i \end{bmatrix} = \begin{bmatrix} X_i' P_i y_i \\ O_i' P_i y_i \end{bmatrix} \quad \text{with } i = 1, 2. \quad (2.3-9)$$

Pre-eliminating $\hat{\gamma}_i$ gives

$$\begin{aligned} \hat{\beta}_i &= \left(X_i' P_i X_i - X_i' P_i O_i (O_i' P_i O_i)^{-1} O_i' P_i X_i \right)^{-1} \\ &\quad \cdot \left(X_i' P_i y_i - X_i' P_i O_i (O_i' P_i O_i)^{-1} O_i' P_i y_i \right) \end{aligned} \quad (2.3-10)$$

$$\begin{aligned} D(\hat{\beta}_i) &= \hat{\sigma}_i^2 \left(X_i' P_i X_i - X_i' P_i O_i (O_i' P_i O_i)^{-1} O_i' P_i X_i \right)^{-1} \\ &= \hat{\sigma}_i^2 \Sigma_i. \end{aligned} \quad (2.3-11)$$

Step 2: Aposteriori LSE

In this aposteriori LSE step the estimation for $\hat{\beta}_c$ is derived using the results of the individual solutions (2.3-10) and (2.3-11) obtained in the first step.

The pseudo-observation equations set up in this second step have the following form

$$y_{II} + e_{II} = X_{II} \hat{\beta}_c \quad \text{with} \quad D(y_{II}) = \sigma_c^2 P_{II}^{-1} \quad (2.3-12)$$

or more explicitly:

$$\begin{bmatrix} \hat{\beta}_1 \\ \hat{\beta}_2 \end{bmatrix} + \begin{bmatrix} e_{1II} \\ e_{2II} \end{bmatrix} = \begin{bmatrix} I \\ I \end{bmatrix} \hat{\beta}_c \quad \text{with} \quad D\left(\begin{bmatrix} \hat{\beta}_1 \\ \hat{\beta}_2 \end{bmatrix} \right) = \sigma_c^2 \begin{bmatrix} \Sigma_1 & \emptyset \\ \emptyset & \Sigma_2 \end{bmatrix}.$$

This means that the results of the individual estimations $\hat{\beta}_i$ and Σ_i are used to form the combined LSE. The interpretation of this pseudo-observation equation system is easy: Each estimation is introduced as a new observation using the associated covariance matrix as the corresponding weight matrix.

The normal equation system may be written as:

$$X_{II}' P_{II} X_{II} \hat{\beta}_c = X_{II}' P_{II} y_{II} \quad (2.3-13)$$

or more explicitly

$$\begin{aligned} &\begin{bmatrix} I', I' \end{bmatrix} \begin{bmatrix} \Sigma_1^{-1} & \emptyset \\ \emptyset & \Sigma_2^{-1} \end{bmatrix} \begin{bmatrix} I \\ I \end{bmatrix} \hat{\beta}_c \\ &= \begin{bmatrix} I', I' \end{bmatrix} \begin{bmatrix} \Sigma_1^{-1} & \emptyset \\ \emptyset & \Sigma_2^{-1} \end{bmatrix} \begin{bmatrix} \hat{\beta}_1 \\ \hat{\beta}_2 \end{bmatrix}. \end{aligned} \quad (2.3-14)$$

With eqn. (2.3-10) and eqn. (2.3-11) we obtain

$$\begin{aligned} & \begin{bmatrix} (\mathbf{X}'_1 \mathbf{P}_1 \mathbf{X}_1 + \mathbf{X}'_2 \mathbf{P}_2 \mathbf{X}_2) - \mathbf{X}'_1 \mathbf{P}_1 \mathbf{O}_1 (\mathbf{O}'_1 \mathbf{P}_1 \mathbf{O}_1)^{-1} \mathbf{O}'_1 \mathbf{P}_1 \mathbf{X}_1 \cdots \\ \cdots - \mathbf{X}'_2 \mathbf{P}_2 \mathbf{O}_2 (\mathbf{O}'_2 \mathbf{P}_2 \mathbf{O}_2)^{-1} \mathbf{O}'_2 \mathbf{P}_2 \mathbf{X}_2 \end{bmatrix} \hat{\boldsymbol{\beta}}_c \\ &= \begin{bmatrix} (\mathbf{X}'_1 \mathbf{P}_1 \mathbf{y}_1 + \mathbf{X}'_2 \mathbf{P}_2 \mathbf{y}_2) - \mathbf{X}'_1 \mathbf{P}_1 \mathbf{O}_1 (\mathbf{O}'_1 \mathbf{P}_1 \mathbf{O}_1)^{-1} \mathbf{O}'_1 \mathbf{P}_1 \mathbf{y}_1 \cdots \\ \cdots - \mathbf{X}'_2 \mathbf{P}_2 \mathbf{O}_2 (\mathbf{O}'_2 \mathbf{P}_2 \mathbf{O}_2)^{-1} \mathbf{O}'_2 \mathbf{P}_2 \mathbf{y}_2 \end{bmatrix} \end{aligned} \quad (2.3-15)$$

which is identical with (2.3-6).

Due to the special notation in the observation equation system the parameters in the vectors $\boldsymbol{\beta}_1$ and $\boldsymbol{\beta}_2$ are ordered in the same way. Generally this will not be the case. To guarantee the combination of the same parameter type the selection matrix \mathbf{S}_i can be used to transform $\mathbf{X}_i \rightarrow \mathbf{S}_i \mathbf{X}_i$ and $\boldsymbol{\beta}_i \rightarrow \mathbf{S}_i \boldsymbol{\beta}_i$, $i = 1, 2$.

2.3.3 Summary of Sequential LSE Formulae

With the results of the previous two subsections we can generalize the LSE procedure to m independent observation series.

Let us illustrate this procedure with an example stemming from processing GPS observations.

Each individual solution may be based on observations pertaining to single days. Common parameters $\boldsymbol{\beta}_c$ are e.g. coordinates, parameters $\boldsymbol{\gamma}_i$ which are only of interest for individual days are ambiguities, troposphere parameters, possibly orbit parameters or earth rotation parameters.

As a result of the least-squares adjustment including all m sequential solutions for the common parameters $\boldsymbol{\beta}_c$ we obtain

$$\begin{aligned} & \left(\sum_{i=1}^m \left(\mathbf{X}'_i \mathbf{P}_i \mathbf{X}_i - \mathbf{X}'_i \mathbf{P}_i \mathbf{O}_i (\mathbf{O}'_i \mathbf{P}_i \mathbf{O}_i)^{-1} \mathbf{O}'_i \mathbf{P}_i \mathbf{X}_i \right) \right) \hat{\boldsymbol{\beta}}_c \\ &= \sum_{i=1}^m \left(\mathbf{X}'_i \mathbf{P}_i \mathbf{y}_i - \mathbf{X}'_i \mathbf{P}_i \mathbf{O}_i (\mathbf{O}'_i \mathbf{P}_i \mathbf{O}_i)^{-1} \mathbf{O}'_i \mathbf{P}_i \mathbf{y}_i \right) \end{aligned} \quad (2.3-16)$$

or, if no parameters $\boldsymbol{\gamma}_i$ are present in eqn. (2.3-8) or the parameters $\boldsymbol{\gamma}_i$ are already pre-eliminated:

$$\left(\sum_{i=1}^m \mathbf{X}'_i \mathbf{P}_i \mathbf{X}_i \right) \hat{\boldsymbol{\beta}}_c = \sum_{i=1}^m \mathbf{X}'_i \mathbf{P}_i \mathbf{y}_i. \quad (2.3-17)$$

This simple superposition of normal equations is always possible if the individual observation series are independent and if the dispersion matrix has the diagonal form (2.3-2).

2.3.4 Computation of the RMS in the Sequential LSE

To complete the proof that the same results are obtained for both LSE methods, the formulae for the computation of the variance factor (variance of unit weight) is derived below. For simplicity we will make the assumption that there are no parameters $\boldsymbol{\gamma}_i$ involved in the sequential solutions (e.g. already pre-eliminated). The simplification means that we may substitute

$$\boldsymbol{\beta}_c^* = \boldsymbol{\beta}_c \quad (2.3-18)$$

in eqn. (2.3-3).

Starting point is the estimation of $\hat{\sigma}_c^2$ resulting from the common LSE. From eqn. (2.1-10) we obtain using eqns. (2.3-18), (2.3-2), and (2.3-3):

$$\hat{\sigma}_c^2 = \Omega_c/f_c = \tilde{\mathbf{e}}_c' \mathbf{P}_c \hat{\mathbf{e}}_c / f_c = \left(\sum_{i=1}^m \tilde{\mathbf{e}}_{i_c}' \mathbf{P}_c \hat{\mathbf{e}}_{i_c} \right) / f_c \quad (2.3-19)$$

where

$$\hat{\mathbf{e}}_c = (\hat{\mathbf{e}}_{1_c}, \dots, \hat{\mathbf{e}}_{m_c})',$$

$$\hat{\mathbf{e}}_c = \mathbf{X}_c \hat{\boldsymbol{\beta}}_c - \mathbf{y}_c: \text{residuals with respect to the combined solution,}$$

\mathbf{X}_c complete first design matrix referring to all observations \mathbf{y}_c ,

$\hat{\boldsymbol{\beta}}_c$ combined parameter estimation vector,

$f_c = n_c - u_c$: redundancy of the combined GMM of full rank,

n_c total number of observations: $\sum_{i=1}^m n_i$,

u_c total number of unknowns: sum over the *different* parameter types,

\cdot_c the index c denotes the estimation with respect to the combined solution, and

m number of the observation series.

In the first step of the sequential LSE we compute the variance of the unit weight in model (2.3-8) as:

$$\hat{\sigma}_i^2 = \Omega_i/f_i = \left(\sum_{i=1}^m \tilde{\mathbf{e}}_i' \mathbf{P}_i \hat{\mathbf{e}}_i \right) / f_i \quad (2.3-20)$$

where

$$\hat{\mathbf{e}}_i = \mathbf{X}_i \hat{\boldsymbol{\beta}}_i - \mathbf{y}_i: \text{residuals with respect to the individual solutions } i,$$

\mathbf{X}_i first design matrix referring to the observation series \mathbf{y}_i ,

$\hat{\boldsymbol{\beta}}_i$ parameter estimation vector of the sequential LSE i ,

$f_i = n_i - u_i$: redundancy of the GMM i of full rank,

n_i number of observations in series i , and

u_i number of unknowns in series i .

The computation of $\hat{\sigma}_c$ in eqn. (2.3-19) using the m values $\hat{\sigma}_i$ from relation (2.3-20) is possible in the following way:

Let us assume that the residuals $\hat{\mathbf{e}}_{i_c}$ are composed of $\hat{\mathbf{e}}_i$ and a correction vector $\Delta\hat{\mathbf{e}}_{i_c}$ due to the different estimations $\hat{\boldsymbol{\beta}}_c$ resp. $\hat{\boldsymbol{\beta}}_i$:

$$\hat{\mathbf{e}}_{i_c} = \hat{\mathbf{e}}_i + \Delta\hat{\mathbf{e}}_{i_c} \quad (2.3-21)$$

or considering $\hat{\mathbf{e}}_i = \mathbf{X}_i\hat{\boldsymbol{\beta}}_i - \mathbf{y}_i$ and $\hat{\mathbf{e}}_{i_c} = \mathbf{X}_i\hat{\boldsymbol{\beta}}_c - \mathbf{y}_i$:

$$\Delta\hat{\mathbf{e}}_{i_c} = \mathbf{X}_i(\hat{\boldsymbol{\beta}}_c - \hat{\boldsymbol{\beta}}_i). \quad (2.3-22)$$

The term $\hat{\mathbf{e}}_{i_c}'\mathbf{P}_c\hat{\mathbf{e}}_{i_c}$ may be expressed with eqns. (2.3-21) and (2.3-22) and the relation $\mathbf{X}_i\mathbf{P}_i\hat{\mathbf{e}}_i = \mathbf{0}$ follows from eqn. (2.1-19):

$$\hat{\mathbf{e}}_{i_c}'\mathbf{P}_c\hat{\mathbf{e}}_{i_c} = \hat{\mathbf{e}}_i'\mathbf{P}_i\hat{\mathbf{e}}_i + (\hat{\boldsymbol{\beta}}_c - \hat{\boldsymbol{\beta}}_i)'\mathbf{X}_i'\mathbf{P}_i\mathbf{X}_i(\hat{\boldsymbol{\beta}}_c - \hat{\boldsymbol{\beta}}_i) \quad (2.3-23)$$

or, in abbreviated from

$$\Omega_{i_c} = \Omega_i + (\hat{\boldsymbol{\beta}}_c - \hat{\boldsymbol{\beta}}_i)'\mathbf{X}_i'\mathbf{P}_i\mathbf{X}_i(\hat{\boldsymbol{\beta}}_c - \hat{\boldsymbol{\beta}}_i). \quad (2.3-24)$$

Introducing eqn. (2.3-24) in eqn. (2.3-19) results in:

$$\Omega_c = \sum_{i=1}^m \Omega_{i_c} = \sum_{i=1}^m \Omega_i + \sum_{i=1}^m (\hat{\boldsymbol{\beta}}_c - \hat{\boldsymbol{\beta}}_i)'\mathbf{X}_i'\mathbf{P}_i\mathbf{X}_i(\hat{\boldsymbol{\beta}}_c - \hat{\boldsymbol{\beta}}_i)$$

and using (2.3-20)

$$\hat{\sigma}_c^2 = \left(\sum_{i=1}^m \hat{\sigma}_i \cdot f_i + \sum_{i=1}^m (\hat{\boldsymbol{\beta}}_c - \hat{\boldsymbol{\beta}}_i)'\mathbf{X}_i'\mathbf{P}_i\mathbf{X}_i(\hat{\boldsymbol{\beta}}_c - \hat{\boldsymbol{\beta}}_i) \right) / f_c. \quad (2.3-25)$$

The first term stems from each individual solution whereas the second term serves as a correction term taking care of the fact that the individual rms computations are not yet referring to the combined parameter estimation.

It is interesting that the correction term $\sum_{i=1}^m (\hat{\beta}_c - \hat{\beta}_i)' \mathbf{X}_i' \mathbf{P}_i \mathbf{X}_i (\hat{\beta}_c - \hat{\beta}_i)$ is equivalent to the quadratic form Ω_{II} following from the analysis of the pseudo-observation equations (2.3-12), (2.3-13). Indeed

$$\Omega_{II} = \hat{\mathbf{e}}_{II}' \mathbf{P}_{II} \hat{\mathbf{e}}_{II} = \sum_{i=1}^m (\hat{\beta}_c - \hat{\beta}_i)' \mathbf{X}_i' \mathbf{P}_i \mathbf{X}_i (\hat{\beta}_c - \hat{\beta}_i) \quad (2.3-26)$$

where

$$\hat{\mathbf{e}}_{II} = \begin{bmatrix} \hat{e}_{1II} \\ \vdots \\ \hat{e}_{mII} \end{bmatrix}; \quad \mathbf{P}_{II} = \begin{bmatrix} \mathbf{P}_{1II} & & \mathbf{0} \\ & \ddots & \\ \mathbf{0} & & \mathbf{P}_{mII} \end{bmatrix} \quad (2.3-27)$$

and

$$\hat{e}_{iII} = (\hat{\beta}_c - \hat{\beta}_i); \quad \mathbf{P}_{iII} = \Sigma_i^{-1} = (\mathbf{X}_i' \mathbf{P}_i \mathbf{X}_i); \quad i = 1, \dots, m. \quad (2.3-28)$$

Therefore relation (2.3-24) may be written as

$$\Omega_{i_c} = \Omega_i + \Omega_{iII}. \quad (2.3-29)$$

With eqn. (2.1-9) we find the equivalent form for Ω_{II}

$$\begin{aligned} \Omega_{II} &= \mathbf{y}_{II}' \mathbf{P}_{II} \mathbf{y}_{II} - \mathbf{y}_{II}' \mathbf{P}_{II} \mathbf{X}_{II} \hat{\beta}_c \\ &= \sum_{i=1}^m \hat{\beta}_i' \mathbf{X}_i' \mathbf{P}_i \mathbf{X}_i (\hat{\beta}_i - \hat{\beta}_c). \end{aligned} \quad (2.3-30)$$

If the combination is done on the basis of normal equations with known matrices $\mathbf{X}_i' \mathbf{P}_i \mathbf{X}_i$, $\mathbf{X}_i' \mathbf{P}_i \mathbf{y}_i$ and $\mathbf{y}_i' \mathbf{P}_i \mathbf{y}_i$ the following formulae may be used instead of eqn. (2.3-25):

$$\Omega_c = \sum_{i=1}^m \mathbf{y}_i' \mathbf{P}_i \mathbf{y}_i - \sum_{i=1}^m \mathbf{y}_i' \mathbf{P}_i \mathbf{X}_i \hat{\beta}_c \quad (2.3-31)$$

$$\hat{\sigma}_c^2 = \left(\sum_{i=1}^m \mathbf{y}_i' \mathbf{P}_i \mathbf{y}_i - \sum_{i=1}^m \mathbf{y}_i' \mathbf{P}_i \mathbf{X}_i \hat{\beta}_c \right) / f_c. \quad (2.3-32)$$

2.4 Applications Related to Sequential LSE

2.4.1 Special Cases of Sequential LSE

Starting from the observation equation (2.3-7) and the pseudo-observation equations (2.3-12) we derived the LSE results (2.3-15), which were identical with the results of the common adjustment (2.3-6). We will derive some special applications which

are frequently used in the practice.

Case 1: $O_1 = \emptyset$, $O_2 = \emptyset$ (zero matrices O)

If there are no additional parameters γ_i in the individual observation series the normal equation system (2.3-6) reads as

$$(\mathbf{X}'_1 \mathbf{P}_1 \mathbf{X}_1 + \mathbf{X}'_2 \mathbf{P}_2 \mathbf{X}_2) \hat{\boldsymbol{\beta}}_c = (\mathbf{X}'_1 \mathbf{P}_1 \mathbf{y}_1 + \mathbf{X}'_2 \mathbf{P}_2 \mathbf{y}_2) . \quad (2.4-1)$$

There are no "correction terms" to be taken care in this example. The "classical" combination of coordinates based on this principle.

Case 2: $O_1 = \emptyset$, $O_2 = \emptyset$ and $\mathbf{X}_1 = \mathbf{I}$, $\mathbf{y}_1 = \emptyset$

This special case corresponds to the introduction of apriori weights \mathbf{P}_1 on the parameters $\boldsymbol{\beta}_c$

From the general form (2.3-6) or (2.3-15) of the NEQs we immediately obtain:

$$(\mathbf{P}_1 + \mathbf{X}'_2 \mathbf{P}_2 \mathbf{X}_2) \hat{\boldsymbol{\beta}}_c = \mathbf{X}'_2 \mathbf{P}_2 \mathbf{y}_2 . \quad (2.4-2)$$

This application will be discussed in more detail in Section 2.6.1.

Case 3: $O_1 = \emptyset$, $O_2 = \emptyset$ and $\mathbf{X}_1 = \emptyset$, $\mathbf{y}_1 = \emptyset$

Under these simple assumptions we obtain the original formulae for the GMM:

$$\begin{aligned} \hat{\boldsymbol{\beta}}_c &= (\mathbf{X}'_2 \mathbf{P}_2 \mathbf{X}_2)^{-1} \mathbf{X}'_2 \mathbf{P}_2 \mathbf{y}_2 \\ \text{with } \mathbf{D}(\hat{\boldsymbol{\beta}}_c) &= (\mathbf{X}'_2 \mathbf{P}_2 \mathbf{X}_2)^{-1} . \end{aligned} \quad (2.4-3)$$

2.4.2 Recursive Parameter Estimation

In this section we will analyse the impact of additional observation series \mathbf{y}_m on the results of the combined solution.

Let us assume that we already produced a combined solution using all observation series up to \mathbf{y}_{m-1} . For all matrices referring to these observations we use the index $m - 1$. Using in addition the observation series \mathbf{y}_m leads in analogy to eqn. (2.3-17) to the normal equation system of the form:

$$\begin{aligned} (\mathbf{X}'_{m-1} \mathbf{P}_{m-1} \mathbf{X}_{m-1} + \mathbf{X}'_m \mathbf{P}_m \mathbf{X}_m) \hat{\boldsymbol{\beta}}_m \\ = (\mathbf{X}'_{m-1} \mathbf{P}_{m-1} \mathbf{y}_{m-1} + \mathbf{X}'_m \mathbf{P}_m \mathbf{y}_m) . \end{aligned} \quad (2.4-4)$$

There are two different observation equations leading to the above normal equation system.

The *first possibility* corresponds to the observation equations (2.3-1):

$$\begin{aligned} \mathbf{y} + \mathbf{e} &= \mathbf{X} \boldsymbol{\beta}_m \quad \text{with } \mathbf{D}(\mathbf{y}) = \sigma^2 \mathbf{P}^{-1} \\ \text{with } \mathbf{X} &= \begin{bmatrix} \mathbf{X}_{m-1} \\ \mathbf{X}_m \end{bmatrix}, \quad \mathbf{y} = \begin{bmatrix} \mathbf{y}_{m-1} \\ \mathbf{y}_m \end{bmatrix} \quad \text{and } \mathbf{D}(\mathbf{y}) = \sigma^2 \begin{bmatrix} \mathbf{P}_{m-1}^{-1} & \emptyset \\ \emptyset & \mathbf{P}_m^{-1} \end{bmatrix} . \end{aligned} \quad (2.4-5)$$

There is a *second interpretation* when using the previously estimated parameters and the associated covariance information instead of the observations:

$$\begin{aligned} \mathbf{y} + \mathbf{e} &= \mathbf{X} \boldsymbol{\beta}_m \quad \text{with} \quad \mathbf{D}(\mathbf{y}) = \sigma^2 \mathbf{P}^{-1} \\ \text{with } \mathbf{X} &= \begin{bmatrix} \mathbf{I}_{m-1} \\ \mathbf{X}_m \end{bmatrix}, \quad \mathbf{y} = \begin{bmatrix} \hat{\boldsymbol{\beta}}_{m-1} \\ \mathbf{y}_m \end{bmatrix} \\ \text{and } \mathbf{D}(\mathbf{y}) &= \sigma^2 \begin{bmatrix} (\mathbf{X}'_{m-1} \mathbf{P}_{m-1} \mathbf{X}_{m-1})^{-1} & \boldsymbol{\emptyset} \\ \boldsymbol{\emptyset} & \mathbf{P}_m^{-1} \end{bmatrix}. \end{aligned}$$

The results for $\hat{\boldsymbol{\beta}}_{m-1}$, $\mathbf{D}(\hat{\boldsymbol{\beta}}_{m-1})$ and Ω_{m-1} up to observation series $m-1$ are given according to eqns. (2.1-5) and (2.1-6) as

$$\hat{\boldsymbol{\beta}}_{m-1} = (\mathbf{X}'_{m-1} \mathbf{P}_{m-1} \mathbf{X}_{m-1})^{-1} \mathbf{X}'_{m-1} \mathbf{P}_{m-1} \mathbf{y}_{m-1}, \quad (2.4-6)$$

$$\mathbf{D}(\hat{\boldsymbol{\beta}}_{m-1}) = \hat{\sigma}_{m-1}^2 (\mathbf{X}'_{m-1} \mathbf{P}_{m-1} \mathbf{X}_{m-1})^{-1} = \hat{\sigma}_{m-1}^2 \boldsymbol{\Sigma}_{m-1} \quad (2.4-7)$$

and with eqn. (2.1-9)

$$\begin{aligned} \Omega_{m-1} &= (\mathbf{y}_{m-1} - \mathbf{X}_{m-1} \hat{\boldsymbol{\beta}}_{m-1})' \mathbf{P}_{m-1} (\mathbf{y}_{m-1} - \mathbf{X}_{m-1} \hat{\boldsymbol{\beta}}_{m-1}) \\ &= \mathbf{y}'_{m-1} \mathbf{P}_{m-1} \mathbf{y}_{m-1} - \mathbf{y}'_{m-1} \mathbf{P}_{m-1} \mathbf{X}_{m-1} \hat{\boldsymbol{\beta}}_{m-1}. \end{aligned} \quad (2.4-8)$$

Solving eqn. (2.4-4) for the unknown parameters $\hat{\boldsymbol{\beta}}_m$ we obtain

$$\begin{aligned} \hat{\boldsymbol{\beta}}_m &= (\mathbf{X}'_{m-1} \mathbf{P}_{m-1} \mathbf{X}_{m-1} + \mathbf{X}'_m \mathbf{P}_m \mathbf{X}_m)^{-1} (\mathbf{X}'_{m-1} \mathbf{P}_{m-1} \mathbf{y}_{m-1} \\ &\quad + \mathbf{X}'_m \mathbf{P}_m \mathbf{y}_m). \end{aligned} \quad (2.4-9)$$

For the dispersion matrix we obtain according to eqns. (2.1-5), (2.1-6), and (2.4-7)

$$\begin{aligned} \mathbf{D}(\hat{\boldsymbol{\beta}}_m) &= \hat{\sigma}_m^2 (\mathbf{X}'_{m-1} \mathbf{P}_{m-1} \mathbf{X}_{m-1} + \mathbf{X}'_m \mathbf{P}_m \mathbf{X}_m)^{-1} \\ &= \hat{\sigma}_m^2 (\boldsymbol{\Sigma}_{m-1}^{-1} + \mathbf{X}'_m \mathbf{P}_m \mathbf{X}_m)^{-1} \\ &= \hat{\sigma}_m^2 \boldsymbol{\Sigma}_m \end{aligned} \quad (2.4-10)$$

using the definition

$$\boldsymbol{\Sigma}_m = (\boldsymbol{\Sigma}_{m-1}^{-1} + \mathbf{X}'_m \mathbf{P}_m \mathbf{X}_m)^{-1} \quad (2.4-11)$$

In analogy to eqn. (2.3-31) we get

$$\Omega_m = (\mathbf{y}'_{m-1} \mathbf{P}_{m-1} \mathbf{y}_{m-1} + \mathbf{y}'_m \mathbf{P}_m \mathbf{y}_m) - (\mathbf{y}'_{m-1} \mathbf{P}_{m-1} \mathbf{X}_{m-1} + \mathbf{y}'_m \mathbf{P}_m \mathbf{X}_m) \hat{\boldsymbol{\beta}}_m. \quad (2.4-12)$$

Using the substitution (2.4-6), (2.4-7), (2.4-11) we conclude from eqn. (2.4-9)

$$\hat{\boldsymbol{\beta}}_m = (\boldsymbol{\Sigma}_{m-1}^{-1} + \mathbf{X}'_m \mathbf{P}_m \mathbf{X}_m)^{-1} (\boldsymbol{\Sigma}_{m-1}^{-1} \hat{\boldsymbol{\beta}}_{m-1} + \mathbf{X}'_m \mathbf{P}_m \mathbf{y}_m) \quad (2.4-13)$$

or

$$\hat{\boldsymbol{\beta}}_m = \boldsymbol{\Sigma}_m \left(\boldsymbol{\Sigma}_{m-1}^{-1} \hat{\boldsymbol{\beta}}_{m-1} + \mathbf{X}'_m \mathbf{P}_m \mathbf{y}_m \right). \quad (2.4-14)$$

Applying the matrix identity (2.2-9) on the right hand side of eqn. (2.4-11) we get

$$\boldsymbol{\Sigma}_m = \boldsymbol{\Sigma}_{m-1} - \mathbf{F}_m \mathbf{X}_m \boldsymbol{\Sigma}_{m-1} \quad (2.4-15)$$

where

$$\mathbf{F}_m = \boldsymbol{\Sigma}_{m-1} \mathbf{X}'_m \bar{\mathbf{P}} \quad (2.4-16)$$

with

$$\bar{\mathbf{P}} = (\mathbf{P}_m^{-1} + \mathbf{X}_m \boldsymbol{\Sigma}_{m-1} \mathbf{X}'_m)^{-1}. \quad (2.4-17)$$

Introducing eqn. (2.4-15) into eqn. (2.4-14) leads to the result

$$\begin{aligned} \hat{\boldsymbol{\beta}}_m &= \hat{\boldsymbol{\beta}}_{m-1} - \mathbf{F}_{m-1} \mathbf{X}_m \hat{\boldsymbol{\beta}}_{m-1} + (\boldsymbol{\Sigma}_{m-1} \mathbf{X}'_m \mathbf{P}_m \\ &\quad - \mathbf{F}_m \mathbf{X}_m \boldsymbol{\Sigma}_{m-1} \mathbf{X}'_m \mathbf{P}_m) \mathbf{y}_m. \end{aligned} \quad (2.4-18)$$

Multiplying eqn. (2.4-16) from the right with $\bar{\mathbf{P}}^{-1} \mathbf{P}_m$ and using eqn. (2.4-17) leads to:

$$\mathbf{F}_m (\mathbf{X}_m \boldsymbol{\Sigma}_{m-1} \mathbf{X}'_m + \mathbf{P}_m^{-1}) \mathbf{P}_m = \boldsymbol{\Sigma}_{m-1} \mathbf{X}'_m \mathbf{P}_m \quad (2.4-19)$$

or

$$\boldsymbol{\Sigma}_{m-1} \mathbf{X}'_m \mathbf{P}_m - \mathbf{F}_m \mathbf{X}_m \boldsymbol{\Sigma}_{m-1} \mathbf{X}'_m \mathbf{P}_m = \mathbf{F}_m. \quad (2.4-20)$$

Substituting the right hand side of this expression into (2.4-18) gives

$$\hat{\boldsymbol{\beta}}_m = \hat{\boldsymbol{\beta}}_{m-1} + \mathbf{F}_m \bar{\mathbf{e}}_m \quad \text{with} \quad \bar{\mathbf{e}}_m = \mathbf{y}_m - \mathbf{X}_m \hat{\boldsymbol{\beta}}_{m-1}. \quad (2.4-21)$$

This relation reflects directly the impact of additional observations \mathbf{y}_m on the estimated parameters $\hat{\boldsymbol{\beta}}_{m-1}$ and it may be written formally as

$$\hat{\boldsymbol{\beta}}_m = \hat{\boldsymbol{\beta}}_{m-1} + \Delta \hat{\boldsymbol{\beta}}_m. \quad (2.4-22)$$

Let us now derive the impact of additional observations on the value of Ω_m .

According to eqn. (2.4-12) we get for Ω_m using (2.4-22):

$$\begin{aligned} \Omega_m &= (\mathbf{y}'_{m-1} \mathbf{P}_{m-1} \mathbf{y}_{m-1} - \mathbf{y}'_{m-1} \mathbf{P}_{m-1} \mathbf{X}_{m-1} \hat{\boldsymbol{\beta}}_{m-1}) + (\mathbf{y}'_m \mathbf{P}_m \mathbf{y}_m \\ &\quad - \mathbf{y}'_{m-1} \mathbf{P}_{m-1} \mathbf{X}_{m-1} \Delta \hat{\boldsymbol{\beta}}_m - \mathbf{y}'_m \mathbf{P}_m \mathbf{X}_m \hat{\boldsymbol{\beta}}_{m-1} - \mathbf{y}'_m \mathbf{P}_m \mathbf{X}_m \Delta \hat{\boldsymbol{\beta}}_m) \\ &= \Omega_{m-1} + \Delta \Omega_m. \end{aligned} \quad (2.4-23)$$

The first term is given by (2.4-8), and for the second term we find:

$$\Delta \Omega_m = \mathbf{y}'_m \mathbf{P}_m \mathbf{y}_m - \mathbf{y}'_{m-1} \mathbf{P}_{m-1} \mathbf{X}_{m-1} \Delta \hat{\boldsymbol{\beta}}_m - \mathbf{y}'_m \mathbf{P}_m \mathbf{X}_m \hat{\boldsymbol{\beta}}_{m-1} - \mathbf{y}'_m \mathbf{P}_m \mathbf{X}_m \Delta \hat{\boldsymbol{\beta}}_m.$$

Using eqns. (2.4-21) and (2.4-22), i.e. $\Delta\hat{\beta}_m = \mathbf{F}_m\bar{\mathbf{e}}_m$, we may write

$$\begin{aligned}\Delta\Omega_m &= \mathbf{y}'_m\mathbf{P}_m\mathbf{y}_m - \mathbf{y}'_{m-1}\mathbf{P}_{m-1}\mathbf{X}_{m-1}\mathbf{F}_m\bar{\mathbf{e}}_m - \mathbf{y}'_m\mathbf{P}_m\mathbf{X}_m\hat{\beta}_{m-1} \\ &\quad - \mathbf{y}'_m\mathbf{P}_m\mathbf{X}_m\mathbf{F}_m\bar{\mathbf{e}}_m, \text{ or using eqn. (2.4-21)} \\ \Delta\Omega_m &= \mathbf{y}'_m\mathbf{P}_m\bar{\mathbf{e}}_m - \mathbf{y}'_{m-1}\mathbf{P}_{m-1}\mathbf{X}_{m-1}\mathbf{F}_m\bar{\mathbf{e}}_m - \mathbf{y}'_m\mathbf{P}_m\mathbf{X}_m\mathbf{F}_m\bar{\mathbf{e}}_m.\end{aligned}$$

Substitution of \mathbf{F}_m in the second and third terms according to eqn. (2.4-16) results with eqn. (2.4-6) to

$$\Delta\Omega_m = \mathbf{y}'_m\mathbf{P}_m\bar{\mathbf{e}}_m - \hat{\beta}'_{m-1}\mathbf{X}'_m\bar{\mathbf{P}}\bar{\mathbf{e}}_m - \mathbf{y}'_m\mathbf{P}_m\mathbf{X}_m\boldsymbol{\Sigma}_{m-1}\mathbf{X}'_m\bar{\mathbf{P}}\bar{\mathbf{e}}_m. \quad (2.4-24)$$

This last term of this expression may also be written in a different form using simple matrix identities:

$$\begin{aligned}\mathbf{y}'_m\mathbf{P}_m\mathbf{X}_m\boldsymbol{\Sigma}_{m-1}\mathbf{X}'_m\bar{\mathbf{P}}\bar{\mathbf{e}}_m &= \mathbf{y}'_m(\mathbf{P}_m - \mathbf{P}_m + \mathbf{P}_m\mathbf{X}_m\boldsymbol{\Sigma}_{m-1}\mathbf{X}'_m\bar{\mathbf{P}})\bar{\mathbf{e}}_m \\ &= \mathbf{y}'_m(\mathbf{P}_m - \mathbf{P}_m\bar{\mathbf{P}}^{-1}\bar{\mathbf{P}} + \mathbf{P}_m\mathbf{X}_m\boldsymbol{\Sigma}_{m-1}\mathbf{X}'_m\bar{\mathbf{P}})\bar{\mathbf{e}}_m.\end{aligned}$$

Substitution for $\bar{\mathbf{P}}^{-1}$ using eqn. (2.4-17) gives

$$\begin{aligned}\mathbf{y}'_m\mathbf{P}_m\mathbf{X}_m\boldsymbol{\Sigma}_{m-1}\mathbf{X}'_m\bar{\mathbf{P}}\bar{\mathbf{e}}_m &= \mathbf{y}'_m\{\mathbf{P}_m + [\mathbf{P}_m\mathbf{X}_m\boldsymbol{\Sigma}_{m-1}\mathbf{X}'_m \\ &\quad - \mathbf{P}_m(\mathbf{P}_m^{-1} + \mathbf{X}_m\boldsymbol{\Sigma}_{m-1}\mathbf{X}'_m)]\bar{\mathbf{P}}\}\bar{\mathbf{e}}_m \\ &= \mathbf{y}'_m(\mathbf{P}_m - \bar{\mathbf{P}})\bar{\mathbf{e}}_m.\end{aligned}$$

Introducing this into (2.4-24) and using eqn. (2.4-21) leaves us with the following equation for $\Delta\Omega_m$:

$$\begin{aligned}\Delta\Omega_m &= \mathbf{y}'_m\mathbf{P}_m\bar{\mathbf{e}}_m - \hat{\beta}'_{m-1}\mathbf{X}'_m\bar{\mathbf{P}}\bar{\mathbf{e}}_m - \mathbf{y}'_m(\mathbf{P}_m - \bar{\mathbf{P}})\bar{\mathbf{e}}_m \\ &= (\mathbf{y}'_m - \hat{\beta}'_{m-1}\mathbf{X}'_m)\bar{\mathbf{P}}\bar{\mathbf{e}}_m \\ &= \bar{\mathbf{e}}'_m\bar{\mathbf{P}}\bar{\mathbf{e}}_m.\end{aligned} \quad (2.4-25)$$

Let us summarize the formulae of the recursive LSE:

$\hat{\beta}_m = \hat{\beta}_{m-1} + \mathbf{F}_m\bar{\mathbf{e}}_m$	(2.4-26a)
$\boldsymbol{\Sigma}_m = \boldsymbol{\Sigma}_{m-1} - \mathbf{F}_m\mathbf{X}_m\boldsymbol{\Sigma}_{m-1}$	(2.4-26b)
$\Omega_m = \Omega_{m-1} + \bar{\mathbf{e}}'_m\bar{\mathbf{P}}\bar{\mathbf{e}}_m$	(2.4-26c)
where	(2.4-26d)
$\bar{\mathbf{e}}_m = \mathbf{y}_m - \mathbf{X}_m\hat{\beta}_{m-1}$	(2.4-26e)
$\mathbf{F}_m = \boldsymbol{\Sigma}_{m-1}\mathbf{X}'_m\bar{\mathbf{P}}$ (= Kalman gain matrix)	(2.4-26f)
$\boldsymbol{\Sigma}_{m-1} = (\mathbf{X}'_{m-1}\mathbf{P}_{m-1}\mathbf{X}_{m-1})^{-1}$	(2.4-26g)
$\bar{\mathbf{P}} = (\mathbf{P}_m^{-1} + \mathbf{X}_m\boldsymbol{\Sigma}_{m-1}\mathbf{X}'_m)^{-1}$	(2.4-26h)

The above set of formulae is equivalent to the *update step* in the *Kalman Filter* procedure.

In general the Kalman filter is subdivided into three parts: A prediction, a time update and an update step. The prediction step enables additional possibilities of the general filter equations. The prediction of the state vector $\hat{\beta}_m$ and the associated covariance information may be based on a dynamical time model and the associated information concerning the *system noise*. Only if the state vector is time-independent and the system noise is negligible the Kalman filter equations are identical with the *parameter-estimation* formulae presented above. In this case the filter problem is reduced to a NEQ representation of the sequential LSE procedure. For more information we refer to GELB [1974], HERRING [1990], LANDAU [1988], and SALZMANN [1993].

The formulae (2.4-26) are very useful if the number of additional observations is small. The formulae are almost trivial if the update is performed using only one observation at the time because in this case the update step of the estimated values simplified from an inversion step to a division step. For large dimensions per iteration step the formulae of the sequential LSE are easier.

Assuming that the observation series \mathbf{y}_m and \mathbf{y}_{m-1} are already a result of least-squares adjustments, in fact pseudo-observations of the parameters $\hat{\beta}$, we may derive the sequential LSE formulae based on covariances.

Using the notation of the corresponding formulae based on normal equations in Section 2.3.2 we make the substitutions $\beta_m = \beta_c$, $\beta_{m-1} = \hat{\beta}_1$, $\mathbf{y}_m = \hat{\beta}_2$, $\mathbf{X}_m = \mathbf{I}_m$, $\mathbf{P}_m^{-1} = \Sigma_2$, $\Sigma_m = \Sigma_c$, $\Sigma_{m-1} = \Sigma_1$, $\Omega_m = \Omega_c$, $\Omega_{m-1} = \Omega_1$ and $\mathbf{e}_m = \hat{\beta}_2 - \hat{\beta}_1$. Eqns. (2.4-26) may then be written as

$$\begin{aligned}\hat{\beta}_c &= \hat{\beta}_1 + \Sigma_1(\Sigma_1 + \Sigma_2)^{-1}(\hat{\beta}_2 - \hat{\beta}_1), \\ \Sigma_c &= \Sigma_1 - \Sigma_1(\Sigma_1 + \Sigma_2)^{-1}\Sigma_1, \quad \text{and} \\ \Omega_c &= \Omega_1 + (\hat{\beta}_2 - \hat{\beta}_1)'(\Sigma_1 + \Sigma_2)^{-1}(\hat{\beta}_2 - \hat{\beta}_1).\end{aligned}\tag{2.4-27}$$

The iterative estimation is based on the simple principle: The addition of a correction term to the actual solution takes care of the impact of a new observation series or a new sequential least-squares estimate on the combined solution.

An example for the impact of a series of sequential adjustments on the coordinate estimates may be found in Figure 5.3.

These formulae are also well suited to study the effect of apriori constraints for the final solution (see also Section 2.6.1). To constrain a parameter to the apriori value

β_{apr} we substitute $\Sigma_1 = \Sigma_{\text{apr}}$, $\hat{\beta}_1 = \beta_{\text{apr}}$, $\Omega_1 = \Omega_{\text{apr}}$, $\Sigma_2 = \Sigma_{\text{free}}$, $\hat{\beta}_2 = \beta_{\text{free}}$, and $\Omega_2 = \Omega_{\text{free}}$.

On the other hand, it is possible to reconstruct the original solution without apriori weights if the matrices β_{apr} , Σ_{apr} , and Ω_{apr} are known. To remove the apriori constraints we have to proceed as follows (using the results from (2.4-27)):

$$\begin{aligned}
 \hat{\beta}_{\text{free}} &= \beta_{\text{apr}} + \Sigma_{\text{apr}}(\Sigma_{\text{apr}} - \Sigma_c)^{-1}(\hat{\beta}_c - \beta_{\text{apr}}) \\
 &= \hat{\beta}_c + (\Sigma_c + \Sigma_c(\Sigma_{\text{apr}} - \Sigma_c)^{-1}\Sigma_c)\Sigma_{\text{apr}}^{-1}(\hat{\beta}_c - \beta_{\text{apr}}) \quad , \\
 \Sigma_{\text{free}} &= \Sigma_{\text{apr}}(\Sigma_{\text{apr}} - \Sigma_c)^{-1}\Sigma_{\text{apr}} - \Sigma_{\text{apr}} \\
 &= \Sigma_c + \Sigma_c(\Sigma_{\text{apr}} - \Sigma_c)^{-1}\Sigma_c \quad , \text{ and} \\
 \Omega_{\text{free}} &= \Omega_c - (\hat{\beta}_c - \hat{\beta}_{\text{apr}})'(\Sigma_{\text{apr}} - \Sigma_c)^{-1}(\hat{\beta}_c - \hat{\beta}_{\text{apr}}).
 \end{aligned} \tag{2.4-28}$$

The operator for the update of covariances is compared to the simple addition in the case of the normal equations much more complicated. In the second case we obtain

$$\Sigma_{\text{free}}^{-1} = \Sigma_c^{-1} - \Sigma_{\text{apr}}^{-1} \tag{2.4-29}$$

which, in view of the matrix identity (2.2-9), is not amazing.

An application of such procedures is the combination of GPS solutions using the *SINEX format* [KOUBA 1996]. The SINEX files contain results mainly for coordinate- and velocity estimates including the covariance information. Additional information concerning the sites (station names, antenna types, receiver types, antenna heights, eccentricities, etc.) is helpful for site identification.

For any institution combining results of different processing centers it is essential to have in addition the information of the applied apriori constraints available. This is in particular true for solutions in which a certain number of sites is tightly constrained to a given value (it is a standard IGS procedure to constrain 13 sites to the ITRF values). Free network solutions are achievable after the removal of the constraints using relations (2.4-28) or (2.4-29) respectively.

2.5 Parameter Transformations

The sequential LSE methods of Section 2.3 are only valid if all normal equations are based on the same apriori values for the unknown parameters. If this is not true the normal equations have to be transformed to the same set of apriori values.

Other applications are shown in the following subsections and also in section 4 dealing with orbit combination where it is necessary to transform orbit parameters referring to different apriori arcs.

2.5.1 Principles

Let us depart again from the observation equations of the GMM in the nonlinear case (2.1-26):

$$\Delta \mathbf{y} + \mathbf{e} = \mathbf{X} \Delta \boldsymbol{\beta} \quad ; \quad \mathbf{D}(\Delta \mathbf{y}) = \sigma^2 \mathbf{P}^{-1} \quad (2.5-1)$$

The corresponding normal equations follows from eqn. (2.1-27):

$$\mathbf{X}' \mathbf{P} \mathbf{X} \Delta \hat{\boldsymbol{\beta}} = \mathbf{X}' \mathbf{P} \Delta \mathbf{y} \quad (2.5-2)$$

or, in the abbreviated form,

$$\mathbf{N} \Delta \hat{\boldsymbol{\beta}} = \mathbf{b} \quad (2.5-3)$$

where

$$\mathbf{N} = \mathbf{X}' \mathbf{P} \mathbf{X} \quad \text{and} \quad \mathbf{b} = \mathbf{X}' \mathbf{P} \Delta \mathbf{y}. \quad (2.5-4)$$

Below we derive the normal equation system corresponding to the new parameter $\Delta \tilde{\boldsymbol{\beta}}$ which is related to the parameter $\Delta \hat{\boldsymbol{\beta}}$ through the linear transformation:

$$\Delta \hat{\boldsymbol{\beta}} = \mathbf{B} \Delta \tilde{\boldsymbol{\beta}} + d\boldsymbol{\beta} \quad (2.5-5)$$

where

\mathbf{B} is the transformation matrix with u rows and u columns ($u \times u$)

$d\boldsymbol{\beta}$ is the vector of constants u rows ($u \times 1$).

Introducing eqn. (2.5-5) into the observation equation (2.5-1) gives

$$\Delta \mathbf{y} - \mathbf{X} d\boldsymbol{\beta} + \mathbf{e} = \mathbf{X} \mathbf{B} \Delta \tilde{\boldsymbol{\beta}}, \quad (2.5-6)$$

which leads to the normal equations

$$\mathbf{B}' \mathbf{X}' \mathbf{P} \mathbf{X} \mathbf{B} \Delta \tilde{\boldsymbol{\beta}} = \mathbf{B}' \mathbf{X}' \mathbf{P} \Delta \tilde{\mathbf{y}} \quad \text{with} \quad \Delta \tilde{\mathbf{y}} = (\Delta \mathbf{y} - \mathbf{X} d\boldsymbol{\beta}) \quad (2.5-7)$$

or comparing with eqn. (2.5-2) and using eqn. (2.5-4)

$$\tilde{\mathbf{N}} \Delta \tilde{\boldsymbol{\beta}} = \tilde{\mathbf{b}} \quad \text{where} \quad (2.5-8)$$

$$\tilde{\mathbf{N}} = \mathbf{B}' \mathbf{N} \mathbf{B} \quad \text{and} \quad (2.5-9)$$

$$\tilde{\mathbf{b}} = \mathbf{B}' (\mathbf{b} - \mathbf{N} d\boldsymbol{\beta}). \quad (2.5-10)$$

The original form of the normal equation system (2.5-2), referring to the parameter $\Delta \hat{\boldsymbol{\beta}}$, is now transformed in a normal equation system with respect to the parameter $\Delta \tilde{\boldsymbol{\beta}}$.

For completeness the transformation for the quadratic form $\Delta \mathbf{y}' \mathbf{P} \Delta \mathbf{y}$ is also given.

With eqns. (2.5-1) and (2.5-7) we get

$$\begin{aligned}
 \Delta \tilde{\mathbf{y}}' \mathbf{P} \Delta \tilde{\mathbf{y}} &= (\Delta \mathbf{y} - \mathbf{X} d\boldsymbol{\beta})' \mathbf{P} (\Delta \mathbf{y} - \mathbf{X} d\boldsymbol{\beta}) \\
 &= \Delta \mathbf{y}' \mathbf{P} \Delta \mathbf{y} - 2\Delta \mathbf{y}' \mathbf{P} \mathbf{X} d\boldsymbol{\beta} + d\boldsymbol{\beta}' \mathbf{X}' \mathbf{P} \mathbf{X} d\boldsymbol{\beta} \\
 &= \Delta \mathbf{y}' \mathbf{P} \Delta \mathbf{y} - 2\mathbf{b}' d\boldsymbol{\beta} + d\boldsymbol{\beta}' \mathbf{N} d\boldsymbol{\beta}.
 \end{aligned} \tag{2.5-11}$$

2.5.2 Applications

2.5.2.1 Superposition of NEQs Derived from Parameter Transformations

Let us assume that we processed m sequential least-squares adjustments for the determination of a common parameter $\hat{\boldsymbol{\beta}}_c$. Each solution $i = 1, 2, \dots, m$ may result in the normal equation system

$$\mathbf{X}'_i \mathbf{P}_i \mathbf{X}_i \hat{\boldsymbol{\beta}}_i = \mathbf{X}'_i \mathbf{P}_i \mathbf{y}_i \tag{2.5-12}$$

from which we may estimate the parameter vector $\hat{\boldsymbol{\beta}}_i$. So far the situation is identical to the first step in Section 2.3.2. In matrix notation we may also write

$$\begin{bmatrix} \mathbf{X}'_1 \mathbf{P}_1 \mathbf{X}_1 & & & \mathbf{0} \\ & \mathbf{X}'_2 \mathbf{P}_2 \mathbf{X}_2 & & \\ & & \ddots & \\ \mathbf{0} & & & \mathbf{X}'_m \mathbf{P}_m \mathbf{X}_m \end{bmatrix} \begin{bmatrix} \hat{\boldsymbol{\beta}}_1 \\ \hat{\boldsymbol{\beta}}_2 \\ \vdots \\ \hat{\boldsymbol{\beta}}_m \end{bmatrix} = \begin{bmatrix} \mathbf{X}'_1 \mathbf{P}_1 \mathbf{y}_1 \\ \mathbf{X}'_2 \mathbf{P}_2 \mathbf{y}_2 \\ \vdots \\ \mathbf{X}'_m \mathbf{P}_m \mathbf{y}_m \end{bmatrix} \tag{2.5-13}$$

or shorter

$$\mathbf{N} \hat{\boldsymbol{\beta}} = \mathbf{b}. \tag{2.5-14}$$

If we interpret the pseudo-observation equation of the second step in Section 2.3.2 as a parameter transformation of the form $\hat{\boldsymbol{\beta}} = \mathbf{B} \hat{\boldsymbol{\beta}}_c$ (according to eqn. (2.5-5) $\hat{\boldsymbol{\beta}} = \Delta \hat{\boldsymbol{\beta}}$, $\hat{\boldsymbol{\beta}}_c = \Delta \tilde{\boldsymbol{\beta}}$, $d\boldsymbol{\beta} = \mathbf{0}$)

$$\begin{bmatrix} \hat{\boldsymbol{\beta}}_1 \\ \hat{\boldsymbol{\beta}}_2 \\ \vdots \\ \hat{\boldsymbol{\beta}}_m \end{bmatrix} = \begin{bmatrix} \mathbf{I} \\ \mathbf{I} \\ \vdots \\ \mathbf{I} \end{bmatrix} \hat{\boldsymbol{\beta}}_c \tag{2.5-15}$$

we can directly verify with using eqns. (2.5-9) and (2.5-10) that the resulting compressed normal equation system (2.5-8) $\tilde{\mathbf{N}} \hat{\boldsymbol{\beta}}_c = \tilde{\mathbf{b}}$ is equivalent with the superposition formulae for the corresponding NEQ (2.3-17).

2.5.2.2 Apriori Parameter Transformation

We may apply a parameter transformation to refer a NEQ system to a different set of apriori parameters.

Let us assume that the normal equations, which are based on the apriori parameters $\beta|_0$, should be transformed to a new set of apriori values $\beta|_{0_c} = \beta|_0 + d\beta$ where $\beta|_{0_c}$ is used e.g. in the combination. The transformation equation for the unknown parameters reads as

$$\Delta\hat{\beta} = \Delta\tilde{\beta} + d\beta. \quad (2.5-16)$$

With $\mathbf{B} = \mathbf{I}$ (see eqn. (2.5-5)) we obtain from eqns. (2.5-8)-(2.5-10) the transformed normal equations $\mathbf{N}\Delta\tilde{\beta} = \mathbf{b} - \mathbf{N}d\beta$ or $\Delta\tilde{\beta} = \mathbf{N}^{-1}\mathbf{b} - d\beta = \Delta\hat{\beta} - d\beta$, which is identical with eqn. (2.5-16).

The final estimation $\hat{\beta}$ must be independent of the apriori values. This may be verified using eqn. (2.5-16):

$$\tilde{\beta} := \beta|_{0_c} + \Delta\tilde{\beta} = (\beta|_0 + d\beta) + \Delta\tilde{\beta} = \beta|_0 + (\Delta\tilde{\beta} + d\beta) = \beta|_0 + \Delta\hat{\beta} = \hat{\beta} \quad (2.5-17)$$

or summarized

$$\tilde{\beta} \equiv \hat{\beta} = \beta|_{0_c} + \Delta\tilde{\beta} = \beta|_0 + \Delta\hat{\beta}. \quad (2.5-18)$$

2.5.2.3 Combination of Parameter Types in the Same NEQ

It may be useful to combine also parameters in the same normal equation and not only parameters of different sequential solutions. Applications are:

- Combining troposphere parameters which are valid for subsequent short time intervals to one common parameter valid for a longer time interval (sum of the subsequent intervals).
- Coordinates are set up and determined frequently to study possible site motions: Combining the coordinates in all those intervals without significant movement into the same parameter to strengthen the solution.

The advantage of this procedure has to be seen in the fact that originally as many parameters may be set up in each solution as necessary for all possible kinds of investigations. This may be done for all time dependent parameters. It is always possible a posteriori to reduce the number of parameters if a high resolution is not required.

Figure 2.2 gives an example for a reduction of the number of troposphere parameters on the normal equation level. The 4-parameter solution was produced from the original normal equations containing 12 parameters per day.

Assuming that we want to change the vector of unknowns from β to $\tilde{\beta}$ in the following way:

$$\beta_{u \times 1} = \left[\dots, \underbrace{\beta_i, \beta_{i+1}, \beta_{i+2}, \dots, \beta_{i+m-1}}_{\downarrow}, \dots \right]'$$

$$\tilde{\beta}_{(u-m+1) \times 1} = \left[\dots, \tilde{\beta}_i, \dots \right]'$$

The corresponding transformation equation which combines the m parameters $\beta_i, \beta_{i+1}, \dots, \beta_{i+m-1}$ into the new parameter $\tilde{\beta}_i$ is given by:

$$\beta = B\tilde{\beta} + d\beta \quad \text{with}$$

$$B' = \begin{array}{cccccc|c} 1 & & & & & & \emptyset \\ & \ddots & & & & & \\ & & 1 & & & & \\ & & & 1 & \dots & 1 & \\ & & & & & & 1 \\ & & \emptyset & & & & \ddots \\ & & & & & & & 1 \\ & & & \uparrow & \uparrow & \uparrow & \uparrow & \\ & & & i & i+1 & i+m-1 & u & \end{array} \begin{array}{l} \\ \\ \leftarrow i \text{ and} \\ \\ \\ \\ \leftarrow (u-m+1) \end{array}$$

$$d\beta = \emptyset. \tag{2.5-19}$$

The transformed NEQ system follows from eqns. (2.5-8)-(2.5-10). The quadratic form $\mathbf{y}'\mathbf{P}\mathbf{y}$ in eqn. (2.5-11) remains unchanged because we have $d\beta = \emptyset$. The new NEQ has the dimension $u - m + 1$ instead of u . In this simple case we can give the explicit formula for the transformed NEQ system

$$\tilde{\mathbf{N}} = \begin{bmatrix} \mathbf{N}_{11} & \tilde{\mathbf{N}}_{12} & \mathbf{N}_{13} \\ \tilde{\mathbf{N}}'_{12} & \tilde{\mathbf{N}}_{22} & \tilde{\mathbf{N}}_{23} \\ \mathbf{N}'_{13} & \tilde{\mathbf{N}}'_{23} & \mathbf{N}_{33} \end{bmatrix} = \mathbf{B}' \begin{bmatrix} \mathbf{N}_{11} & \mathbf{N}_{12} & \mathbf{N}_{13} \\ \mathbf{N}'_{12} & \mathbf{N}_{22} & \mathbf{N}_{23} \\ \mathbf{N}'_{13} & \mathbf{N}'_{23} & \mathbf{N}_{33} \end{bmatrix} \mathbf{B}; \tag{2.5-20}$$

$$\tilde{\mathbf{b}} = \begin{bmatrix} \mathbf{b}_1 \\ \tilde{\mathbf{b}}_2 \\ \mathbf{b}_3 \end{bmatrix} = \mathbf{B}' \begin{bmatrix} \mathbf{b}_1 \\ \mathbf{b}_2 \\ \mathbf{b}_3 \end{bmatrix} \quad \text{with} \tag{2.5-21}$$

$$(\tilde{\mathbf{N}}_{12})_{k1} = \sum_{j=1}^m (\mathbf{N}_{12})_{kj}$$

$$(\widetilde{\mathbf{N}}_{23})_{1k} = \sum_{i=1}^m (\mathbf{N}_{23})_{ik} \quad (2.5-22)$$

$$(\widetilde{\mathbf{N}}_{22})_{11} = \sum_{i=1}^m \sum_{j=1}^m (\mathbf{N}_{22})_{ij}$$

$$\widetilde{\mathbf{b}}_2 = \sum_{i=1}^m (\mathbf{b}_2)_i \quad (2.5-23)$$

which actually corresponds to a pure addition of the involved rows and columns.

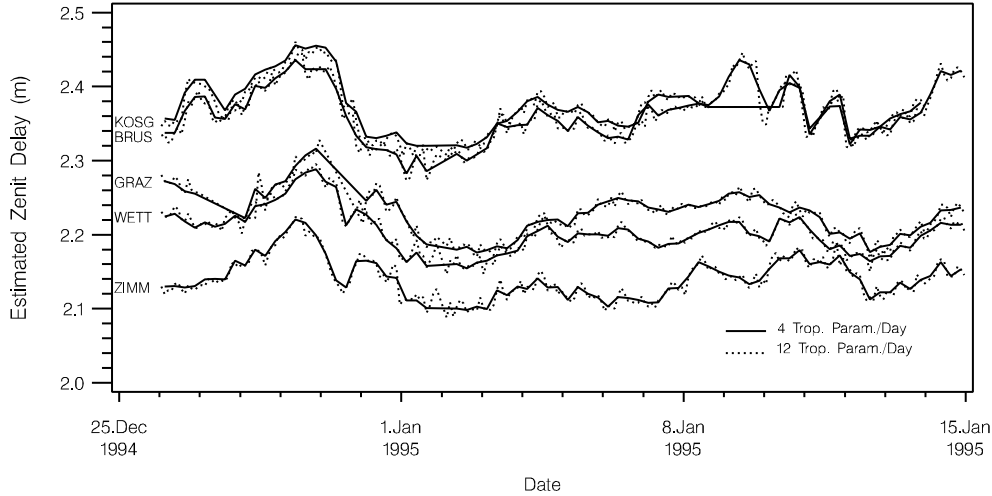


Figure 2.2: Tropospheric zenit delay for some European stations: Time resolution of 2 resp. 6 hours (12 / 4 parameters per day).

2.5.2.4 Normalization

Normalization is an important procedure to avoid numerical instabilities in the solution of the normal equations. Singular normal equations are not the only reason for numerical problems. In principle, the NEQ system $\mathbf{N}\hat{\boldsymbol{\beta}} = \mathbf{b}$ is regular if $\det(\mathbf{N}) \neq 0$. The smaller the value of $\det(\mathbf{N})$ the more unreliable the solution for $\hat{\boldsymbol{\beta}}$. A badly conditioned system causes large relative changes in $\hat{\boldsymbol{\beta}}$ coming from only small relative changes in \mathbf{b} . A rule of thumb for well conditioned systems is: big and well distributed main diagonal values and small off diagonal element. More information concerning badly conditioned equations may be found in ZURMÜHL [1964] or in SCHWARZ ET AL. [1972].

Even an inconvenient unit of a parameter may cause numerical problems. The principle of normalization is the following:

To obtain a value of "1" on all diagonals of \mathbf{N} we have to apply a transformation of type (2.5-5) to $\Delta\hat{\boldsymbol{\beta}}$:

$$\Delta\hat{\boldsymbol{\beta}} = \text{diag}(N_{ii}^{-\frac{1}{2}})\Delta\tilde{\boldsymbol{\beta}}. \quad (2.5-24)$$

The transformed normal equation parts result from eqns. (2.5-8)-(2.5-10): $\tilde{\mathbf{N}} = \mathbf{B}'\mathbf{N}\mathbf{B} = \text{diag}(N_{ii}^{-1/2})'\mathbf{N}\text{diag}(N_{ii}^{-1/2}) = (N_{ij}/\sqrt{N_{ii}N_{jj}})$ and $\tilde{\mathbf{b}} = \mathbf{B}'\mathbf{b} = \text{diag}(N_{ii}^{-1/2})'\mathbf{b} = (b_i/\sqrt{N_{ii}})$ and for the quadratic form according to (2.5-11) we find: $\Delta\tilde{\mathbf{y}}'\mathbf{P}\Delta\tilde{\mathbf{y}} = \Delta\mathbf{y}'\mathbf{P}\Delta\mathbf{y}$ which is not amazing because the dimensions of $\Delta\mathbf{y}$ and \mathbf{P} are not changed.

In the case of normalization the transformation is reduced to a scaling.

2.5.2.5 Introduction of Additional Unknown Parameters

It is possible to introduce a posteriori new parameters, which are not set up in the sequential NEQs. The only restriction is that the influence of the additional parameters in the sequential solution is negligible. Applications are for example the estimation of station velocities.

Let us assume that there is a relationship between the parameters $\boldsymbol{\beta}_i$ of the m sequential solutions and the new parameters $\boldsymbol{\delta}_1$ and $\boldsymbol{\delta}_2$ given as

$$\boldsymbol{\beta}_i = f(\boldsymbol{\delta}_1) + g(\boldsymbol{\delta}_2) \quad \text{with } i = 1, m.$$

In linearized form we obtain

$$\boldsymbol{\beta}_i = \mathbf{F}_i\boldsymbol{\delta}_1 + \mathbf{G}_i\boldsymbol{\delta}_2 + \mathbf{c}_i. \quad (2.5-25)$$

With relation (2.5-5) we find the substitutions

$$\mathbf{B} = [\mathbf{F}_i, \mathbf{G}_i] \quad \text{and} \quad d\boldsymbol{\beta} = \mathbf{c}_i \quad (2.5-26)$$

and the transformed normal equation system

$$\tilde{\mathbf{N}}\tilde{\boldsymbol{\beta}} = \tilde{\mathbf{b}} \quad \text{with} \quad (2.5-27)$$

$$\begin{aligned} \tilde{\boldsymbol{\beta}} &= [\boldsymbol{\delta}_1, \boldsymbol{\delta}_2]' \quad , \\ \tilde{\mathbf{N}} &= \begin{bmatrix} \mathbf{F}'_i\mathbf{N}_i\mathbf{F}_i & \mathbf{F}'_i\mathbf{N}_i\mathbf{G}_i \\ \mathbf{G}'_i\mathbf{N}_i\mathbf{F}_i & \mathbf{G}'_i\mathbf{N}_i\mathbf{G}_i \end{bmatrix} \quad \text{and} \\ \tilde{\mathbf{b}} &= \begin{bmatrix} \mathbf{F}'_i(\mathbf{b}_i - \mathbf{N}_i\mathbf{c}_i) \\ \mathbf{G}'_i(\mathbf{b}_i - \mathbf{N}_i\mathbf{c}_i) \end{bmatrix}. \end{aligned}$$

Accumulation of two sequential solutions according to (2.3-17) results e.g. in

$$\begin{aligned} & \begin{bmatrix} \mathbf{F}'_1 \mathbf{X}'_1 \mathbf{P}_1 \mathbf{X}_1 \mathbf{F}_1 + \mathbf{F}'_2 \mathbf{X}'_2 \mathbf{P}_2 \mathbf{X}_2 \mathbf{F}_2 & \mathbf{F}'_1 \mathbf{X}'_1 \mathbf{P}_1 \mathbf{X}_1 \mathbf{G}_1 + \mathbf{F}'_2 \mathbf{X}'_2 \mathbf{P}_2 \mathbf{X}_2 \mathbf{G}_2 \\ \mathbf{G}'_1 \mathbf{X}'_1 \mathbf{P}_1 \mathbf{X}_1 \mathbf{F}_1 + \mathbf{G}'_2 \mathbf{X}'_2 \mathbf{P}_2 \mathbf{X}_2 \mathbf{F}_2 & \mathbf{G}'_1 \mathbf{X}'_1 \mathbf{P}_1 \mathbf{X}_1 \mathbf{G}_1 + \mathbf{G}'_2 \mathbf{X}'_2 \mathbf{P}_2 \mathbf{X}_2 \mathbf{G}_2 \end{bmatrix} \begin{bmatrix} \hat{\delta}_1 \\ \hat{\delta}_2 \end{bmatrix} \\ & = \begin{bmatrix} \mathbf{F}'_1 \mathbf{X}'_1 \mathbf{P}_1 \mathbf{y}_1 + \mathbf{F}'_2 \mathbf{X}'_2 \mathbf{P}_2 \mathbf{y}_2 - \mathbf{F}'_1 \mathbf{X}'_1 \mathbf{P}_1 \mathbf{X}_1 \mathbf{c}_1 - \mathbf{F}'_2 \mathbf{X}'_2 \mathbf{P}_2 \mathbf{X}_2 \mathbf{c}_2 \\ \mathbf{G}'_1 \mathbf{X}'_1 \mathbf{P}_1 \mathbf{y}_1 + \mathbf{G}'_2 \mathbf{X}'_2 \mathbf{P}_2 \mathbf{y}_2 - \mathbf{G}'_1 \mathbf{X}'_1 \mathbf{P}_1 \mathbf{X}_1 \mathbf{c}_1 - \mathbf{G}'_2 \mathbf{X}'_2 \mathbf{P}_2 \mathbf{X}_2 \mathbf{c}_2 \end{bmatrix}. \end{aligned} \quad (2.5-28)$$

The estimation of drift rates of coordinates is a good example for the above formulae.

Example: Aposteriori estimation of coordinate drift rates

Assuming a linear model in time for the coordinates we may write the relationship between the parameter β_i (coordinates at epoch t_i) and the new parameters β_{t_0} (reference coordinate concerning an arbitrary reference epoch t_0) and \mathbf{v}_{t_0} (drift rate) as

$$\beta_i = \beta_{t_0} + \Delta t_i \mathbf{v}_{t_0}, \quad (2.5-29)$$

where Δt_i is the time difference for each individual solution between the epoch t_i of solution no. i and the reference epoch t_0 .

Comparison of eqn. (2.5-29) with (2.5-25) gives

$$\mathbf{c}_i = \emptyset, \quad \mathbf{F}_i = \mathbf{I}_i \quad \text{and} \quad \mathbf{G}_i = \Delta t_i \mathbf{I}_i.$$

We have to assume of course that for the time span covered by any of the individual solutions $\hat{\beta}_i$ the effect due to the velocity is negligible.

The estimation of station velocities needs a minimum of two sequential solutions at different epochs to ensure that the normal equation below is not singular. Instead of eqn. (2.5-28) we obtain

$$\begin{aligned} & \begin{bmatrix} \mathbf{X}'_1 \mathbf{P}_1 \mathbf{X}_1 + \mathbf{X}'_2 \mathbf{P}_2 \mathbf{X}_2 & \Delta t_1 (\mathbf{X}'_1 \mathbf{P}_1 \mathbf{X}_1) + \Delta t_2 (\mathbf{X}'_2 \mathbf{P}_2 \mathbf{X}_2) \\ \Delta t_1 (\mathbf{X}'_1 \mathbf{P}_1 \mathbf{X}_1) + \Delta t_2 (\mathbf{X}'_2 \mathbf{P}_2 \mathbf{X}_2) & \Delta t_1^2 (\mathbf{X}'_1 \mathbf{P}_1 \mathbf{X}_1) + \Delta t_2^2 (\mathbf{X}'_2 \mathbf{P}_2 \mathbf{X}_2) \end{bmatrix} \begin{bmatrix} \hat{\beta}_{t_0} \\ \hat{\mathbf{v}}_{t_0} \end{bmatrix} \\ & = \begin{bmatrix} \mathbf{X}'_1 \mathbf{P}_1 \mathbf{y}_1 + \mathbf{X}'_2 \mathbf{P}_2 \mathbf{y}_2 \\ \Delta t_1 (\mathbf{X}'_1 \mathbf{P}_1 \mathbf{y}_1) + \Delta t_2 (\mathbf{X}'_2 \mathbf{P}_2 \mathbf{y}_2) \end{bmatrix}. \end{aligned} \quad (2.5-30)$$

Comparison of eqn. (2.5-30) with eqn. (2.4-1) shows that we "blew up" the NEQ system to include the additional parameter $\hat{\mathbf{v}}_0$. On the other hand we combine, when processing m NEQ systems, m independent parameter vector estimates into the mentioned two parameters vectors (thus reducing the number of unknowns from m to 2 parameter vectors).

An apriori introduction of the velocity parameters in each particular least-squares adjustment is not necessary as long as the effect of the velocities is negligible in the individual solutions.

2.5.2.6 Helmert Parameter Estimation

Introduction of seven *Helmert parameters* for each individual NEQ system (translation, rotation and a scale with respect to the combined solution) is possible, too. Applied to two sequential solutions this is similar to a Helmert transformation using the full variance-covariance information of both solutions. The difference resides in the fact that we estimate one combined coordinate set together with the Helmert parameters.

Applications of introducing transformation parameters are:

- Combination of global GPS network solutions with different definitions of the center of mass (estimation versus non-estimation versus the use of different first order terms in the gravity field).
Three translation parameters are necessary to absorb the effect of the different definitions of the origin of the terrestrial reference frames.

- combination of solutions based on different techniques: e.g. combining classical geodetic networks with GPS networks.

Assuming that a free GPS solution would not contribute to the "translational definition" of the network indicates that this degree of freedom can be eliminated by constraining the coordinates of one site to predefined values or by applying the no-net-translation conditions (2.6-29) to the free GPS solution. The orientation of both networks is usually well determined. An estimation of rotation parameters between the two systems is therefore better suited than forcing the orientation of the GPS network with the rotation and scale constraints of type (2.6-33) to that of the classical terrestrial network.

We should point out that for the majority of combinations of different GPS solutions it is not necessary to specify additional Helmert parameters. Setting up such parameters weakens the combined solution.

Let us start using eqn. (2.3-13)

$$\begin{bmatrix} \hat{\beta}_1 \\ \hat{\beta}_2 \end{bmatrix} + \begin{bmatrix} e_{1II} \\ e_{2II} \end{bmatrix} = \begin{bmatrix} I \\ I \end{bmatrix} \hat{\beta}_c \text{ with } D\left(\begin{bmatrix} \hat{\beta}_1 \\ \hat{\beta}_2 \end{bmatrix}\right) = \begin{bmatrix} \Sigma_1 & \emptyset \\ \emptyset & \Sigma_2 \end{bmatrix}$$

representing two pseudo-observation equations of the parameter estimates $\hat{\beta}_1$ and $\hat{\beta}_2$ and their corresponding covariance information resulting from independent solutions.

Let us assume furthermore that the parameter vector $\hat{\beta}_c$ consists only of the n coordinate triples \hat{x}_i : $\hat{\beta}_c = [\hat{x}_1, \hat{x}_2, \dots, \hat{x}_n]'$.

If both solutions are referring to different systems we have to allow for a maximum of seven Helmert parameters $t_x, t_y, t_z, \alpha, \beta, \gamma$, and the scale parameter f .

If introduce Helmert parameters for the system i , $i \in \{1, 2\}$, with respect to the combined solution $\hat{\beta}_c$, we may write:

$$\hat{\beta}_i + \mathbf{e}_{iII} = (\hat{\beta}_c + \mathbf{T}_i) \cdot f_i \cdot \mathbf{U}_i \quad (2.5-31)$$

with the $(3 \cdot n \times 1)$ matrix \mathbf{T} describing the translational part

$$\mathbf{T}_i = \begin{bmatrix} \mathbf{t}_i \\ \mathbf{t}_i \\ \vdots \\ \mathbf{t}_i \end{bmatrix} \quad \text{and} \quad \mathbf{t}_i = \begin{bmatrix} t_{x_i} \\ t_{y_i} \\ t_{z_i} \end{bmatrix}, \quad (2.5-32)$$

the scale factor f_i , and the $(3 \cdot n \times 3)$ matrix \mathbf{U}_i describing the rotation in the following way:

$$\mathbf{U}_i = \begin{bmatrix} \mathbf{u}_i \\ \mathbf{u}_i \\ \vdots \\ \mathbf{u}_i \end{bmatrix} \quad \text{and} \quad \mathbf{u}_i = \mathbf{R}_x(\alpha_i) \cdot \mathbf{R}_y(\beta_i) \cdot \mathbf{R}_z(\gamma_i). \quad (2.5-33)$$

The rotation matrices may be written as

$$\begin{aligned} \mathbf{R}_x(\alpha_i) &= \begin{bmatrix} 1 & 0 & 0 \\ 0 & \cos \alpha_i & \sin \alpha_i \\ 0 & -\sin \alpha_i & \cos \alpha_i \end{bmatrix}; \quad \mathbf{R}_y(\beta_i) = \begin{bmatrix} \cos \beta_i & 0 & -\sin \beta_i \\ 0 & 1 & 0 \\ \sin \beta_i & 0 & \cos \beta_i \end{bmatrix}; \\ \mathbf{R}_z(\gamma_i) &= \begin{bmatrix} \cos \gamma_i & \sin \gamma_i & 0 \\ -\sin \gamma_i & \cos \gamma_i & 0 \\ 0 & 0 & 1 \end{bmatrix}. \end{aligned} \quad (2.5-34)$$

Equation (2.5-31) is not linear in the unknown parameters. Linearization results in:

$$\Delta \hat{\beta}_i = \mathbf{E}_{1_i} \Delta \hat{\beta}_c + \mathbf{E}_{2_i} \Delta \mathbf{t}_i + \mathbf{E}_{3_i} \Delta \mathbf{s}_i + \mathbf{E}_{4_i} \Delta f_i + (\hat{\beta}_c|_0 - \hat{\beta}_i|_0) \quad (2.5-35)$$

with

$$\hat{\beta}_i|_0 = (\hat{\beta}_c|_0 + \mathbf{T}_i|_0) \cdot f_i|_0 \cdot \mathbf{U}_i|_0 \quad (2.5-36)$$

$$\hat{\beta}_c|_0 = \text{apriori value of the combination for } \hat{\beta}_c \quad (2.5-37)$$

$$\mathbf{E}_{1_i} = \begin{bmatrix} f|_0 \mathbf{u}_i|_0 & 0 & \cdots & 0 \\ 0 & f|_0 \mathbf{u}_i|_0 & \cdots & 0 \\ & & \ddots & \\ 0 & 0 & \cdots & f_i|_0 \mathbf{u}_i|_0 \end{bmatrix}, \quad (2.5-38)$$

$$\mathbf{E}_{2_i} = \begin{bmatrix} f|_0 \mathbf{u}_i|_0 \\ f|_0 \mathbf{u}_i|_0 \\ \vdots \\ f|_0 \mathbf{u}_i|_0 \end{bmatrix}, \quad (2.5-39)$$

$$\mathbf{E}_{3_i} = \begin{bmatrix} \mathbf{S}_{1_i} \\ \mathbf{S}_{2_i} \\ \vdots \\ \mathbf{S}_{n_i} \end{bmatrix}, \quad \Delta \mathbf{s}_i = \begin{bmatrix} \Delta \alpha_i \\ \Delta \beta_i \\ \Delta \gamma_i \end{bmatrix} \quad \text{and} \quad (2.5-40)$$

$$\mathbf{S}_{j_i} = (\hat{\mathbf{x}}_j|_0 + \mathbf{t}_i|_0) \cdot f_i|_0 \cdot \left[\frac{\Delta \mathbf{u}_i}{\Delta \alpha_i}|_0 \quad \frac{\Delta \mathbf{u}_i}{\Delta \beta_i}|_0 \quad \frac{\Delta \mathbf{u}_i}{\Delta \gamma_i}|_0 \right], \quad j = 1, \dots, n \quad (2.5-41)$$

$$\mathbf{E}_{4_i} = \begin{bmatrix} (\hat{\mathbf{x}}_1|_0 + \mathbf{t}_i|_0) \mathbf{u}_i|_0 \\ (\hat{\mathbf{x}}_2|_0 + \mathbf{t}_i|_0) \mathbf{u}_i|_0 \\ \vdots \\ (\hat{\mathbf{x}}_n|_0 + \mathbf{t}_i|_0) \mathbf{u}_i|_0 \end{bmatrix}. \quad (2.5-42)$$

The unknown parameters may be summarized in the new parameter estimation vector

$$\Delta \tilde{\boldsymbol{\beta}}_i = [\Delta \hat{\boldsymbol{\beta}}_c, \Delta \mathbf{h}'_i]^T = [\Delta \hat{\boldsymbol{\beta}}_c, \Delta t_{x_i}, \Delta t_{y_i}, \Delta t_{z_i}, \Delta \alpha_i, \Delta \beta_i, \Delta \gamma_i, \Delta f_i]^T. \quad (2.5-43)$$

For the free network conditions of Section 2.6.4 we will assume that the two systems show only small rotation-, translation- and scale differences. The rotation matrices (2.5-34) may then be simplified. A comparison with eqns. (2.6-21) and (2.6-22) leads to the same results using simplified transformation equations and using the apriori values $\mathbf{h}'_i|_0 = [0, 0, 0, 0, 0, 0, 1]$.

Eqn. (2.5-35) in matrix notation reads as

$$\Delta \hat{\boldsymbol{\beta}}_i = \mathbf{E}_i \Delta \tilde{\boldsymbol{\beta}}_i = [\mathbf{E}_{1_i} \quad \mathbf{E}_{2_i} \quad \mathbf{E}_{3_i} \quad \mathbf{E}_{4_i}] \begin{bmatrix} \Delta \hat{\boldsymbol{\beta}}_c \\ \Delta \mathbf{t}_i \\ \Delta \mathbf{s}_i \\ \Delta f_i \end{bmatrix} + (\hat{\boldsymbol{\beta}}_c|_0 - \hat{\boldsymbol{\beta}}_i|_0) \quad (2.5-44)$$

and may be interpreted as a parameter transformation of type (2.5-5): $\Delta \hat{\boldsymbol{\beta}} = \mathbf{B} \Delta \tilde{\boldsymbol{\beta}} + d\boldsymbol{\beta}$. The corresponding normal equation system derived from the given parameter estimation $\hat{\boldsymbol{\beta}}_i$ and its covariance matrix $\boldsymbol{\Sigma}_i$ is transformed according to eqns. (2.5-8)-(2.5-10). The quadratic form $\mathbf{y}' \mathbf{P} \mathbf{y}$ is transformed using eqn. (2.5-11).

The estimation of Helmert parameters thus implies to perform these transformations prior to the accumulation of the normal equation systems.

Note that it is not possible to invert the resulting expanded NEQ system because the Helmert parameters are one-to-one correlated with the coordinate parameters.

A combination of several (instead of only two) sequential solutions including Helmert parameters for each solution is possible in general. In any case we have to select one solution as a reference without specifying any translation, rotation and scale parameters with respect to the combined solution. An alternative would be to set up Helmert parameters for each solution and to constrain e.g. the sums of all Helmert parameters to zeros.

Such a procedure corresponds rather to a *multi-Helmert transformation* than to an estimation of a combined coordinate set.

We should emphasize that this procedure (using only two sequential solutions) is slightly different to the commonly applied seven parameter Helmert transformation between two coordinate sets because we estimate in our case coordinates and Helmert parameters together instead of Helmert parameters only. Constraining the combined solution $\hat{\beta}_c$ to $\hat{\beta}_1$ would include the second case also: $\hat{\beta}_2 = (\hat{\beta}_1 + \mathbf{T}_2) \cdot f_2 \cdot \mathbf{U}_2$.

We should also point out that this method takes into account the full variance covariance information.

The nonlinearity of equation (2.5-31) makes it necessary to iterate the combination in case of bad apriori values or in case of larger values for the Helmert parameters.

2.5.2.7 Other Applications

The estimation of parameters introduced a posteriori in the combination may be extended to other parameter types in the model of the GPS observations. For the "history" of more than 2 years of the GPS derived earth rotation parameters within IGS it is possible to set up Fourier parameters to analyse possible oscillations (see next section).

Potential candidates for such applications are all parameters which occur in the sequential solutions (center of mass, gravity field parameter, satellite antenna offsets, etc.) and should be modeled with a new parameter representation valid for the entire period of time.

Such an analysis is mostly done using the raw day-by-day earth rotation values without considering the correlations to other parameters. Introducing Fourier parameters directly in the combined solution includes all correlations automatically and makes it possible to study the influences on the other parameters.

2.5.3 Estimation of Fourier Coefficients

Let us assume that we estimate in the sequential least-squares adjustments (no. i) the values x_i which are valid for the time interval $t \in [t_i, t_{i+1}]$. If we suspect a

periodical signal of a given frequency in the data we may try to estimate Fourier coefficients as new unknown parameters. Let us adopt the one-frequency model:

$$x_i = a \cdot \cos(\Theta_i + \phi) = a_{xr} \cos \Theta_i + a_{xi} \sin \Theta_i \quad (2.5-45)$$

with

x_i time series of estimated parameters $x(t_i)$

a, ϕ unknown amplitude and phase offset

a_{xr}, a_{xi} unknown *in-phase-* (real,r) coefficient and *out-of-phase-* (imaginary,i) coefficients

$\Theta_i = \omega \cdot (t - t_i)$: given phase argument of an oscillation with frequency ω with respect to the reference epoch t_i

From eqn. (2.5-45) we can conclude:

$$a_{xr} = a \cdot \cos \phi \quad \text{and} \quad a_{xi} = -a \cdot \sin \phi. \quad (2.5-46)$$

Let us further assume that in the time interval $[t_i, t_{i+1}]$ of the i -th observation sequence we represent x_i by a polynomial in time t of degree q with the coefficients x_{ik} as the unknown parameters:

$$x_i(t) = \sum_{k=0}^q x_{ik} \cdot (t - t_i)^k \quad (2.5-47)$$

The sequence of observations $x_i(t)$ is therefore modeled by $q + 1$ parameters x_{ik} , $k = 0, 1, \dots, q$.

From eqn. (2.5-47) we may obtain the partial derivatives

$$x_i^{(k)}(t) := \frac{d^k}{dt^k} x_i(t) = \sum_{k=r}^q \frac{r!}{(r-k)!} x_{ik} (t - t_i)^{r-k} \quad (2.5-48)$$

and with $t := t_i$:

$$x_{ik} = \frac{1}{k!} x_i^{(k)}(t_i). \quad (2.5-49)$$

Introducing the right hand side of eqn. (2.5-45) in this expression gives the transformation equations for the parameters x_{ik} for the reference epoch $t = t_i$ and $k = 0, 1, \dots, q$:

$$x_{ik} = \frac{1}{k!} [a_{xr} (\cos \Theta_i)^{(k)} + a_{xi} (\sin \Theta_i)^{(k)}]. \quad (2.5-50)$$

In matrix notation we find for the parameters of the interval $[t_i, t_{i+1}]$:

$$\mathbf{x}_i = \begin{bmatrix} x_{i0} \\ \vdots \\ x_{iq} \end{bmatrix}_{(q+1) \times 1} = \mathbf{B}_i \tilde{\mathbf{x}} \quad (2.5-51)$$

with

$$\mathbf{B}_i = \begin{bmatrix} \cos \Theta_i & \sin \Theta_i \\ \vdots & \vdots \\ (\frac{1}{q!} \cos \Theta_i)^{(q)} & (\frac{1}{q!} \sin \Theta_i)^{(q)} \end{bmatrix}_{(q+1) \times 2} ; \quad \tilde{\mathbf{x}} = \begin{bmatrix} a_{xr} \\ a_{xi} \end{bmatrix}_{2 \times 1} . \quad (2.5-52)$$

Taking into account all n intervals of the time series we end up with the following transformation equations:

$$\mathbf{x} = \begin{bmatrix} \mathbf{x}_1 \\ \vdots \\ \mathbf{x}_n \end{bmatrix}_{n \cdot (q+1) \times 1} = \mathbf{B} \tilde{\mathbf{x}} \quad (2.5-53)$$

with

$$\mathbf{B} = \begin{bmatrix} \mathbf{B}_1 \\ \vdots \\ \mathbf{B}_n \end{bmatrix}_{n \cdot (q+1) \times 2} ; \quad \tilde{\mathbf{x}} = \begin{bmatrix} a_{xr} \\ a_{xi} \end{bmatrix}_{2 \times 1} . \quad (2.5-54)$$

In the case of polar motion or nutation we have to consider two parameter types together. Assuming that we estimate the coefficients with respect to the same frequency ω we end up with the two equations

$$\begin{aligned} x_i &= a_{xr} \cos \Theta_i + a_{xi} \sin \Theta_i \\ y_i &= a_{yr} \sin \Theta_i + a_{yi} \cos \Theta_i. \end{aligned} \quad (2.5-55)$$

An equivalent formulation is the splitting up in *prograde* and *retrograde* coefficients in the following way:

$$\left. \begin{aligned} x_i &= A^+ \cdot \cos(\Theta_i + \phi^+) = a_r^+ \cos \Theta_i - a_i^+ \sin \Theta_i \\ y_i &= A^+ \cdot \sin(\Theta_i + \phi^+) = a_r^+ \sin \Theta_i + a_i^+ \cos \Theta_i \end{aligned} \right\} \text{prograde} \quad (2.5-56)$$

$$\left. \begin{aligned} x_i &= A^- \cdot \cos(-\Theta_i + \phi^-) = a_r^- \cos \Theta_i + a_i^- \sin \Theta_i \\ y_i &= A^- \cdot \sin(-\Theta_i + \phi^-) = -a_r^- \sin \Theta_i + a_i^- \cos \Theta_i \end{aligned} \right\} \text{retrograde.}$$

The identity of eqns. (2.5-56) and (2.5-55) is confirmed through the following relations

$$\begin{aligned} a_{xr} &= (a_r^+ + a_r^-)/2 ; & a_r^- &= (a_{xr} - a_{yr}) \\ a_{xi} &= -(a_i^+ - a_i^-)/2 ; & a_i^- &= (a_{xi} + a_{yi}) \\ a_{yr} &= (a_i^+ - a_r^-)/2 ; & a_r^+ &= (a_{xr} + a_{yr}) \\ a_{yi} &= (a_i^+ + a_i^-)/2 ; & a_i^+ &= -(a_{xi} - a_{yi}) \end{aligned} \quad (2.5-57)$$

allowing a transformation from one set to the other by

$$\begin{bmatrix} a_{xr} \\ a_{xi} \\ a_{yr} \\ a_{yi} \end{bmatrix} = \frac{1}{2} \begin{bmatrix} 1 & 0 & 1 & 0 \\ 0 & 1 & 0 & -1 \\ -1 & 0 & 1 & 0 \\ 0 & 1 & 0 & 1 \end{bmatrix} \begin{bmatrix} a_r^- \\ a_i^- \\ a_r^+ \\ a_i^+ \end{bmatrix} ; \quad (2.5-58)$$

$$\begin{bmatrix} a_r^- \\ a_i^- \\ a_r^+ \\ a_i^+ \end{bmatrix} = \begin{bmatrix} 1 & 0 & -1 & 0 \\ 0 & 1 & 0 & 1 \\ 1 & 0 & 1 & 0 \\ 0 & -1 & 0 & 1 \end{bmatrix} \begin{bmatrix} a_{xr} \\ a_{xi} \\ a_{yr} \\ a_{yi} \end{bmatrix} . \quad (2.5-59)$$

This procedure is useful because we know for many applications from theory that significant signals are expected only either for the prograde terms or for the retrograde terms. Instead of solving for the unknowns a_r^+ , a_i^+ , a_r^- and a_i^- we may only solve for either a_r^+ and a_i^+ or a_r^- and a_i^- .

Below we derive formulae for the estimation of retrograde and prograde coefficients separately. The procedure is identical to the steps (2.5-50) - (2.5-54).

Let us start with the retrograde part: From eqn. (2.5-56) we get $2 \cdot (q + 1)$ transformation equations using the epoch $t = t_i$ as reference for $k = 0, 1, \dots, q$:

$$\begin{aligned} x_{ik} &= \frac{1}{k!} [a_r^- (\cos \Theta_i)^{(k)} + a_i^- (\sin \Theta_i)^{(k)}] \\ y_{ik} &= \frac{1}{k!} [-a_r^- (\sin \Theta_i)^{(k)} + a_i^- (\cos \Theta_i)^{(k)}] \end{aligned} \quad (2.5-60)$$

or in matrix notation

$$\mathbf{xy}|_i = \begin{bmatrix} x_{i0} \\ y_{i0} \\ \vdots \\ x_{iq} \\ y_{iq} \end{bmatrix}_{2 \cdot (q+1) \times 1} = \mathbf{B}_i^- \widetilde{\mathbf{xy}}|^- \quad (2.5-61)$$

with

$$\mathbf{B}_i^- = \begin{bmatrix} \cos \Theta_i & \sin \Theta_i \\ -\sin \Theta_i & \cos \Theta_i \\ \cdots & \cdots \\ \cdots & \cdots \\ \frac{1}{q!} (\cos \Theta_i)^{(q)} & \frac{1}{q!} (\sin \Theta_i)^{(q)} \\ -\frac{1}{q!} (\sin \Theta_i)^{(q)} & \frac{1}{q!} (\cos \Theta_i)^{(q)} \end{bmatrix}_{2 \cdot (q+1) \times 2} ; \quad \widetilde{\mathbf{xy}}|^- = \begin{bmatrix} a_r^- \\ a_i^- \end{bmatrix}_{2 \times 1} . \quad (2.5-62)$$

For an estimation of the prograde frequencies we get a similar expression:

$$\mathbf{xy}|_i = \mathbf{B}_i^+ \widetilde{\mathbf{xy}}|^+ \quad (2.5-63)$$

with

$$\mathbf{B}_i^+ = \begin{bmatrix} \cos \Theta_i & -\sin \Theta_i \\ \sin \Theta_i & \cos \Theta_i \\ \dots & \dots \\ \dots & \dots \\ \frac{1}{q!}(\cos \Theta_i)^{(q)} & -\frac{1}{q!}(\sin \Theta_i)^{(q)} \\ \frac{1}{q!}(\sin \Theta_i)^{(q)} & \frac{1}{q!}(\cos \Theta_i)^{(q)} \end{bmatrix}_{2 \cdot (q+1) \times 2} ; \quad \widetilde{\mathbf{xy}}|^+ = \begin{bmatrix} a_r^+ \\ a_i^+ \end{bmatrix}_{2 \times 1} . \quad (2.5-64)$$

Taking into account all n intervals of the time series we end up with the following transformation equations for the estimation of the coefficients of the retrograde frequency ω :

$$\mathbf{xy}| = \begin{bmatrix} \mathbf{xy}|_1 \\ \vdots \\ \mathbf{xy}|_n \end{bmatrix}_{2 \cdot n \cdot (q+1) \times 2} = \mathbf{B}^- \widetilde{\mathbf{xy}}|^- \quad (2.5-65)$$

with

$$\mathbf{B}^- = \begin{bmatrix} \mathbf{B}_1^- \\ \vdots \\ \mathbf{B}_n^- \end{bmatrix}_{2 \cdot n \cdot (q+1) \times 2} ; \quad \widetilde{\mathbf{xy}}|^- = \begin{bmatrix} a_r^- \\ a_i^- \end{bmatrix}_{2 \times 1} . \quad (2.5-66)$$

Similar equations with the index $..^+$ instead of $..^-$ may be derived for the coefficients corresponding to the prograde terms.

Both, pro- and retrograde coefficients, may be easily estimated using the transformation equation

$$\mathbf{xy}| = \begin{bmatrix} \mathbf{B}^+ & \mathbf{B}^- \end{bmatrix} \begin{bmatrix} \widetilde{\mathbf{xy}}|^+ \\ \widetilde{\mathbf{xy}}|^- \end{bmatrix} . \quad (2.5-67)$$

The equations (2.5-53), (2.5-65) or (2.5-67) have the form (2.5-5). The corresponding NEQ system can be transformed according to eqns. (2.5-8)-(2.5-10) and (2.5-11). Equation (2.5-67) causes for example a reduction of the effective number of parameters for each component $x(t)$ and $y(t)$ from $2 \cdot n \cdot (q+1)$ parameters to four Fourier coefficients with respect to the given frequency ω . If we want to estimate coefficients for additional frequencies we can extend the transformation equations (2.5-54), (2.5-65) or (2.5-67) with additional coefficients. The estimation of an offset and a drift may be performed in a similar way as in the example of the estimation of station coordinates and velocities.

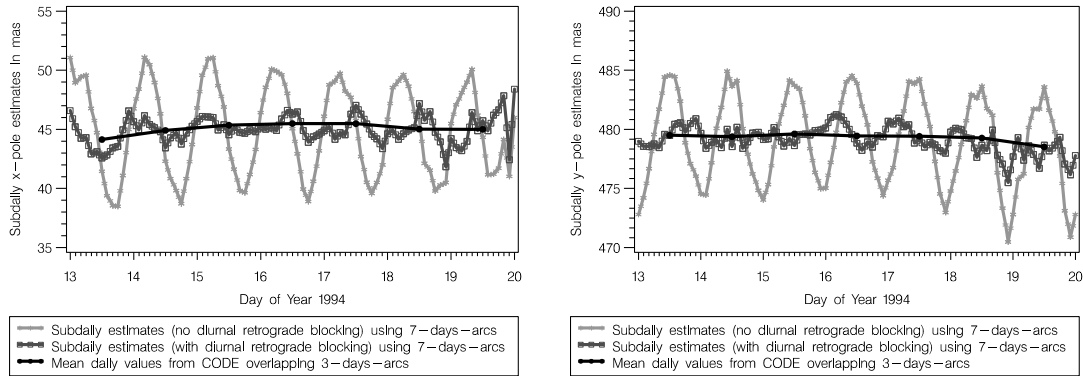
In the case of the nutation parameters we can derive with the described method the amplitudes and phases for selected prograde and retrograde frequencies based on the analysis of the sequential NEQ system taking into account all parameters of

the GPS model. That there are already important signals with respect to the IAU 1990 nutation model is demonstrated by WEBER ET AL. [1995A].

The earth rotation estimates x and y base on predicted apriori information. The estimated parameter increments $\Delta\beta$ are not suited to search for signals. It is necessary to transform the NEQ systems first to a well-defined apriori pole.

2.5.4 Blocking Frequencies

Blocking certain frequencies is explained for a special application: Retrograde diurnal terms in the polar motion cannot be estimated with GPS because these terms are one-to-one correlated with a constant rotation of the entire orbit system [BEUTLER 1995]. If we intend to solve for subdiurnal signals in the earth rotation we must be able to constrain (block) the diurnal retrograde signal especially if we simultaneously solve for the orbit parameters.



(a) x-pole

(b) y-pole

Figure 2.3: Sub-diurnal pole estimates of a 7-days-arc with and without blocking the retrograde diurnal frequency. For comparison we refer also to the values of the CODE solution stemming from the middle day of overlapping 3-days-arcs.

If we are not interested in the orbits we are free to leave these signals in the estimates and to interpret only for the coefficients corresponding to the other frequencies. Figure 2.3 show a typical example for the signal in the x and the y pole if we block and resp. if we do not block the retrograde diurnal signal. We solved for one set

of orbital parameters valid for seven days based on the combination of 1-day-arcs (see Chapter 4) allowing stochastic pulses every 12 hours for all satellites. The pole estimates (of degree 1 for each one hour subinterval) are made continuous with the constraints (2.6-12). For comparison the values of the middle day of overlapping 3-days-solutions are given also. To avoid the slightly larger noise at the beginning and the end of the 7-days-arc it might be useful to analyse the spectrum of the sub-diurnal estimates only the middle three to five days. We can easily verify that the main oscillation is a *retrograde* diurnal signal: the amplitudes of y are a quarter of a revolution earlier on its maxima than the x estimates. We may illustrate this fact if we consider an eastward rotation in the usual left hand pole coordinate system.

The procedure of the blocking of a particular frequency is similar to the estimation of Fourier coefficients (section 2.5.3).

If we apply the parameter transformation equation (2.5-65) to the corresponding NEQ system $\mathbf{N}\mathbf{xy}| = \mathbf{b}$ we find according to eqns. (2.5-8)-(2.5-10):

$$\mathbf{B}^{-'} \mathbf{N} \mathbf{B}^{-} \widetilde{\mathbf{xy}}|^{-} = \mathbf{B}^{-'} \mathbf{b} \quad (2.5-68)$$

and therefore

$$\widetilde{\mathbf{xy}}|^{-} = (\mathbf{B}^{-'} \mathbf{N} \mathbf{B}^{-})^{-1} \mathbf{B}^{-'} \mathbf{b} = (\mathbf{B}^{-'} \mathbf{N} \mathbf{B}^{-})^{-1} \mathbf{B}^{-'} \mathbf{N} \mathbf{xy}| \quad (2.5-69)$$

To constrain the retrograde diurnal signal we have to set up the condition $\widetilde{\mathbf{xy}}|^{-} \equiv \mathbf{0}$. This can be achieved by introducing a fictitious observation with a large weight (or a small variance σ_w^2) which, according to Section 2.6.2, is equivalent to the introduction of real constraints in the least-squares adjustment. With eqn. (2.5-69) we get the pseudo-observation equation

$$(\mathbf{B}^{-'} \mathbf{N} \mathbf{B}^{-})^{-1} \mathbf{B}^{-'} \mathbf{N} \mathbf{xy}| + \mathbf{e} = \mathbf{0} \quad \text{with} \quad \mathbf{D}(\mathbf{0}) = \frac{\sigma_0^2}{\sigma_w^2} \mathbf{I}. \quad (2.5-70)$$

Using eqn. (2.6-3) thus leads to a superposition of the left hand side of the normal equations in the following way:

$$\widetilde{\mathbf{N}} = \mathbf{N} + \frac{\sigma_0^2}{\sigma_w^2} \mathbf{N} \mathbf{B}^{-} (\mathbf{B}^{-'} \mathbf{N} \mathbf{B}^{-})^{-1} (\mathbf{B}^{-'} \mathbf{N} \mathbf{B}^{-})^{-1} \mathbf{B}^{-'} \mathbf{N} \quad (2.5-71)$$

The constraints are much simpler if we assume that all parameters $\mathbf{xy}|$ are determined with the same quality and that there are no correlations between the subsequent pole intervals ($\mathbf{N} = c \cdot \mathbf{I}$). For the blocking of the retrograde diurnal terms such an assumption is justified, because this signal cannot be estimated by GPS. Due to the simple structure of the matrix \mathbf{B}^{-} we find according to eqns. (2.5-62) and (2.5-66):

$$(\mathbf{B}^{-'} \mathbf{B}^{-})^{-1} = \frac{1}{n \cdot (q+1)} \mathbf{I} \quad (2.5-72)$$

and instead of eqn. (2.5-71) we have

$$\widetilde{\mathbf{N}} = \mathbf{N} + \frac{\sigma_0^2}{\sigma_w^2 n^2 (q+1)^2} \mathbf{B}^- \mathbf{B}^{-'} \quad (2.5-73)$$

with

$$\mathbf{B}^- \mathbf{B}^{-'} = \begin{bmatrix} \mathbf{B}_{11} & \mathbf{B}_{12} & \dots & \mathbf{B}_{1n} \\ \mathbf{B}_{12} & \mathbf{B}_{22} & \dots & \mathbf{B}_{2n} \\ \vdots & \vdots & \ddots & \vdots \\ \mathbf{B}_{1n} & \mathbf{B}_{1n} & \dots & \mathbf{B}_{nn} \end{bmatrix}_{2 \cdot n \cdot (q+1) \times 2 \cdot n \cdot (q+1)}. \quad (2.5-74)$$

The blocking of the prograde frequencies - for which we have in case of GPS no reason - might be done in an analogous way to the above procedure. We would end up with a matrix $\mathbf{B}^+ \mathbf{B}^{+'}$ with opposite signs for all terms which are mixed in x_{ik} and y_{ik} . This is a logical consequence because the superposition of $\mathbf{B}^- \mathbf{B}^{-'}$ and $\mathbf{B}^+ \mathbf{B}^{+'}$ has to result in a matrix with no correlations between the parameters of the time series of x and those of y . Blocking both, the prograde and the retrograde part of the oscillation is therefore identical with blocking the frequency ω in x independently of the blocking for y . The corresponding equations to block ω only in one time series are given by replacing every second column and row by zeros.

The procedure described above is an elegant way to protect the sub-diurnal estimates from the presence of retrograde diurnal signals without setting up Fourier parameters explicitly in the normal equations.

2.6 Constraints for Normal Equations

2.6.1 Apriori Constraints as Fictitious Observations

In general, the observations from a given measurement type are not sensitive to *all* parameters in the theoretical model. In this case the normal equations (NEQs) $\mathbf{N}\boldsymbol{\beta} = \mathbf{b}$ are singular which is equivalent to $\det \mathbf{N} = 0$.

For example, distance measurements contain no information concerning the orientation of the geodetic datum.

Additional information must be introduced in the least-squares solution to make the normal equations non-singular. One way is to hold the coordinates of at least one station fixed. This is equivalent to form the NEQs without this parameter.

Also for many other applications it is useful to be able to incorporate exterior information about parameters of the form

$$\mathbf{H}\boldsymbol{\beta} = \mathbf{w} + \mathbf{e}_w \quad \text{with} \quad \mathbf{D}(\mathbf{w}) = \sigma^2 \mathbf{P}_w^{-1} \quad (2.6-1)$$

where

- \mathbf{H} $r \times u$ matrix with given coefficients with $\text{rg } \mathbf{H} = r$,
- r number of constraining equations with $r < u$,
- $\boldsymbol{\beta}$ vector of unknown parameters with dimension $u \times 1$,
- \mathbf{w} $r \times 1$ vector of known constants,
- \mathbf{e}_w $r \times 1$ residual vector, and
- \mathbf{P}_w^{-1} dispersion matrix of the introduced constraining equation with dimension $r \times r$.

There is one important difference of such constraints in comparison to exact constraints in the GMM (Section 2.1.2): In eqn. (2.6-1) a dispersion matrix of the constraining equation is specified whereas in the GMM with constraints the dispersion matrix is implicitly defined as $\mathbf{P}_w^{-1} \rightarrow \emptyset$ respectively $\mathbf{P}_w \rightarrow \infty$. The proof is given in the following of this section. The GMM with constraints minimizes the squared sum of the residuals and fulfills also the introduced constraints. For the observation equations (2.6-1) this is only valid in the frame of the specified dispersion matrix \mathbf{P}_w^{-1} .

If the constraints are nonlinear a linearization has to be performed through a first order Taylor series expansion.

We may interpret the constraints (2.6-1) as additional pseudo-observations, or to distinguish it, as *fictitious observations*. That leads us to the observation equations:

$$\begin{bmatrix} \mathbf{y} \\ \mathbf{w} \end{bmatrix} + \begin{bmatrix} \mathbf{e}_y \\ \mathbf{e}_w \end{bmatrix} = \begin{bmatrix} \mathbf{X} \\ \mathbf{H} \end{bmatrix} \tilde{\boldsymbol{\beta}} \text{ with } \mathbf{D}\left(\begin{bmatrix} \mathbf{y} \\ \mathbf{w} \end{bmatrix}\right) = \sigma^2 \begin{bmatrix} \mathbf{P}^{-1} & \emptyset \\ \emptyset & \mathbf{P}_w^{-1} \end{bmatrix} \quad (2.6-2)$$

or to the associated NEQ system $\tilde{\mathbf{N}}\tilde{\boldsymbol{\beta}} = \tilde{\mathbf{b}}$:

$$(\mathbf{X}'\mathbf{P}\mathbf{X} + \mathbf{H}'\mathbf{P}_w\mathbf{H})\tilde{\boldsymbol{\beta}} = \mathbf{X}'\mathbf{P}\mathbf{y} + \mathbf{H}'\mathbf{P}_w\mathbf{w}. \quad (2.6-3)$$

To constrain the parameter β_j in $\boldsymbol{\beta} = (\beta_1, \dots, \beta_j, \dots, \beta_u)$ with the help of the specified weight P_j to its apriori value β_j we set up the fictitious observation equation $\beta_j + e_j = 0$ and $\mathbf{D}(\beta_j) = \sigma^2 P_j^{-1}$. This results in

$$r = 1, \quad \mathbf{w} = w_j = 0, \quad \mathbf{H} = \mathbf{I}_j = \begin{pmatrix} 0, 0, \dots, 1, 0, \dots, 0 \\ \vdots \\ 0, 0, \dots, 1, 0, \dots, 0 \end{pmatrix} \text{ and}$$

$$\mathbf{P}_w = \text{diag} \begin{pmatrix} 0, 0, \dots, 1, 0, \dots, 0 \end{pmatrix}.$$

To complete the estimation procedure the formula for the computation of the estimated variance of unit weight $\tilde{\sigma}^2$ respectively $\tilde{\Omega}$ is given below.

From eqns. (2.6-2) and (2.1-9) we obtain

$$\tilde{\Omega} = \mathbf{e}'_y \mathbf{P} \mathbf{e}_y + \mathbf{e}'_w \mathbf{P}_w \mathbf{e}_w. \quad (2.6-4)$$

This means that in comparison to the model without additional observation equations the form $\mathbf{e}'_y \mathbf{P} \mathbf{e}_y + \mathbf{e}'_w \mathbf{P}_w \mathbf{e}_w$ is minimized in the LSE instead of $\mathbf{e}'_y \mathbf{P} \mathbf{e}_y$, only.

Using $\mathbf{e}_y = \mathbf{X}\tilde{\boldsymbol{\beta}} - \mathbf{y}$ and $\mathbf{e}_w = \mathbf{H}\tilde{\boldsymbol{\beta}} - \mathbf{w}$ and eqn. (2.6-3) we may also write

$$\tilde{\Omega} = \mathbf{y}' \mathbf{P} \mathbf{y} + \mathbf{w}' \mathbf{P}_w \mathbf{w} - (\mathbf{y}' \mathbf{P} \mathbf{X} + \mathbf{w}' \mathbf{P}_w \mathbf{H}) \tilde{\boldsymbol{\beta}} \quad (2.6-5)$$

$$= \mathbf{y}' \mathbf{P} \mathbf{y} + \tilde{\mathbf{b}} \tilde{\boldsymbol{\beta}} + \mathbf{w}' \mathbf{P}_w \mathbf{w}. \quad (2.6-6)$$

The estimated variance of the unit weight is computed as

$$\tilde{\sigma}^2 = \frac{\tilde{\Omega}}{n_y - u_y + n_w}. \quad (2.6-7)$$

This procedure is very useful to constrain parameters to special values without using the more complex formulae of the GMM with constraints. Nevertheless, constraining of parameters using this simple method must be applied very carefully, because we should be able to answer the question: Is the resulting estimation of a parameter a consequence of the original observations or is the result already strongly influenced by the additional fictitious observation equation.

Problematic is the dependence of the specified apriori weight matrix \mathbf{P}_w on the number of observation equations used in the original NEQ system.

If only a very small number of observations is involved, a small weight may be sufficient to constrain a particular parameter to a special value. This may not be true for a NEQ system based on a large amount of observations.

The same weight may in this case not be able to constrain the parameter on the wished value.

Using too large weights may generate numerical problems for the inversion step and for the computation of the variance of the unit weight. The "correction" terms $\mathbf{H}' \mathbf{P}_w \mathbf{H}$, $\mathbf{w}'_w \mathbf{P}_w \mathbf{H}$ and $\mathbf{w}'_w \mathbf{P}_w \mathbf{w}_w$ are responsible for this. Especially if the values for \mathbf{P}_w are large and the values for \mathbf{w} are small, numerical problems may occur.

Constraining should therefore only be applied to set up all parameter types in the sequential solutions even if a parameter estimate is not significant. Parameters, which may cause singularity problems are potential candidates for the constraining, too. In the accumulation step of sequential normal equations it will be possible to estimate in a second step these parameters without any constraints.

2.6.2 Constraints as Fictitious Observations with Large Weights

We can transform the formulae derived above into the formulae of the GMM with constraints of section 2.1.2 using infinitely large weights \mathbf{P}_w . The identity is useful because it is much easier to handle the introduction of apriori constraints. Furthermore a steady transition from loose constraints to an exact constraints is possible. Using $\mathbf{P}_w^{-1} = \sigma_w^2 \mathbf{I}$ with σ_w^2 as a very small value which causes a strong weighting for the additional fictitious observations \mathbf{w} we get from eqn. (2.6-3)

$$\tilde{\boldsymbol{\beta}} = (\mathbf{X}'\mathbf{P}\mathbf{X} + \mathbf{H}'\mathbf{H}/\sigma_w^2)^{-1}(\mathbf{X}'\mathbf{P}\mathbf{y} + \mathbf{H}'\mathbf{w}/\sigma_w^2). \quad (2.6-8)$$

Using the matrix identity (2.2-9) ($\mathbf{A}^{-1} = \mathbf{X}'\mathbf{P}\mathbf{X}$, $\mathbf{B} = \mathbf{H}'$, $\mathbf{C} = -\mathbf{H}$, $\mathbf{D}^{-1} = \mathbf{I}/\sigma_w^2$) and taking into account eqn. (2.1-32) we find

$$\begin{aligned} \lim_{\sigma_w^2 \rightarrow 0} \tilde{\boldsymbol{\beta}} &= \lim_{\sigma_w^2 \rightarrow 0} [(\mathbf{X}'\mathbf{P}\mathbf{X})^{-1}(\mathbf{X}'\mathbf{P}\mathbf{y} \\ &\quad + \mathbf{H}'(\sigma_w^2 \mathbf{I} + \mathbf{H}(\mathbf{X}'\mathbf{P}\mathbf{X})^{-1}\mathbf{H}')^{-1}(\mathbf{w} - \mathbf{H}'(\mathbf{X}'\mathbf{P}\mathbf{X})^{-1}\mathbf{X}'\mathbf{P}\mathbf{y}))] \\ &\quad + \lim_{\sigma_w^2 \rightarrow 0} [(\mathbf{X}'\mathbf{P}\mathbf{X})^{-1}(\mathbf{H}'(\sigma_w^2 \mathbf{I} + \mathbf{H}(\mathbf{X}'\mathbf{P}\mathbf{X})^{-1}\mathbf{H}')^{-1}\mathbf{w} + (1/\sigma_w^2)\mathbf{H}'\mathbf{w} \\ &\quad - (1/\sigma_w^2)\mathbf{H}'(\sigma_w^2 \mathbf{I} + \mathbf{H}(\mathbf{X}'\mathbf{P}\mathbf{X})^{-1}\mathbf{H}')^{-1}\mathbf{H}(\mathbf{X}'\mathbf{P}\mathbf{X})^{-1}\mathbf{H}'\mathbf{w})] \\ &= \tilde{\boldsymbol{\beta}} + \lim_{\sigma_w^2 \rightarrow 0} [(1/\sigma_w^2)\mathbf{H}'\mathbf{w} - (1/\sigma_w^2)\mathbf{H}'\mathbf{w}] \\ &= \tilde{\boldsymbol{\beta}}. \end{aligned} \quad (2.6-9)$$

For small variances of the additional fictitious observations the introduction of apriori constraints is identical to the case of the GMM with constraints.

In the following sections we will mainly use the expression *conditions* if we mean *constraints* which are realized using a strong constraining weight or using the methods of parameter transformation (Section 2.5).

The same is also true for the estimates $\mathbf{D}(\tilde{\boldsymbol{\beta}})$:

$$\lim_{\sigma_w^2 \rightarrow 0} \mathbf{D}(\tilde{\boldsymbol{\beta}}) = \mathbf{D}(\tilde{\boldsymbol{\beta}})$$

and for $\tilde{\Omega}$ and $\tilde{\sigma}^2$, because with eqns. (2.6-5) and (2.6-9) we obtain

$$\begin{aligned} \lim_{\sigma_w^2 \rightarrow 0} \tilde{\Omega} &= \lim_{\sigma_w^2 \rightarrow 0} [\mathbf{y}'\mathbf{P}\mathbf{y} + (1/\sigma_w^2)\mathbf{w}'\mathbf{w} - (\mathbf{y}'\mathbf{P}\mathbf{X} + (1/\sigma_w^2)\mathbf{w}'\mathbf{H})\tilde{\boldsymbol{\beta}}] \\ &= \mathbf{y}'\mathbf{P}\mathbf{y} - \mathbf{y}'\mathbf{P}\mathbf{X}\tilde{\boldsymbol{\beta}} - \mathbf{w}'\mathbf{k} \\ &= \tilde{\Omega} \\ \lim_{\sigma_w^2 \rightarrow 0} \tilde{\sigma} &= \tilde{\sigma}. \end{aligned} \quad (2.6-10)$$

That $\lim_{\sigma_w^2 \rightarrow 0} [(1/\sigma_w^2)(\mathbf{H}\tilde{\boldsymbol{\beta}} - \mathbf{w})] = \mathbf{k}$ may be verified with eqn. (2.6-3) and with the relation $\mathbf{H}'\mathbf{k} = \mathbf{X}'\mathbf{P}\mathbf{y} - \mathbf{X}'\mathbf{P}\mathbf{X}\tilde{\boldsymbol{\beta}}$ using eqn. (2.1-31).

2.6.3 Applications for Apriori Constraints

The introduction of apriori constraints is not only used for defining the geodetic datum. Most of the parameters in the model of the GPS observations may be constrained.

Constraints using $\mathbf{w} = \mathbf{0}$ in eqn. (2.6-1) are frequently used for the following parameter types:

- coordinates (absolute constraints, free network conditions)
- velocities (absolute and relative constraints)
- troposphere (absolute and relative constraints)
- orbit (keplerian-, dynamical-, stochastic-) parameters
- center of mass
- earth rotation parameters (UT1 and nutation absolute value has to be constrained to a VLBI value and continuity constraints)
- satellite antenna offsets

Table 2.1: Constraints and constraining options used in the program ADDNEQ.

$\mathbf{H}\boldsymbol{\beta} = \mathbf{w} + \mathbf{e}$	\mathbf{H}	\mathbf{w}	\mathbf{P}_w
Constraining and fixing on apriori values $\beta_i = 0 + e_i$	$[0, \dots, 0, 1, 0, \dots, 0]$	$[0]$	$[\sigma_0^2 / \sigma_{\text{abs}}^2]$
Constraining and fixing on apriori values $\beta_{0\text{new}}$ $\beta_i = \beta_{0\text{new}} - \beta_0 + e_i$	$[0, \dots, 0, 1, 0, \dots, 0]$	$[\beta_{0\text{new}} - \beta_0]$	$[\sigma_0^2 / \sigma_{\text{abs}}^2]$
Relative constraints between parameters $\beta_i - \beta_{i+1} = 0 + e_i$	$[0, \dots, 0, 1, -1, 0, \dots, 0]$	$[0]$	$[\sigma_0^2 / \sigma_{\text{rel}}^2]^a$
Continuity between subsequent polynomials: see eqns. (2.6-12), (2.6-13)			
Common polynomials in subsequent time intervals: eqn. (2.6-16)			
"Absolute" polynomials: eqns. (2.6-16), (2.6.3.3)			
Free networks: eqns. (2.6-18), (2.6-21)			

^aused for troposphere parameters; can be derived from power spectral density of random walk process [ROTHACHER, 1992], also used for relative velocity constraints

Constraints using $\mathbf{w} \neq \mathbf{0}$ are implemented only for coordinates, velocities and earth rotation parameters. In this case it is possible to constrain a parameter to a value different from the apriori value used in the individual NEQs.

In the following we will focus on some useful constraints implemented in the program ADDNEQ, which was developed for combining NEQs. Table 2.1 summarizes the discussed applications. Let us discuss below the options in Table 2.1 in more detail.

2.6.3.1 Continuity of Polynomials Referring to Consecutive Time Intervals

Let us assume that a process (e.g. earth rotation) is modeled in the time interval $I = [t_i, t_{i+1}]$ (interval length $\Delta t_{i,i+1}$) with polynomials of degree m (see Figure 2.4):

$$p_i(t) = \sum_{j=0}^m \beta_{j,i} (t - t_i)^j. \quad (2.6-11)$$

Let us assume that in the next time interval $I = [t_{i+1}, t_{i+2}]$ the model parameters are $\beta_{0,i+1}, \dots, \beta_{m,i+1}$.

A least-squares estimation of all parameters results in general in a discontinuity at the time interval boundary t_{i+1} . To make the estimation continuous we have to set up the constraining equation

$$\sum_{j=0}^m \beta_{j,i} \Delta t_{i,i+1}^j - \beta_{0,i+1} = 0 \text{ where } \Delta t_{i,i+1}^j = (t_{i+1} - t_i)^j \quad (2.6-12)$$

and we have to specify a corresponding weighting. In matrix representation we obtain from eqn. (2.6-1) $\mathbf{H}\boldsymbol{\beta} = \mathbf{w} + \mathbf{e}_w$ and $\mathbf{D}(\mathbf{w}) = \sigma^2 \mathbf{P}_w^{-1}$ with

$$\begin{aligned} \mathbf{H} &= [0 \quad \dots \quad 0 \quad 1 \quad \Delta t_{i,i+1} \quad \dots \quad \Delta t_{i,i+1}^m \quad -1 \quad 0 \quad \dots \quad 0] \\ \boldsymbol{\beta} &= [\dots \quad \beta_{0,i} \quad \beta_{1,i} \quad \dots \quad \beta_{m,i} \quad \beta_{0,i+1} \quad \dots] \\ \mathbf{w} &= [0] \\ \mathbf{P}_w &= [\sigma_0^2 / \sigma_{\text{fix}}^2]. \end{aligned} \quad (2.6-13)$$

If we ask for continuity at subsequent interval boundaries we have to set up for each interval boundary one equation of the form (2.6-13).

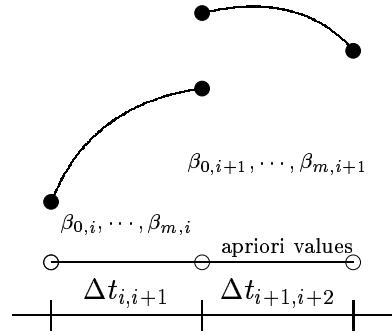


Figure 2.4: Discontinuous Polynomials.

2.6.3.2 Common Polynomials in Subsequent Time Intervals

As an example for a modification of the polynomial degree in subsequent intervals we mention the special case of changing a model characterized by degree 1 polynomials (offset plus drift) in all n subintervals to *one* degree 1 polynomial valid for the entire interval (covering all subintervals). Figure 2.5 illustrates this application. We have to ensure continuity between the intervals and we have to ask in addition for identical first order coefficients.

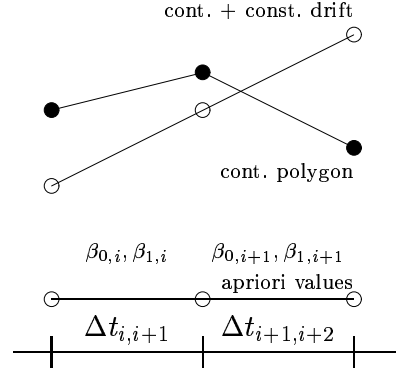


Figure 2.5: Common Polynomials in subsequent time intervals.

With $m = 1$ we obtain from eqn. (2.6-12):

$$\beta_{0,i} + \beta_{1,i} \Delta t_{i,i+1} - \beta_{0,i+1} = 0, \quad i = 1, 2, \dots, n-1. \quad (2.6-14)$$

Identical linear terms result if we ask for

$$\beta_{1,i} - \beta_{1,i+1} = 0, \quad i = 1, 2, \dots, n-1. \quad (2.6-15)$$

The latter two equations may be written in matrix representation $\mathbf{H}\boldsymbol{\beta} = \mathbf{w}$ where

$$\begin{aligned} \mathbf{H} &= \begin{bmatrix} 0 & \cdots & 0 & 1 & \Delta t_{i,i+1} & -1 & 0 & 0 & \cdots & 0 \\ 0 & \cdots & 0 & 0 & 1 & 0 & -1 & 0 & \cdots & 0 \end{bmatrix} \\ \boldsymbol{\beta} &= [\cdots, \beta_{0,i}, \beta_{1,i}, \beta_{0,i+1}, \beta_{1,i+1}, \cdots]' \\ \mathbf{w} &= \begin{bmatrix} 0 \\ 0 \end{bmatrix} \\ \mathbf{P}_w &= \begin{bmatrix} \sigma_0^2 / \sigma_{\text{fix1}}^2 & 0 \\ 0 & \sigma_0^2 / \sigma_{\text{fix2}}^2 \end{bmatrix}. \end{aligned} \quad (2.6-16)$$

The value σ_{fix2}^2 has to ensure that the constraint of the identical linear terms (2.6-15) is fulfilled. Eqns. (2.6-14) and (2.6-15) are two constraints for four parameters $\beta_{0,i}, \beta_{1,i}, \beta_{0,i+1}, \beta_{1,i+1}$, so only two of them are independent (needed to represent a degree 1 polynomial).

For more than two intervals we have to introduce two constraints of type (2.6-16) for each additional interval.

In the IGS processing at CODE this procedure is used to set up earth rotation parameters of degree 1 for each day. The ERP estimates are showing at present a better consistency and reasonable drift rates if we solve in the 3-days-solutions only for one linear model covering all 3 days (see Figure 8.14).

2.6.3.3 Constraints Concerning the "Absolute" Estimates

If the apriori pole for each interval shows a behavior as shown in Figure 2.6 the equations (2.6-16) are forcing the estimates to be linear and continuous, but the resulting parameters (apriori value + estimated value) still is "contaminated" by the changing drifts of the apriori model.

Using

$$\mathbf{w} = \begin{bmatrix} 0 \\ d_{i+1,i+2} - d_{i,i+1} \end{bmatrix} \quad (2.6-17)$$

in eqn. (2.6-16) (instead of a zero vector) we have condition equations which enforce a linear behavior for the resulting "absolute" estimate.

Examples are given in Section 8.4.

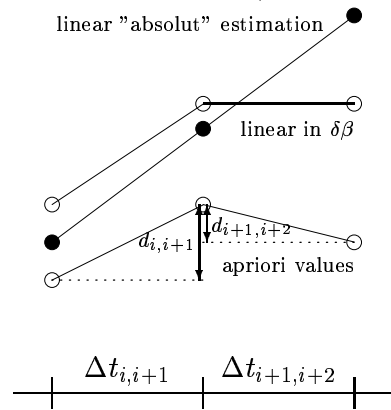


Figure 2.6: "Absolute" estimation.

2.6.4 Free Network Adjustment

The theoretical model for the GPS observables makes it impossible to determine the coordinates of all stations *together with* the orbits and earth rotation parameters *without* defining the geodetic datum for any of the used GPS sites.

In general, a (static) reference frame needs a minimum of seven parameters to define the location, the orientation and the scale of the coordinate system. Allowing also for constant (in time) site velocities leaves us with the twice the number of parameters to define the reference frame unambiguously.

The *No-Net-Translation and Rotation Conditions* are a useful instrument to define the geodetic datum without fixing coordinates to predefined values. Possible problems in all coordinates are detectable without relying on the specific values of some fix stations.

The derivation of these equations is similar as in conventional 3-dimensional geodetic methods (*minimal and inner constraint adjustment*). Assuming that only the inner geometry of a network may actually be determined (if e.g. only distance measurements are available) the whole network can be translated, rotated and rescaled without affecting the original observations. The resulting NEQ system has a rank defect of 7 in the three-dimensional space.

Without going into the detail of other one-to-one correlations in the GPS system (especially with pole coordinates, orbits and gravity field parameters) we will discuss only the rank defect due to the definition of the geodetic datum.

Regarding the GPS observations as an observation type without any "absolute" information we can directly apply the methods of the conventional 3-dimensional

geodesy.

Without changing the inner geometry it is possible to apply the following linear transformation to the unknown parameters:

$$\boldsymbol{\beta}_a = \boldsymbol{\beta}_c + \mathbf{H}'\mathbf{h} \quad (2.6-18)$$

where

$\boldsymbol{\beta}_c$ Parameter vector (only coordinates) before transformation (with respect to apriori coordinates \mathbf{X}_{i_0}),

$$\boldsymbol{\beta}_c' = [\boldsymbol{\beta}_{1_c}, \dots, \boldsymbol{\beta}_{i_c}, \dots], \quad \boldsymbol{\beta}_{i_c} = [x_{i_c}, y_{i_c}, z_{i_c}], \quad (2.6-19)$$

$\boldsymbol{\beta}_a$ Parameter vector after transformation (with respect to apriori coordinates \mathbf{X}_{i_0}),

$$\boldsymbol{\beta}_a' = [\boldsymbol{\beta}_{1_a}, \dots, \boldsymbol{\beta}_{i_a}, \dots], \quad \boldsymbol{\beta}_{i_a} = [x_{i_a}, y_{i_a}, z_{i_a}], \quad (2.6-20)$$

\mathbf{H}' Transformation matrix (*inner constraint matrix*) with $\text{rg}(\mathbf{H}') = 7$:

$$\mathbf{H}' = \begin{bmatrix} \mathbf{I}_3 & \mathbf{S}_1 & \mathbf{X}_{1_0} \\ \dots & \dots & \dots \\ \mathbf{I}_3 & \mathbf{S}_i & \mathbf{X}_{i_0} \\ \dots & \dots & \dots \end{bmatrix}, \quad (2.6-21)$$

\mathbf{I}_3 Identity matrix of dimension 3,

\mathbf{S}_i Rotation matrix (valid only for small rotations) with

$$\mathbf{S}_i = \begin{bmatrix} \emptyset & z_{i_0} & -y_{i_0} \\ -z_{i_0} & \emptyset & x_{i_0} \\ y_{i_0} & -x_{i_0} & \emptyset \end{bmatrix}, \quad (2.6-22)$$

\mathbf{X}_{i_0} Apriori coordinates with

$$\mathbf{X}_{i_0}' == [\boldsymbol{\beta}_{1_0}, \dots, \boldsymbol{\beta}_{i_0}, \dots], \quad \boldsymbol{\beta}_{i_0} = [x_{i_0}, y_{i_0}, z_{i_0}] \text{ and} \quad (2.6-23)$$

\mathbf{h} Translation, rotation and scale parameter vector

$$\mathbf{h}' = [t_x, t_y, t_z, \alpha, \beta, \gamma, f]'. \quad (2.6-24)$$

Introducing eqns. (2.6-18) and (2.6-21) into the observation equation of the GMM (2.1-2) gives

$$\mathbf{X}\boldsymbol{\beta}_a + \mathbf{e}_a = \mathbf{X}\boldsymbol{\beta}_c + \mathbf{X}\mathbf{H}'\mathbf{t} + \mathbf{e}_a \equiv \mathbf{E}(\mathbf{y}). \quad (2.6-25)$$

From this we conclude

$$\mathbf{X}\mathbf{H}' = \mathbf{0}. \quad (2.6-26)$$

KOCH [1988] showed that the matrix

$$\mathbf{D} = \begin{bmatrix} \mathbf{X}'\mathbf{P}\mathbf{X} & \mathbf{H}' \\ \mathbf{H} & \mathbf{0} \end{bmatrix} \quad (2.6-27)$$

is in this case non-singular, even if $\mathbf{X}'\mathbf{P}\mathbf{X}$ is singular.

The matrix \mathbf{D} is equal to the left hand part of the NEQ system (2.1-31) of the GMM with constraints on parameters (see eqn. (2.1-30)):

$$\mathbf{E}(\mathbf{y}) = \mathbf{X}\boldsymbol{\beta} \quad \text{and} \quad \mathbf{H}\boldsymbol{\beta} = \mathbf{0} \quad ; \quad \mathbf{D}(\mathbf{y}) = \sigma^2\mathbf{P}^{-1}. \quad (2.6-28)$$

The additional r constraints enable the inversion of the NEQ matrix which means that now the parameter vector $\boldsymbol{\beta} \in \mathcal{R}^u$ is estimable in the space \mathcal{R}^{u-r} .

Depending on the actual choice of the matrix \mathbf{H}' we get for the inverse of \mathbf{D} the *reflexive generalized inverse* or the *pseudoinverse*. These two inverse matrices have different properties concerning the trace of the matrix. Sites can be excluded if we set the corresponding rows of the matrix \mathbf{H}' to zero. Let us assume that k sites should be used for the setting up of the matrix \mathbf{H} . In our implementation station selection for the datum definition is possible with a selection matrix \mathbf{S} which is in principle the identity matrix, but contains zero on all main diagonals for the stations which should be excluded: $\overline{\mathbf{H}} = \mathbf{S}\mathbf{H}$.

The first three equations of $\mathbf{H}\boldsymbol{\beta} = \mathbf{0}$ may be written as:

$$\sum_{i=1}^k \delta x_i = 0, \quad \sum_{i=1}^k \delta y_i = 0, \quad \sum_{i=1}^k \delta z_i = 0 \quad (2.6-29)$$

where $\delta x_i, \delta y_i, \delta z_i$ are the estimates for the coordinates of one of the k sites referring to the apriori values $x_{i_0}, y_{i_0}, z_{i_0}$.

This means that the coordinate origin (x_s, y_s, z_s) , given by the apriori coordinates of the k sites

$$x_s = 1/k \sum_{i=1}^k x_{i_0}, \quad y_s = 1/k \sum_{i=1}^k y_{i_0}, \quad z_s = 1/k \sum_{i=1}^k z_{i_0}, \quad (2.6-30)$$

is identical to the one of the estimated coordinates $(x_{s_a}, y_{s_a}, z_{s_a})$. For the x -coordinates we may verify this statement using eqns. (2.6-29) and (2.6-30):

$$x_{s_a} := 1/k \sum_{i=1}^k x_i = 1/k \sum_{i=1}^k (x_{i_0} + \delta x_i) = 1/k \sum_{i=1}^k x_{i_0} + 1/k \sum_{i=1}^k \delta x_i = x_s. \quad (2.6-31)$$

Let the other 4 conditions be given by the matrix \mathbf{H}_o as a submatrix of \mathbf{H} . The corresponding subset of constraints (2.6-28) then reads

$$\mathbf{H}_o\boldsymbol{\beta} = \boldsymbol{\emptyset}. \quad (2.6-32)$$

Assuming that the parameter vector $\boldsymbol{\beta}$ plus an error vector \mathbf{e} may be derived by a rotation and a scale (analogous to (2.6-18)) results in the observation equation

$$\mathbf{H}'_o\mathbf{o} = \boldsymbol{\beta} + \mathbf{e}; \quad \mathbf{o} = [\alpha, \beta, \gamma, f]'; \quad \mathbf{H}'_o = \begin{bmatrix} \mathbf{S}_1 & \mathbf{X}_{1_0} \\ \cdots & \cdots \\ \mathbf{S}_i & \mathbf{X}_{i_0} \\ \cdots & \cdots \end{bmatrix}. \quad (2.6-33)$$

Interpreting this equation as an observation equation with $\mathbf{D}(\boldsymbol{\beta}) = \sigma^2\mathbf{I}$ leads us using eqns. (2.1-5) (2.1-30), and (2.6-32) to the least-squares estimate:

$$\hat{\mathbf{o}} = (\mathbf{H}_o\mathbf{H}'_o)^{-1}\mathbf{H}_o\boldsymbol{\beta} = \boldsymbol{\emptyset}. \quad (2.6-34)$$

In other words: The last four conditions force the estimates of $\boldsymbol{\beta}$ to have no rotation and no scale change with respect to the used apriori coordinates.

The definition of the geodetic datum of the network is based on the used apriori coordinates. With the results of Section 2.5.2 we are almost free in the selection of the apriori coordinates. Instead of transformation of the normal equations to a different set of apriori coordinates we may also introduce the conditions $\mathbf{H}\boldsymbol{\beta} = \mathbf{w}$ with $\mathbf{w} = \mathbf{H}d\boldsymbol{\beta}$ and $d\boldsymbol{\beta}$ as the difference between the new coordinate set and the originally used one.

An alignment of the free solution with different systems (e.g. different ITRF systems) is therefore easily possible.

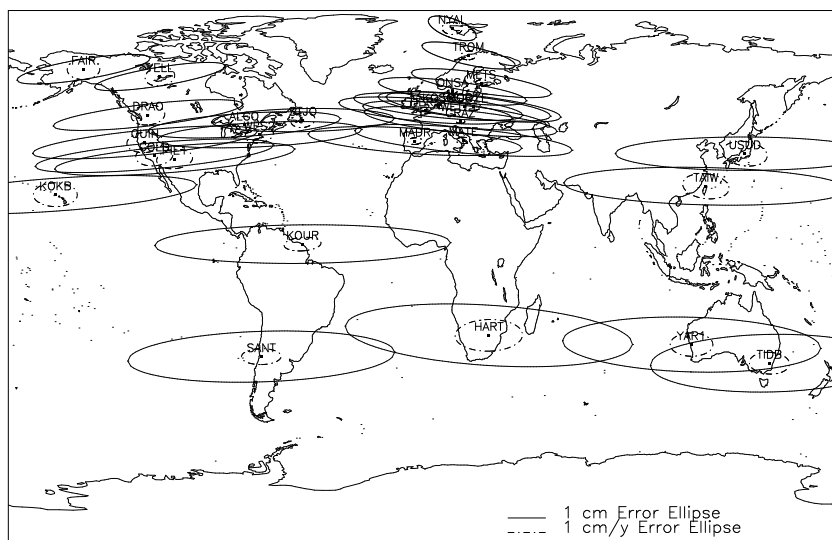
Lets us underline that with free network solutions we estimate coordinates for *all* involved sites without fixing a minimum of 7 coordinates on predefined values.

The estimation of parameters $\hat{\boldsymbol{\beta}}^*$ and the associated estimation of the covariance matrix $\mathbf{D}(\hat{\boldsymbol{\beta}}^*)$ in the GMM not of full rank is given by KOCH [1988]:

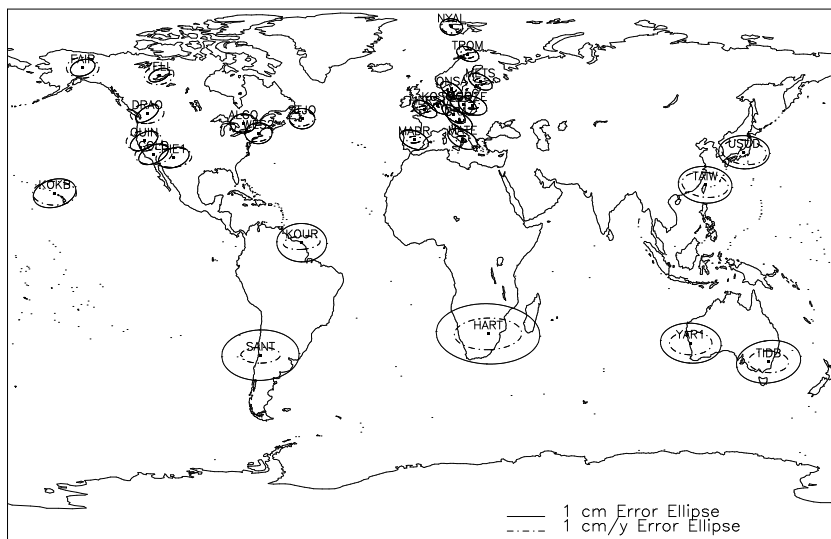
$$\hat{\boldsymbol{\beta}}^* = (\mathbf{X}'\mathbf{P}\mathbf{X} + \overline{\mathbf{H}'\mathbf{H}})^{-1}\mathbf{X}'\mathbf{P}\mathbf{y} \text{ and} \quad (2.6-35)$$

$$\mathbf{D}(\hat{\boldsymbol{\beta}}^*) = \sigma^2\mathbf{D}^{-1} = \sigma^2 \left\{ (\mathbf{X}'\mathbf{P}\mathbf{X} + \overline{\mathbf{H}'\mathbf{H}})^{-1} - \mathbf{H}'(\mathbf{H}\overline{\mathbf{H}'\mathbf{H}}\mathbf{H}')^{-1}\mathbf{H} \right\}. \quad (2.6-36)$$

Comparison of eqn. (2.6-35) with the normal equation (2.6-3) shows the identity for the estimates of the GMM not of full rank with the GMM with constraints ($\mathbf{P}_w = \mathbf{I}$, $\mathbf{w} = \boldsymbol{\emptyset}$). In practice we use *constraints* according to Section 2.6.1 and Section 2.6.2 to realize the free network conditions.



(a) No-net-translation conditions applied



(b) No-net-translation plus z-rotation conditions applied

Figure 2.7: Error ellipses for coordinates and velocities of a 2-years free network solution (1993-1994) using different conditions.

The same is not true for $D(\hat{\beta}^*)$. The term $-\mathbf{H}'(\mathbf{H}\overline{\mathbf{H}}'\overline{\mathbf{H}}\mathbf{H}')^{-1}\mathbf{H}$ is a specialty of the GMM not of full rank.

The usage of the free network conditions (2.6-28) is also possible if no rank defect is present.

In the case when velocities are estimated together with site coordinates we may introduce "free velocity" conditions to enable a velocity estimation for *all* sites without relying on specific predefined values. If the estimation should be based on a reference velocity field we may define the necessary conditions by selecting a list of stations which serve as the reference.

Figure 2.7 demonstrates the effect of free network conditions on the global IGS network. In both cases we selected 13 IGS core sites to define with their ITRF93 coordinates an apriori network. We established in both cases a free network solution with coordinate and velocity estimation for each site. The datum definition for the velocities was simplified to the constraining of the three velocity components of the site (WETT) to the ITRF93 values.

In case (a) we implemented only the three condition equations with respect to the translation which means that the center given by the estimated coordinates of the 13 sites is identical to the center given by their ITRF93 coordinates.

The error ellipses indicate that the longitudes are weakly determined by GPS. In case (b) we add the condition equation for the rotation about the z-axis to reduce the uncertainties in the estimation of the longitudes. An equivalent and frequently used possibility for the definition of the reference frame consists of fixing three components of one particular site and the latitude of a second site on predefined values [MA ET AL. 1995]. The resulting error ellipses are typical for GPS: Slightly larger uncertainties for the longitudes than for the latitudes are due to the dominant north-south motion of the satellites.

The formal errors of the velocities are identical in both cases.

Introducing more than four condition equations would not help to reduce the formal errors. We find already small differences in the coordinate estimates of solution (b) if we use more than the mentioned four conditions. This indicates that additional conditions would noticeable bias the GPS solutions.

It is not clear at present which is the minimum number of conditions necessary for the definition of the velocities. The use of the three translational free network conditions may align the velocity estimates with a given apriori velocity field (for example ITRF93 [BOUCHER AND ALTAMIMI 1994] or NUVEL1 [DEMETTS ET AL. 1990]). Such a procedure is equivalent to fixing three components of one site on predefined values (method applied for the solutions in Figure 2.7).

The *integration of GPS networks* into a given reference frame is a candidate for the use of the free network conditions. In the official surveying applications of a country it is in most cases not allowed to change the coordinates of the reference frame. Even if the final solution will fix all reference sites, a free network solution should be performed to detect possible inconsistencies between the GPS network and the reference frame. Because of such problems GPS serves in many cases only as a baseline length generator ignoring the full information of a network solution. The combination/integration is done with the help of standard geodetic adjustment programs [EISELE 1991].

The number of condition equations may also be reduced. In small networks (< 10 km) based on fixed GPS orbits it may useful to permit only a translation (which is identical with the fixing of the 3 coordinates of one station) and take over the orientation and the scale from GPS. The datum information coming from GPS is completely ignored if the full number of 7 conditions is used.

2.7 Equivalence of Combining Normal Equations and Covariances

In this section we demonstrate the equivalence of sequential LSE estimates using normal equations or using covariances.

In Table 2.2 we give the two possibilities to store the necessary information to produce a combined solution.

Table 2.2: Required information from each sequential solution for the production of a combined solution.

Combination based on	
Covariances	Normal equations
$(\mathbf{X}'\mathbf{P}\mathbf{X})^{-1}$	$\mathbf{X}'\mathbf{P}\mathbf{X}$
$\hat{\boldsymbol{\beta}}$	$\mathbf{X}'\mathbf{P}\mathbf{y}; \boldsymbol{\beta} _0$
$\hat{\sigma}^2$	$\mathbf{y}'\mathbf{P}\mathbf{y}$
$n; u$	$n; u$

The difference between the first line elements in Table (2.2) is obvious: The left hand side NEQ matrix is saved in case of normal equations, the inverted matrix (the cofactor matrix) in case of the other storage type. The information with respect to the computation of the variance of unit weight is given in the lines three and four. The last line elements are identical and the equivalence of the third line elements is given with the eqns. (2.1-9) and (2.1-10).

The difference in the second line is essential. The right hand side of the NEQ system $\mathbf{X}'\mathbf{P}\mathbf{y}$ is directly dependent on the used apriori information because of (2.1-27). Therefore we have to store the associated apriori information $\beta|_0$. In case of storing directly $\hat{\beta}$ this is not necessary because we can recompute $\mathbf{X}'\mathbf{P}\mathbf{y}$ using (2.1-27) in the following way:

$$\mathbf{X}'\mathbf{P}\mathbf{y} = \mathbf{X}'\mathbf{P}\mathbf{X}(\hat{\beta} - \beta|_{arb}). \quad (2.7-1)$$

The selection of the arbitrary apriori information $\beta|_{arb}$ has to ensure that the linearized Taylor series expansion is still valid and that the effect on the computation of the design matrix \mathbf{X} (which was originally computed using $\beta|_0$) is negligible.

The above statement is true for both methods because the combination of the sequential solutions has to be performed using a common apriori value for each parameter. To make sure that all sequential adjustments meet these requirements it is therefore useful to store also the used apriori information together with the estimates, in particular if the estimates show larger discrepancies. Under unfavourable circumstances this implies repetition of the individual sequential solutions or exclusion of the solution from the combined solution.

As already shown at the end of Section 2.4.2 with equation (2.4-28) we need also the apriori information if apriori constraints are applied.

From the point of view of computing time the storing of normal equations is much more efficient because the combinations based according to Section 2.3 on a pure superposition of normal equations.

The combination based on covariances requires an inversion and a reconstruction of the normal equation part $\mathbf{X}'\mathbf{P}\mathbf{y}$ according to (2.7-1) or the use of the more complicated combination formulae (2.4-27).

This statement is also valid for the removal of apriori constraints if we compare eqns. (2.4-28) with eqns. (2.6-3) and (2.6-5).

The covariances are on the other hand much more suited to give information about the quality of the solutions. The rms of each parameter, the three-dimensional error ellipses for each site and correlations between the parameters are directly accessible. Another advantage has to be seen in the fact that one may easily exclude parameters from the system by skipping the corresponding rows and columns in the parameter estimation vector and in the covariance matrix whereas we have to apply the pre-elimination formulae in the case of normal equation storage (see Section 2.2).

Both methods are implemented in two different programs in the Bernese software package [ROTHACHER ET AL. 1993].

The combination program COMPAR is based on the covariance storing method corresponding to the first column in Table 2.2. It is closely related to the classical

geodetic application: Combination using only the coordinate estimations of each individual LSE together with the corresponding covariance information.

The second storage type is underlying the more general program ADDNEQ which is used to combine all parameter types of the GPS observation model.

2.8 Estimation of Group RMS Values

2.8.1 General Estimation Formulae

To get an idea of the contribution and the quality of different types of observations we divide the total rms into rms values for different groups.

This procedure approximates the more general *variance component estimation* where variance-covariance components are estimated for each observation group. These additional unknowns allows it to model different observation qualities. A more realistic dispersion matrix will lead us to a more reliable estimation of the primary unknown parameters β .

On the normal equation level we have no connection to the original observations. Therefore we assume that each sequential solution is already performed with a realistic weighting matrix. In Section 2.3.2 we proved the concept that the combination of normal equations is identical with introducing simple pseudo-observation equations of type (2.3-12) consisting only of the results of each individual solution. Therefore we may split up the pseudo-observations in different observation groups also on normal equation level. Each group may consist of different types of parameters or may consist of sets of different parameters.

The group rms is well suited to give additional information concerning the quality of each parameter. We will see a close relationship to an rms value derived from repeatabilities.

Let us split up the observation equations into two parts. As opposed to Section 2.3.2 we assume $\gamma_1 = \gamma_2 = \emptyset$. From eqns.(2.3-17) and (2.3-31) we find

$$\begin{aligned} \Omega_c &= \mathbf{y}'_1 \mathbf{P}_1 \mathbf{y}_1 + \mathbf{y}'_2 \mathbf{P}_2 \mathbf{y}_2 - (\mathbf{y}'_1 \mathbf{P}_1 \mathbf{X}_1 + \mathbf{y}'_2 \mathbf{P}_2 \mathbf{X}_2) \hat{\beta}_c \quad \text{with} & (2.8-1) \\ \hat{\beta}_c &= (\mathbf{X}'_1 \mathbf{P}_1 \mathbf{X}_1 + \mathbf{X}'_2 \mathbf{P}_2 \mathbf{X}_2)^{-1} (\mathbf{X}'_1 \mathbf{P}_1 \mathbf{y}_1 + \mathbf{X}'_2 \mathbf{P}_2 \mathbf{y}_2) = \mathbf{Q}_{\hat{\beta}_c} \hat{\beta}_c \mathbf{b}_{\hat{\beta}_c} \end{aligned}$$

and the total rms results in

$$\hat{\sigma}_c^2 = \frac{\Omega_c}{f_c} \quad \text{with the total redundancy } f_c \text{ from eqn. (2.3-20).} \quad (2.8-2)$$

The group rms for each individual observation series is given by

$$\Omega_{1_c} = \hat{\mathbf{e}}_{1_c} \mathbf{P}_{1_c} \hat{\mathbf{e}}_{1_c} \neq \Omega_1 \quad ; \quad \hat{\sigma}_{1_c}^2 = \frac{\Omega_{1_c}}{f_{1_c}} \quad (2.8-3)$$

$$\Omega_{2_c} = \hat{\mathbf{e}}_{2_c} \mathbf{P}_{2_c} \hat{\mathbf{e}}_{2_c} \neq \Omega_2 \quad ; \quad \hat{\sigma}_{2_c}^2 = \frac{\Omega_{2_c}}{f_{2_c}} \quad (2.8-4)$$

with the relation to the combined solution given by eqn. (2.3-25)

$$\Omega_c = \Omega_{1_c} + \Omega_{2_c} \text{ and } f_c = f_{1_c} + f_{2_c}. \quad (2.8-5)$$

The vector $\hat{\mathbf{e}}_{i_c}$ refers to the combined solution and is different from the residuals $\hat{\mathbf{e}}_i$ of the sequential solution. This was already pointed out in Section 2.3.4.

The redundancies f_{1_c} and f_{2_c} respectively are computed using (2.1-11):

$$\begin{aligned} \mathbf{F} &= \begin{bmatrix} \mathbf{F}_{11} & \mathbf{F}_{12} \\ \mathbf{F}_{21} & \mathbf{F}_{22} \end{bmatrix} = \begin{bmatrix} \mathbf{I}_1 - \mathbf{P}_1 \mathbf{X}_1 \mathbf{Q}_{\hat{\beta}_c \hat{\beta}_c} \mathbf{X}'_1 & -\mathbf{P}_1 \mathbf{X}_1 \mathbf{Q}_{\hat{\beta}_c \hat{\beta}_c} \mathbf{X}'_2 \\ -\mathbf{P}_2 \mathbf{X}_2 \mathbf{Q}_{\hat{\beta}_c \hat{\beta}_c} \mathbf{X}'_1 & \mathbf{I}_2 - \mathbf{P}_2 \mathbf{X}_2 \mathbf{Q}_{\hat{\beta}_c \hat{\beta}_c} \mathbf{X}'_2 \end{bmatrix} \\ f_{1_c} &= \text{Sp} (\mathbf{I}_1 - \mathbf{P}_1 \mathbf{X}_1 \mathbf{Q}_{\hat{\beta}_c \hat{\beta}_c} \mathbf{X}'_1) = n_1 - \text{Sp} (\mathbf{P}_1 \mathbf{X}_1 \mathbf{Q}_{\hat{\beta}_c \hat{\beta}_c} \mathbf{X}'_1) \\ f_{2_c} &= \text{Sp} (\mathbf{I}_2 - \mathbf{P}_2 \mathbf{X}_2 \mathbf{Q}_{\hat{\beta}_c \hat{\beta}_c} \mathbf{X}'_2) = n_2 - \text{Sp} (\mathbf{P}_2 \mathbf{X}_2 \mathbf{Q}_{\hat{\beta}_c \hat{\beta}_c} \mathbf{X}'_2). \end{aligned} \quad (2.8-6)$$

A comparison of f_{1_c} and f_{2_c} with eqn. (2.3-20) shows the difference to the redundancy f_1 and f_2 of each individual solution. There we found $f_i = n_i - \text{Sp} (\mathbf{P}_i \mathbf{X}_i (\mathbf{X}'_i \mathbf{P}_i \mathbf{X}_i)^{-1} \mathbf{X}'_i) = n_i - u_i$ because $\mathbf{P}_i \mathbf{X}_i (\mathbf{X}'_i \mathbf{P}_i \mathbf{X}_i)^{-1} \mathbf{X}'_i$ is idempotent (property $\mathbf{A}^2 = \mathbf{A}$).

2.8.2 Applications of the Group RMS

In this section the following important applications will be discussed:

- Group rms of one apriori constraint
- Group rms of all apriori constraints
- Group rms of a single parameter type
- Group rms of a set of parameter types

2.8.2.1 Group RMS of One Apriori Constraint

For the simple constraining of the parameter β_k of vector $\boldsymbol{\beta}$ according to Table 2.1 we find with $\mathbf{y}_{2_c} = \mathbf{w} = 0$, $n_{2_c} = r = 1$, $\mathbf{X}_2 = \mathbf{H} = [0, \dots, 0, 1, 0, \dots, 0]$,

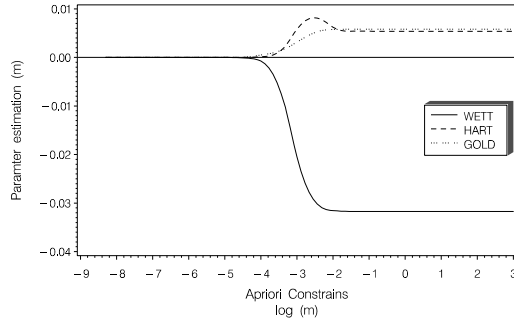
$\mathbf{P}_2 = \mathbf{P}_w = \sigma_0^2 / \sigma_{\text{abs}}^2$ and $\hat{\mathbf{e}}_{2c} = \hat{\mathbf{e}}_w = \beta_k$:

$$f_{2c} = 1 - \frac{\sigma_0^2}{\sigma_{\text{abs}}^2} \cdot (\mathbf{Q}_{\hat{\beta}_c \hat{\beta}_c})_{kk} ; (\mathbf{Q}_{\hat{\beta}_c \hat{\beta}_c})_{kk} = \left(\mathbf{X}'_1 \mathbf{P}_1 \mathbf{X}_1 + \frac{\sigma_0^2}{\sigma_{\text{abs}}^2} \mathbf{H}' \mathbf{H} \right)^{-1}_{kk}$$

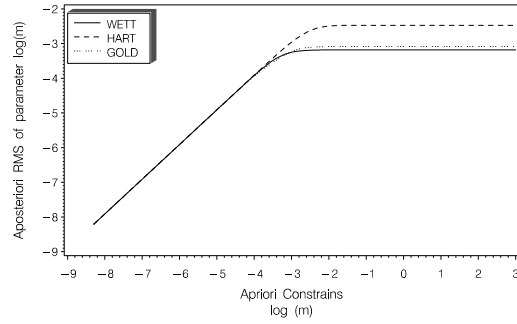
$$\Omega_{2c} = (\hat{\beta}_c)_k^2 \cdot \frac{\sigma_0^2}{\sigma_{\text{abs}}^2} ; \hat{\sigma}_{2c} = \frac{\Omega_{2c}}{f_{2c}} \quad (2.8-7)$$

and with eqn. (2.8-5)

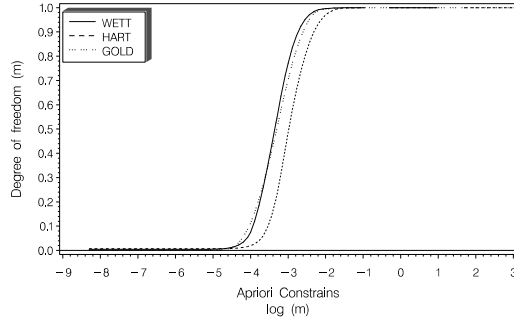
$$f_{1c} = f_c - f_{2c} ; \Omega_{1c} = \Omega_c - \Omega_{2c} ; \hat{\sigma}_{1c}^2 = \frac{\Omega_{1c}}{f_{1c}}. \quad (2.8-8)$$



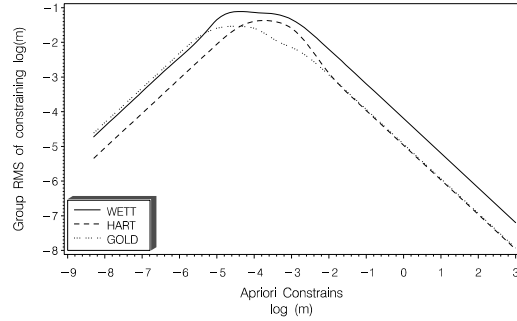
(a) Coordinate estimates



(b) Aposteriori rms



(c) Redundancy



(d) Group rms

Figure 2.8: Influence of constraints on the estimation (a) and the associated rms (b), the degree of freedom (c) and the group rms of the constraint equation (d) for the coordinate component x of three different IGS stations. The example was extracted from a monthly solution of 53 globally distributed IGS stations of January 1995.

For small variances $\lim \sigma_{\text{abs}}^2 \rightarrow 0$ we obtain $f_{2_c} = 0$ and $f_c = f_{1_c}$. The constraint equation is in this case more than an additional (fictitious) observation because the weight forces the combined estimation to the apriori value. For large variances $\lim \sigma_{\text{abs}}^2 \rightarrow \infty$ we get $f_{2_c} = 1$ and $f_c = f_{1_c} + 1$.

Figure 2.8 shows the dependencies between constraints and parameter estimates for a monthly solution for three different stations. Constraints $> 10^{-2}m$ enable a free parameter estimation. Apriori constraints of about 1 mm influence already the solution. With values of $< 10^{-5}m$ (0.01 mm) the parameters are fixed on the apriori values with an aposteriori rms which is equivalent to the introduced constraint. The degree of freedom of the constraint equation and the group rms are important information to judge the influence on the solution. Apriori constraints ranging between $10^{-2}m$ and $10^{-5}m$ ($1 \text{ mm} - 0.01 \text{ mm}$) are critical because they realize neither a free parameter estimation nor a fixed solution.

2.8.2.2 Group RMS of All Apriori Constraints

The group rms values of all r constraint equations can easily be derived analogous to the previous section. We obtain

$$\begin{aligned} f_{2_c} &= r - \sum_{i=1}^r \frac{\sigma_0^2}{\sigma_{\text{abs}_i}^2} \cdot (\mathbf{Q}_{\hat{\beta}_c \hat{\beta}_c})_{ii} ; (\mathbf{Q}_{\hat{\beta}_c \hat{\beta}_c})_{ii} = \left(\mathbf{X}'_1 \mathbf{P}_1 \mathbf{X}_1 + \frac{\sigma_0^2}{\sigma_{\text{abs}_i}^2} \mathbf{H}' \mathbf{H} \right)_{ii}^{-1} \\ \Omega_{2_c} &= \sum_{i=1}^r (\hat{\beta}_c)_i^2 \cdot \frac{\sigma_0^2}{\sigma_{\text{abs}_i}^2} ; \hat{\sigma}_{2_c} = \frac{\Omega_{2_c}}{f_{2_c}}. \end{aligned} \quad (2.8-9)$$

2.8.2.3 Group RMS of a Single Parameter Type

The group rms of a parameter is a useful information concerning the quality of the parameter in addition to the resulting rms of the combination. Let us assume that we sort the observation vector in a way that all pseudo-observations of a certain parameter are contained in \mathbf{y}_{2_c} whereas all other parameter estimations of all sequential solution are located in \mathbf{y}_{1_c} . Let us in particular assume that all n_2 estimations of the parameter β_k are contained in \mathbf{y}_{2_c} . The observation equations (2.3-12) lead to the following substitutions:

$$\begin{aligned} \mathbf{y}_2 &= [(\hat{\beta}_1)_k, \dots, (\hat{\beta}_{n_2})_k]_{(n_2 \times 1)}' ; \\ \mathbf{X}_2 &= [1, 1, \dots, 1]_{(n_2 \times 1)}' ; \\ \mathbf{P}_2 &= \text{diag}((\mathbf{X}'_i \mathbf{P}_i \mathbf{X}_i)_{kk}) = \begin{bmatrix} (\mathbf{X}'_1 \mathbf{P}_1 \mathbf{X}_1)_{kk} & & 0 \\ & \ddots & \\ 0 & & (\mathbf{X}'_{n_2} \mathbf{P}_{n_2} \mathbf{X}_{n_2})_{kk} \end{bmatrix}_{(n_2 \times n_2)} ; \end{aligned}$$

$$\hat{\mathbf{e}}_{2_c} = \left[(\hat{\boldsymbol{\beta}}_c)_k - (\hat{\boldsymbol{\beta}}_1)_k, \dots, (\hat{\boldsymbol{\beta}}_c)_k - (\hat{\boldsymbol{\beta}}_{n_2})_k \right]'_{(n_2 \times 1)}. \quad (2.8-10)$$

Using these substitutions in eqns. (2.8-4) and (2.8-6) the group rms for the parameter β_k may be computed as:

$$\begin{aligned} f_{2_c} &= n_2 - (\mathbf{Q}_{\hat{\boldsymbol{\beta}}_c \hat{\boldsymbol{\beta}}_c})_{kk} \sum_{i=1}^{n_2} (\mathbf{X}'_i \mathbf{P}_i \mathbf{X}_i)_{kk} \\ \Omega_{2_c} &= \sum_{i=1}^{n_2} ((\hat{\boldsymbol{\beta}}_c)_k - (\hat{\boldsymbol{\beta}}_i)_k)^2 (\mathbf{X}'_i \mathbf{P}_i \mathbf{X}_i)_{kk} \\ \hat{\sigma}_{2_c}^2 &= \frac{\Omega_{2_c}}{f_{2_c}}. \end{aligned} \quad (2.8-11)$$

Equation $(\mathbf{Q}_{\hat{\boldsymbol{\beta}}_c \hat{\boldsymbol{\beta}}_c})_{kk} = (\sum_{i=1}^{n_2} ((\mathbf{X}'_i \mathbf{P}_i \mathbf{X}_i)_{kk}))^{-1}$ only holds if the individual parameter estimates $(\hat{\boldsymbol{\beta}}_i)_k$, $i = 1, \dots, n_2$ are totally independent determined from all other parameters. In this case we get $f_{2_c} = n_2 - 1$. The group rms of the parameter $(\hat{\boldsymbol{\beta}}_c)_k$ is reduced to the *weighted mean rms*.

This simplification indicates that the group rms of a parameter is a quality value which is comparable to the rms value derived from *repeatabilities*.

2.8.2.4 Group RMS of a Set of Parameter Types

The coordinate triple of a single site is an example for a set of parameters. It may also be very useful to derive a group rms for all coordinates. This value may be interpreted as the variance of unit weight of a coordinate observation and may therefore be used as the scaling factor for the associated coordinate covariances instead of using the derived variance of the unit weight of the original observations (phase observation in case of GPS).

For the sake of completeness we include the relevant formulae below. For u_c coordinate values we find from the observation equations the substitutions:

$$\begin{aligned} \mathbf{y}_2 &= \left[\hat{\boldsymbol{\beta}}_1, \dots, \hat{\boldsymbol{\beta}}_{n_2} \right]'_{(n_2 \cdot u_c \times u_c)} ; \\ \mathbf{X}_2 &= [\mathbf{I}_1, \mathbf{I}_2, \dots, \mathbf{I}_{n_2}]'_{(n_2 \cdot u_c \times u_c)} ; \\ \mathbf{P}_2 &= \text{diag}(\mathbf{X}'_i \mathbf{P}_i \mathbf{X}_i) = \begin{bmatrix} \mathbf{X}'_1 \mathbf{P}_1 \mathbf{X}_1 & & 0 \\ & \ddots & \\ 0 & & \mathbf{X}'_{n_2} \mathbf{P}_{n_2} \mathbf{X}_{n_2} \end{bmatrix}_{(n_2 \cdot u_c \times n_2 \cdot u_c)} ; \\ \hat{\mathbf{e}}_{2_c} &= \left[\hat{\boldsymbol{\beta}}_c - \hat{\boldsymbol{\beta}}_1, \dots, \hat{\boldsymbol{\beta}}_c - \hat{\boldsymbol{\beta}}_{n_2} \right]'_{(n_2 \cdot u_c \times u_c)}. \end{aligned} \quad (2.8-12)$$

With eqns. (2.8-4) and (2.8-6) we obtain the group rms for all coordinates:

$$\begin{aligned}
 f_{2_c} &= n_2 - \sum_{k=1}^{u_c} \sum_{i=1}^{n_2} (\mathbf{X}'_i \mathbf{P}_i \mathbf{X}_i \mathbf{Q}_{\hat{\beta}_c \hat{\beta}_c})_{kk} \\
 \Omega_{2_c} &= \sum_{i=1}^{n_2} (\hat{\beta}_c - \hat{\beta}_i)' \mathbf{X}'_i \mathbf{P}_i \mathbf{X}_i (\hat{\beta}_c - \hat{\beta}_i) \\
 \hat{\sigma}_{2_c}^2 &= \frac{\Omega_{2_c}}{f_{2_c}}.
 \end{aligned} \tag{2.8-13}$$

With eqn. (2.1-9) Ω_{2_c} may be computed as:

$$\Omega_{2_c} = \sum_{i=1}^{n_2} \hat{\beta}'_i \mathbf{X}'_i \mathbf{P}_i \mathbf{X}_i (\hat{\beta}_i - \hat{\beta}_c) \tag{2.8-14}$$

$$= \sum_{i=1}^{n_2} \mathbf{b}_{\hat{\beta}_i}' (\hat{\beta}_i - \hat{\beta}_c). \tag{2.8-15}$$

This method is more efficient computationally because $\mathbf{b}_{\hat{\beta}_i}$ is already given from the left hand side normal equation vector $\mathbf{b}_{\hat{\beta}_i} = \mathbf{y}' \mathbf{P} \mathbf{X}$.

2.8.2.5 Example

We demonstrated that the group rms values are in a certain sense comparable to quality values derived from repeatabilities.

In the most cases the latter values are a more realistic quality indicator than the formal errors of the combined solution.

The main difference between internal precision and group rms values resides in the used degree of freedom. In eqn. (2.8-11) the redundancy is of the order of the number of sequential estimations for the specific parameter, whereas the combined solution refers to the total number of original observations. The difference comes from the introduction of the pseudo-observation equation (2.3-12) using already derived parameter values as new observations. This ignores the fact that each parameter was already a product of many different observations.

That the rule of thumb "Multiplication of the combined solution rms with an empirical factor of 3-5" gives a more realistic value for the accuracy of a parameter is shown in Table 2.3.

The averaged discrepancies between the estimated precision and the group rms of each coordinate component is a factor of 5.9. A value of similar order of magnitude (5.4) results for the discrepancies between the estimated variance of unit weight of a single difference observation and the derived unit weight of a coordinate estimation according to (2.8-13).

Table 2.3: Estimated rms values from a monthly solution: January 1995, 9 stations fixed on ITRF93 apriori values. rms1 is the formal rms derived from the combination and rms2 is the group rms for each parameter according to eqn. (2.8-11).

Station-name	# days	Fixed Stat.	rms in x [mm]		rms in y [mm]		rms in z [mm]		Mean Ratio rms2/rms1
			rms1	rms2	rms1	rms2	rms1	rms2	
ALGO	30		0.6	3.3	0.8	4.2	0.8	3.4	5.3
WES2	30		0.5	2.9	0.7	4.0	0.6	4.0	6.1
AREQ	30		1.7	14.2	1.6	8.3	0.7	6.8	8.4
BOGT	15		1.2	2.9	1.7	9.8	0.6	6.6	8.4
SANT	30		1.8	16.3	1.6	9.7	1.0	8.2	8.2
KOUR	30		1.2	9.6	1.2	6.3	0.5	5.1	8.3
BRMU	30		0.7	3.4	0.8	5.0	0.6	4.0	6.4
STJO	30		0.6	2.7	0.6	4.6	0.7	5.6	6.2
BRUS	30		0.7	1.9	0.4	0.8	0.8	2.2	1.9
ONSA	27		0.5	2.8	0.3	1.1	0.7	3.9	3.7
ZIMM	30		0.5	2.0	0.3	1.4	0.5	1.3	3.9
CAS1	30		0.7	2.3	0.8	4.8	1.1	5.7	4.6
DAV1	30		0.8	3.0	0.9	5.1	1.3	4.1	4.5
MCMU	15		1.1	5.4	0.9	7.1	2.5	11.3	5.2
TIDB	30	F	0.0	0.0	0.0	0.0	0.0	0.0	—
KOKB	30		1.3	5.3	0.9	5.4	0.8	3.9	5.7
YAR1	30	F	0.0	0.0	0.0	0.0	0.0	0.0	—
MDO1	30		0.5	1.2	0.8	5.2	0.5	4.0	6.6
PIE1	30		0.4	2.0	0.7	5.3	0.5	4.3	7.1
RCM5	30		0.6	2.7	0.8	5.5	0.5	4.4	7.2
DRAO	30		0.4	1.4	0.5	3.0	0.6	3.7	4.8
QUIN	30		0.4	3.0	0.5	5.6	0.5	5.2	10.1
YELL	30	F	0.0	0.0	0.0	0.0	0.0	0.0	—
KERG	30		0.8	3.5	1.0	3.6	1.0	2.6	3.9
FAIR	30	F	0.0	0.0	0.0	0.0	0.0	0.0	—
FORT	30		1.6	16.3	1.5	6.6	0.6	5.4	8.8
GOLD	30	F	0.0	0.0	0.0	0.0	0.0	0.0	—
GRAZ	30		0.5	1.7	0.3	1.1	0.6	2.1	2.9
LJUB	30		0.6	1.7	0.4	1.2	0.7	1.7	2.5
MATE	30		1.1	3.3	0.6	1.4	0.9	3.0	2.3
WETT	30	F	0.0	0.0	0.0	0.0	0.0	0.0	—
KOSG	30	F	0.0	0.0	0.0	0.0	0.0	0.0	—
LAMA	30		0.5	2.0	0.3	1.5	0.7	3.4	3.4
METS	27		0.4	1.9	0.3	1.4	0.7	3.7	3.9
MASP	30		1.0	5.2	0.6	1.8	0.6	2.7	3.7
MADR	30	F	0.0	0.0	0.0	0.0	0.0	0.0	—
PAMA	30		4.3	14.3	4.6	23.1	1.5	5.4	7.7
TROM	30	F	0.0	0.0	0.0	0.0	0.0	0.0	—
TAIW	30		1.0	8.0	1.3	7.4	0.8	5.8	7.6
NYAL	30		0.4	1.0	0.3	1.3	1.6	3.3	2.3
TSKB	30		0.9	3.1	0.9	4.4	0.8	3.2	4.5
HERS	30		0.4	16.4	0.2	3.3	0.5	21.2	19.0
Variance of unit weight of a singl.-diff. observation [mm]:								3.5	
Variance of unit weight of a coordinate observation (2.8-13) [mm]:								18.9	
Ratio:								5.4	5.9

The group rms of each coordinate component is also a useful instrument to detect station problems. Whereas the estimated internal precision of the site HERS is

comparable to the quality of other European sites we find much higher group rms values for the x-y-z-components. This indicates that particular days are showing large deviations to the combined solution.

3. Orbit Determination

There are interesting applications for combining normal equations in the context of satellite orbit modeling.

In a first part we briefly introduce some modeling aspects. This includes a review of the important perturbing forces acting on the GPS satellites. Most forces are known with sufficient accuracy to allow introducing them as known. Other forces, such as the radiation pressure, need to be estimated in the orbit determination process. The same is true for so-called pseudo-stochastic parameters. Due to modeling problems in particular for longer arcs (> 1 day) it is necessary to allow for velocity changes at predefined time epochs. The principles of "classical" orbit determination will conclude this first part.

In the second part (next chapter) we present a method to produce n -days-arcs based on n consecutive 1-day-arcs. The advantages of this method in comparison to the "classical" method lie in the flexibility and the speed of computation. In the combination step we do no longer have to process GPS observations but only normal equations. This does not only saves time, but disk space, too. The combination methods allow to generate long-arcs which would not be possible with the classical approach due to computer memory and processing-time limitations.

3.1 Modeling the GPS Satellite Orbits

3.1.1 Equation of Motion for GPS Satellites

The *equation of motion* in a central force field is (according to Newton and Euler) given by

$$m \cdot \ddot{\mathbf{r}} = \mathbf{F} \quad \text{or} \quad \ddot{\mathbf{r}} = \mathbf{a} \tag{3.1-1}$$

where

m the constant mass of a particle (satellite)

\mathbf{r} , $\ddot{\mathbf{r}}$ position respectively acceleration vector in the inertial space

F external forces acting on the particle

a accelerations acting on the particle.

If the force field is reduced to the gravity attraction of a spherical earth, the above equation characterizes the *two-body problem*.

Eqn. (3.1-1) is a differential equation of second order in the three-dimensional Euclidian space. To specify a particular solution we have to define e.g. 6 initial conditions. Usually this is done by the

initial values for $\mathbf{r}(t_0)|_0$ (position) and $\dot{\mathbf{r}}(t_0)|_0$ (velocity) at epoch t_0 or by

boundary values $\mathbf{r}(t_1)|_0$ and $\mathbf{r}(t_2)|_0$ at different time epochs t_1 and t_2 .

The six osculating *Keplerian elements* at epoch t_0 are an equivalent representation to the initial conditions and therefore also suited to describe a particular solution of the problem.

In general we have to take into account all accelerations **a** acting on the satellite. Let us split up the acceleration vector **a** into the gravitational part **a_G** (main effect) and a perturbing part **a_P**:

$$\mathbf{a} = \mathbf{a}_G + \mathbf{a}_P. \quad (3.1-2)$$

The two-body acceleration **a_G** may be written according to the *Newtonian law of gravitation* as

$$\mathbf{a}_G = -\frac{GM}{r^2} \frac{\mathbf{r}}{r} \quad (3.1-3)$$

where

r geocentric distance of the satellite

G, M Newtonian gravitational constant and mass of the Earth; for satellite methods we have: $GM = 3.986004415 \cdot 10^{14} \text{ m}^3\text{s}^{-2}$ [IERS 1992; SEIDELMANN AND FUKUSHIMA 1992]

whereas the perturbing acceleration may be expressed as

$$\mathbf{a}_P = \mathbf{a}_P(t, \mathbf{r}, \dot{\mathbf{r}}, q_1, q_2, \dots, q_n) \quad (3.1-4)$$

with q_1, q_2, \dots, q_n as unknown parameters of the force field.

3.1.2 Perturbing Forces

In the following subsections we will give a brief summary of the most important external forces acting on the GPS satellites. Table 3.1 gives a first impression of the relevant perturbing accelerations for orbit dynamics.

Table 3.1: Effect of gravitational and non-gravitational perturbing forces on GPS satellites (from LANDAU 1988).

Perturbing Force	Acceleration [m/s ²]	Orbit Effect [m]	
		After 1 Day	After 7 Days
Earth's oblateness (C_{20})	$5 \cdot 10^{-5}$	10 000	100 000
Non-sphericity of the earth ($C_{nm}, S_{nm}, n, m \leq 8$)	$3 \cdot 10^{-7}$	200	3 400
Non-sphericity of the earth ($C_{nm}, S_{nm}, n, m > 8$)		0.03	0.1
Attraction by the moon	$5 \cdot 10^{-6}$	3 000	8 000
Attraction by the sun	$2 \cdot 10^{-6}$	800	3 500
Earth's tidal potential	$1 \cdot 10^{-9}$	0.3	1.2
Ocean tides	$5 \cdot 10^{-10}$	0.04	0.2
Direct solar rad. pressure	$6 \cdot 10^{-8}$	200	1 000
y -bias effect	$5 \cdot 10^{-10}$	1.4	51
Albedo	$4 \cdot 10^{-10}$	0.03	
Relativistic effects	$3 \cdot 10^{-10}$		

3.1.2.1 The Earth's Gravity Field

The most important perturbing accelerations are resulting from the Earth's gravity field. Because of the high altitudes of the GPS satellites the effect due to the shorter wavelengths of the gravity field is relatively small. Therefore it is usually sufficient to use an earth potential model up to degree and order 8 [BEUTLER ET AL. 1985]. The coefficients of the gravity field are very well determined by the long history of laser, altimetry and surface gravity data. The IERS standards recommend the use of the GEM-T3 model [IERS 1992; LERCH ET AL. 1994] with the exception of the terms C_{20} , C_{21} , and S_{21} . The reasons are explained below.

The gravity field of the Earth is a consequence of the mass distribution in the Earth's interior. The mathematical description of the potential field is usually performed using a *development in spherical harmonics* [HEISKANEN AND MORITZ 1967] with the *harmonic geopotential coefficients* C_{nm} and S_{nm} of degree n and order m as model parameters. An equivalent approximation is the development in a *series of mass moments* [HEITZ 1986].

The coefficient of *zero order* is fixing the total mass of the Earth. The corresponding term in the potential is the so-called *Kepler term*.

The three *first order* coefficients are equivalent to the definition of the center of mass. Setting these values to zero means to select the center of mass as the origin of the terrestrial reference frame (which is actually the case for the ITRF).

The *second order terms* are also of great importance. The mass moments of order two (or the coefficients C_{2m} and S_{2m}) are functions of the components of the tensor of inertia.

The geopotential of the non-rigid Earth is time dependent due to the solid tides. This effect is usually modeled as a variation of the geopotential coefficients C_{nm} and S_{nm} [EANES ET AL. 1983]. SEIDELMANN [1992] summarizes an efficient two-step computing procedure treating in the first step only the second order terms and in the second step all higher order terms (to a large extent not important for the GPS applications). The mean value of the tidal disturbance in C_{20} is not zero. SEIDELMANN [1992] published a mean value of $\overline{C}_{20} = -1.39119 \cdot 10^{-8} \cdot k_2$, which depends on the *Love number of degree two* k_2 . The current IERS recommended geopotential model GEM-T3 does not include this permanent tidal disturbance. To be consistent with the corresponding solid Earth tide model of IERS which is used to define the terrestrial reference frame a corrected \overline{C}_{20} value (including the permanent effect) should be used.

The coefficients C_{21} and S_{21} describe the position of the Earth's figure axis with respect to the ITRF pole. The figure axis should closely coincide with the observed position of the rotation axis averaged over a period of many years. Therefore we can assume that the estimated values correspond to the mean pole position. If this mean pole is identical to the ITRF pole we can use $C_{21} = S_{21} = 0$. To be consistent with the IERS pole series it is recommended to use the normalized values $\overline{C}_{21} = -0.17 \cdot 10^{-9}$ and $\overline{S}_{21} = 1.19 \cdot 10^{-9}$ instead of the GEM-T3 values [IERS 1992].

It is worth to mention that the term C_{20} (like the other zonal coefficients) is responsible for secular perturbations of the satellite orbits such as the movement of the orbit nodes (for GPS satellites about $-14.2^0/\text{year}$) [BEUTLER 1995].

The osculating elements are showing perturbations in the semi-major axis a of 1.7 km with periods of 6 hours - also mainly due to the flattening of the Earth.

The geopotential coefficients with and up to order two are therefore essential for the definition of the terrestrial reference frame.

All *coefficients of higher orders* are representing the irregular shape of the gravity field corresponding to the mass distribution in the earth.

HUGENTOBLER AND BEUTLER [1993] found that the non-central gravity field

(mainly the potential term $n = 2, m = 3$) is responsible for *resonance effects*. Due to the revolution period of exactly half a sidereal day, which is a perfect 2:1 resonance with the earth rotation, the orbits of the GPS satellites are considerably affected. Typical periods of orbital disturbances in the semi-major axis a resulting from resonance effects are ranging from 8 to 25 years with amplitudes of about 4 km. ROTHACHER [1992] pointed out that a drastic reduction would be obtained already if the revolution period would be changed by two minutes.

It is possible to try to solve for some of these parameters using for example the data of the global IGS network. The partial derivatives are given in LANDAU [1988]. First attempts were presented by BEUTLER ET AL. [1994]. Results of center of mass estimates are shown in Section 8.5.

3.1.2.2 Gravity Effect of Sun, Moon and other Third Body's

In addition to the Earth gravitation we have to take into account the perturbation forces of the Sun, the Moon and other planets.

The perturbing force of the third body is identical with the tidal force with respect to the Earth's center of mass. The effect of the other planets is small. The largest effect would result from Venus with $1.5 \cdot 10^{-10} \text{ m/s}^2$ perturbation acceleration.

The perturbing acceleration caused by a third body mass shows a period of six hours in an earth-fixed system as a consequence of the combined effect of the periods of the satellites orbit and the Earth rotation.

The mean orbital elements, in which the higher frequency parts due to the Earth's non-central gravity field are removed, are dominated by annual, semianual, monthly, semimonthly etc. oscillations caused by the tidal forces of the Sun and the Moon. BEUTLER [1995] demonstrated this fact with his analysis of 2.5 years of IGS orbit determination.

The use of the new DE400/LE400 [STANDISH 1995] ephemerides for Sun and Moon is proposed in the IERS standards (1995) [IERS 1995].

3.1.2.3 Solid Earth Tide Effects

The gravity attraction of the Moon and the Sun has primary an effect on the deformation of the Earth. The satellite orbits are affected because with the tidal deformation also the gravity field changes. The perturbation acceleration depends on the Love number k_2 . Second order approximation formulae are given in LAMBECK [1974].

3.1.2.4 Direct Solar Radiation Pressure and y-Bias

Direct Radiation

The *direct radiation pressure* results from the interaction (absorption and reflection) of the light emitted by the Sun with the surface of the satellite. All radiation models are therefore strongly depending on the knowledge of the shape, the reflection coefficients of the illuminated planes and the orientation of the satellite with respect to the Sun.

The satellite orientates its solar panels always in a plane which is perpendicular to the Sun. Only eclipses (when the satellite is in the shadow of the Earth) are an exception (see section 3.1.3). The perturbing force points in the direction sun \rightarrow satellite. This is the reason for the commonly used expression *direct* radiation pressure.

Due to the ellipticity of the Earth's orbit around the Sun and the changing angle between the normal to the orbital plane and the unit vector pointing to the Sun we have dominating annual variations in the radiation pressure. BEUTLER [1995] shows an annual effect with an amplitude of 4 % of the total effect using the parameter estimates of 2.5 years of IGS processing at CODE.

The perturbation acceleration formulae are given in [CAPPELLARI ET AL. 1976].

The IERS standards [IERS 1995] recommend the use of the so-called *Rock 4 (Block I) and Rock42 (Block II)* models [FLIEGEL ET AL. 1992]. Furthermore, a distinction has to be made between the standard (S) models and the T-model which includes thermal re-radiation.

The radiation pressure models are of importance only if we do not solve for radiation parameters. For high precision applications these models are not sufficient enough. If we determine in the least-squares adjustment a scale parameter (for the radiation pressure) the resulting orbit is widely independent of the used apriori model [ROTHACHER ET AL. 1995].

y-Bias

If the solar panels are not perfectly normal to the direction to the Sun there is also an effect in the *y*-direction, the so-called *y-bias*. The real physical meaning of this parameter is controversial discussed.

Extended Radiation Model

BEUTLER ET AL. [1994] demonstrated that GPS orbits with an arc length of several days (up to 10 days) can be successfully represented with a modeling of the radiation pressure in the following way:

$$\mathbf{a}_{rpr} = a_{\text{Rock}} + X_1(t)\mathbf{e}_1 + X_2(t)\mathbf{e}_2 + X_3(t)\mathbf{e}_3 \quad (3.1-5)$$

with

a_{Rock} apriori radiation model (i.e. ROCK4 / Rock42 model)

$\mathbf{e}_1 = \frac{\mathbf{r} - \mathbf{r}_\odot}{|\mathbf{r} - \mathbf{r}_\odot|}$; direction of the direct radiation pressure (Sun (\odot) \rightarrow satellite),

$\mathbf{e}_2 = \mathbf{e}_y = \frac{\mathbf{e}_z \times (\mathbf{r} - \mathbf{r}_\odot)}{|\mathbf{e}_z \times (\mathbf{r} - \mathbf{r}_\odot)|}$ direction of the y -bias; $\mathbf{e}_z = -\frac{\mathbf{r}}{|\mathbf{r}|}$,

$\mathbf{e}_3 = \mathbf{e}_1 \times \mathbf{e}_2$, and

$X_i = X_{0i} + X_{ci} \cos u(t) + X_{si} \sin u(t)$, $i = 1, 2, 3$; $u(t)$ argument of latitude.

Instead of only two parameters p_0 and p_2 for the modeling of the radiation pressure we end up with nine parameters X_{0i} , X_{ci} , and X_{si} , $i = 1, 2, 3$. These parameter types are implemented in a parameter estimation program of the Bernese Software (ORBIMP) treating the orbital positions as pseudo-observations. The program is used by KOUBA [1995B] to check the long-arc quality of the orbits of the IGS Analysis Centers.

Recently the model has also been implemented in the main parameter estimation program GPSEST and the combination program ADDNEQ. High quality long-arc orbits (below 10 *cm*) are possible using this model together with pseudo-stochastic orbit modeling (see Section 3.1.4).

3.1.2.5 Other Perturbations

Other effects with a perturbation acceleration smaller than $1 \cdot 10^{-9}$ are usually not modeled

- Albedo radiation pressure (radiation of lights which is reflected by the Earth)
- Gravitational effects of the ocean tides
- Relativistic effects due to the Earth's gravity field
- Thermal emission of the satellite
- Drag

3.1.3 Eclipsing Satellites

About twice per year, for usually two months twice per day, a GPS satellite is moving through the shadow of the Earth. The maximum duration of an eclipse is about 55 minutes.

The modeling of GPS satellites during eclipse seasons is extremely difficult. On board solar sensors are not able to determine the direction to the Sun during the

eclipse periods. The satellite is rotating with a constant rotation rate during the eclipse phase. After the shadow exit the satellite has an arbitrary orientation with respect to the Sun. On the shortest possible way the satellite turns back to its usually orientation. The rotation direction is ambiguous and depends on the orientation of the satellite at the shadow exit.

More details are reported by BAR-SEVER [1994].

A possible corrective action for the orbit determination of eclipsing satellites is the removal of data (about 1 hour) after the shadow exit and the introduction of pseudo-stochastic parameters (see next section).

According to the weekly orbit comparisons performed by the IGS Analysis Center Coordinator [KOUBA 1995B] the orbit quality of the eclipsing satellites is considerably degraded compared to the other satellites.

3.1.4 Stochastic Orbit Modeling

Pseudo-stochastic parameters are included as additional orbit parameters to absorb unmodeled perturbations.

The physical meaning of the pseudo-stochastic parameters is a pulse s at a predefined time τ in a predefined direction characterized by the unit vector \mathbf{e} . The resulting orbit is continuous. Only the satellite's velocity is allowed to have a discontinuity at the time τ of the pulse:

$$\mathbf{v}_{\text{new}} = \mathbf{v}_{\text{old}} + s \cdot \mathbf{e}.$$

Allowed directions are usually radial (R), along-track (S) and out-of-plane (W). We make use of this type of orbit parameters with much success for the following applications:

a) Modeling Eclipsing Satellites:

Due to the sometimes unpredictable behavior of an eclipsing satellite (see section 3.1.3) it is useful to set up these parameters to absorb a part of the modeling prob-

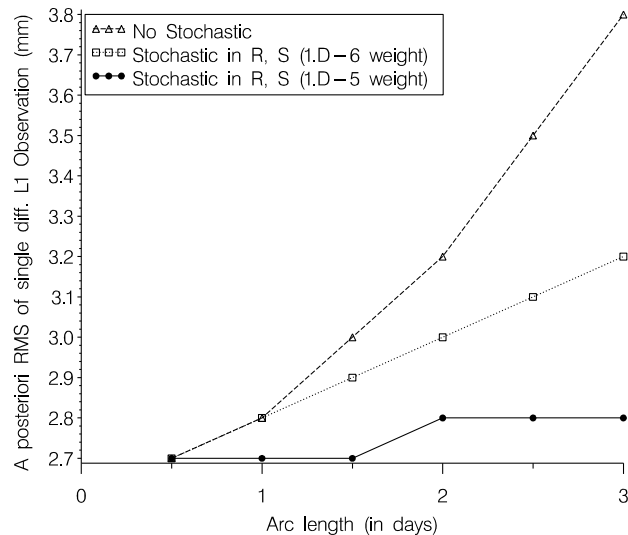


Figure 3.1: Improvement of the estimated rms a posteriori of single difference L_1 observations using pseudo-stochastic parameters for longer arcs. Unit of the specified pseudo-stochastic weights is m/s^2 .

lems. The quality of the 3-days-orbits increases significantly even if it does not reach the quality of the non-eclipsing satellites. Usually we set up stochastic parameters in the R and S direction twice a day (at midnight and noon UT). Parameters in the W direction are set up, but they are tightly constrained for the parameter estimation.

b) Introducing Pseudo-Stochastic Pulses for All Satellites for Long Arcs (> 1 Day):

Figure 3.1 reflects the orbit model deficit for longer arcs showing an increase of the estimated rms aposteriori of single difference L_1 phase observations. It is clearly visible that pseudo-stochastic parameters with apriori rms values $> 1 \cdot 10^{-5} m/s^2$ for the R and the S direction are able to keep the increase of the rms for longer arcs small. Additional parameters for the W directions create no improvement.

The longer the arcs the more important is stochastic orbit modeling. Long-arc computation is the topic of Chapter 4. The quality of 7-days-arcs is shown in Figure 3.2. The rms values are obtained from a Helmert comparison of the orbits of a

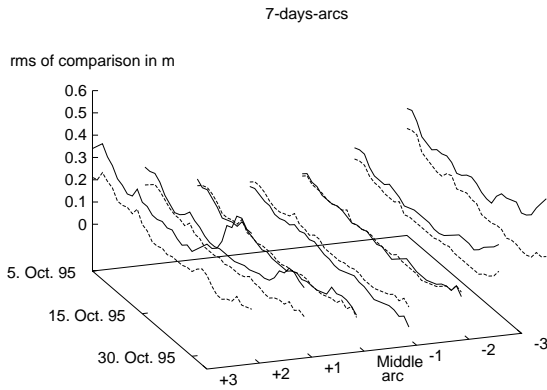


Figure 3.2: Quality of 7-days-arcs using different apriori weights for the pseudo-stochastic parameters. Radiation pressure model: direct radiation and y -bias.

particular day (within the 7-days-arc) with the CODE orbit (middle day of a 3-days-arc, stochastic applied for all satellites, apriori weights 1.d-6 m/s^2 (R), 1.d-5 m/s^2 (S), 1.d-9 m/s^2 (W), direct and y -bias radiation pressure parameters). The upper (solid) line corresponds to an orbit for which all satellites are modeled with identical options as for the 3-days-arcs. For the days at the arc boundaries (day 3 and -3 of the arc) we see differences of up to 50 cm . The quality of the middle days is not degraded by the longer arc length. The agreement is of the order of 6-8 cm . Using apriori weights of 1.d-4 m/s^2 for the

R , S , and W component helps to reduce the problems at the arc boundaries. Nevertheless there is a considerable loss of quality (rms values of about 20 cm for the days 3 and -3). The limits for the use of the *standard radiation pressure model together with pseudo-stochastic parameters* is given by arc lengths of about 3 days.

Most of the effect of the stochastic parameters is absorbed by the extended radiation pressure model (3.1-5), which is, as already mentioned, now also implemented in the parameter estimation program GPSEST and the stacking program ADDNEQ.

Using *extended radiation model together with pseudo-stochastic parameters* (weights identical to the values of the 3-days-arcs) we are able to keep the rms values of Figure 3.2 for all days of the 7-days-arc below the 10 *cm* level. This means that there is almost no difference in the quality between the orbits of the boundary days and the orbits of the middle days [SPRINGER ET AL. 1996].

In spite of the larger degree of freedom it is useful even for shorter arc lengths (including 1-day-arcs) to model all satellites using stochastic parameters. For 3-days-arcs the advantage is clear (see e.g. the estimation of the center of mass in Section 8.5).

c) Flexibility of the Modeling Using Normal Equations

The method of the orbit determination based on normal equations allows a very flexible handling of the stochastic parameters. Setting up stochastic parameters for *all* satellites in the daily solutions allows it to select the stochastic model later on in the combination step. For satellites which behave well we may tightly constrain the estimates, for others we may specify only loose constraints (see section 2.6.1). We refer to Section 4.4 for setting up additional stochastic parameters at the day boundaries of consecutive arcs.

3.2 Estimation of Satellite Orbits

The estimation of orbit parameters with the help of observations (GPS carrier phase and pseudorange observations, observations of geocentric satellite positions in form of broadcast messages [DIERENDONCK ET AL. 1978] or in form of precise orbits [REMONDI 1989]) is the task of the orbit determination.

Below we review the principles of a "classical" orbit determination.

The linearized observation equations, taking into account only the orbital parameters as unknowns, may be written as:

$$\mathbf{y}(t, \mathbf{r}, \dot{\mathbf{r}}, q_1, q_2, \dots, q_n) + \mathbf{e} = \mathbf{y}(t, \mathbf{r}_0, \dot{\mathbf{r}}|_0, q_1|_0, q_2|_0, \dots, q_n|_0) \quad (3.2-1)$$

$$+ \begin{bmatrix} \mathbf{B}_{rv} & \mathbf{B}_q \end{bmatrix} \begin{bmatrix} \Delta \mathbf{rv} \\ \Delta \mathbf{q} \end{bmatrix}$$

where

\mathbf{y} , $\mathbf{y}|_0$ observation vector and the corresponding apriori values of dimension n_{obs} , $\Delta \mathbf{rv}$ parameters characterizing initial conditions; vector contains geocentric position \mathbf{r} and velocity $\dot{\mathbf{r}}$ of the satellite; $\Delta \mathbf{rv} = \mathbf{rv} - \mathbf{rv}|_0$,

- $\Delta \mathbf{q}$ dynamical parameters $q_i, i = 1, \dots, n_q$; $\Delta \mathbf{q} = \mathbf{q} - \mathbf{q}|_0$,
 \mathbf{B}_{rv} partial derivatives with respect to \mathbf{rv} :
 $(\mathbf{B}_{rv})_{ij} = \frac{\partial (\mathbf{y})_i}{\partial (\mathbf{rv})_j}|_0$; $i = 1, \dots, n_{obs}$, $j = 1, \dots, 6$, and
 \mathbf{B}_q partial derivatives with respect to the dynamical parameters \mathbf{q} :
 $(\mathbf{B}_q)_{ij} = \frac{\partial (\mathbf{y})_i}{\partial (q)_j}|_0$; $i = 1, \dots, n_{obs}$, $j = 1, \dots, n_q$.

The orbit determination process asks not only for a best fitting approximation of the observations, it also asks for the validity of the equation of motion (3.1-1) for the resulting orbit.

We solve the orbit determination problem iteratively. The apriori orbit used for the least-squares adjustment is obtained by solving the following initial value problem

$$\ddot{\mathbf{r}}|_0 = (\mathbf{a}_G + \mathbf{a}_P)|_0 = -\frac{GM}{r|_0^3}\mathbf{r} + \mathbf{a}_P(t, \mathbf{rv}|_0, \mathbf{q}|_0) \quad (3.2-2)$$

where the initial conditions

$$\begin{aligned} \mathbf{r}(t_0)|_0 &= \mathbf{r}(t_0, \mathbf{rv}|_0) \\ \dot{\mathbf{r}}(t_0)|_0 &= \dot{\mathbf{r}}(t_0, \mathbf{rv}|_0) \\ \text{and} \quad \mathbf{q}|_0 & \end{aligned} \quad (3.2-3)$$

are assumed known. The apriori values for the dynamical parameters $\mathbf{q}|_0$ may be assumed to be e.g. zero. In practice the program DEFSTD computes an apriori orbit $\mathbf{r}(t)|_0$ which is not an ephemeris table of satellite positions, but consists of several sets of q polynomial coefficients (usually one set per hour and $q = 11$) to allow at any time t the computation of the satellite's position and velocity [ROTHACHER ET AL. 1993; ROTHACHER 1992]. The approximation error with respect to the true solution of the equation of motion can be reduced to any given limit with the selection of the polynomial degree.

The polynomial coefficients and the partials with respect to the dynamical parameters are stored for later use in the main parameter estimation process (program GPSEST). The partials with respect to the Keplerian elements do not have to be saved because they can be computed using analytical formulae.

The principles, advantages and disadvantages of analytical and numerical integration methods are not discussed here. We refer to BEUTLER [1990] for detailed informations. From now on, eqn. (3.2-1) represents a standard parameter estimation process.

The improved orbit $\mathbf{r}(t)$ may be expressed using the apriori orbit $\mathbf{r}(t)|_0$ and the increments $\Delta \mathbf{rv}$ and $\Delta \mathbf{q}$ (linearization with respect to the unknowns necessary for the least-squares adjustment) as:

$$\mathbf{r}(t) = \mathbf{r}(t)|_0 + \begin{bmatrix} \mathbf{C}_{rv}(t) & \mathbf{C}_q(t) \end{bmatrix} \begin{bmatrix} \Delta \mathbf{rv} \\ \Delta \mathbf{q} \end{bmatrix} \quad (3.2-4)$$

with

$\mathbf{C}_{rv}(t)$ partial derivatives with respect to \mathbf{rv} :

$$(\mathbf{C}_{rv}(t))_{ij} = \frac{\partial(\mathbf{r}(t))_i}{\partial(\mathbf{rv})_j}|_0 ; i = 1, \dots, 3, j = 1, \dots, 6$$

$\mathbf{C}_q(t)$ partial derivatives with respect to the dynamical parameters \mathbf{q} :

$$(\mathbf{C}_q(t))_{ij} = \frac{\partial(\mathbf{r}(t))_i}{\partial(\mathbf{q})_j}|_0 ; i = 1, \dots, 3, j = 1, \dots, n_q.$$

The partial derivatives in the matrices $\mathbf{C}_{rv}(t)$ and $\mathbf{C}_q(t)$ are solutions of the derivative of the (primary) initial value problem (3.2-2) and (3.2-3) with respect to the parameters \mathbf{rv} and \mathbf{q} . The resulting set of differential equations expressed in matrix notation are also called *variational equations*:

$$\begin{bmatrix} \ddot{\mathbf{C}}_{rv}(t) \\ \ddot{\mathbf{C}}_q(t) \end{bmatrix} = \begin{bmatrix} \mathbf{C}_{rv}(t) & \dot{\mathbf{C}}_{rv}(t) \\ \mathbf{C}_q(t) & \dot{\mathbf{C}}_q(t) \end{bmatrix} \begin{bmatrix} \mathbf{A}_r \\ \mathbf{A}_v \end{bmatrix} + \begin{bmatrix} \mathbf{\emptyset} \\ \mathbf{A}_q \end{bmatrix} \quad (3.2-5)$$

with the given initial conditions

$$\begin{aligned} \mathbf{C}_{rv}(t_0) &= \frac{\partial(\mathbf{r}(t_0))}{\partial\mathbf{rv}}|_0 ; & \dot{\mathbf{C}}_{rv}(t_0) &= \frac{\partial(\dot{\mathbf{r}}(t_0))}{\partial\mathbf{rv}}|_0 \\ \mathbf{C}_q(t_0) &= \mathbf{\emptyset} ; & \dot{\mathbf{C}}_q(t_0) &= \mathbf{\emptyset}, \end{aligned} \quad (3.2-6)$$

the 3×3 matrices

$$(\mathbf{A}_r)_{ij} = \frac{\partial(\mathbf{a}_G + \mathbf{a}_P)_i}{\partial(\mathbf{r})_j}|_0 ; (\mathbf{A}_v)_{ij} = \frac{\partial(\mathbf{a}_G + \mathbf{a}_P)_i}{\partial(\dot{\mathbf{r}})_j}|_0 \quad (3.2-7)$$

and $3 \times n_q$ matrices containing the elements

$$(\mathbf{A}_q)_{ik} = \frac{\partial(\mathbf{a}_G + \mathbf{a}_P)_i}{\partial(\mathbf{q})_k}|_0. \quad (3.2-8)$$

The simplifications $\mathbf{A}_v = \mathbf{\emptyset}$ are valid if no velocity-dependent accelerations are acting on the satellites (which is true for GPS) and $\mathbf{A}_r = -\frac{GM}{r^3}(\mathbf{I} - 3 \cdot \frac{\mathbf{r}\mathbf{r}'}{r^2})$ if we can neglect the perturbation accelerations \mathbf{a}_p [BEUTLER 1982].

The accuracy requirements for the integration of the variational equations are less stringent than for the integration of the equation of motion. An approximate solution decreasing considerably the computational burden of the solution of the variational equations may be found in [BEUTLER ET AL. 1994].

Such approximations are helpful because in each iteration step for the orbit improvement we have to solve the non-linear differential equation of motion (3.2-2), (3.2-3) and the $6 + n_q$ linear differential equations (3.2-5), (3.2-6).

It should be mentioned, however, that the solutions of the variational equations are produced using numerical integration, today.

The resulting orbit, computed by a new numerical integration using the improved orbital elements, is a solution of the equation of motion and is the best fit to the observations in a least-squares sense.

4. Combination of Consecutive Daily Arcs

4.1 Introduction

The combination of parameters on normal equation systems level is only possible if the parameters are referring to the same apriori information. If this is not the case we have to perform a parameter transformation (2.5-5) to make them identical. For this procedure we need to know the apriori information for each particular solution. This principle was applied to many examples in Section 2.5.2. We only have to make sure that the linearization is still valid.

In the following sections we will apply the parameter transformation method for the combination of the orbits:

Based on daily normal equation systems (NEQs) containing all parameters (including orbit parameters referring to a well-defined 1-day apriori arc) we will develop the formulae which are needed to form n -days-arcs. These developments were published in [BEUTLER ET AL. 1996]. We review them below in view of our general considerations in Chapter 2.

4.2 Problem Definition

We assume that each daily solution i (out of totally n daily solutions) may contain the following orbit parameters for a particular satellite:

- *osculating orbital elements* E_{ik} , $i = 1, 2, \dots, n$; $k = 1, 2, \dots, 6$:
Keplerian orbital elements referring to the osculation epoch t_{0i} of the arc for day i (usually 0^h GPS-time for the particular day). We use the representation $\mathbf{E}_i = (E_{i1}, E_{i2}, \dots, E_{i6}) = (a, e, i, \Omega, \omega, u)_i$.
- *dynamical parameters* q_{ik} , $i = 1, 2, \dots, n$; $k = 1, 2, \dots, m_1$:
orbital parameters to model the perturbation forces due to solar radiation (section 3.1.2.4). Usually only two radiation parameters (direct term and y -bias)

are estimated: $\mathbf{q}_i = (a_d, a_y)_i$; $m_1 = 2$. Additional parameters characterizing radiation pressure according to eqn. (3.1-5) are implemented, too.

- *pseudo-stochastic parameters* s_{ik} , $i = 1, 2, \dots, n$; $k = 1, 2, \dots, m_2$ characterize velocity changes at predetermined times in predetermined directions. The stochastic parameters are very useful to absorb unmodeled perturbation forces (see Section 3.1.4) and therefore important for long-arc evaluations.

Let us summarize all $m = 6 + m_1 + m_2$ orbital parameters of a particular satellite of day i in the following way:

$$\mathbf{o}_i = (o_{i1}, o_{i2}, \dots, o_{im}) = (E_{i1}, E_{i2}, \dots, E_{i6}, q_{i1}, q_{i2}, \dots, q_{im_1}, s_{i1}, s_{i2}, \dots, s_{im_2}) \quad (4.2-1)$$

For simplification we assume that each day i contain the same number of dynamical and stochastic parameters m_1 and m_2 respectively (which is in general not the case).

The daily normal equations refer to the used apriori arc

$$\mathbf{r}_i(t)|_0 = \mathbf{r}(t; o_{i1}|_0, o_{i2}|_0, \dots, o_{im}|_0) \quad (4.2-2)$$

We store the apriori arc as a set of polynomials for each component (resulting from the solution of the equation of motion in a perturbed gravity field) allowing a computation of the position and the velocity of the satellites at any time. Apriori values for the radiation pressure parameters can be specified (see Section 3.1.2.4) and the apriori values for the stochastic parameters are zero. We need this piece of information together with the normal equations as input for the combination program ADDNEQ.

The estimated orbit of day i is given by

$$\mathbf{r}_i(t) = \mathbf{r}(t; o_{i1}, o_{i2}, \dots, o_{im}) \quad (4.2-3)$$

using the "improved" parameters $\mathbf{o}_i = \mathbf{o}_i|_0 + \delta\mathbf{o}_i$ for the orbit integration.

The combined orbit $\mathbf{r}_c(t)$ is defined as

$$\begin{aligned} \mathbf{r}_c(t) &= \mathbf{r}(t; o_{c1}, o_{c2}, \dots, o_{c\tilde{m}}) \\ &= \mathbf{r}(t; E_{c1}, E_{c2}, \dots, E_{c6}, q_{c1}, q_{c2}, \dots, q_{cm_1}, \\ &\quad s_{11}, s_{12}, \dots, s_{1m_2}, s_{21}, s_{22}, \dots, s_{2m_2}, \dots, s_{n1}, s_{n2}, \dots, s_{nm_2}). \end{aligned} \quad (4.2-4)$$

The vector $\mathbf{r}_c(t)$ is now expressed for the entire n -days-arc as a function of one set of six Keplerian elements, one set of m_1 dynamical parameters and n sets of m_2 pseudo stochastic parameters. As reference we use the initial epoch t_1 of arc number 1.

This means that the Keplerian elements of the arcs $i = 2, 3, \dots, n$ have to be expressed by those of the first day.

The dynamical parameters \mathbf{q}_i of the different days are combined to \mathbf{q}_c with a simple superposition of the relevant NEQ-parts if the apriori models are identical.

It is also possible to solve for dynamical parameters each day separately even if we solve for common osculating elements which will be demonstrated later on.

In addition, all $(n \cdot m_2)$ pseudo-stochastic parameters remain as unknown parameters in the combined orbit (4.2-4) because of the fact that the stochastic parameters s_{ik} of day i have an influence on the orbit for all following days $i + 1, i + 2, \dots, n$.

It is also possible to set up additional stochastic parameters in three linear independent directions (for example R, S, W) between two subsequent days. In this case we have to add stochastical parameters s_{ik}^* to the model for the combined orbit (4.2-4).

All the described combination possibilities for the different parameter types can be realized using the parameter transformation (2.5-5). For simplification we discuss the combination in the following steps:

- combination of the osculating elements and the dynamical parameters
- combination of the stochastic parameters
- combination of all orbit parameters together

4.3 Combination of Osculating Elements and Dynamical Parameters

4.3.1 One Set of Dynamical Parameters for the Combined Arc

Because the six osculating elements of day i $\mathbf{E}_i = (a, e, i, \Omega, \omega, u)_i$ at epoch t are equivalent to the position $\mathbf{r}_i(t)$ and velocity $\mathbf{r}_i^{(1)}(t)$ of the satellite at this epoch, we have to ask for continuity of position velocity at the day boundary (labeled with the time argument t_{i+1}) if we try to express the orbital parameters of the day $i + 1$ by those of day i . For the dynamical parameters we have to ask for identical estimates. The corresponding $6 + m_1$ condition equations then read as:

$$\begin{aligned} \mathbf{r}_i(t_{i+1}) &= \mathbf{r}_{i+1}(t_{i+1}) \\ \mathbf{r}_i^{(1)}(t_{i+1}) &= \mathbf{r}_{i+1}^{(1)}(t_{i+1}) \\ \mathbf{q}_i &= \mathbf{q}_{i+1} = \mathbf{q}_c \end{aligned} \tag{4.3-1}$$

The linearized condition equations give directly the transformation equations from day $i + 1$ to day i . In order to simplify the notation we leave out the time argument t_{i+1} which is the same in all the time dependent functions:

$$\begin{aligned}
 & \mathbf{r}_i|_0 + \sum_{k=1}^6 \frac{d\mathbf{r}_i|_0}{dE_{ik}} \cdot \Delta E_{ik} + \sum_{k=1}^{m_1} \frac{d\mathbf{r}_i|_0}{dq_{ik}} \cdot \Delta q_{ik} = \\
 = & \mathbf{r}_{i+1}|_0 + \sum_{k=1}^6 \frac{d\mathbf{r}_{i+1}|_0}{dE_{i+1,k}} \cdot \Delta E_{i+1,k} + \sum_{k=1}^{m_1} \frac{d\mathbf{r}_{i+1}|_0}{dq_{i+1,k}} \cdot \Delta q_{i+1,k}
 \end{aligned} \tag{4.3-2}$$

$$\begin{aligned}
 & \mathbf{r}_i^{(1)}|_0 + \sum_{k=1}^6 \frac{d\mathbf{r}_i^{(1)}|_0}{dE_{ik}} \cdot \Delta E_{ik} + \sum_{k=1}^{m_1} \frac{d\mathbf{r}_i^{(1)}|_0}{dq_{ik}} \cdot \Delta q_{ik} = \\
 = & \mathbf{r}_{i+1}^{(1)}|_0 + \sum_{k=1}^6 \frac{d\mathbf{r}_{i+1}^{(1)}|_0}{dE_{i+1,k}} \cdot \Delta E_{i+1,k} + \sum_{k=1}^{m_1} \frac{d\mathbf{r}_{i+1}^{(1)}|_0}{dq_{i+1,k}} \cdot \Delta q_{i+1,k} \\
 & \mathbf{q}_i|_0 + \Delta \mathbf{q}_i = \mathbf{q}_{i+1}|_0 + \Delta \mathbf{q}_{i+1}.
 \end{aligned} \tag{4.3-3}$$

Let us summarize the position- and velocity- vectors $\mathbf{r}_i|_0$ and $\mathbf{r}_i^{(1)}|_0$ into the one column matrix

$$\mathbf{r}_i = \begin{bmatrix} \mathbf{r}_i|_0 \\ \mathbf{r}_i^{(1)}|_0 \end{bmatrix}. \tag{4.3-4}$$

In matrix notation the condition equations (4.3-2) are given as

$$\begin{bmatrix} \mathbf{H}_{i+1} & \mathbf{Q}_{i+1} \\ \emptyset & \mathbf{I} \end{bmatrix} \begin{bmatrix} \Delta \mathbf{E}_{i+1} \\ \Delta \mathbf{q}_{i+1} \end{bmatrix} = \begin{bmatrix} \mathbf{H}_i & \mathbf{Q}_i \\ \emptyset & \mathbf{I} \end{bmatrix} \begin{bmatrix} \Delta \mathbf{E}_i \\ \Delta \mathbf{q}_i \end{bmatrix} + \begin{bmatrix} \mathbf{r}\mathbf{v}_i|_0 - \mathbf{r}\mathbf{v}_{i+1}|_0 \\ \mathbf{q}_i|_0 - \mathbf{q}_{i+1}|_0 \end{bmatrix} \tag{4.3-5}$$

with

i day number

\mathbf{H}_i Jacobian matrix of the transition from a set of osculating elements to initial coordinates and velocities at time t_{i+1} ; analytical formulae are given in [BEUTLER ET AL. 1996]:

$$\left[\begin{array}{cc} \frac{d(\mathbf{r}_i)_j}{dE_{ik}}|_0 & \frac{d(\mathbf{r}_i^{(1)})_j}{dE_{ik}}|_0 \end{array} \right]_{(6 \times 6)} ; \quad j = 1, 2, 3; \quad k = 1, 2, \dots, 6, \tag{4.3-6}$$

$(\mathbf{r}_i)_j$ and $(\mathbf{r}_i^{(1)})_j$ being the j -th component of the vector \mathbf{r}_i and $\mathbf{r}_i^{(1)}$

\mathbf{Q}_i partials with respect to the dynamical parameters; numerical computation according to Section 3.2:

$$\left[\begin{array}{cc} \frac{d(\mathbf{r}_i)_j}{dq_{ik}}|_0 & \frac{d(\mathbf{r}_i^{(1)})_j}{dq_{ik}}|_0 \end{array} \right]_{(6 \times m_1)} ; \quad j = 1, 2, 3; \quad k = 1, 2, \dots, m_1 \tag{4.3-7}$$

$\Delta \mathbf{E}_i$ estimated osculating elements of day i :

$$= [E_{ij} - E_{ij}|_0]_{(6 \times 1)} ; \quad j = 1, 2, \dots, 6 \tag{4.3-8}$$

$\Delta \mathbf{q}_i$ estimated dynamical parameters of day i :

$$[q_{ij} - q_{ij}|_0]_{(m_1 \times 1)} \quad ; \quad j = 1, 2, \dots, m_1 \quad (4.3-9)$$

$\mathbf{E}_i|_0$ apriori osculating orbital elements of the daily orbits at $t = t_{i+1}$:

$$\mathbf{E}_i|_0 = (E_{i1}, E_{i2}, \dots, E_{i6})|_0 \quad (4.3-10)$$

$\mathbf{rv}_i|_0$ apriori positions and velocities of the daily orbit arcs at $t = t_{i+1}$

$\mathbf{q}_i|_0$ apriori dynamical parameters of the daily orbits:

$$\mathbf{q}_i|_0 = (q_{i1}, q_{i2}, \dots, q_{im_1})|_0. \quad (4.3-11)$$

To derive a transformation equation which is identical to eqn. (2.5-5) $\Delta \hat{\boldsymbol{\beta}} = \mathbf{B} \Delta \tilde{\boldsymbol{\beta}} + d\boldsymbol{\beta}$ we have to solve eqn. (4.3-5) for the parameters $\Delta \hat{\boldsymbol{\beta}} \equiv [\Delta \mathbf{E}_{i+1}, \mathbf{q}_{i+1}]'$. With

$$\begin{bmatrix} \mathbf{H}_{i+1} & \mathbf{Q}_{i+1} \\ \boldsymbol{\emptyset} & \mathbf{I} \end{bmatrix}^{-1} = \begin{bmatrix} \mathbf{H}_{i+1}^{-1} & -\mathbf{H}_{i+1}^{-1} \mathbf{Q}_{i+1} \\ \boldsymbol{\emptyset} & \mathbf{I} \end{bmatrix} \quad (4.3-12)$$

we find that:

$$\begin{bmatrix} \Delta \mathbf{E}_{i+1} \\ \Delta \mathbf{q}_{i+1} \end{bmatrix} = \begin{bmatrix} \mathbf{K}_{i+1,i} & \mathbf{L}_{i+1,i} \\ \boldsymbol{\emptyset} & \mathbf{I} \end{bmatrix} \begin{bmatrix} \Delta \mathbf{E}_i \\ \Delta \mathbf{q}_i \end{bmatrix} + \begin{bmatrix} \mathbf{M}_{i+1,i} \\ \mathbf{N}_{i+1,i} \end{bmatrix} \quad (4.3-13)$$

with

$$\begin{aligned} \mathbf{K}_{i+1,i} &= \mathbf{H}_{i+1}^{-1} \cdot \mathbf{H}_i \\ \mathbf{L}_{i+1,i} &= \mathbf{H}_{i+1}^{-1} \cdot (\mathbf{Q}_i - \mathbf{Q}_{i+1}) \\ \mathbf{M}_{i+1,i} &= \mathbf{H}_{i+1}^{-1} \cdot \{(\mathbf{rv}_i|_0 - \mathbf{rv}_{i+1}|_0) - \mathbf{Q}_{i+1} \cdot (\mathbf{q}_i|_0 - \mathbf{q}_{i+1}|_0)\} \\ \mathbf{N}_{i+1,i} &= \mathbf{q}_i|_0 - \mathbf{q}_{i+1}|_0. \end{aligned} \quad (4.3-14)$$

In a final step we have to apply a sequence of transformations of type (4.3-13) to express the parameters of day $i+1$ by those of the first day. This can be done, without numerical integrations of the equation of motion, using the recursion formulae:

$$\begin{bmatrix} \Delta \mathbf{E}_{i+1} \\ \Delta \mathbf{q}_{i+1} \end{bmatrix} = \begin{bmatrix} \mathbf{K}_{i+1,1} & \mathbf{L}_{i+1,1} \\ \boldsymbol{\emptyset} & \mathbf{I} \end{bmatrix} \begin{bmatrix} \Delta \mathbf{E}_1 \\ \Delta \mathbf{q}_1 \end{bmatrix} + \begin{bmatrix} \mathbf{M}_{i+1,1} \\ \mathbf{N}_{i+1,1} \end{bmatrix} \quad (4.3-15)$$

with

$$\begin{aligned} \mathbf{K}_{i+1,1} &= \mathbf{K}_{i+1,i} \cdot \mathbf{K}_{i,1} \\ \mathbf{L}_{i+1,1} &= \mathbf{L}_{i+1,i} + \mathbf{K}_{i+1,i} \cdot \mathbf{L}_{i,1} \\ \mathbf{M}_{i+1,1} &= \mathbf{M}_{i+1,i} + \mathbf{L}_{i+1,i} \cdot (\mathbf{q}_1|_0 - \mathbf{q}_i|_0) + \mathbf{K}_{i+1,i} \cdot \mathbf{M}_{i,1} \\ \mathbf{N}_{i+1,1} &= \mathbf{q}_1|_0 - \mathbf{q}_{i+1}|_0. \end{aligned} \quad (4.3-16)$$

The corresponding normal equation system of day $i + 1$ has to be transformed according to eqns. (2.5-8)-(2.5-10) and (2.5-11) prior to the superposition to the combined NEQ (containing the parameters $\mathbf{E}_c \equiv \mathbf{E}_1$ and $\mathbf{q}_c \equiv \mathbf{q}_1$).

An alternative is the introduction of the transformation equations (4.3-15) as pseudo-observations with heavy weights which is according to 2.6.2 identical to the GMM with constraints. Such a procedure has the disadvantage that all orbit parameters \mathbf{E}_i and \mathbf{q}_i of the days $i = 2, 3, \dots, n$ remain in the combined normal equation system. The condition equations are linking these parameters to the ones of the first day. The parameter transformation is an elegant method keeping the combined normal equation system as small as possible using the parameters \mathbf{E}_c and \mathbf{q}_c only.

4.3.2 n Sets of Dynamical Parameters for the Combined Arc

If we solve for $n \cdot m_1$ dynamical parameters q_{ik} for the n -days-arc instead for q_{1k} , $k = 1, \dots, m_1$ we just have to skip the third condition equation in (4.3-1). In this case the linearized transformation equations (4.3-13) are simplified to

$$\Delta \mathbf{E}_{i+1} = \begin{bmatrix} \mathbf{K}_{i+1,i} & \tilde{\mathbf{L}}_{i+1,i} & \tilde{\mathbf{L}}_{i+1,i+1} \end{bmatrix} \begin{bmatrix} \Delta \mathbf{E}_i \\ \Delta \mathbf{q}_i \\ \Delta \mathbf{q}_{i+1} \end{bmatrix} + \tilde{\mathbf{M}}_{i+1,i} \quad (4.3-17)$$

with

$$\begin{aligned} \mathbf{K}_{i+1,i} &= \mathbf{H}_{i+1}^{-1} \cdot \mathbf{H}_i \quad (\text{same as in the previous section}) \\ \tilde{\mathbf{L}}_{i+1,i} &= \mathbf{H}_{i+1}^{-1} \cdot \mathbf{Q}_i \\ \tilde{\mathbf{L}}_{i+1,i+1} &= -\mathbf{H}_{i+1}^{-1} \cdot \mathbf{Q}_{i+1} \\ \tilde{\mathbf{M}}_{i+1,i} &= \mathbf{H}_{i+1}^{-1} \cdot (\mathbf{r}\mathbf{v}_i|_0 - \mathbf{r}\mathbf{v}_{i+1}|_0). \end{aligned} \quad (4.3-18)$$

The corresponding recursive formulae then read as:

$$\Delta \mathbf{E}_{i+1} = \begin{bmatrix} \mathbf{K}_{i+1,1} & \tilde{\tilde{\mathbf{N}}}_{i+1,1} & \dots & \tilde{\tilde{\mathbf{N}}}_{i+1,i+1} \end{bmatrix} \begin{bmatrix} \Delta \mathbf{E}_1 \\ \Delta \mathbf{q}_1 \\ \vdots \\ \Delta \mathbf{q}_{i+1} \end{bmatrix} + \tilde{\tilde{\mathbf{M}}}_{i+1,1} \quad (4.3-19)$$

with

$$\begin{aligned} \mathbf{K}_{i+1,1} &= \mathbf{K}_{i+1,i} \cdot \mathbf{K}_{i,1} \quad (\text{same as in the previous section}) \\ \tilde{\tilde{\mathbf{N}}}_{i+1,j} &= \begin{cases} \tilde{\mathbf{L}}_{i+1,i+1} & \text{for } j = i + 1 \\ \tilde{\mathbf{L}}_{i+1,i} + \mathbf{K}_{i+1,i} \cdot \tilde{\tilde{\mathbf{N}}}_{i,i} & \text{for } j = i \\ \mathbf{K}_{i+1,i} \cdot \tilde{\tilde{\mathbf{N}}}_{i,j} & \text{for } j \leq i - 1 \end{cases} \\ \tilde{\tilde{\mathbf{M}}}_{i+1,1} &= \tilde{\tilde{\mathbf{M}}}_{i+1,i} + \mathbf{K}_{i+1,i} \cdot \tilde{\tilde{\mathbf{M}}}_{i,1}. \end{aligned} \quad (4.3-20)$$

The above recursive formulae are the transformation equations for the orbital parameters $\Delta \mathbf{E}_{i+1}$ of day $i + 1$. The parameter transformation has to be applied, as in the previous section, prior to the superposition to the combined normal equation system.

4.4 Combination of Stochastic Parameters

Let us start with a brief definition of pseudo-stochastic parameters. We consider the particular day i with the day boundaries t_i and t_{i+1} . A pseudo-stochastic pulse s in the direction \mathbf{e} at the time $\tau \leq t_i$ allow according to Section 3.1.4 a velocity change at that time:

$$\mathbf{v}_{new}(\tau) = \mathbf{v}_{old}(\tau) + s \cdot \mathbf{e} \quad (4.4-1)$$

It is of greatest importance for the orbit combination that we can compute the effect of that specific pulse on the orbital elements at the time t_i and all following osculating epochs. Using the special perturbation theory of celestial mechanics we are able to express the induced effect in the osculating elements as linear functions of the pulse components of $s \cdot \mathbf{e}$.

A stochastic pulse $s \cdot \mathbf{e}$ at time τ changes for example the semi-major axis [BEUTLER ET AL. 1996]:

$$\Delta a_s(\tau) = s \cdot \frac{2}{n \cdot \sqrt{1 - e^2}} \cdot (e \cdot \sin v \cdot e_R + \frac{a \cdot (1 - e^2)}{r} \cdot e_S). \quad (4.4-2)$$

Similar equations also exist for the other osculating elements as functions of e_R , e_S and e_W which are the components of the vector \mathbf{e} in R -, S - and W - directions. In matrix notation we can simplify the equations to

$$\Delta \mathbf{E}_s(\tau) = \boldsymbol{\kappa}_s(\tau) \cdot s \quad (4.4-3)$$

For the case $\tau = t_i$ this already proves that the changes induced into the osculating elements are linear functions of the pulse s .

For the case $\tau < t_i$ we have to solve the perturbation equations starting from the elements $\mathbf{E}_i = \mathbf{E}(t_i)$. In linearized form neglecting all terms higher than the first order in the Taylor series development we may write:

$$\Delta \mathbf{E}_s(\tau) = \mathbf{M}_s(t_i, \tau) \cdot \Delta \mathbf{E}_s(t_i) \quad (4.4-4)$$

with

$$(\mathbf{M}_s(t_i, \tau))_{jk} = \frac{d(\mathbf{E}_i(\tau))_j}{d(\mathbf{E}(t_i))_k}. \quad (4.4-5)$$

\mathbf{M}_s results from the solution of the variational equations (3.2-5) taking into account all perturbation forces used in the orbit model.

Only in case of the simple Keplerian approximation we may assume $\mathbf{M}_s = \mathbf{I}$ which is sufficient for short arcs.

On the other hand we are able with eqns. (4.4-3) and (4.4-4) to take into account the effect of a stochastic pulse s at time τ onto the osculating elements at epoch t_i by the linear transformation equations

$$\Delta \mathbf{E}_s(t_i) = \mathbf{M}_s^{-1}(t_i, \tau) \cdot \boldsymbol{\kappa}_s(\tau) \cdot s. \quad (4.4-6)$$

This result opens also the possibility to set up additional stochastic parameters (up to three pulses in three linearly independent directions) at the arc boundary t_i . The osculating elements at time t_i - which are figuring in the NEQ system of day i - may be written as a linear function of these introduced stochastical parameters according to (4.4-6). But even if we do not do that the osculating elements of day i are in any case functions of the stochastic parameters pertaining to epoch t_i .

Let us assume that $\Delta \tilde{\boldsymbol{\beta}}_i$ contain all parameters of the NEQ system i plus all pseudo-stochastical parameters which were set up in the previous days plus all the additional ones at the day boundaries t_j ; $j = 2, \dots, i$. With (4.4-6) we get the parameter transformation equations of type (2.5-5) $\Delta \hat{\boldsymbol{\beta}}_i = \mathbf{B} \Delta \tilde{\boldsymbol{\beta}}$:

$$\Delta \hat{\boldsymbol{\beta}}_i := \Delta \tilde{\mathbf{E}}_i = \begin{bmatrix} \mathbf{I} & \mathbf{T}_1 & \dots & \mathbf{T}_{i-1} & \mathbf{T}_2^* & \dots & \mathbf{T}_i^* \end{bmatrix} \begin{bmatrix} \Delta \hat{\mathbf{E}}_i \\ \hat{\mathbf{s}}_1 \\ \vdots \\ \hat{\mathbf{s}}_{i-1} \\ \hat{\mathbf{s}}_2^* \\ \vdots \\ \hat{\mathbf{s}}_i^* \end{bmatrix} \quad (4.4-7)$$

with

$\Delta \hat{\mathbf{E}}_i$ Keplerian parameters of NEQ system i :

$\hat{\mathbf{s}}_j$ pseudo-stochastical parameters of NEQ system j : $s_{j1}, s_{j2}, \dots, s_{jm_2}$; $j = 1, 2, \dots, i - 1$

$\hat{\mathbf{s}}_j^*$ additional pseudo-stochastical parameters at the day boundary to the previous arc: $s_{j1}^*, s_{j2}^*, \dots, s_{jm_2}^*$; $j = 2, \dots, i$

\mathbf{T}_j transition matrix of pseudo-stochastic parameters set up in the previous arcs $j = 1, 2, \dots, i - 1$ according to (4.4-6)

\mathbf{T}_j^* transition matrix of additional pseudo-stochastic parameters set up at the arc boundaries $j = 2, 3, \dots, i$ according to (4.4-6)

Applying transformations (2.5-8)-(2.5-10) and (2.5-11) we get an *expanded* NEQ system i which can be superposed in the conventional way to the accumulated NEQ system.

It should be mentioned that the expanded NEQ system will be singular because the additional rows and columns are according to (4.4-6) linear functions of the rows and columns of the osculating parameters in the original NEQ system. This singularity disappears after the combination into the n -days-arc.

We have thus demonstrated that it is possible to take into account the changes of the orbital elements at the osculating epoch induced by stochastic pulses set up prior to that epoch and that it is possible to set up additional pseudo-stochastic parameters at the day boundaries for any satellite. For an estimation of stochastic pulses more frequently than once per day it is necessary to set up these parameters already in the 1-day-solutions.

4.5 Combination of Osculating Elements, Dynamical Parameters and Stochastic Parameters

We developed in the previous subsections the orbit combination step separately for osculating elements and dynamical parameters on the one hand and for pseudo-stochastic parameters on the other hand. For the osculating elements and the dynamical parameters the recursive transformation equations (4.3-15) (common dynamical parameters) and (4.3-19) (separate dynamical parameters) were derived, for the stochastic parameters the transformation equations (4.4-7) have to be applied.

The realization of the orbit combination covering all the kinds of orbital parameters is merely the addition of the transformation equations.

In practice we proceed sequentially. After the parameter transformation for the stochastic parameters leading to an expanded NEQ system the necessary transformations are applied for the osculating elements and the dynamical parameters in the daily normal equations.

4.6 Implementation Aspects

The described feature of computing n -days-arcs from n 1-day-arcs is implemented in the program ADDNEQ of the Bernese Software V3.6.

The primary motivation was the reduction of the processing time of the CODE processing center of the IGS without loss of accuracy. This was necessary because with the steadily increasing data volume (Table 1.2 illustrates this statement) the

turn around time for the daily solutions (and the final overlapping 3-days-solutions) increased considerably leaving not enough time in the case of problems. Section 5.5 shows the effort of a new processing scheme based on daily solutions in comparison with the conventional processing using the original observations for the overlapping 3-days-solutions.

Additional motivation came from the fact that the estimation of UT1-UTC and probably also subdiurnal variations in the earth's rotation rate are more stable for longer arcs. See Section 8.4 for more details.

For all the long-arc applications it is important that we are independent of a "limit" of the arc length. This is true for the demonstrated method even if we consider only arc lengths of up to ten days. The only input we need is the daily NEQ systems and the corresponding apriori arc information whereas the conventional method always needs an apriori arc of the lengths of n days.

It is also true that the CPU requirements would never allow processing of arcs longer than three to four days using the conventional method based on the original observations. Table 5.3 shows that the storage requirements of the original observations are not negligible either.

The availability of a flexible and comfortable tool in case of satellite problems is a necessary but also very helpful consequence of the long-arc evaluations. Satellites which behave not properly are showing larger residuals with respect to the observations (increasing estimated rms of the phase observations). Other test criteria like fitting a 7-days-arc through the resulting daily orbits according to BEUTLER ET AL. [1994] and differences between consecutive daily orbits are also very helpful to detect such problems.

The following options are available to the user:

- arbitrary arc-lengths are possible. For longer arcs (≥ 2 days) additional stochastic parameters are necessary to absorb unmodeled perturbation forces (see Section 3.1.4).
- New arcs (new osculating elements and new dynamical parameters) may be set up at any day boundary for any satellite.
- New stochastic parameters in the R -, S -, W - directions may be set up at the day boundaries for any satellite with any apriori weight.
- If a satellite is missing in a file we can bridge the gap (same orbital elements before and after the gap) or we can set up new orbital elements after the gap.
- One manoeuver per satellite and per n -days-arc allow a setting up of a new arc within a particular day without losing data. For security it may be useful to

delete one hour of data centered around the manoeuvre. This and the setting up of a new arc within the day has to be handled by the main parameter estimation.

- It is possible to ask for one and the same set of dynamical parameters for the entire n -days-arc (see Section 4.3.1) or to set up day-specific dynamical parameters (see Sections 4.3.2)

The main gain of these options is the fact that a re-processing of the daily solutions can be avoided in most cases.

4.7 Partial Derivatives: Computation and Accuracy

An important characteristic of the least-squares adjustment is the fact that the partial derivatives with respect to the unknowns parameters can be computed with a moderate accuracy if we iterate the least-squares adjustment process.

To avoid these iterations we have to compute the partial derivatives with an accuracy which will not affect the resulting parameter estimation. This is usually the case if the products (*partial derivative*) · (*parameter increment*) are well below the formal errors of the particular parameters.

The product indicates already the dependence on the partial derivative but also on the quality of the apriori information of the parameter.

Let us assume that the Keplerian orbit deviates with respect to the true orbit by 10 *km* after a day and 100 *km* after 3 days (see Table 3.1). This seems to be a bad approximation but in view of the absolute distance to the satellite of 20000 *km* the relative error is only 0.5 %. The same error can be expected for the partial derivatives using Keplerian approximation. This means that with each iteration the parameter increments are reduced by a factor of 2000.

The orbit combination based on 1-day-solutions shows an accuracy of the order of 20 *cm* (see Figure 4.1) with respect to a 3-days-solution. The last iteration of the conventional solution is not contaminated by this error source because the maximum parameter increments are of the order of 2–3 *cm*. The effect of a relative error of 0.5 % in the partial derivatives and a parameter increment of 20 *cm* is well below the 1 *mm* for the resulting orbit. The error propagation of an error in the semi-major axis of $\Delta a = 1$ *mm* causes because of Kepler's third law $n^2 a^3 = GM$ an along track error of $-3\pi N \Delta a = 2.5$ *cm* · N after N revolutions. This quality becomes important for longer arcs.

To be on the safe side we compute the partial derivatives in (4.3-5) with analytical formulae more accurately using the perturbation theory [BEUTLER ET AL. 1996]. Actually only the effect of the earth's oblateness (C_{20} term) is taken into account

which improves the accuracy with respect to the Keplerian approximation by a factor of 10.

The partials with respect to the dynamical parameters are computed using numerical integration in a simplified force field according to Section 3.2. That is satisfactory from the point of view of the quality of the results but not from the storage point of view (0.5 Mbyte per day and 1-day-arc).

After several promising attempts to compute the partials analytically, we ended up by actually computing *all* partials through *numerical integration*. The disk storage requirements were minimized by a very efficient way to store the partials (to be published).

4.8 Equivalence of the Orbit Combination with the Conventional Orbit Determination

Figure 4.1 demonstrates the equivalence of the conventional method (improvement of a 3-days-arc with original observations) and the new developed method based on the combination of daily NEQ systems. For a month (since day 226 of year 1994) the orbits of the two methods were compared using a seven parameter Helmert transformations between the two orbit systems. The rms values of transformation are of the order of 1 *cm* in the cases in which no stochastic parameters are set up (no eclipsing satellites in the time period of the days 248 - 260). Before and after these days we have rms values of up to 8 *cm*. The reason for this is a different selection of stochastic parameters for the eclipsing satellites for the 1-day- and the 3-days-solutions. If a particular satel-

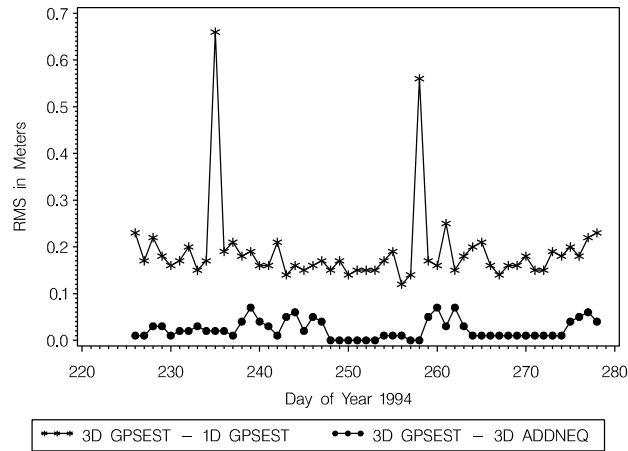


Figure 4.1: Rms error of a seven parameter Helmert transformation between the orbit systems generated using the conventional method (GPSEST) and the new method based on the combination of daily solutions (ADDNEQ). The rms of transformation between the 1-day- and the 3-days-orbits is also included.

lite was eclipsed for the first time on day 3 of the 3-days-arc, stochastical parameters were set up all 12 hours for all the days (totally 6 stochastic time epochs) in the conventional, but only within the last day and for the arc boundaries (totally 3 stochastic time epochs) with the new procedure.

In all other cases (identical stochastical parameters) we find an agreement of 1-2 *cm*. Actually we assume that the quality of the 3-days-orbits is (in the years 1994 and 1995) of the order of 10 *cm* [KOUBA 1995B] which is about five times larger than the effect coming from the new processing method.

A similar picture results from the comparison of the earth rotation parameters. The derivations are below 0.03 *mas* for the x- and the y-component and 0.002 *msec/day* for UT1-UTC which is a comfortable factor 10 below the current accuracy level given by the annual comparisons of the different space techniques by the IERS annual reports [IERS 1994].

The method was used operationally since January 1995 without causing any problems.

With the mentioned computation of the partials using analytically methods (see previous section) the equivalence of orbit combination and conventional orbit determination is of the order of 1-3 *mm* for the orbits - a necessary improvement in view of the increased orbit quality in 1996.

5. Processing Strategies using Normal Equations

Sequential LSE has a big variety of applications in the processing of GPS observations, ranging from near-real time applications to multi-annual solutions.

The modularity in the handling of normal equations allows furthermore a combination between the different applications. Let us discuss some of these applications.

5.1 Multi-Session Solutions

Multi-session solutions is the application for which the program `ADDNEQ` was originally designed. The increasing number of permanent GPS tracking networks all over the world (mostly regional networks for the monitoring of crustal deformations or federal networks as local GPS reference frames, but also the global IGS network) asked for tools to condense the numerous observations to a final site coordinate and velocity set.

Usually such networks are processed day-by-day independently. The stacking program `ADDNEQ` combines the daily solutions on the basis of normal equations (NEQs). For global networks geophysical parameters (center of mass and gravitational parameters) are of great interest. To find a reliable estimation for these parameters it is important to summarize the information of all the individual solutions for the final estimation.

Figure 5.1 shows statistical information for a 2-years-solution performed at the CODE Analysis Center using data from the permanent IGS network.

The combination is statistically correct. All correlations between the original observations have to be applied in the daily solutions. We focus on these aspects in the next section. Assuming that there are no correlations between the observations of different days - which is probably correct - leads us to a final least-squares adjustment which is, according to the results of Section 2.3, identical with a (theoretical) processing of all observations in one step.

It is also worth to mention that in the individual daily solutions all parameters can be stored, even those which are only of interest for the individual solutions. Troposphere parameters may be kept in the normal equation systems to be able to change the number of relevant parameters according to Section 2.5.2 or to change the absolute and relative constraints without going back to the original observations. In the IGS network we store also earth rotation parameters including nutation parameters. Opening or constraining the nutation parameters, modifying the effective number of parameters according to Section 2.6.3 are useful applications.

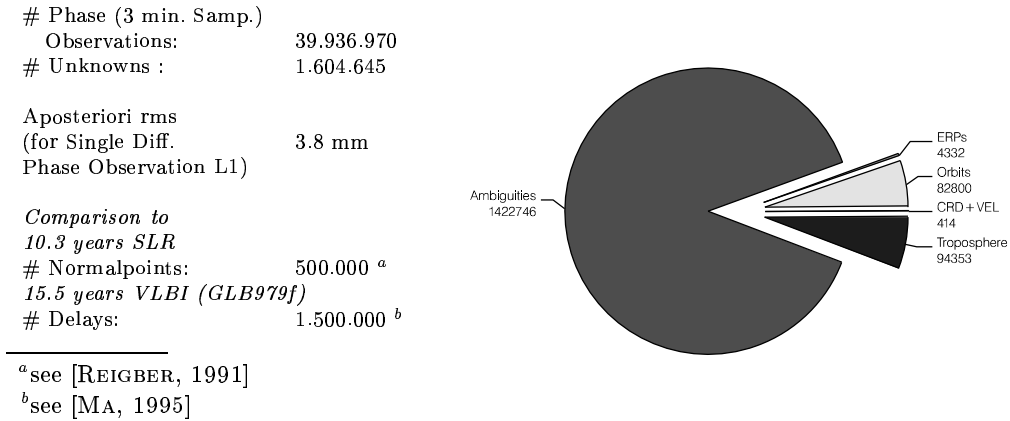


Figure 5.1: Solution statistics of a combined 2-years-solution.

For the accumulation of NEQs the nuisance parameters may be pre-eliminated according to the scheme developed in Section 2.2 to keep the dimension of the final normal equation system as small as possible. That is of particular importance for the ambiguity parameters. Because of their big number (Figure 5.1) we pre-eliminate them usually before the storing of the normal equations.

For many applications the parameters common to all solutions are the coordinates only. In this case the combination is performed using considerably reduced individual NEQs. New parameters such as station velocities may be set up now (Section 2.5.2).

The pre-eliminated parameters (orbits, earth rotation parameters, troposphere, etc.) may also be determined in a second step by introducing the parameter values of the combined solution into each sequential solution as known.

Figure 5.2 gives a schematic description of the handling of the individual normal equations.

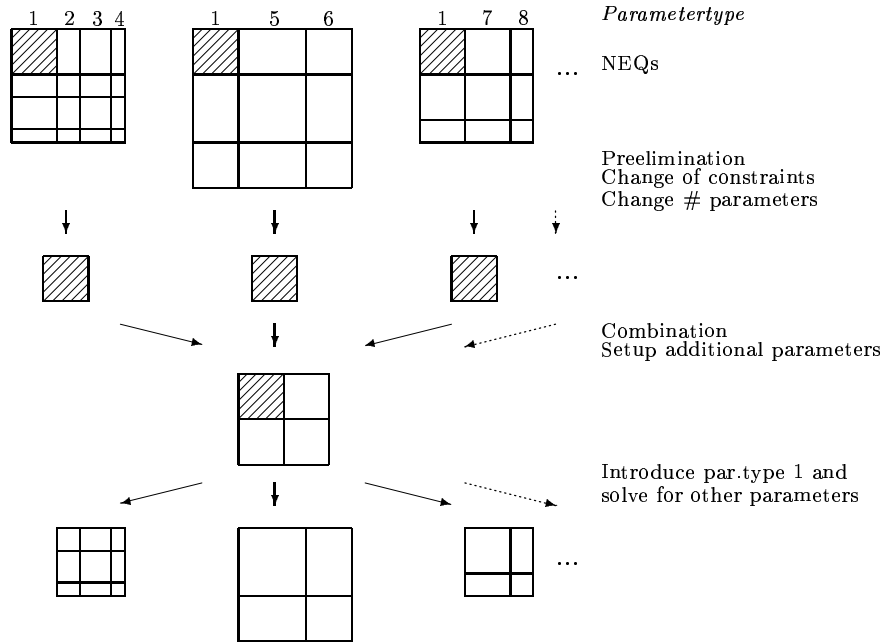


Figure 5.2: Processing scheme for multi-session solutions.

Additional remarks are required concerning the use of the covariance information of the parameters which are common to all solutions (e.g. coordinates).

Figure 5.3 shows the impact on the resulting parameter estimation for the coordinates of KOSG when adding more and more sessions (days) to a multi-session solution. Each data point represents the solution obtained from combining all sessions up to that day. The offset to zero expresses the difference between the mean and the combination solution.

The result is not astonishing and in agreement with the *theorem by Tschebyscheff* [BRONSTEIN AND SEMENDJAJEW 1985]: The results are more and more independent of the used covariance information. After 100 days or 3 months we cannot expect any important contributions to the final parameter values by additional sequential solutions. The offset to the zero line is no longer visible which proves the statement that for long time intervals the combination converges to the pure mean value.

The use of the full information in the normal equations is of course important for the backward substitution in the last step in Figure 5.2. The parameters which refer to one individual solution only cannot profit from the smoothing effect due to the big number of parameter estimates. They are in essence determined only by the information in the associated normal equations.

For the estimation of site velocities a longer time interval is of much more relevance for the reliability of the estimation. See Chapter 6 for more details.

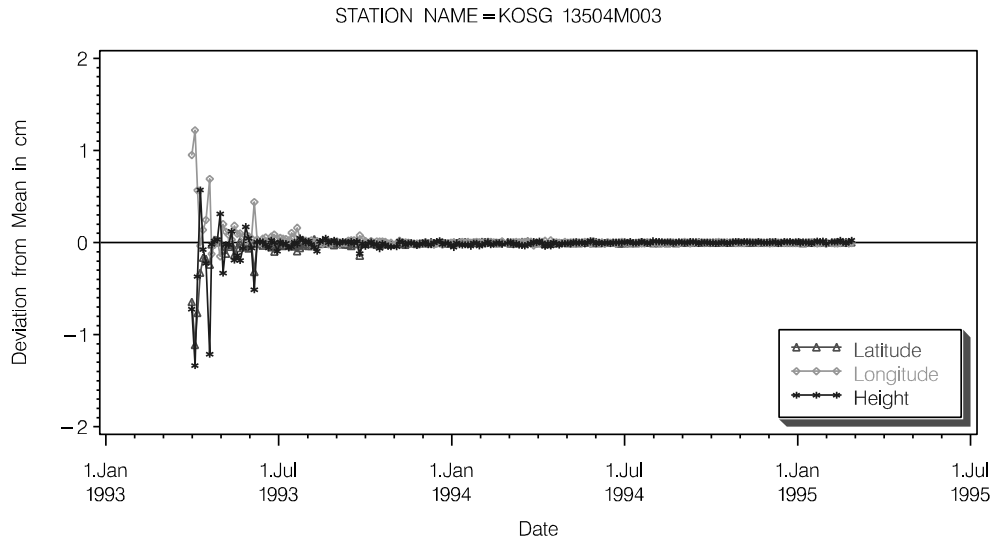


Figure 5.3: Impact of additional observations on the coordinate estimates for KOSG. Reference is a 23 months free GPS solution including velocity estimation. The offset to zero, actually negligible, represents the difference between the combined solution and the pure mean.

5.2 Processing in the Baseline Mode

5.2.1 Differences to a Network Solution

A network solution is usually computed using the correct correlations between the observations of the different stations. Even on the double difference level the correlations may be taken into account in a correct way [BEUTLER ET AL. 1986; BEUTLER ET AL. 1987].

In the *baseline processing mode* each baseline is processed independently. The correlations between the observations of different baselines are neglected.

For big networks (24 hour data, > 30 stations) the correct computation procedure is rather time consuming (for an ambiguity-free solution about 2-3 times longer than the less correct baseline processing).

For a baseline processing mode the situation is better, because after the processing of each baseline the non-common parameters (such as ambiguities) may be pre-eliminated. That keeps the NEQ system small. In addition, the processing time

increases only *linearly* with the number of baselines in the baseline mode. More details about the baseline processing mode are given in Section 5.2.2.

The impact of the correct handling of correlations was analyzed using a test campaign of 25-30 European permanent GPS sites (see Figure 5.4). These sites are processed with a time delay of about 10 days to the time of the observations. For about two months (September and October 1995) we produced solutions based on a baseline mode (also called solution *A*) as well as solutions with a correct handling of the correlations (solution *B*).

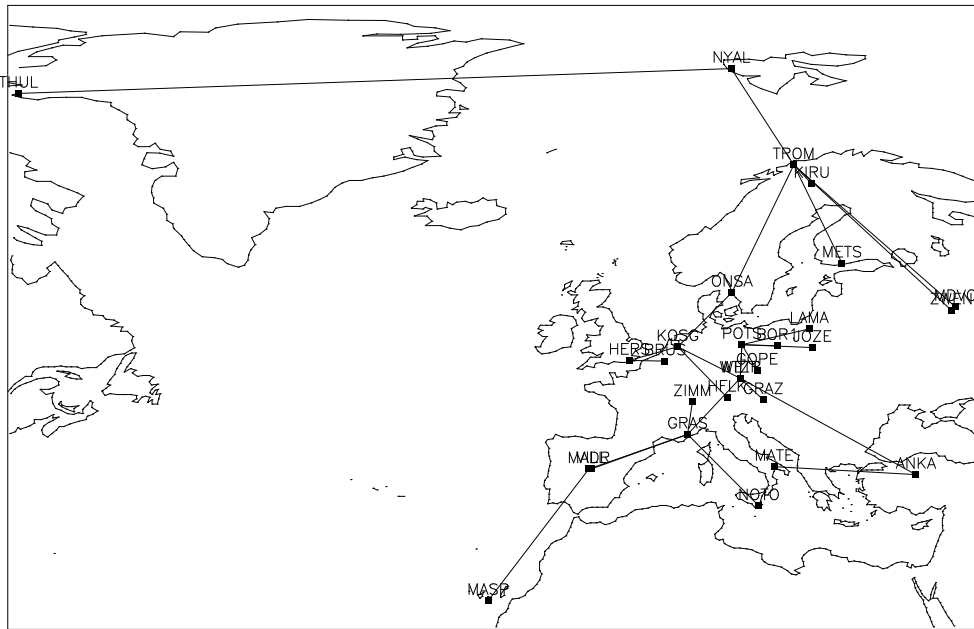
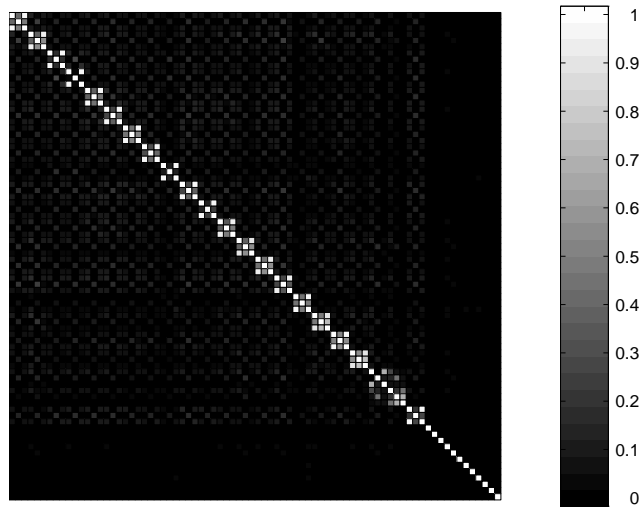
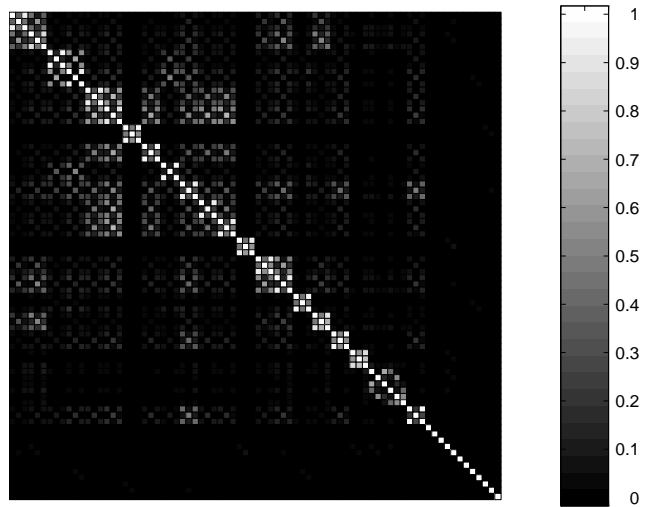


Figure 5.4: Baseline selection of DOY 300 for the separately processed European Test Campaign: All days are processed in a baseline mode as well as in a network mode with a correct handling of the correlations.

The other processing options, identical for both solution types, are: 12 troposphere parameters estimated (without apriori weights), no ambiguity fixing, 180 sec sampling, 20 degree elevation cutoff, CODE orbits and CODE Earth rotation parameters used, baseline selection maximizing the number of single difference observations.



(a) Network solution: Correct modeling of the correlations



(b) Baseline Processing: Correlations modeled only within the baseline

Figure 5.5: Absolute values of the a posteriori derived correlation matrix of a daily solution containing 26 European sites. The correlations are given in the x-y-z geocentric coordinate system.

5.2.1.1 Correlation Matrix A posteriori

A graphical presentation of the correlation matrix of a daily solution containing 26 sites (or 78 coordinate estimates) is given in Figure 5.5. Zero correlation elements are black, a correlation ± 1 corresponds to the white color.

With a full observation scenario without gaps and with about the same satellites for all sites we expect that all sites are determined with about the same accuracy (the sites on the periphery of the network may be slightly degraded) and that the covariance information between the components of different sites is approximately identical for all station pairs. This implies for the resulting correlation matrix, that the correlation values between the components of each site contain about the same information and that the correlation values between the sites are small and similar for all station pairs.

Both statements are true only for solution *B*, the correlation matrix of the baseline processed solution *A* is strongly influenced by the baseline selection. We find higher correlation values between sites which are connected by a baseline.

We should mention that

- the pattern of the last four sites (no correlations of the off-side diagonal elements at all) is a consequence of the constraining of these sites for the definition of the geodetic datum and that
- the repeated 3×3 pattern with non-zero off-diagonal elements (in particular the x-z correlation) are demonstrating that the axes of the error ellipses are not identical with the x-y-z coordinate axes. The GPS determined error ellipses are quite well aligned with the local geodetic system (see 6.5). In that coordinate system the off-diagonal elements, corresponding to latitude, longitude and height, are negligible.

From this point of view the correlation matrix of the network solution seems to be much better suited to represent the precision information of the daily solution.

Selecting identical baselines for all days may cause systematic effects in the resulting correlation matrix. In our case the baselines are selected using the criterion of a maximum number of observations, which generally leads to different baselines for different days. Two neighbor sites are observing the same satellites at about the same elevation angle. The probability that these two sites are connected to a baseline using this criterion is much higher than for sites with a larger distance. For a network of a size of about $5000 \text{ km} \times 5000 \text{ km}$ we never will obtain a random distribution of the baselines in time.

Table 5.1: Rms values of the between-site correlations as an indicator of a correct stochastic model for the GPS phase observations: For different time spans a combined solution was produced for the European subnetwork and the resulting correlation matrix analysed.

		Rms values of between-site correlations in [-]					
		Inter-baseline correlations applied:					
		NO			YES		
Interval	Correl. type	x-x	x-y	x-z	x-x	x-y	x-z
1 week	x-x	0.13	0.01	0.10	0.02	0.00	0.02
	y-x		0.23	0.01		0.04	0.00
	z-x			0.12			0.02
2 weeks	x-x	0.12	0.01	0.09	0.02	0.00	0.02
	y-x		0.21	0.01		0.04	0.00
	z-x			0.11			0.02
1 month	x-x	0.10	0.01	0.08	0.03	0.00	0.02
	y-x		0.16	0.01		0.04	0.00
	z-x			0.09			0.02
2 months	x-x	0.09	0.01	0.07	0.03	0.00	0.02
	y-x		0.11	0.01		0.05	0.00
	z-x			0.08			0.02

We definitely find an improvement if we analyze the correlation matrix of combined solutions covering a longer time interval. If we have a look at the correlation values between two coordinate parameters (e.g. x-y) of all possible combinations of different sites (with the exception of the fixed sites), we may derive a mean correlation value as well as an rms value representing the variations. Table 5.1 presents the rms values for each inter-coordinate value (x-x,x-y,x-z,y-y,y-z,z-z) for different combination intervals (1 week up to 2 months). Assuming that e.g. all x-y correlation values between different sites are identical we would obtain an rms of zero. In other words: The smaller the rms value the regular the pattern in the graphical representation of the correlation matrix (Figure 5.5). For the solution type *B* the pattern remains the same independent of the interval of combination. A reduction of the rms can be acknowledged for solution *A*. A regular pattern as in the case of solution *B* was not reached, not even after 2 months of combination.

5.2.1.2 Coordinate Estimates

The quality of the coordinate estimates is also an important indicator of the influence of the inter-baseline correlations.

The repeatability values in Figure 5.6 were achieved by performing a 2-months free solution of each solution series and comparing each daily free solution with the combined solution using a Helmert transformation. The quality of the network solution (solution *B*) is considerably better for the height components. The mean rms value of Figure 5.6 using all sites is 7.6 mm for solution *B* and to 9.9 mm for the baseline mode (solution *A*).

We skipped a presentation for the other components because of an almost identical quality for both solution types (mean rms, North: 2.5 mm versus 2.5 mm, East: 3.8 mm versus 4.3 mm).

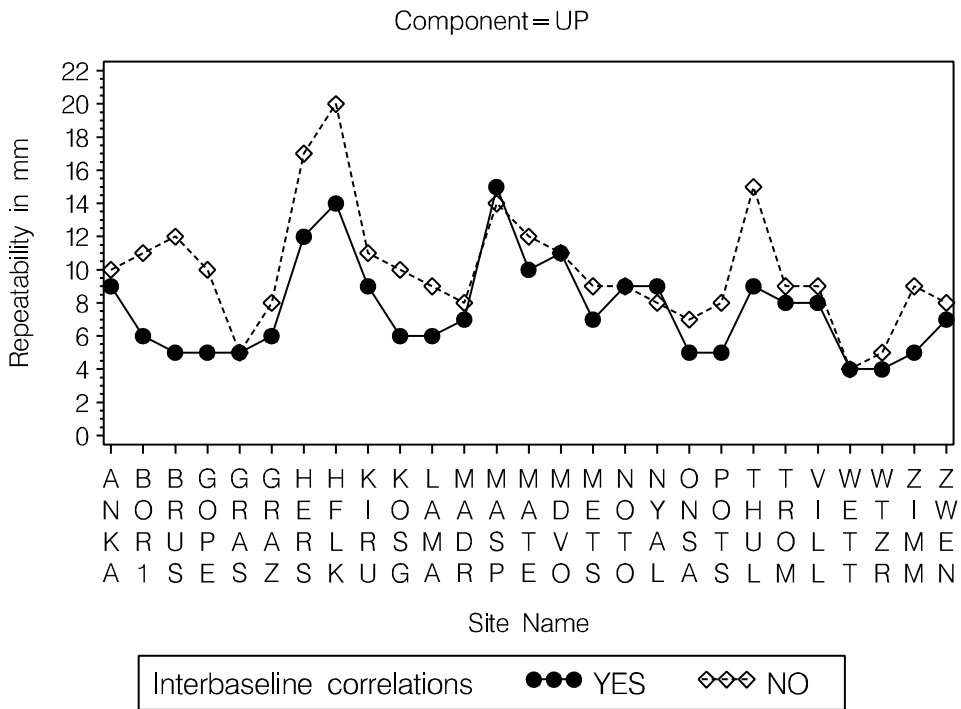


Figure 5.6: Repeatability for the vertical components of the European sites: network solution versus baseline processing.

The combined coordinate estimates are not very much affected by the processing mode: Table 5.2 shows the rms of a Helmert transformation for the three components (in a the local coordinate system) for different combination intervals. The

differences in the horizontal components are of the order of 1 *mm*, the height differences are larger especially if the border sites MASP, THUL and KIRU (noisy data) are also included in the comparison. Height residuals for these sites of up to 2 *cm* are responsible for the increased rms values.

Table 5.2: Rms values of Helmert transformation between two combined solutions with and without processing the daily solutions using correct inter-baseline correlations.

interval	rms of Helmert transformation in [mm]					
	All sites used			THUL, MASP, KIRU excl.		
	North	East	Up	North	East	Up
1 week	1.3	1.4	5.3	0.9	1.3	3.0
2 weeks	1.2	1.5	5.6	0.8	1.0	3.0
1 month	0.9	1.1	5.8	0.7	0.8	2.9
2 months	0.8	1.1	4.9	0.6	0.8	2.2

5.2.1.3 Summary

The inter-baseline correlations have an influence especially on the resulting covariance matrix. The estimates for the vertical components are more consistent in the case of the network solution. Nevertheless we found only a very small influence on the coordinate estimates. If errors of this magnitude may be neglected we are able to split up the network into smaller parts (baselines or subnetworks).

5.2.2 Baseline Processing Concept

Figure 5.7 demonstrates the combination procedure based on baselines.

Only one baseline file at the time is used as input for the parameter estimation program **GPSEST**. All parameters of interest have to be set up in this step even if the parameters cannot significantly be estimated using the observations of one baseline only (center of mass, orbits, earth rotation parameters, etc.). Apriori weights have to be set up according to Section 2.6.1 for those parameters which may cause singularity problems. It also may occur that the number of unknowns is greater than the actual number of observations.

Today we set up as unknown parameters coordinates, 12 troposphere parameters per day and station, ERPs with a 2-hour time resolution including nutation drifts, orbit parameters for each satellite (6 Keplerian elements and 9 parameters of the new radiation pressure model according to Section 3.1.2.4), three stochastic pulses at noon UT for each satellite, center of mass parameters, and satellite antenna offsets.

The final network solution is produced by the program `ADDNEQ` using as input the NEQs of the individual baselines. The constraints are removed for the accumulation, new constraints can be specified for the final solution (see Figure A.1).

The residuals for each baseline are saved on a file. In case of outliers only the affected baselines have to be re-processed which saves considerable CPU time.

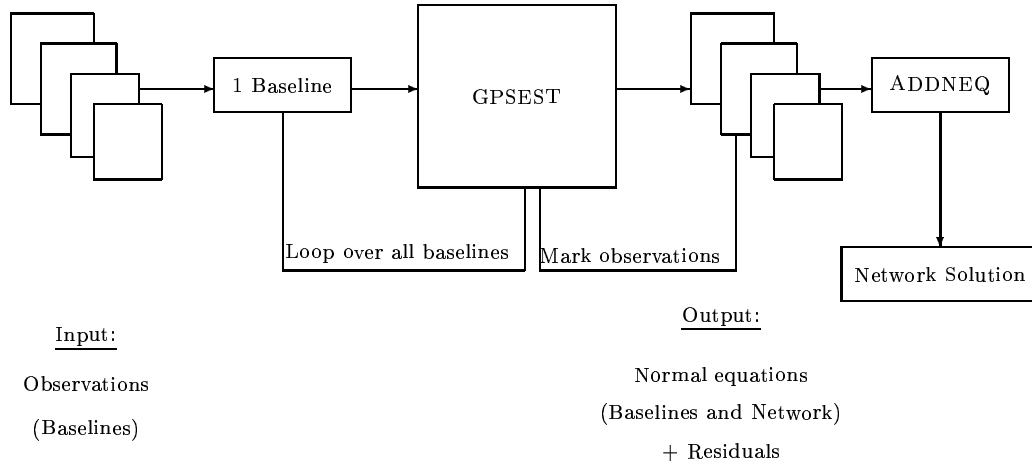


Figure 5.7: Processing scheme based on Baseline processing.

If the correlations are neglected this method allows an efficient processing of big networks: The computing time grows only *linearly* with the number of stations in this case.

The individual baselines can also be computed in parallel on different CPU's. The processing time thus decreases with the number of processors available.

This procedure is used at the CODE processing center to compute the daily solutions of the first iteration step.

5.3 Network Solutions based on Subnetwork Results

5.3.1 Processing Scheme

Dividing a big network into subnetworks (clusters) and modeling correlations in a correct way within the subnetworks, then combining these results into a network solution may be a valuable compromise between processing considerations and statistical exactness of the method.

The division into subnetworks is, similarly to the baseline processing, suited to reduce the processing time, especially if multiple CPU's are available. The processing procedure is as shown in Figure 5.7 if we replace a single baseline by a subnetwork solution consisting of a cluster.

5.3.2 Impact of Subnetworks on Network Solutions

Since June 1995 the final daily network solutions at the CODE processing center consists of five clusters (see Figure 5.8) where within each cluster the correlations are modeled correctly. The clusters are: An European cluster, a North American cluster, a South American cluster, an Asian cluster, and an Australian cluster. A sixth cluster is used for additional (extremely long) baselines which are processed without a correct handling of the correlations. The idea is to gain additional observations, which are not yet used in the observation clusters.

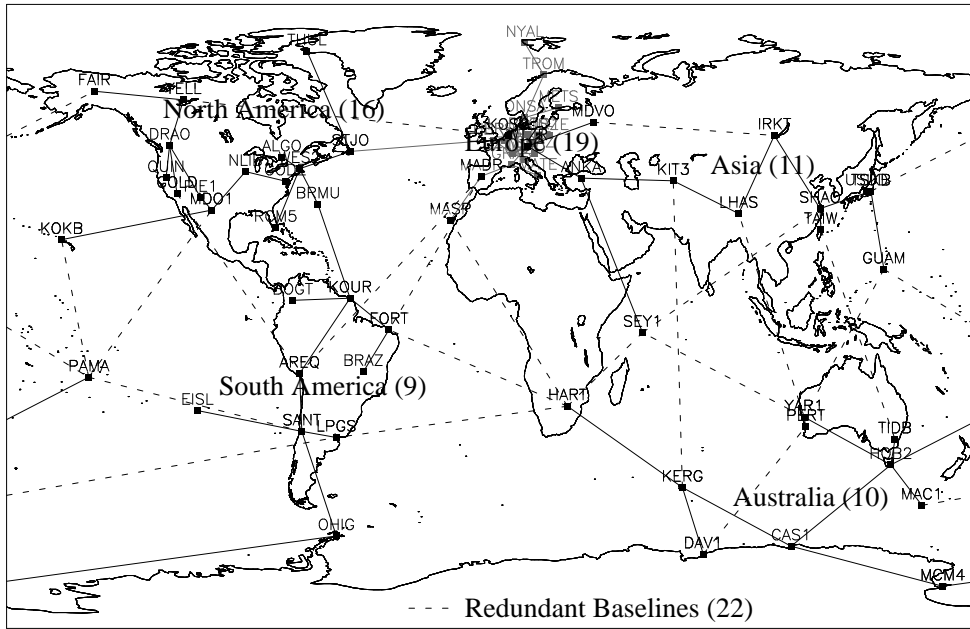


Figure 5.8: Subdivision of the global IGS network in subnetworks. Each cluster, with the exception of the redundant baselines, is processed with a correct handling of the inter-baseline correlations.

Directly as a by-product of such a processing scheme we are able to analyze the

impact of each cluster on the combined solution. Figure 5.9 shows the quality of the orbits, obtained from different single clusters or different sets of clusters. We compare each 3-days-orbit with a 3-days-orbit, which is produced using the normal equation systems of all subnetworks. The following examples are analyzed: Using Europe only, North America only, all clusters without the redundant baselines, and finally Europe plus North America only. The presented rms values are derived from the 7-parameter Helmert transformation of two orbit systems including all satellites. For the single-cluster solutions we also give the rms values for an orbit comparison over the particular region, only.

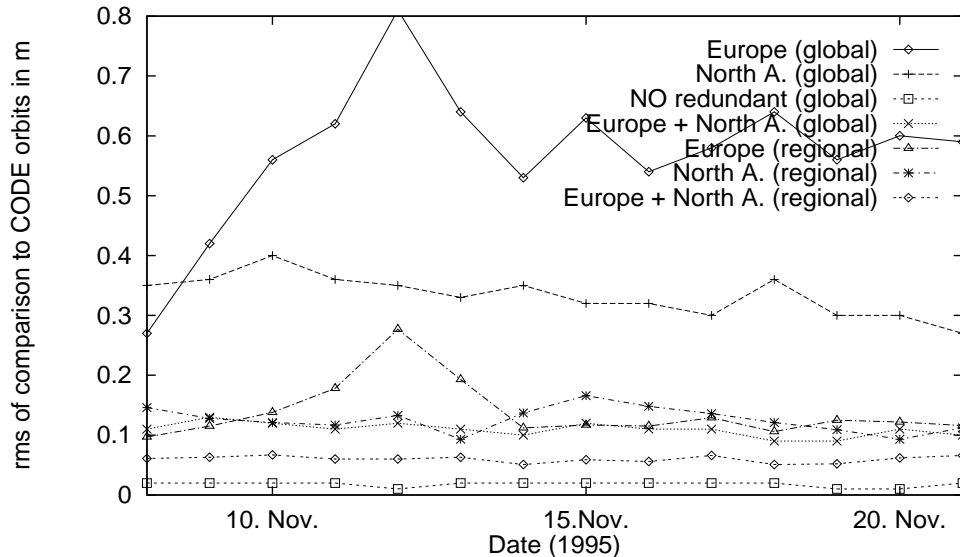


Figure 5.9: Orbit quality derived from subnetworks. Reference is a 3-days-orbit (official CODE solution) obtained from the observations of all clusters.

We may conclude:

- The global orbits derived from the observations of one cluster only show rms values of about 40 *cm* (North America) and 60 *cm* (Europe). For the reference orbit (official CODE solution) we may assume a quality of about 10 *cm* from the weekly IGS orbit comparisons [KOUBA 1995B].
The biases determined by the Helmert parameters are of the order of up to 5-7 *cm* for the translations, and up to 2 *mas* for the rotations. Nevertheless, the orbits are well suited for regional purposes (agreement below 20 *cm*). BROCKMANN ET AL. [1993] showed the high quality of regionally determined orbits using coordinate repeatabilities.
- Both clusters together (Europe and North America) are providing orbits with

the excellent agreement of better than 15 *cm* compared to the globally determined orbits. The biases are negligible (maximum of 4 *mm* translation and 0.2 *mas* rotation). This result indicates that the orbits derived from all sub-networks are dominated by the observations of these two subnetworks.

- The impact of the redundant baselines (1-2 *cm* rms values) is negligible. On the one hand the redundant baselines are contributing only with a small number of observations to the daily solutions (about 10-15 %) due to the extremely long baselines. Nevertheless these additional baselines may stabilize the solution in case of weak connections between the different clusters.

We should mention that we get qualitatively the same results for other "global" parameters. The Earth rotation parameters, determined by the European sites only, are showing e.g. an agreement of 2-3 *mas* compared to the C04 pole, the European plus the North American cluster gives an agreement with C04 clearly below the 1 *mas* level.

5.4 Processing in Sequences of Sub-Diurnal Intervals

For near-real time applications it may be useful or required to process the GPS data at a higher frequency than the generally used once-per-day rate. Typical applications are detection of *crustal deformations* or determination of the *atmospheric behavior* using GPS.

For the sequential processing procedure intervals of up to 0.5-1 hours are conceivable. The expression "near-real time" has to be understood in this sense. Higher than once per 30 minutes rates are at present unrealistic in view of the communication links and the management of the data for permanent networks.

The *stacking methods* presented here are *not* the optimal tool for real kinematic applications. The *filter algorithms* of Section 2.4.2 are better suited for such applications.

Here we have applications in mind, where results have to be available *few hours* rather than *few days* after the observations.

Principles of the processing are the same as in the previous section. For each interval and each baseline we have to actually process the GPS observations. Afterwards the stored NEQs of the same interval are stacked to a network solution valid for this specific interval. Daily solutions may then be created by stacking all intervals of e.g. the previous 24 hours.

The actual implementation of such a processing scheme is strongly dependent on the particular goal (coordinates or troposphere) and the network size. Some general considerations are:

- Orbit estimation requires in any case a longer time interval. We do not consider it here. In future there might be applications where high accuracy orbits (or even predictions) with a very short delay are required.
- The processing scheme has to be independent of the availability of precise orbits of "IGS-quality". That is in particular important for ambiguity resolution.
- The resulting network solution based on e.g. a 2-hour interval is much weaker than a network solution stemming from a 24 hour interval because at the beginning of each interval new ambiguities have to be set up for all satellites. This is an important disadvantage of this processing mode.
- The combination of troposphere parameters is handled by `ADDNEQ`. It is possible to connect different troposphere intervals by specifying relative constraints and to combine troposphere parameters of several intervals to one common parameter (see Section 2.6.3 and 2.5.2).

Such processing schemes are e.g. used at *UNAVCO* [ROCKEN ET AL. 1994] for the purpose of near-real time troposphere estimation.

5.5 Long-Arc Computation

The motivation for computing arcs longer than one day was already mentioned in Section 4.6. The `UT1-UTC` estimates, but also the intrinsic orbit quality are much better for 3-days-arcs than for 1-day-arcs. The theoretical background and the very flexible processing options for dealing with satellite problems were already discussed in Section 4.6.

With these methods we are free to combine the 1-day normal equations and the associated 1-day-orbits to longer arcs. The actual limitations are given by the quality of the orbit model (see Section 3.1.4) and the linearization errors.

The computation of longer arcs based on 1-day-arcs is an elegant way to be independent of the original GPS observations and the length of the a priori orbit. Figure 5.10 shows the processing scheme for the overlapping 3-days-solutions as implemented at `CODE` for orbit and earth rotation estimation.

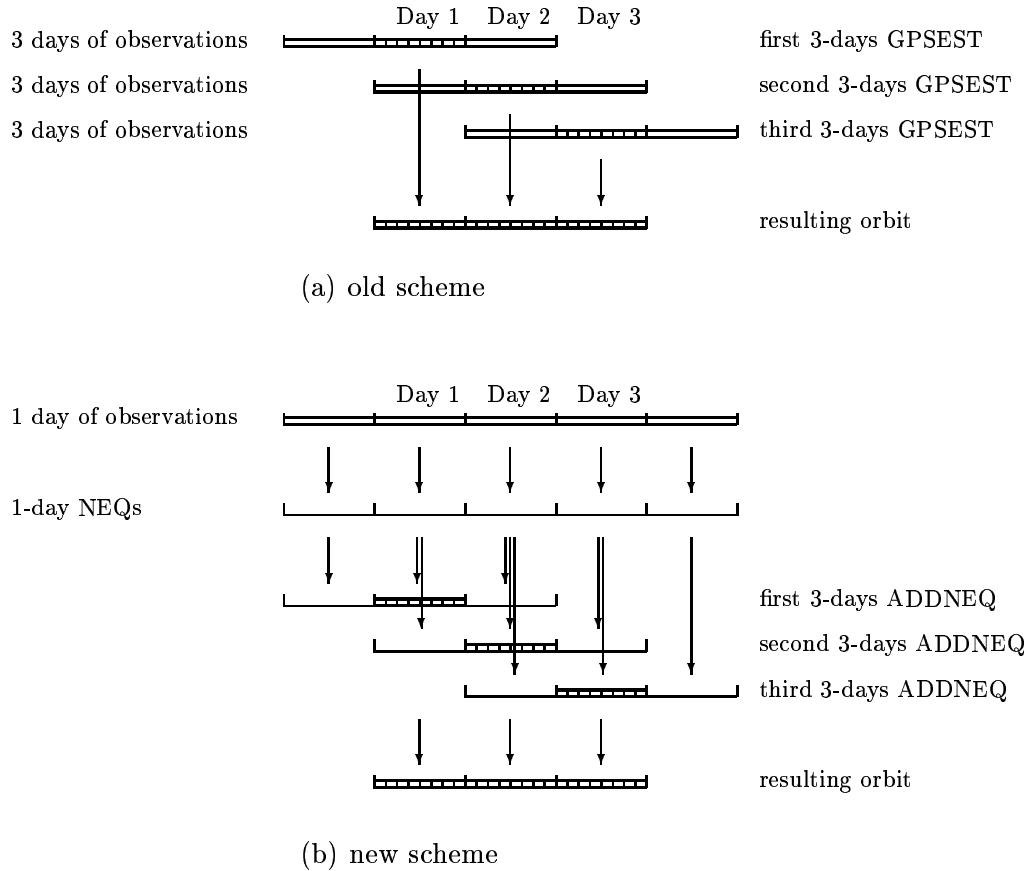


Figure 5.10: Computation of overlapping 3-days-solutions at the CODE Analysis Center of the IGS according to (a) the actual reprocessing of three days of GPS observations and according to (b) the new processing scheme based on the stacking of three daily normal equation files.

The old processing scheme was based on processing the original observations. In the case of the overlapping 3-days-processing, each day is actually processed 3 times whereas the new processing scheme needs the observations of one day only once to create the daily NEQs. Table 5.3 proves that the new method brings a gain of more than a factor of 10 of CPU-time.

We should underline that the long-arc methods are also very effective for the com-

putation of *rapid orbits*, which are of great importance in particular for near-real time applications (see previous section). The quality of daily orbits, which are computed 12 to 24 hours after the end of a day, strongly depends on the availability of sites. Data transfer problems may cause a drastically reduced network for specific days. Long-arcs of about 5-7 days are suited to minimize this effect. The radiation pressure model (3.1-5) and the stochastic orbit modeling (see Section 3.1.4) ensures a sufficiently accurate orbit model (below 10 *cm* for one week). An update of the normal equations of the older days using sites, which became later available, can improve the orbits of the latest day and with this also the prediction into the future. Orbits available in real-time for the actual day (predicted from the last processed long-arc combination) of high quality (below 0.5 - 1 *m*) are possible with such a procedure.

5.6 Modularity of Combination Strategies

Thanks to the modularity in the handling of the normal equations we may combine solutions which are already a result of a combination. This can be done without loss of information assuming that there are no correlations between the solutions which should be combined.

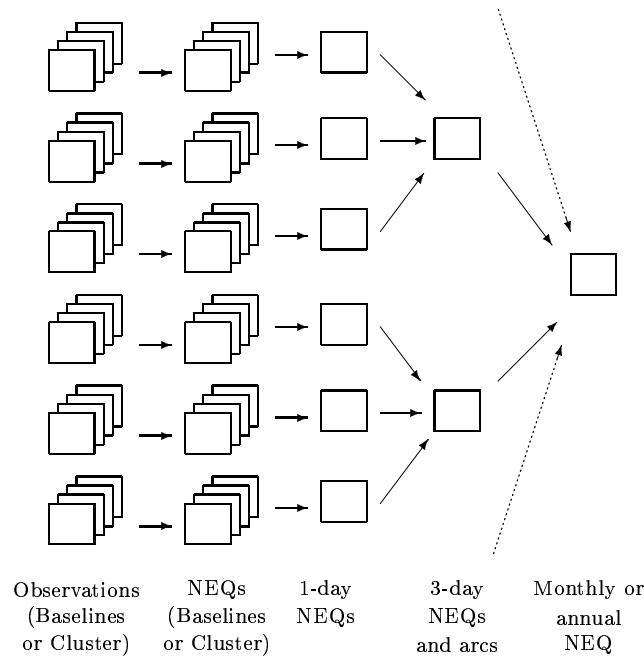


Figure 5.11: Combination of the normal equations of different processing steps.

Figure 5.11 shows the processing scheme implemented at the CODE processing center. Starting with the normal equations for each baseline (or each cluster of baselines), continuing with daily network solutions, and 3-days-arc computations for the daily earth rotation- and orbit estimation we are free to stack these results in an additional step to longer (monthly, annual) solutions.

Table 5.3 gives an overview of the processing times and the disk space required by the procedures based on normal equations in comparison to the processing based on the original observations.

Using normal equations instead of going back to the original observations saves not only much processing time. If we store only the minimum number of parameters (e.g. site coordinates and earth rotation parameters) in the files the necessary disk space is vanishingly small when compared to the single difference observation files.

Table 5.3: Required CPU times and disk space for different processing schemes.

	NEQ		Observations*	
	4 Trop.	12 Trop.	4 Trop.	12 Trop.
	CPU **			
Parameter estimation: Baselines or 6 Cluster	15 min.	30 min.	20 min.***	40 min.***
Network solution (1 day)	2 min.	6 min.		
3 days + Orbit combination	8 min.	16 min.	120 min.	-
3-days-solution (only CRD, ERP)	0.2 min.			
2-years-solution	60 min.			
	Diskspace			
Baselines (1 day, CRD, ERP, ORB, TRP) or 6 Cluster	7.5 Mbyte 2.5 Mbyte	25 Mbyte 8 Mbyte	25 Mbyte	
Network solution (1 day, CRD, ERP, ORB, TRP)	1.5 Mbyte	6 Mbyte		
3-days-solution (CRD, ERP, ORB)	1 Mbyte		75 Mbyte	
3-days-solution (CRD, ERP)	0.2 Mbyte			
2-years-solution (CRD, VEL)	0.6 Mbyte		18 GByte	

* compressed Rinex files (same size as Bernese binary zero diff. phase files); 50 sites; 24 h data

** DEC 3000 M 600 - Alpha processor

*** no correct correlations

CRD, VEL: coordinate and velocity parameters

ERP: Earth rotation and nutation parameters (polyn. degree 1 (2 par.) for $x, y, UT1 - UTC, \delta\psi, \delta\epsilon$

ORB: 6 Keplerian elements, 2 rad. pressure, 1 stoch. pulse (3 comp. R, S, W) per sat.

TRP: Troposphere parameters (4 or 12 par. per day and site)

In the case of the baseline processing using 12 troposphere parameters per day and station the disk space is comparable to the size of the daily observation files. These NEQ files are only of temporary nature, however, and are deleted as soon as the daily network solution has been performed. The normal equations referring to one baseline contain not much more information than the daily network solution. Storing

these files is therefore senseless.

The same statement is also valid for the processing of clusters as the smallest unit.

It should be pointed out that the information in the normal equations is not equivalent to the information contained in the original observations. Many model modifications may be performed using only NEQs (see Chapter 2), others require an actual reprocessing of data. Comparing CPU and disk space only makes sense if no model modification of the second kind (like troposphere a priori model, elevation cutoff, tide modeling, etc.) are intended.

The *distributed processing concept* suggested by the IGS [BLEWITT ET AL. 1995] is an attempt to use this modularity in the handling of normal equations for the aspects of the densifications of the global reference frame. We refer to Chapter 7 for more details.

Part II

Results

6. Estimation of Coordinates and Velocities

6.1 Introduction

Below we develop algorithms to compute the rms of station velocities (site motions) as a function of the estimated coordinate rms values stemming from GPS solutions. The same formulas may be used to develop an idea of the required observation scheme (quality, frequency, time span) to obtain station velocities of a given quality.

6.2 Accuracy of the Coordinate and Velocity Estimation

Figure 6.1 illustrates an observation scenario of n homogeneously distributed coordinate determinations y_i , $i = 1, \dots, n$ in a time interval t_{n-1} . In the case of GPS we may e.g. assume that each data point is the result of a daily solution. For our consideration it is however not important how the sets were produced.

Furthermore we assume that all estimates have the same quality and that they are uncorrelated.

If we model the observations of the coordinate component y as a linear function of time $\mathbf{y} + \mathbf{e} = \mathbf{a}t + b = \mathbf{X}\boldsymbol{\beta}$ with $\mathbf{D}(\mathbf{y}) = \sigma_0^2 \mathbf{I}$ we may compute the unknown parameters $\boldsymbol{\beta} = [a, b]'$ according to the method of least-squares using eqns. (2.1-4)-(2.1-22):

$$\begin{bmatrix} a \\ b \end{bmatrix} = (\mathbf{X}'\mathbf{X})^{-1} \mathbf{X}'\mathbf{y} = \begin{bmatrix} \sum_{i=1}^n t_i^2 & \sum_{i=1}^n t_i \\ \sum_{i=1}^n t_i & n \end{bmatrix}^{-1} \begin{bmatrix} \sum_{i=1}^n t_i y_i \\ \sum_{i=1}^n y_i \end{bmatrix} \quad (6.2-1)$$

$$\mathbf{D}\left(\begin{bmatrix} a \\ b \end{bmatrix}\right) = \hat{\sigma}_0^2 \mathbf{Q}_{\hat{\beta}\hat{\beta}} = \hat{\sigma}_0^2 \begin{bmatrix} \sum_{i=1}^n t_i^2 & \sum_{i=1}^n t_i \\ \sum_{i=1}^n t_i & n \end{bmatrix}^{-1} \quad (6.2-2)$$

$$\hat{\sigma}_0^2 = \left(\sum_{i=1}^n (y_i - (at_i + b))^2 \right) / (n - 2). \quad (6.2-3)$$

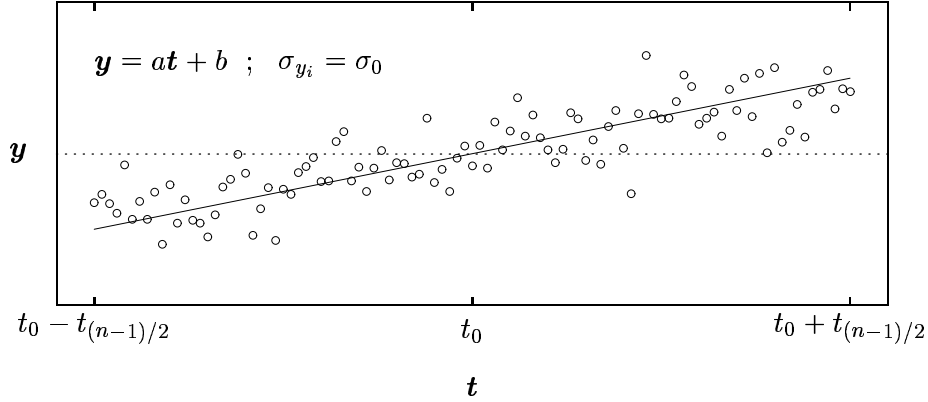


Figure 6.1: Continuous observations of a coordinate component.

We may derive much simpler equations if we center the observations around the middle of the time interval. In this case we find with $\sum_{i=1}^n t_i = 0$ and $\sum_{i=1}^n y_i = 0$ for our result (6.2-2)

$$\begin{bmatrix} a \\ b \end{bmatrix} = \begin{bmatrix} \frac{\sum_{i=1}^n t_i y_i}{\sum_{i=1}^n t_i^2} \\ 0 \end{bmatrix} \quad (6.2-4)$$

$$\mathbf{D}\left(\begin{bmatrix} a \\ b \end{bmatrix}\right) = \hat{\sigma}_0^2 \mathbf{Q}_{\hat{\beta}\hat{\beta}} = \hat{\sigma}_0^2 \begin{bmatrix} \frac{1}{\sum_{i=1}^n t_i^2} & 0 \\ 0 & \frac{1}{n} \end{bmatrix} \quad (6.2-5)$$

$$\hat{\sigma}_0^2 = \left(\sum_{i=1}^n (y_i - (at_i + b))^2 \right) / (n - 2). \quad (6.2-6)$$

The estimation $b = 0$ is a consequence of our definition of the reference time, only. The covariance matrix $\mathbf{D}(\boldsymbol{\beta})$ shows that statements concerning the accuracy of both parameters can be made independently of each other.

A first trivial consequence of this result is that

- $\sigma_{\text{vel}} = \sigma_a = \hat{\sigma}_0 \sqrt{\frac{1}{n \sum_{i=1}^n t_i^2}};$

the longer the time interval, the better the precision of the estimated velocity.

- $\sigma_{\text{COO}} = \sigma_b = \hat{\sigma}_0 \sqrt{\frac{1}{n}};$

The precision of the mean coordinate increases with the square root of the number of observations independently of their chronological order.

- Estimated mean errors for coordinates and velocities are proportional to the rms $\hat{\sigma}_0$ of the measurement.
- the formulae are independent of the motion rates.

These simple formulae are well suited to compute the gain or loss in precision of coordinates and velocities for different observation strategies.

6.3 Accuracy for Different Processing Strategies

In this section we derive the formula for a gain factor g for different observation scenarios by comparing the computed rms values with those corresponding to the uniform, continuous observation scheme of Figure 6.1.

The formulae are explicitly given as a function of the input parameters. An analysis of simulated normally distributed data would confirm these results.

Statements and predictions are made only in a relative sense. The gain factors are therefore independent of an exact knowledge of the precision of any of the different processing strategies.

Longer Time Interval with Continuous Daily Observations

Observing (with the same rate of one observation per day) over $k \cdot n$ days instead of n days leads to the following gain factor (using eqn. (6.2-5) and $\sum_{i=1}^n i^2 = 1/6 \cdot n(n+1)(2n+1)$)

Coordinates:

$$g_1 = \sqrt{(ki)/i} = \sqrt{k} \tag{6.3-1}$$

Velocities:

$$g_1 = \frac{\sqrt{\sum_{i=1}^{kn} i^2}}{\sqrt{\sum_{i=1}^n i^2}} = \sqrt{\frac{k(1+kn)(1+2kn)}{(1+n)(1+2n)}} \stackrel{n \gg 1}{=} \sqrt{k^3}. \quad (6.3-2)$$

The following table shows the differences in the gain for different values of k :

Table 6.1: Quality increase of coordinates and velocities with a k times longer continuous observation interval.

	k			
Type	2	3	4	5
Coordinates:	1.4	1.7	2.0	2.2
Velocities:	2.8	5.2	8.0	11.2

As expected, the gain associated with the length of the time interval is much more important for the velocities than for the coordinates.

Longer Time Interval with the Same Number of Daily Observations

Let us assume that we have on one hand a campaign 1 with $2n/k$ observations centered around the mean and on the other hand a campaign 2 consisting of 2 parts (2a and 2b). Campaign 2 has the same number of observations as campaign 1 but it covers a much longer time interval (Figure 6.2). The spacing between subsequent observations is identical for campaigns 1 and 2.

The gain g_2 of the processing of two separated campaigns with a longer time interval is in comparison to the continuous observations

Coordinates:

$$g_2 = 1 \quad (\text{same number of observations}) \quad (6.3-3)$$

Velocities:

$$g_2 = \frac{\sqrt{2 \cdot \sum_{i=n-n/k}^n i^2}}{\sqrt{2 \cdot \sum_{i=1}^{n/k} i^2}} = \sqrt{\frac{k + 2n - 6kn + 6k^2n}{1 + 2n}}$$

$$\stackrel{n \gg k}{=} \sqrt{3k^2 - 3k + 1}, \quad (6.3-4)$$

which is independent of the number n of observations n .

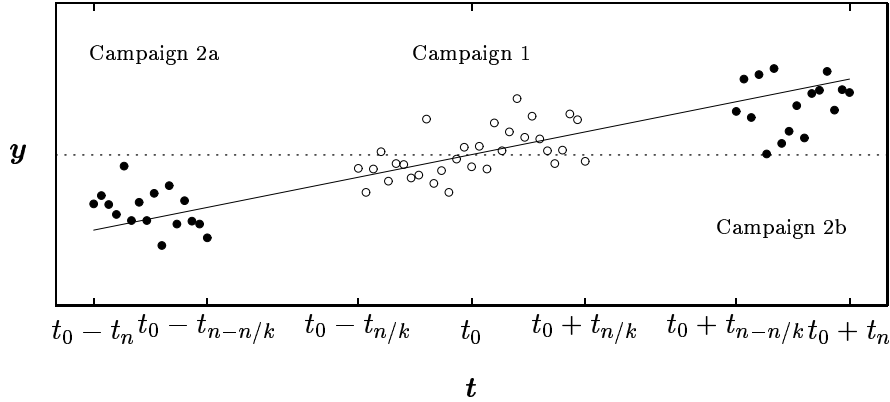


Figure 6.2: Continuous observation of coordinates versus epoch campaigns.

The following Table demonstrates the improvement for the velocities due to a longer time span.

Table 6.2: Quality increase of coordinates and velocities with a k times longer time interval with an unchanged number of observations.

	k			
Type	2	3	4	5
Coordinates:	1.0	1.0	1.0	1.0
Velocities:	2.6	4.3	6.0	7.8

The covered time interval is thus the dominating factor for the quality of velocity estimates. A continuous observation series filling up the gaps between the two campaigns improves the coordinates more than the velocities (see Table 6.1) - a fact which is probably not relevant anyway.

Using Different Sampling Rates

A sampling of k gives the following gains:

Coordinates:

$$g_3 = \sqrt{i/(ki)} = \sqrt{1/k} \tag{6.3-5}$$

Velocities:

$$g_3 = \frac{\sqrt{\sum_{i=1}^{n/k} i^2}}{\sqrt{\sum_{i=1}^n i^2}} = \sqrt{\frac{(k+n)(k+2n)}{k(1+n)(1+2n)}} \quad n \gg k \quad = \sqrt{1/k} \quad (6.3-6)$$

The derivation of the gain factor is more of theoretical interest. In this specific case coordinates and velocities are degraded by the well known factor $\sqrt{1/k}$.

Intermittent Campaigns

IGS Analysis Centers may include additional sites from a particular region into their daily solutions from time to time only for densification purposes. This reduces the computational burden significantly.

Lets us assume that we process in a total time interval of n days at intervals of r days a campaign of a length of d days. The actual number f of such intermittent campaigns is thus $f = n/r$.

The loss of precision for coordinates and velocities in comparison to a continuous observation covering all n days can be computed as following:

Coordinates:

$$g_4 = \sqrt{\frac{\sum_{i=0}^f \sum_{j=1}^n 1}{n}} = \sqrt{\frac{d(f+1)}{rf}} \quad f \gg 1 \quad = \sqrt{d/r} \quad (6.3-7)$$

Velocities:

$$\begin{aligned} g_4 &= \sqrt{\frac{\sum_{i=0}^f \sum_{j=1}^n (i \cdot n/f - d/2 + j)^2}{\sum_{i=1}^n i^2}} \\ &= \sqrt{\frac{d(f+1)(2f + d^2f + 6fn + 2n^2 + 4fn^2)}{rf(2f + 6fn + 4fn^2)}} \\ &\quad n \gg d, n \gg r \quad = \sqrt{d/r} \quad (6.3-8) \end{aligned}$$

For high repetition rates or long time intervals this is completely equivalent to a sampling (decimation) of data with a sampling rate of r/d .

Assuming a time interval of longer than 4 years we get for typical repetition rates in comparison to a permanent network the following "gains" for coordinates and velocities:

- one week campaign every half year ($d = 7, r = 182$): $g_4=0.21$
- one week campaign every year ($d = 7, r = 365$): $g_4=0.15$
- one month campaign every half year ($d = 30, r = 182$): $g_4=0.42$
- one month campaign every year ($d = 30, r = 365$): $g_4=0.32$

Organizing a one month campaign every year thus already gives an precision of about 1/3 of the precision achievable with a permanent network. This is an important aspect for the densification issue within the IGS.

All above statements concerning the gain in the precision of a particular processing method assume that there are no systematic effects associated with the campaign-type operation. In particular one has to be afraid of the "human factor" (local eccentricity vectors, antenna heights) but also of changing receiver/antenna combinations used in the network.

6.4 Error Propagation for the Coordinate Precision

All the above estimates for the coordinate precision refer to the middle time t_0 of the observation interval. For an arbitrary observation epoch we have to write

$$y(t_i) = (t_i - t_0)a + b. \tag{6.4-1}$$

With eqn. (6.2-5) we find according to the law of the error propagation:

$$\sigma_{y(t_i)} = \sqrt{(t_i - t_0)^2 \sigma_a^2 + \sigma_b^2}. \tag{6.4-2}$$

Figure 6.3 demonstrates the fact that the coordinates are determined with the best quality for the middle observation epoch whereas for longer extrapolations the effect due to the uncertainty of the velocity estimation dominates.

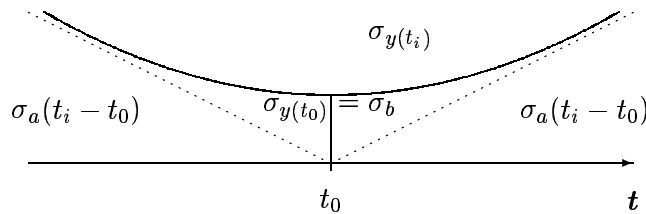


Figure 6.3: Error propagation for coordinates with estimated velocities.

6.5 Expected Precision of Long Time Series of Continuous Observations

We apply the results of the previous section to derive precision values for coordinates and velocities. Afterwards we will compare these results with real results using the data of the global IGS network.

Eqn. (6.2-5) gives all relations of interest: With a given precision of a single coordinate estimation and a given time interval of continuous daily observations we are able to derive the associated precision values for the coordinate estimates σ_b at the mean epoch of all observations, and also the precision for the velocity estimation σ_a . Table 6.3 shows these values for different observation times and qualities.

Table 6.3: Resulting coordinate and velocity precision using different data quality σ_0 and time intervals of continuous 3-days-solutions. σ_0 is the rms error of one individual coordinate estimate.

k (yr)	g_1^a	σ_{coo} (mm)					g_1^b	σ_{vel} (mm/yr)				
		σ_0 (mm)						σ_0 (mm)				
		10	15	30	50	100		10	15	30	50	100
0.5	1/8	1.3	1.9	3.8	6.4	12.8	1/2.2	4.5	6.7	13.4	22.3	44.6
1	1/11	0.9	1.4	2.7	4.5	9.0	1/6.3	1.6	2.3	4.7	7.9	15.8
2	1/16	0.6	1.0	1.9	3.2	6.4	1/18	0.6	0.8	1.6	2.8	5.6
3	1/19	0.5	0.8	1.5	2.6	5.2	1/33	0.3	0.5	0.9	1.5	3.0
4	1/22	0.5	0.7	1.3	2.3	4.5	1/51	0.2	0.3	0.6	1.0	2.0
5	1/25	0.4	0.6	1.2	2.0	4.0	1/71	0.1	0.2	0.4	0.7	1.4

^again according to (6.3-1) divided by $\sqrt{3}$

^bgain according to (6.3-2) divided by $\sqrt{3}$

The usually adopted processing strategy at the CODE processing center is to use 3-days-solutions (to make use of the strength of the 3-days-orbits). Therefore the gain factors of Table 6.1 are reduced according to eqns. (6.3-5) and (6.3-6) by a factor of $\sqrt{3}$.

With 2 years of observations all rms errors for coordinates and velocities are below the 1 cm or 1 cm/yr level even if the accuracy of a single solution is of the order of 10 cm.

The improvement of the velocity estimates with time is demonstrated in Figure 6.4 using the results of 2 years IGS processing of the CODE Analysis Center. For time intervals of different lengths we solved for coordinates and velocities. The formal velocity rms values of the combined solution for a selected number of stations and also the predicted reduction according to eqn. (6.3-2) for a fictive rms estimation (60 mm rms for the first monthly solution) are drawn. The law of error propagation

($\sim \sqrt{k^3}$) can easily be verified. Comparisons of the velocity estimates with ITRF are shown in Figure 8.10. From these results we can conclude that the improvement of the internal precision means also an improvement of the accuracy of the site velocities.

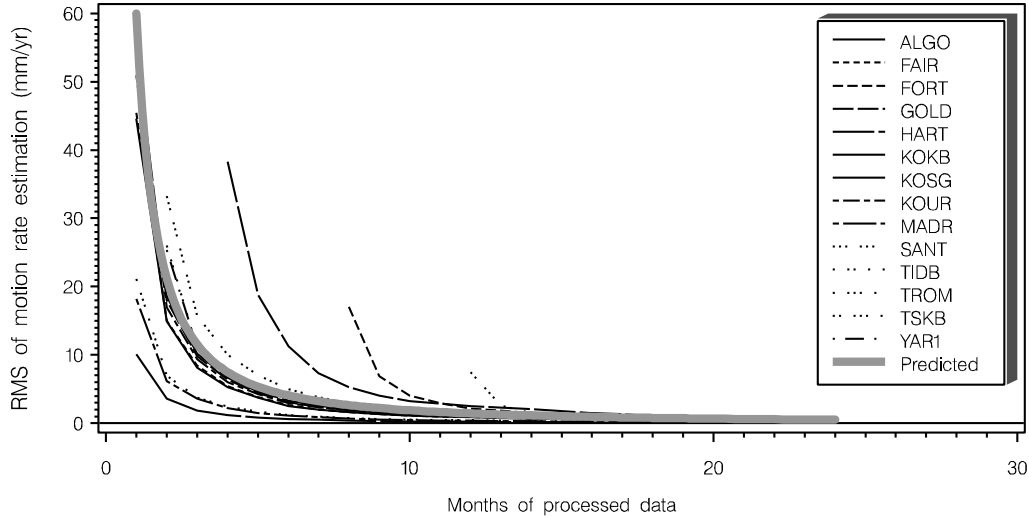
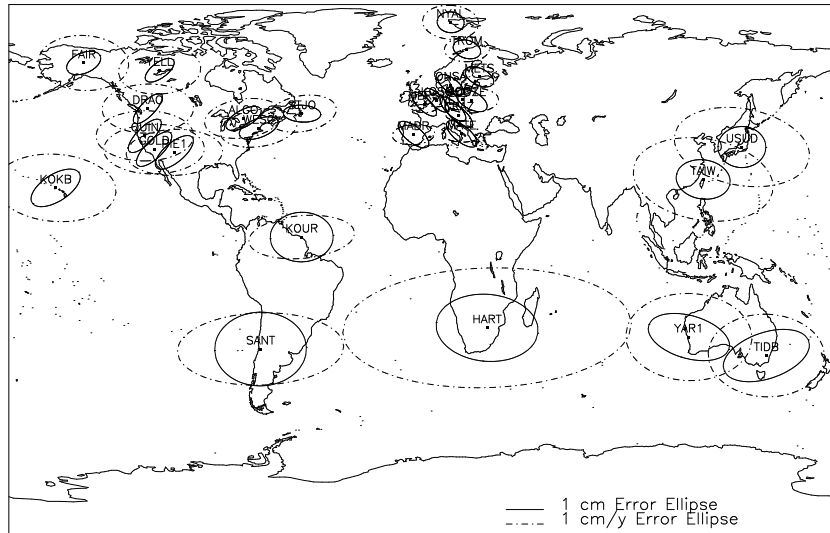


Figure 6.4: Estimated rms errors for site velocities. The predicted rms reduction using eqn. (6.3-2) (for a station observing since month 0) is given for an adopted precision of 60 mm/yr for the first monthly solution.

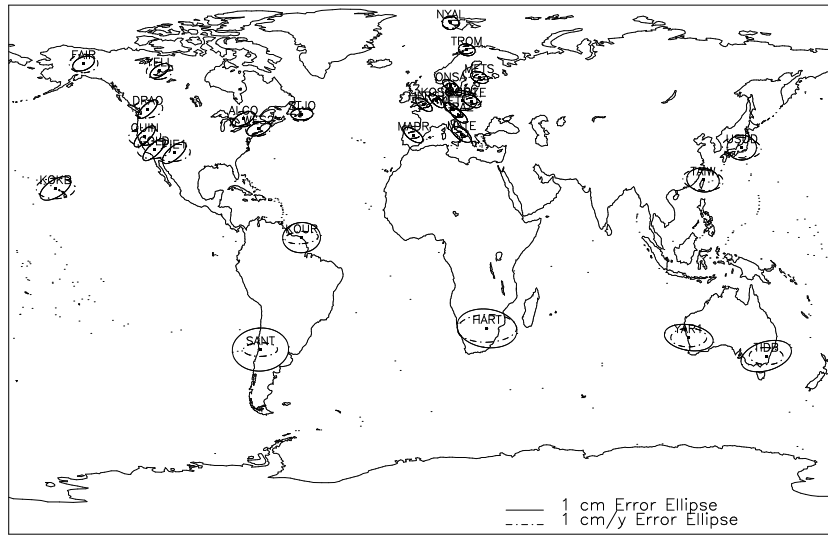
Figure 6.5 illustrates the estimated internal precision of an annual solution using the CODE results of 1993 (a) and a 2-years-solution covering the years 1993 and 1994 (b). The error ellipses represent the internally achieved precision in the local north and east directions. The internal rms values are multiplied by an empirical factor of 10 to align the degree of freedom of the combined solution (based on the original GPS phase observations) with the degree of freedom of this simple approach (based on coordinate estimates).

As opposed to the assumptions we made to obtain the values in Table 6.3 (a particular coordinate parameter is uncorrelated to other coordinate parameters and is determined in all sequential solutions with the same precision) the full covariance matrices of the sequential solutions are taken into account.

The statement that the coordinate quality increases with a factor of $\sqrt{2} = 1.4$ and that the velocity estimation increases with a factor of $\sqrt{8} = 2.8$ is easily seen in Figure 6.5.



(a) Error ellipses from the annual solution 1993



(b) Error ellipses from a 2-years-solution 1993-1994

Figure 6.5: Estimated internal precision of coordinates and velocities using different time intervals. The formal rms values are scaled with an empirical factor of 10.

If we compare the (unitless) values in Table 6.3 for 1 and 2 years of observations we find that with a 2-years-solution the site movements per year can be determined better (in mm/yr) than the coordinates (in mm). This is also illustrated by Figure 6.5 showing smaller error ellipses for the velocities than for the coordinates.

The Sections 8.2.2 and 8.3.1.3 show that not only the formal errors decrease with a longer time series. The agreement with ITRF is also considerably improved.

That the simple error propagation formulae (6.2-2) or (6.2-5) are capable of predicting the accuracy level for real results is due to the fact that with the increased number of observations the influence of a correct handling of the covariances diminishes. We pointed out this effect already in Section 5.1.

The consequence of Table 6.3 is very encouraging for the future of the IGS. With additional 3 years of observations the precision- (and also the accuracy-) level for the velocities can be improved by a factor of 4.

For the *coordinate estimates* we expect with the same data a gain of 1.5 only. The coordinate estimates are furthermore problematic because systematic effects cannot be detected by looking at internal consistencies. The realization of a physically accessible reference point is difficult on the mm level. Effects due to elevation (and azimuth) dependent phase center variations of an antenna may introduce systematic effects of up to 10 cm in a combination of different receiver types [ROTHACHER ET AL. 1995] (see also Figure 7.8).

For the *velocity estimates* the situation better. In spite of possible systematic errors in the coordinates the absolute values of the velocities are unaffected as long as the same antenna / receiver combinations and processing options are used.

7. Combination of GPS solutions of Different Analysis Centers

The combination of GPS solutions of different analysis centers is important for the maintenance of reference systems and for densification purposes. We divide this chapter into two parts. The densification is the subject of the first part. A case study demonstrates the principles of the combinations and compares the quality of different processing and combination strategies. Applications conclude this first part. The subject of the second part is the combination of weekly coordinate estimates (and the associated covariance information) computed by the IGS Analysis Centers.

7.1 Combination of Regional Solutions with Global Network Solutions

7.1.1 Introduction

The correct combination of regional campaigns with global networks is an important task in view of the steadily increasing number of permanent GPS networks all over the world.

The creation of a software independent exchange format for coordinates (and associated site- and covariance information), *SINEX* [KOUBA 1996], allows the exchange of results from different GPS Analysis Centers using different software tools.

It is also possible to combine results achieved by different space techniques (VLBI, SLR, PRARE, or DORIS) using such methods.

In this chapter we discuss different methods to densify the global IGS network and the quality associated with these methods.

7.1.2 Existing Global and Regional Networks

The first *global GPS network* was the Cooperative International GPS Network (CIGNET) consisting of 8 stations in North America, Europe and Japan starting its operations in July 1988. The importance of the establishment of a denser tracking network was widely recognized. With the 3-weeks campaign called GIG'91

[MELBOURNE 1991] a first attempt was made with a global GPS network of about 100 receivers around the world. The IGS operations started in July 1992 with about 20 permanent sites [BEUTLER ET AL. 1994]. At the beginning of the year 1996 the network consisted of about 60 sites (see Table 1.2). New permanent sites are coming up almost every month.

Parallel to the global activities a variety of *regional permanent arrays* are built up. We mention in particular the *Permanent GPS Geodetic Array (PGGA)* in California [BOCK 1991; LINDQWISTER ET AL. 1991] for the detection of deformations at the North American - Pacific plate boundary, the *Canadian Active Control System (CACS)* [DELIKARAGKOU ET AL. 1986; KOUBA AND POPELAR 1994] to provide Canada with orbits of sufficient quality for all geodetic purposes (most of them are also part of the IGS network), the *Continuously Operating Reference Station (CORS)* network of the US National Geodetic Survey (NGS) [STRANGE ET AL. 1994] (which will be expanded in 1995 by 50 sites of the US Coast Guard and also by about 30 site of the Federal Aviation Administration FAA), two *Japanese arrays* for the detection of crustal deformations (a dense local network in the Tokyo area with a point separation of about 15 km and a nation-wide network consisting together of about (at present) 600 sites [TSUJI ET AL. 1995], and the *Swedish network (SWEPOS)* [HEDLING AND JONSSON 1995] of about 20 sites.

In addition to these big networks there exist already many *nation-wide networks*. In Europe such activities are coordinated under the umbrella of the EUREF (European Reference Frame) subcommission of the IAG (International Association of Geodesy) (see also Section 7.1.4).

We should not forget either numerous *non-permanent regional campaigns* with observing sessions of some days up to some weeks.

For all the listed activities there is the necessity of a correct integration into a global reference frame.

The distinction between the global IGS network for the orbit determination and regional networks for the densification of the ITRF is mainly a consequence of the increasing number of sites. Processing procedures based on the combination of normal equations are the only possibility to handle such permanent regional networks of more than 100 sites in a more or less correct way.

If the processing is organized by regional agencies we call such a procedure *distributed processing*.

Regional and local agencies have the possibility to work as *Regional Network Associated Analysis Centers (RNAAC)* (also called *Associated Analysis Centers Type 1*), to process their own data and to contribute to the global densification with their solutions using the mentioned SINEX format.

Global Network Associated Analysis Centers (GNAAC) (sometimes also called *Associated Analysis Centers Type 2*) may perform the integration in the global reference system (see Section 7.2).

A common least-squares adjustment of all available sites together including orbit determination is on one hand the best option from a theoretical point of view. It is on the other hand not realistic in view of the workload involved. Some of the IGS Analysis Centers prove furthermore that excellent global products (orbits and Earth rotation parameters) may be derived using a sparse global network (EMR of Natural Resources Canada achieves its results using 30 sites only).

7.1.3 Distributed Processing in Europe: A Case Study

7.1.3.1 The Solution Types

In order to study different processing strategies for a regional network, the European observations used by the CODE Analysis Center referring to the time interval 1 Nov 1994 - 31 Dec 1994 were processed in different ways. First of all we made the (artificial) distinction between "global" and "regional" sites. In Figure 7.1 the "global" sites are marked with large, the "regional" sites with smaller capital letters. All in all we have 18 European sites, 9 of them are "global", 9 are "regional".

Two kinds of *global network solutions* were produced for the mentioned time interval:

- a solution where the data of *all* European sites and the sites from outside Europe were used to generate orbits and ERPs. This global solution corresponds to the CODE routine solution. We may regard this solution as the "truth" and will refer to it as *global solution type I*.
- a solution using the same data as in the global solution *with the exception* of the 9 "regional" European sites. We may call the processed network *global solution type II*.

In addition to these two network solutions we process a third solution type:

- *Regional* network solutions with characteristics specified in Section 7.1.3.4. To allow a link to the global network we also process some of the global sites. We call the global sites, which are processed also in the regional campaign, *anchor sites*.

Baselines of doy 355 (21.12.1994) in Europe

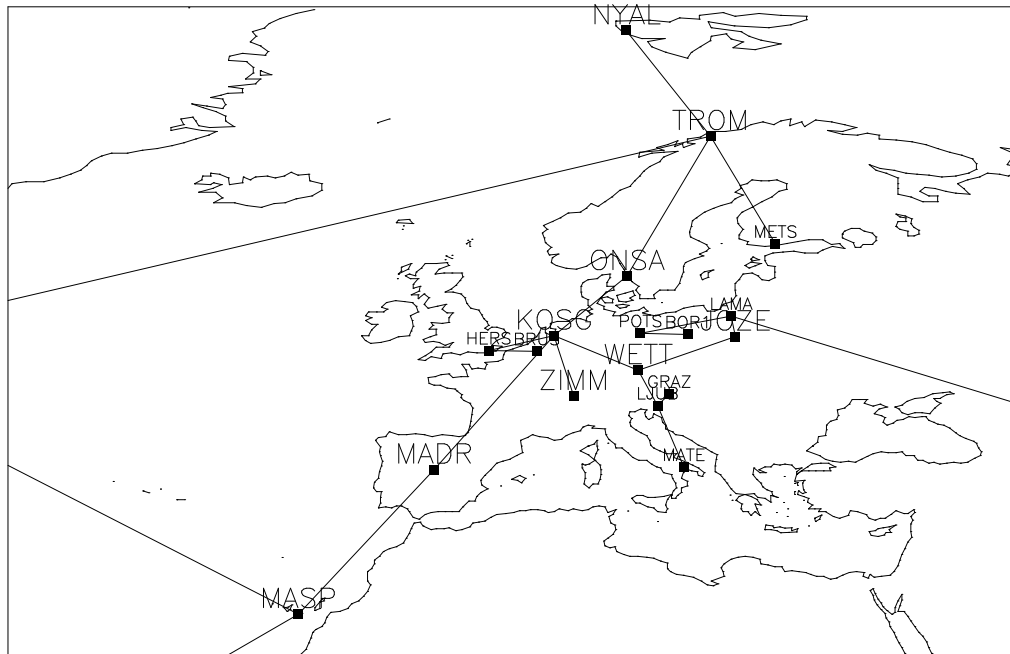


Figure 7.1: Baseline configuration of the European subnetwork (DOY 355 / 21 Dec 1994). Stations printed in a large font are the global stations, sites in a small font are considered as regional sites.

Let us conclude this overview with the remark, that on each day the baselines were formed independently using a criterion maximizing the number of single difference observations for the global network. Figure 7.1 also shows the baseline selection of one day of this 2-months experiment.

The goal of our experiment is to combine the results of the global solution type II with the regional network solutions. The differences to our "true" solution (global solution type I) will give us an idea of the quality of different processing- and combination strategies. We will focus on these aspects in Sections 7.1.3.4 and 7.1.3.6.

7.1.3.2 Processing Aspects

Let us mention that we used a *baseline-wise* processing scheme for all the three solution types. The more correct approach of the *cluster-processing* was not considered. Due to the fact that the daily solutions are based on baseline NEQs we get the total

global network solutions by stacking all available normal equations of the day (see Section 5.2). The daily global solution type II is achieved by excluding the NEQs of all baselines which contain one of the mentioned 9 regional sites. The 3-days-solution is obtained by stacking the daily normal equations according to Section 5.5.

The result of solution type II consists of normal equation files containing all (with the exception of the ambiguity parameters) unknown parameters. This is true for the 3-days-solutions and for the 1-day-solutions.

The differences in the orbit parameters and also in the earth rotation parameters between solution types I and II are showing directly the impact of the 9 European regional stations. These results are presented in the next section.

7.1.3.3 Impact of the Regional Solution on the Global Solution

Figure 7.2 shows the rms errors of the Helmert transformation between different orbit systems. The improvement of the global solution due to the 9 European regional sites (with a maximum rms difference of 3 cm) is negligible. This is true in view of the rms values we obtain if we compare the global 1- and 3-days-orbits with the IGS orbits. In the average we get 3 to 5 times larger values.

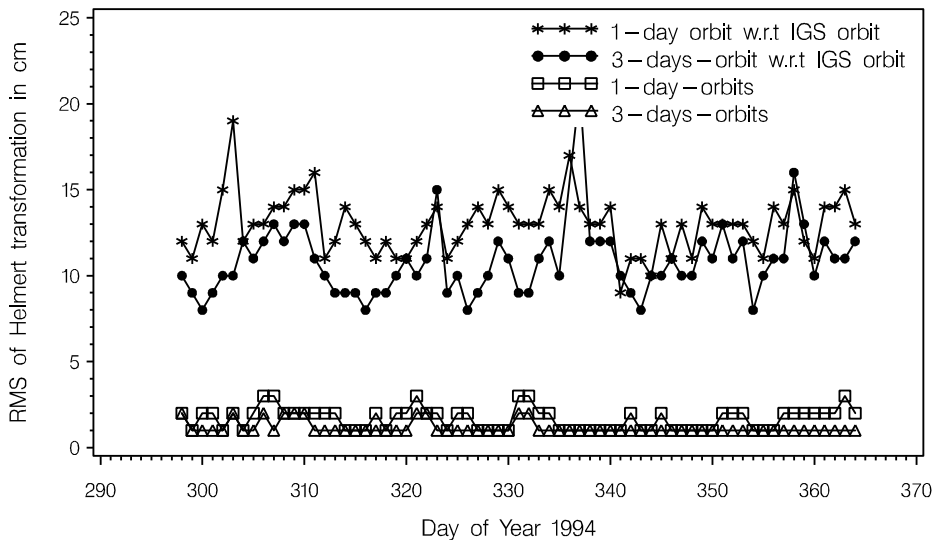


Figure 7.2: Rms of Helmert transformation between orbit systems achieved with (global solution type I) and without European regional sites (type II). For comparison the values of the complete global solution type I with respect to the final IGS orbits are also included.

The impact of the additional regional sites on the Earth rotation parameters is

contained in Table 7.1.

Table 7.1: Rms error of the differences between the two global solutions of type I and II (with and without additional European sites) derived from 2 months of processing.

	rms of the differences	
	3-days-solution	1-day-solution
x-pole	0.02 <i>mas</i>	0.03 <i>mas</i>
y-pole	0.02 <i>mas</i>	0.03 <i>mas</i>
UT1-UTC drift	0.002 <i>msec/day</i>	0.003 <i>msec/day</i>

For the 3-days-solution the influence is slightly smaller than for the 1-day-solutions, which is consistent with the orbit quality achievable with these arc lengths.

We conclude that the reduction of the dense European GPS network by 9 sites showed no significant reduction of the quality of our global products.

If we consider an extremely inhomogeneous network of e.g. 100 sites in a particular region and a very low density for other regions we may get a different result because the combined solution using all sites together might result in an orbit system which is best suited for that particular region.

The influence of a station on the orbits is in general proportional to the length of the baseline (inversion of the Bauersimas rule [BAUERSIMA 1983]). Sites which would be important for the orbit determination should not be selected as regional sites.

7.1.3.4 Processing Procedures for Regional Campaigns

Let us now study different ways of processing regional campaigns and of combining the results with the global solutions. The strategies are different in their degree of correctness. It should be mentioned, however, that less correct methods are in general easier to implement in the case of a distributed processing.

The following five different processing strategies are studied:

Strategy A is as correct as possible (with respect to the daily solution of the total daily network solution):

We use the pole- and orbit information derived from the global solution type II. The regional sites are therefore not contributing to the pole and orbits used. This is the only inconsistency with respect to the complete global network (type I) where all stations are used for the determination of the orbits and the Earth rotation.

Unknown parameters of this strategy are all site coordinates, 12 troposphere parameters per day and station, and the ambiguities.^a

The ambiguities are (similar to all other strategies) pre-eliminated from the normal equation system. We save therefore normal equations containing only site coordinates *and* troposphere parameters.

Troposphere parameters and the corresponding covariance information are (at present) not supported by the SINEX format. A combination of global and regional campaign including troposphere information is therefore only possible for agencies using the same software.

Strategy *B* Software independence is a characteristic for this strategy. The combination of troposphere parameters in the NEQs is avoided by introducing the troposphere estimates of the anchor stations from the global network as known apriori values into the least-squares adjustment process for the regional campaign. We thus have to solve for troposphere parameters for the regional sites only.

In the NEQs we store only the coordinate information because the troposphere parameters for the regional sites will find no counterpart in the combination with the global network.

The MET RINEX format [GURTNER AND MADER 1990] is well suited to store the estimated zenith path delays of the stations of the global solution type II. Most scientific software tools support the MET RINEX format.

Strategy *B* is less correct from the mathematical point of view than strategy *A* because the troposphere estimates for the global sites in the regional campaign will not contribute to the troposphere parameter estimates in the combination. This is not really a problem for small networks (diameter < 50 km) because the absolute troposphere cannot be separated from the heights [ROTHACHER ET AL. 1990]. It is a common procedure in small networks to constrain the troposphere of one site to a model and to estimate troposphere parameters only for the other sites.

Strategy *B* takes over the troposphere estimates for the global stations from the global analysis.

^aThat it is possible to perform a regional solution which also contributes to the orbits was already proved with the concepts developed in Section 5.2. In this case we have to set up in the regional campaign orbit- and Earth rotation parameters, too. We consider such a method as not feasible for regional processing agencies and moreover unnecessary if the effect on the orbits is small.

Strategy *C* This strategy was defined to illustrate the influence of different apriori orbit information on the processing of the regional campaign. Instead of the 1-day-orbits and ERPs we used slightly different orbit and pole information for the regional campaign, taken from the 3-days-solution (CODE orbits and ERPs). The Helmert transformation between 1- and 3-days-orbits gives - similar to that underlying Figure 7.2 - an average rms of transformation of 15-20 *cm*. Apart from using inconsistent orbits and ERPs strategy *C* is identical with strategy *A*.

Strategy *D* We set up troposphere parameters for all sites (including the anchor stations) but do not store them in the NEQs. A combination of troposphere parameters is therefore in contrast to strategy *A* not possible. We expect that neglecting the troposphere has consequences mainly for the coordinate heights of the regional sites.

Strategy *E* We separate the troposphere estimation of the global solution and the estimation in the regional solution as in strategy *D*. In addition to this we use the slightly inconsistent IGS orbits (according to Figure 7.2 the IGS orbits and 1-day-orbits differ by about 15 *cm* rms after Helmert transformation). The C04 pole differs from the daily Earth rotation parameters as estimated by CODE by a constant offset of 0.5 *mas* for the x-pole and 0.8 *mas* for the y-pole. The scatter is of the order of 0.25 *mas*. From the point of view of internal inconsistency this strategy is the worst studied here, from the point of view of easiness and practicality for processing and combination this strategy is well suited for a distributed processing.

The impact of using broadcast orbits is not studied here. BROCKMANN ET AL. [1993] showed that the repeatabilities of European baselines are degraded by a factor of about 5-10 when using broadcast orbits and not IGS orbits.

Baselines and anchor sites were identical in all strategies. Because we maximize the number of observations we obtain different anchor sites for each day. A fixed number of anchor sites (e.g. 3-4 sites) not changing from day to day is probably better suited for a typical processing of a regional campaign. We come back to the selection of the anchor sites in Section 7.1.5.

7.1.3.5 Combination of Global Solution (Type II) and Regional Solution

Figure 7.3 shows the principles of combining the normal equations of the regional campaign with the NEQs of the global solution type II.

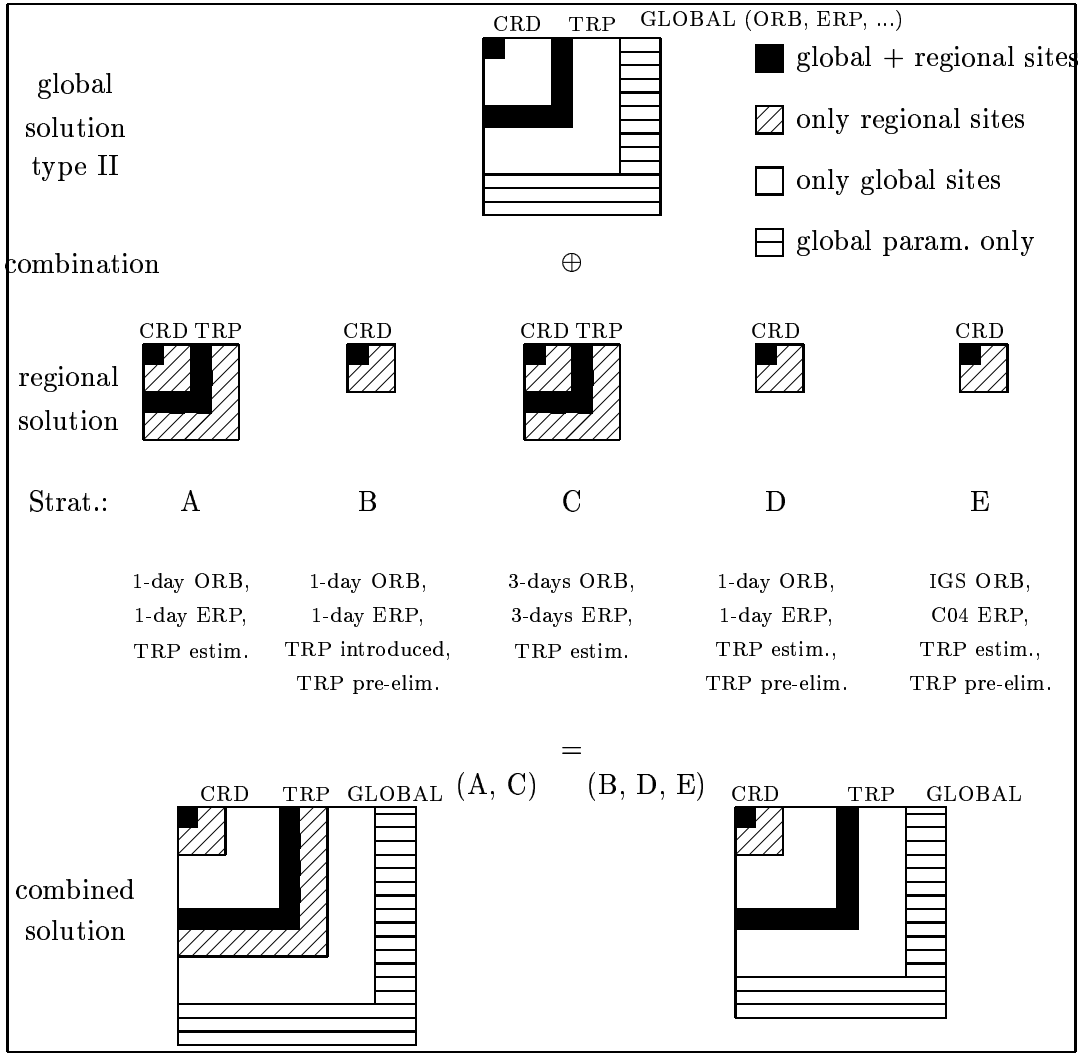


Figure 7.3: Combination of the regional solution with the global solution type II for different processing strategies.

We have to distinguish between two cases. Whereas we have to combine only the coordinate parameters for the strategies *B*, *D*, and *E*, we have to combine also the troposphere parameters for the other two strategies.

Combination means superposition (stacking) of the NEQ elements referring to the same parameters in both normal equation systems and appending the elements for parameters which occur only in one NEQ system. This is how the symbol \oplus in Figure 7.3 has to be interpreted.

Due to the approximations made in the different processing strategies we cannot expect to obtain results identical with those of a correct combination. The impact of the approximations is studied in the next section.

7.1.3.6 Quality of Different Processing Strategies

Comparison of daily solutions

For the time span of about two months we compared the daily coordinates of the combined solution (global solution type II and regional solution) using different strategies with the results of the global solution type I.

We mention that we defined the geodetic datum of the global solution and of the combined solutions by fixing (tightly constraining) the coordinates of the 13 IGS core sites (see Figure 1.1) on the ITRF93 values. No Helmert transformation is thus required for these comparisons.

Figure 7.4 shows the differences for the site GRAZ using strategy *A* and *E*. It is obvious that strategy *A* is superior to strategy *E*.

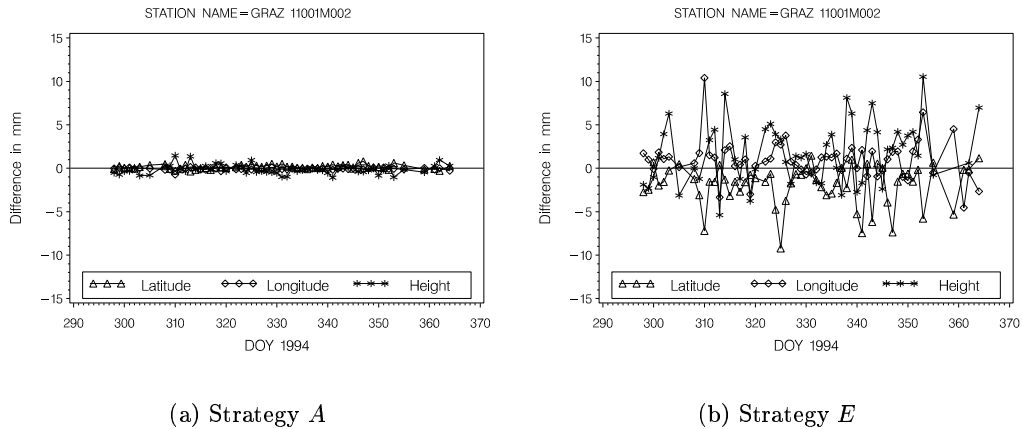


Figure 7.4: Comparison of the combination results with the global network solution type I. Using strategy *A* we obtain a repeatability of ± 0.1 mm (North), ± 0.2 mm (East), and ± 0.5 mm (UP) for GRAZ, strategy *E* gives ± 2.2 mm (North), ± 2.4 mm (East), and ± 6.4 mm (UP).

Table 7.2: Repeatability of the comparisons of the combination results with the global network solutions type I (averaged over all regional sites).

Strategy	rms of the difference [mm]		
	North	East	Up
<i>A</i>	0.2	0.5	1.1
<i>B</i>	1.7	1.3	3.1
<i>C</i>	1.5	2.9	5.0
<i>D</i>	3.4	3.0	8.4
<i>E</i>	4.3	4.1	8.9

Table 7.2 compares the quality achieved with strategy *A-E* (repeatability means rms error of the differences with respect to the correct solution). The stations LAMB, LJUB and POTS are not included in the rms computation because these sites were not always available for our time interval of two months. It makes sense to present the results in latitude, longitude and height because we suspect a strong correlation between station heights and troposphere estimates. Table 7.2 shows that, when the troposphere estimates are correctly handled, the station heights are not influenced. Only strategies *A* and *B* are satisfactory.

Table 7.2 documents that all strategies are consistent with the "true" solution below the 1 *cm* level. The largest differences are found in the up-direction for all strategies. Nevertheless there are significant differences in the achieved results: Strategy *A* is better by a factor 8 than strategy *E*. The corresponding ratio for the north component is even more pronounced.

Obviously the approximation made in strategy *A* (regional European sites do not contribute to orbits and ERPs) is not relevant for the combination.

Strategy *B* shows very small differences to the results of the global network, too. This confirms the assumption that most of the information concerning the troposphere of the anchor stations stems from the global network. The assumption underlying this strategy (that the observations of the regional network have no influence on the troposphere estimation of the anchor stations) seems close to truth.

The impact of neglecting the troposphere parameters in the combination is seen in the comparison of strategies *D* and *A*. Strategy *A* is about 8 times better.

The comparison of strategies *C* and *A* illustrates the impact of a slightly inconsistent orbit. Instead of the daily orbits of the global solution type II, which agree with those of solution I on the 1-3 *cm* level, we use the orbits derived from a 3-days-solution (the official CODE solution) showing an agreement of about 15 *cm* rms after a Helmert transformation. We obtain similar values if we compare the IGS orbits with Analysis

Center specific orbits. Apart from that, the combination strategy is the best possible - combining all coordinates and troposphere parameters. The results are worse than those of strategies *A* and *B* but with about 5 mm for the vertical component still acceptable.

Looking at the rms value of strategy *D* leads us to conclude that the combination strategy of the troposphere parameters plays a key role in the combination strategies. This statement is also confirmed by the results of strategy *E*. The quality of strategy *E* is almost the same as strategy *D*, although we even used inconsistent orbit information in addition to the incorrect troposphere handling.

Systematic Effects in Multi-Days Solutions

In addition to the day to day agreement of the combined solution with the "true" solution we studied multi-days combinations to see whether the coordinate differences (with respect to the "truth") are of random nature with zero expectation value for longer time periods or if systematic differences remain.

The combination procedure is the same as that presented in Section 5.6. For each time interval (1 day, 1 week, 2 weeks, 1 month, 2 months) we generate a combined solution by stacking the "true" daily normal equations and also a solution using the daily NEQs resulting from the combination of regional- and global solution (type II). Such combinations would be performed e.g. by regional analysis centers to include a multi-days regional solution into a global network solution.

The absolute values of the vector differences (labeled as bias) are given in Figure 7.5. From Table 7.2 we know already that the biases in Figure 7.5 are mainly height differences.

We confine ourselves to present the sites BOR1, BRUS, GRAZ, and MATE. The other regional sites show a similar behavior.

We may conclude:

- In general the biases are greatly reduced with the length of the multi-days solution. For longer time spans we actually may assume that the bias has a zero expectation value. This is an important result for densification purposes.
- The reduction with time is very small for strategy *C*. Even an increase is observed for the sites GRAZ and MATE. Inconsistent orbit information seems to have a systematic influence which is the dominating error source even for longer time periods.
- There are quality differences between the results of different stations. GRAZ and BOR1 are good examples, MATE was the worst case in our comparisons. These differences are mainly a consequence of the *distance to the next anchor station* and the data quality of each site.

- To ensure the best possible agreement with the correct global solution strategies *A* or *B* should be used. The biases actually are negligible for these strategies.

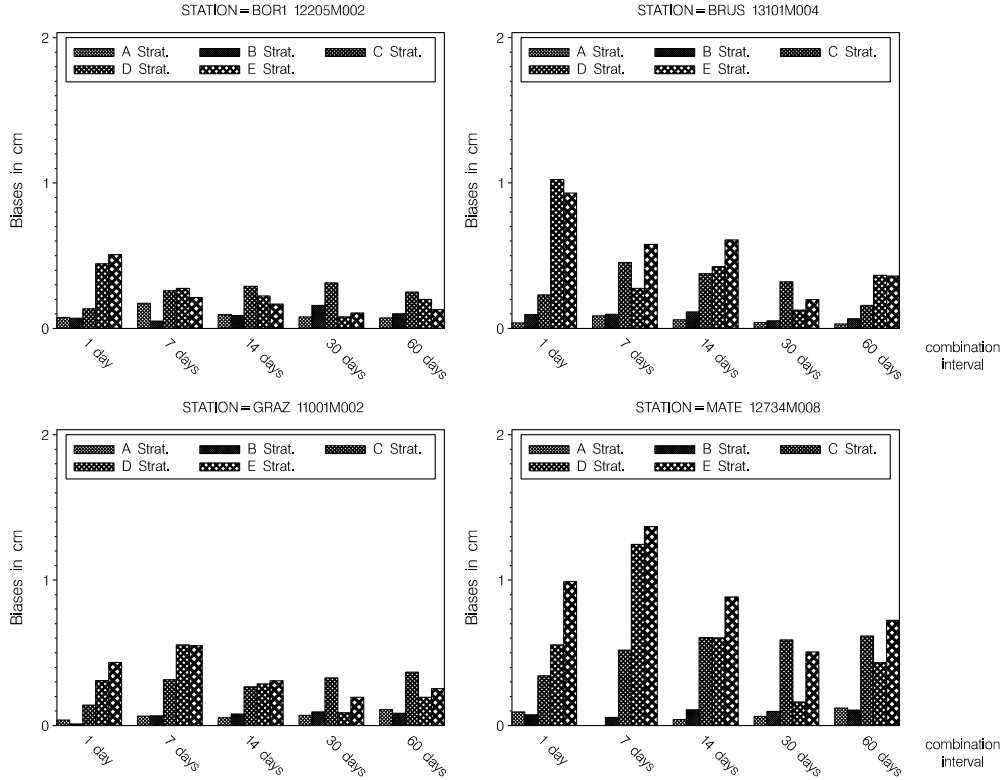


Figure 7.5: Biases of multi-days combined solutions (of regional and global solutions type II) with respect to the corresponding correct solution (type I).

Although there are significant differences between different strategies, we would like to mention that the achieved results are excellent in all cases. But in view of the precision of the daily coordinate components of the European sites the mentioned biases are not negligible. From repeatability studies of the global network solution type I we obtain precision values for a daily coordinate estimation of the order of 5 mm (north), 7 mm (east) and about 10 mm (heights) (see also Section 8.2.1.2). The combined two-months solution has (according to Section 6.3) an internal precision which is by a factor of about $1/\sqrt{60} \approx 8$ smaller than that of the daily solutions. This 1-2 mm consistency is observed for strategies *A* and *B*, only. The results of the other strategies are much worse which means that the combination strategy is an important error source.

7.1.4 Applications

For the *IGS Analysis Centers* the division of the processing into a global part used for orbit determination and into a regional part for densification is a most attractive tool to reduce the computational burden of the daily processing. In view of the density of stations in Europe and in North America such a separation of the processing into a global and a regional part makes sense in both cases. A combination of the global and regional solutions allows it to provide the IERS - without a quality reduction (in case of strategy *A* or *B*) - with site coordinates and velocities in a consistent terrestrial reference frame.

Regional agencies have the possibility to process their own network using the methods presented here. Including some well established sites (anchor sites) of the global IGS network makes it possible to determine their sites in the ITRF and to contribute to a densified terrestrial reference frame.

The division of the network into subnetworks has moreover additional advantages. In smaller network it is possible to resolve most of the ambiguities for baselines up to 2000 *km*. MERVART [1995] demonstrated a quality improvement of the daily solutions for the east component by a factor of two with respect to the ambiguity-free solution. For the other components we cannot expect significant improvements.

For combinations using the same software system we recommend strategy *A* (combination including troposphere).

In the other cases strategy *B* offers an elegant way to deal in an (almost) correct way with this problem. The available exchange format of troposphere estimates (MET RINEX and in future also SINEX) makes this strategy suitable for a software independent combination.

For highest consistency requirements it is furthermore necessary that the used troposphere-, orbit-, and ERP-information is consistent with the associated covariances used for the combination. That is actually true only if the results of a particular IGS Analysis Centers are used. At present combined IGS products are available for orbits, ERPs, and coordinates together with the associated covariance information (weekly combinations performed by the *Global Network Associated Analysis Centers (GNAAC)* using the weekly SINEX submissions of the IGS Analysis Centers; see also Section 7.2, which demonstrates the quality of such combinations). Combined troposphere estimates are planned. GENDT AND BEUTLER [1995] demonstrated an excellent agreement of the 2-hour troposphere estimates of different processing centers.

The dependence on a particular processing center is thus not given any longer (assuming that all the IGS products are consistent) to achieve the best possible qualities.

Such a dependence is not given for strategy E , too. The use of IGS orbits ensures a certain quality level and the storage of the coordinate results in the SINEX format allows for a later combination with a global network solution. The price for this independence is a somewhat reduced consistency of the results.

Since the beginning of the year 1996 four European Regional Analysis Centers produce, under the umbrella of EUREF, on a regular (weekly) basis coordinate results together with the associated covariance information. The *Institute for Applied Geodesy in Germany (IfAG)* process 13 European sites, the *International Commission for Global Geodesy of the Bavarian Academy of Sciences (BEK)* process 12 IGS sites located near the Mediterranean area, the *Royal Observatory of Belgium (ROB)* process the data of 4 Belgian permanent sites and 6 additional European sites involved in IGS, and the *Warsaw University of Technology (WUT)* process 3 Polish stations (all available within IGS) together with 7 European IGS sites.

The exchange format used from the first two agencies is SINEX, the exchange format used by ROB and WUT is a *Bernese 3.5* specific format based on normal equations. A first step in the direction of a distributed processing is done, even if at present only the 3 Belgian sites are not processed by the CODE Analysis Center. Comparisons of the regional solutions with the solutions derived at CODE prove that the combination concepts are working and that the quality of an integration in a common reference frame can be achieved with an excellent precision [BROCKMANN AND GURTNER 1996]. The ITRF95 contribution of the CODE Analysis Center contains already the solutions of the mentioned European Regional Analysis Centers.

7.1.5 Problem Areas

There are problems which were not yet discussed:

- No correlations between (the same) observations used in the global network and the regional network can be taken into account:
A compromise is the use of three to five anchor stations in the regional network solution to achieve a best possible fit of the regional network into the global network. From the statistical point of view this is also not correct because we introduce the same observations twice.
- Different sampling rates for global solution and regional solution:
The combination procedure is based on the implicit assumption that all normal equations were created using the same sampling rate for the observations. A higher sampling rate by a factor of k in a regional subnetwork would artificially scales the normal equation matrices approximately by a factor of $1/k^2$. This has to be taken into account in the combination.

- Scaling of covariance matrices of different software packages:
The scaling of the covariance matrix is different for different software packages. For a combination using covariance information the *scaling plays a key role*. When giving a considerable weight to a particular solution, this solution will dominate the resulting combined solution. *Variance-covariance component estimation* is a well-suited tool to estimate the cofactor values of particular solutions or groups of solutions together with the combined coordinates [KOCH 1988]. The associated formulae are extremely computing-time consuming because we have to deal with full covariance matrices. In Section 7.2 we present a simple algorithm to determine cofactor values.
- Improvements of the global network solution using the results of regional campaigns:
It is clear that the combination of a global solution with a regional solution using the full covariance information will have an impact on all site coordinates, even on those of the global solution. In our study the biases (according to Figure 7.5) are below 0.5 mm for all European global sites for a combination interval longer than 2 weeks.

One might argue, in analogy to the situation of the first order reference networks in classical geodesy, that the global site coordinates should not change with the combination of additional regional campaigns. In this case we have to perform a *hierarchical* least-squares adjustment. We obtain the coordinates of the regional solution by introducing the results of the global solution as known values into the regional campaign. That means that we have to fix all global site coordinates on predefined values.

- The frequency of the combination:
Typical combination frequencies are ranging from one day to a year. From the point of practicality it is of course much easier to work with NEQs, which are already a product of a (weekly or monthly) combination, than to work with daily NEQs. On the other hand we lose information concerning the site velocities if the combination intervals are too long (e.g. combination of annual solutions).

For some applications it may be useful to perform the combination more frequently. The IGS Analysis Centers for example decided to compare their coordinate results including the full covariance matrix using the SINEX format on a weekly basis to be consistent with the generation of the other official IGS products and because of the fact that the handling of the site velocity is not critical for a weekly combination.

7.2 Combination of Global Solutions of the IGS Analysis Centers

At the 1994 IGS workshop *Densification of the IERS Terrestrial Reference Frame through Regional GPS networks* (JPL, Pasadena, Dec. 1994) it was decided to start a pilot project to proof the concepts of a *distributed processing*.

A test format of a software independent exchange format, called SINEX (Version 0.05) [KOUBA 1995A], was defined by a working group. Since GPS week 817 (Sept. 3, 1994) most of the IGS Analysis Centers produce weekly coordinate solutions in the mentioned format. The SINEX format contains - besides the coordinate estimates and their corresponding covariance information - other important informations like site names (DOMES numbers), antenna types, antenna eccentricities, phase center values, receiver types, and information on apriori weights (apriori values and apriori covariance matrix).

In the following we will present results, combinations, and comparisons based on this data material. The analysis methods are simple from the combination point of view (only coordinates are involved). We will show that the covariance factor used for each Analysis Center is essential for the combination.

7.2.1 Analyzed Data

The results presented here are derived from an analysis of all available SINEX contributions of about half a year (between GPS weeks 817 and 845).

A summary is given in Table 7.3. The meaning of the 3-character abbreviation for the Analysis Centers is given in Table 1.1. Three Global Network Associated Analysis Centers (GNAAC) are also included in our comparisons: NCL (University of Newcastle-upon-Tyne), MIT (Massachusetts Institute of Technology), and JPL (Jet Propulsion Laboratories). They produce weekly combined solutions based on the results of the IGS Analysis Centers and a report about the quality of the submissions (e.g. comparisons of individual solutions w.r.t the combination and w.r.t ITRF, comparisons between solutions of different Analysis Centers). The combined data files are available at the global data center CDDIS (Crustal Dynamics Data Information System), the reports are submitted by e-mail (IGSREPORT mail distribution).

7.2.2 Processing Methods

A conversion program `SNXNEQ` was written to convert SINEX files in corresponding normal equation (NEQ) files, which are the input for the `ADDNEQ` program. Apriori constraints, available in the individual SINEX files, are removed (see Section 2.6.1). The equivalence of covariances and normal equations was mentioned already in Section 2.7.

Apriori values for the *covariance factors* are also derived in this conversion step. The used method is simple: For a number of sites (e.g. all sites which are observed by all Analysis Centers or the 13 IGS core sites) we estimate for each Analysis Center i and each week k a mean formal rms $\sigma_{i_k}^*$ of a coordinate estimation. Due to the fact that we deal with free network solutions, this mean formal rms is computed using the main diagonal elements of the corresponding normal equation matrix instead of using the covariance matrix. Selecting the first Analysis Center as the reference $\sigma_{1_k} = 1.0$ (covariance factor 1) we obtain apriori cofactor values for the other centers of the same week: $\sigma_{i_k}^2 = (\sigma_{i_k}^* / \sigma_{1_k}^*)^2$.

We obtain a reliable value σ_i^2 for a center specific covariance factor if we process several weeks and if we take the mean value over this time interval. The value $1/\sigma_i^2$ is the corresponding scaling factor for the normal equations.

We perform two types of combinations:

- (A) combination using the results of a particular Analysis Center only,
- (B) combinations of different Analysis Centers.

For the first solution type (A) a covariance factor is not necessary (same scaling of all covariance matrices of a particular Analysis Center assumed).

For the second solution type (B) the use of cofactor values is essential. This is true especially when combining a small number of different solutions, only. The scaling mentioned above ensures that the different solutions get about the same weights in the combined solution.

Solution type (A) is useful to provide additional information concerning the quality of an Analysis Center. That may lead to different cofactor values.

The NEQ files together with the apriori cofactor values are the input of the combination program `ADDNEQ`. We perform free network solutions (see Section 2.6.4) to judge the quality of the solutions. Assuming that no geocenter coordinates are estimated by the Analysis Centers (translation is fixed), we specify only three rotation conditions (with respect to the ITRF93 coordinates of the 13 IGS core sites) for the definition of the geodetic datum of the individual solutions as well as for the combined weekly solution.

Free network solutions are possible, because constraints in the SINEX files, as already mentioned, are removed.

A special case is the handling of the NGS files. Because NGS is submitting daily files we first combine seven daily normal equation files to a weekly file.

We should mention that the recent SINEX format 1.0 [KOUBA 1996] is also fully implemented in the programs `ADDNEQ` and `SNXNEQ` of the *Bernese Software 4.0*.

7.2.3 Results

7.2.3.1 Repeatabilities

Solutions of type (A) are analyzed in this section. The week-to-week repeatability for a particular Analysis Center is given in Table 7.3. The values are derived from 7-parameter Helmert transformations of the free weekly solutions with the combined solution of the entire time interval. The high quality (internal accuracy or precision) of the weekly network solutions will also be addressed in Section 8.2.1. The correct handling of the velocities can be neglected for the analyzed time span. For the COD series we found an rms improvement of below 0.5 *mm* when applying a velocity model derived from more than 2 years of GPS observations (see Section 8.3).

Remarks in Table 7.3 indicate unresolved problems. We discovered problems with the specified antenna eccentricity values, we found changes of several meters of a priori coordinate values between weekly solutions, inconsistencies of antenna/receiver informations, SINEX format problems, numerical problems with covariance matrices, and files which were binary - instead of ascii - transferred. These circumstances together with the differing long lengths of the comparison intervals makes it difficult to substitute the listed values into a quality value of an Analysis Center.

Nevertheless we find a good agreement of the quality values derived here with those given for the orbits in the weekly orbit comparisons [KOUBA 1995B]. We can also see, that the internal consistency of the combined solutions (MIT-G, NCL-G, JPL-G) is excellent. In Table 7.3 we included a fourth combined solution (COD-G). The computation of this solution is described in the next section.

7.2.3.2 Combination of Different Analysis Centers

For the total time interval of about half a year we produced a combined solution, which we call COD-G. Proper cofactor values are, as already mentioned, essential for the combination of solutions of different Analysis Centers. In a first iteration we used the cofactor values σ_i^2 (derived using the procedure in Section 7.2.2), which is equivalent to give all contributing solutions about the same weight in the combination. The resulting combined solution showed a repeatability which was considerably worse in comparison to the repeatability values of the "best" Analysis Centers. In addition we found quite large residuals between the individual solutions and the combined solution - much higher than we would expect that from comparisons between different Analysis Centers. That was not what we want for a combined solution.

We requested the criterion of a good week-to-week repeatability of the combined solution. This criterion is theoretically independent of the criterion of a good agreement of most of the Analysis Centers. Nevertheless we found from experimental combination solutions that with a better week-to-week repeatability the agreement of most of the Analysis Centers increased, too.

Table 7.3: Analyzed SINEX files: data used, number of sites, and repeatability for each Analysis Center. The repeatability for the components North (N), East (E), and Up (U) is derived from Helmert transformations comparing each free weekly network solution (using *all sites*) with the free combined solution of the entire time interval. The values in the column labeled "*CORE sites*" are derived using only the 13 IGS core sites shown in Figure 1.1 to estimate the Helmert transformations and the rms values. ITRF93 velocities are applied for this case only. The sites PAMA and IISC have been excluded for all Analysis Centers.

Analysis Center	GPS weeks	number of sites	comp.	Helmert rms in <i>mm</i>		remarks
				all sites	CORE sites	
COD	817	74	N	4.8	5.8	-
	-		E	6.3	7.5	
	845		U	11.5	11.2	
EMR	817	39	N	8.8	8.6	excl. 823, 834, 841, 843 TROM (829, 830) KOSG (838)
	-		E	8.4	8.0	
	845		U	14.7	14.5	
ESA	840	59	N	8.4	6.1	-
	-		E	13.4	12.7	
	845		U	30.1	19.1	
GFZ	817	53	N	6.4	6.6	-
	-		E	8.1	12.7	
	845		U	16.8	16.4	
JPL	817	92	N	4.9	4.2	819 excl.
	-		E	6.4	6.1	
	845		U	9.6	11.4	
NGS	821	55	N	14.7	19.2	IICS, MASP, EISL, KELY, TAEJ excl. 826, 843 excluded
	-		E	16.0	13.8	
	845		U	31.3	21.5	
SIO	825	71	N	6.6	9.0	836 wrong site ID 830 excl.
	-		E	7.3	18.3	
	845		U	18.1	23.7	
COD-G	817	106	N	4.4	4.4	-
	-		E	6.1	8.0	
	845		U	12.7	10.6	
JPL-G	837	93	N	3.3	2.4	841, 842 not readable HART, KELY for particular days excl.
	-		E	4.3	3.7	
	845		U	9.6	6.2	
MIT-G	821	142 ^a	N	4.3	4.9	BRAZ, KELY, KOSG, HART for particular days excl.
	-		E	6.0	6.3	
	845		U	14.0	9.8	
NCL-G	817	104	N	5.2	5.4	817, 818, 819 different scaling
	-		E	6.7	7.5	
	845		U	13.7	12.3	

^aadditional PGGA sites included

For the presented combination solution COD-G we used the scaling values listed in

Table 7.4. In comparison to the apriori values σ_i^2 we found values which are for the ESA solution by a factor of about $\sqrt{3}$, for the EMR and GFZ solutions by a factor of $\sqrt{2}$, and for the NGS solution by a factor of about $\sqrt{5}$ higher. Alternative methods for the estimation of cofactor values are addressed at the end of this section.

Table 7.4: Scaling factors $1/\sigma_i^2$ for normal equations used for the combination of the different weekly solutions.

Weekly IGS Analysis Center Solutions						
COD	EMR	ESA	GFZ	JPL	NGS	SIO
1.0	8.0	3.0	2.5	7.7	1.0	7.3

Combined Weekly Solutions			
COD-G	MIT-G	NCL-G	JPL-G
0.2	7.3	1.2	0.2

In addition to the creation of the COD-G series we produced a combined solution called MEAN consisting of the contributions of the combined solutions only, to compare the results of the GNAACs. Therefore we included the cofactor values used to produce this "combined-combined" solution in Table 7.4. These values are derived using the simple approach described in Section 7.2.2. The JPL-G solution was not included because of the very short time interval available.

In the following we will give some examples. We concentrate on the results for the vertical components, because this coordinate component is the most critical one. The comparison of the free solutions is done, identical to the previous section, using 7-parameter Helmert transformations.

A comparison of the results of a particular site and a particular coordinate component (WETT, up component) is shown in Figure 7.6. The differences between the Analysis Centers are below 4 *cm*, the differences with respect to the combined solution are below 2 *cm*.

An unweighted rms is computed from the residuals of all contributing sites of a particular Analysis Center. Figure 7.7a shows these values for the vertical coordinate component. Most Analysis Centers agree for all weeks processed on the 2 *cm* level. Larger differences may be found only for the Analysis Centers ESA and NGS.

The agreement of the combined solutions of the Associated Analysis Centers (and the COD-G solution) shown in Figure 7.7b, is not only excellent, the stability over the interval of comparison is very impressive, too.

For each solution series in Figure 7.7 we compute from the entire time interval a mean rms. Table 7.5 lists also the values for the horizontal components.

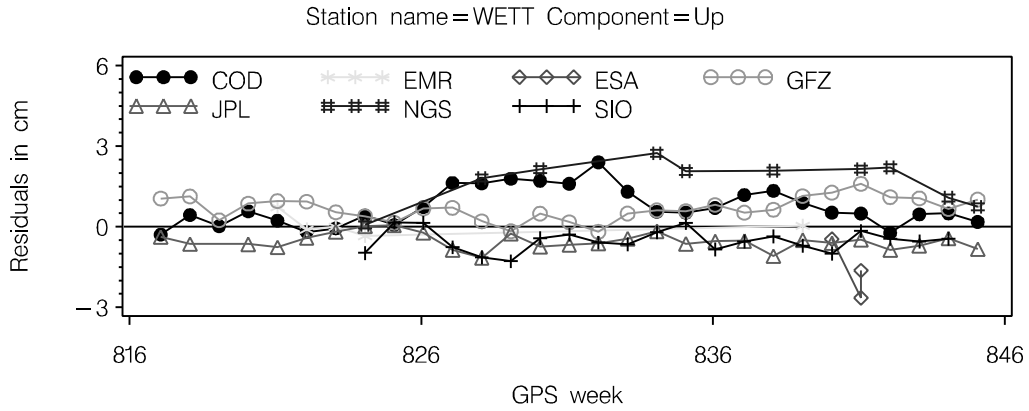


Figure 7.6: Residuals in vertical direction for site WETT.

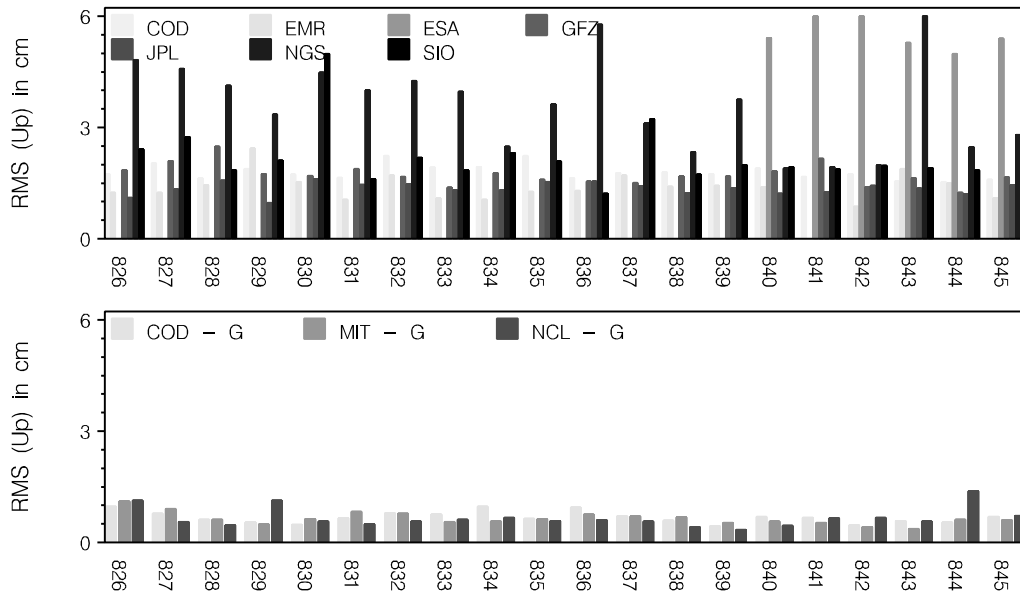


Figure 7.7: (a) Unweighted rms values for vertical components after a 7-parameter Helmert transformation comparing the weekly free Analysis Center results with the weekly combined COD-G solution. All sites (with the exception of the problem sites of Table 7.3) are used. (b) The combined solutions (-G) are compared in the same way with the "MEAN" solution.

Table 7.5: Mean rms of coordinate components derived from the comparison (using 7-parameter Helmert transformations) of each Analysis Center with the combined COD-G solution (derived from the GPS weeks 826-845). In the lower part of the table the rms values obtained from the comparison of the combined (-G) solutions with the "MEAN" solution are given (derived from GPS weeks 817-845).

Center	# Weeks	Component	Mean rms in mm
COD	21	North	5.9
		East	5.7
		Up	17.8
EMR	20	North	5.7
		East	8.8
		Up	14.3
ESA	6	North	10.8
		East	13.3
		Up	56.4
GFZ	21	North	6.0
		East	8.3
		Up	17.3
JPL	21	North	4.6
		East	5.2
		Up	13.5
NGS	21	North	24.3
		East	29.6
		Up	60.3
SIO	21	North	6.2
		East	6.5
		Up	21.5
COG-G	29	North	2.0
		East	2.5
		Up	6.6
MIT-G	25	North	2.4
		East	3.0
		Up	6.2
NCL-G	29	North	2.3
		East	2.7
		Up	7.1

We may conclude that the agreement between the different IGS Analysis Centers is only slightly worse than the week-to-week agreement of a particular Analysis Center (see Table 7.3). We may also conclude that the influence of a different combination procedure (mainly the cofactor values used) is clearly below the 1 cm level. This may seem small for a weekly, global coordinate estimation. In view of the high internal (week-to-week) precision and also the excellent agreement between the Analysis Centers, however, the impact of the combination strategy is not negligible. Other combination strategies, like the *variance-covariance component estimation* (mentioned already in Section 7.1.5), allow an estimation of cofactor values for the Analysis Centers together with the combined coordinate estimation. This iterative

method results in non-negative and reliable variance components only, if a large number of observations (coordinate estimates of several weeks for each Analysis Center) is used. One week is therefore critical. Furthermore the expense of computing-time is considerable in the case of processing several weeks including the full covariance information of each Analysis Center. Other proposals are made by DAVIES AND BLEWITT [1995].

In addition to the problems listed in Table 7.3 we should mention that *systematic differences* between individual solutions can be detected in our comparisons. The modeling of elevation dependent antenna phase center variations has mainly an effect on the station heights. Whereas most Analysis Centers do not apply any model, the CODE processing center takes the Rogue/TurboRouge antenna as reference (no modeling of elevation dependent phase center variations) and applies the difference of the Schupler values (estimated from chamber tests) [SCHUPLER ET AL. 1994] for other antenna types (e.g. Trimble in ZIMM and JOZE) [ROTHACHER ET AL. 1995; ROTHACHER ET AL. 1996]. Comparisons with SLR/ITRF results shows that this modeling removes the major effect of the phase center variations between different antennas.

The big effect on the station heights is shown in Figure 7.8 for the site JOZE. We find differences of 5-8 cm. The effect for ZIMM is even bigger (up to 12 cm).

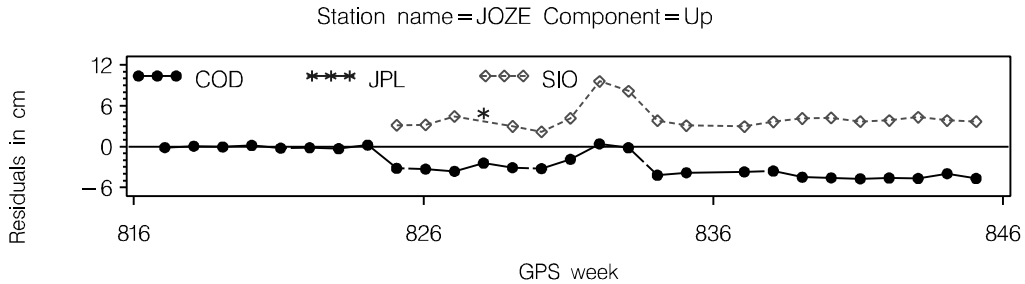


Figure 7.8: Residuals in vertical direction for site JOZE.

8. Selected Results from Multi-Annual GPS Solutions

In the following sections we give an overview of results achieved through an analysis of more than two years of IGS data. We focus on those parameters which take profit out of a long time interval, namely coordinates, velocities, center of mass, and satellite antenna offsets. Because of the high degree of correlation between coordinates and velocities on one hand and Earth rotation parameters on the other hand, we add the Earth rotation to our list.

8.1 Multi-Annual Combined Solutions: A Description

Combined multi-annual solutions with the following characteristics were performed:

- 33 months of GPS data were analyzed (based on the normal equations of non-overlapping 3-days-solutions) from April 1993 to the end of 1995. An idea of the parameter statistics and the involved number of unknowns is given in Figure 5.1.
- All coordinates were solved for; the geodetic datum was defined by forcing the free coordinate solution to have *no translation* and *no rotation* (for a selection of sites) with respect to the ITRF93 (see Section 2.6.4). We set up 4 conditions equations for the six sites which agree best with the ITRF93 (KOSG, WETT, TROM, FAIR, GOLD, YAR1). A z -rotation condition is necessary to define the orientation (see Figure 2.7), the x - and y -rotation can be determined by GPS. Three translation conditions are necessary because the geocenter coordinates are included as unknown parameters.
- *Horizontal* site velocities were solved for if the available data span is longer than half a year. All other velocities were constrained - if available - to ITRF, otherwise to NNR-NUVEL1 [DEMETS ET AL. 1990; ARGUS AND GORDON 1991]. The geodetic datum might be defined in different ways: Constraining the velocity of the site WETT to the ITRF93 values is one option, an alternative way is to apply no-net-rotation conditions similar to those for the site

coordinates. An opening of the vertical velocities is only realized in Section 8.3.2.

8.2 Coordinates

8.2.1 Coordinate Repeatabilities

The Global Positioning System (GPS) is first and foremost an *interferometric technique*. For regional networks this statement means that differences between sites are significantly better determined than their absolute positions relative to the Geocenter.

Global networks are connecting the sites around the globe, which implies that the higher quality of the difference information can be transferred to a "global" but not a "geocentric" coordinate accuracy.

The comparison of the results of each individual solution in a sequence with the combined solution gives an idea about the quality of each individual solution (*repeatability study*).

The geodetic datum of free network solutions, as described above, is mainly defined by the observations. A small number of observations on a specific day for one of the six reference site may cause a mis-orientation of all sites for that day with respect to the other days. This is also a reason to focus on *baseline results* rather than on site *coordinate repeatabilities*, in the case of free solutions.

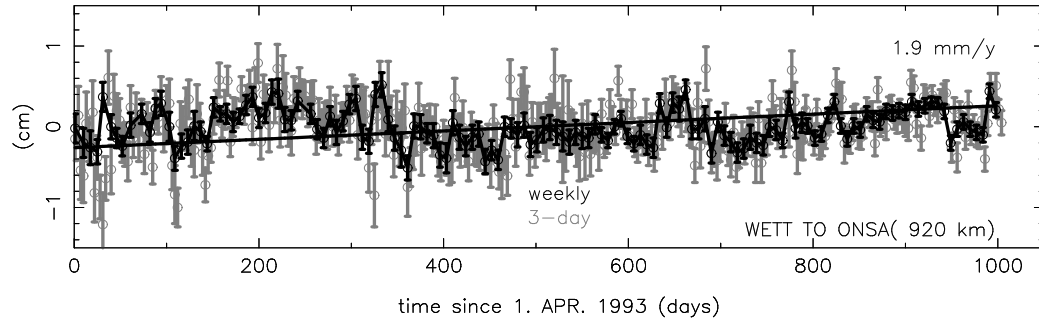
A comparison of the coordinate components is only useful if the geodetic datum is equally well-defined for all individual solutions. Free solutions can only be compared if a Helmert transformation is used to take out differences in the datum definitions. Coordinate repeatabilities are shown in Section 8.2.2.

8.2.1.1 Baseline Length

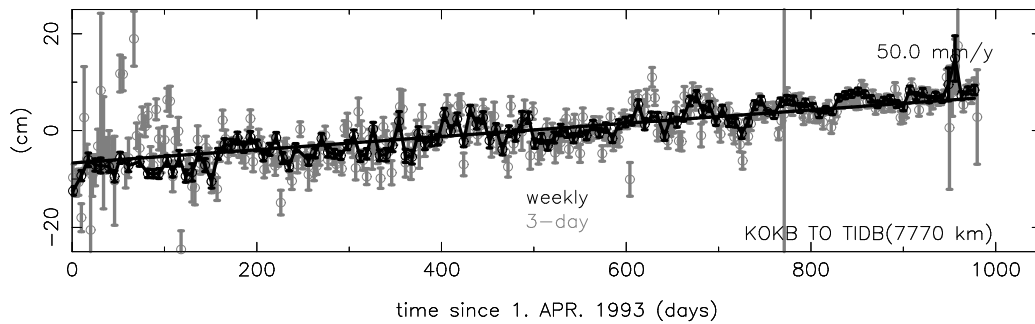
Precision of 3- and 7- Days-Solutions

The baseline length is usually the best determined value of a baseline. Figure 8.1 shows an example of two different baselines, (a) a relatively short European baseline WETT-ONSA and (b) the 7770 km baseline KOKB-TIDB connecting two sites located on different geotectonic plates. In the second case the relative motion of the two sites, estimated by the combined solution to 50 mm/y, is clearly visible, whereas the European baseline shows only a very small, but still significant, relative motion (observe, that the two examples in Figure 8.1 are not in the same scale).

To estimate the quality of each sequential solution we have to take into account only the variation with respect to the straight line. The quality of the two kinds of solutions, weekly solutions (solid) and 3-days-solutions (gray), points out the smoothing effect due for the longer combination interval according to eqn.(6.3-5).



(a) European baseline WETT-ONSA



(b) Baseline KOKB-TIDB

Figure 8.1: Baseline length development for two different baselines. The solid line represents the weekly estimates, the gray line results from the 3-days-solutions. The error bars are the $3\text{-}\sigma$ rms values derived from the estimated formal rms of the individual coordinate estimates. The straight line is not a line fit through the lengths residuals, but a result of the coordinate velocity estimation of the combined multi-annual solution.

The quality of a single baseline length estimation (for 3-days-solutions and weekly solutions) as a function of the baseline length is the topic in Figures 8.2. We analyzed all baselines relative to one of the 13 IGS core sites. To get a realistic rms estimation we excluded only the baselines which were observed on fewer than 100 days during the total time interval of about 1000 days.

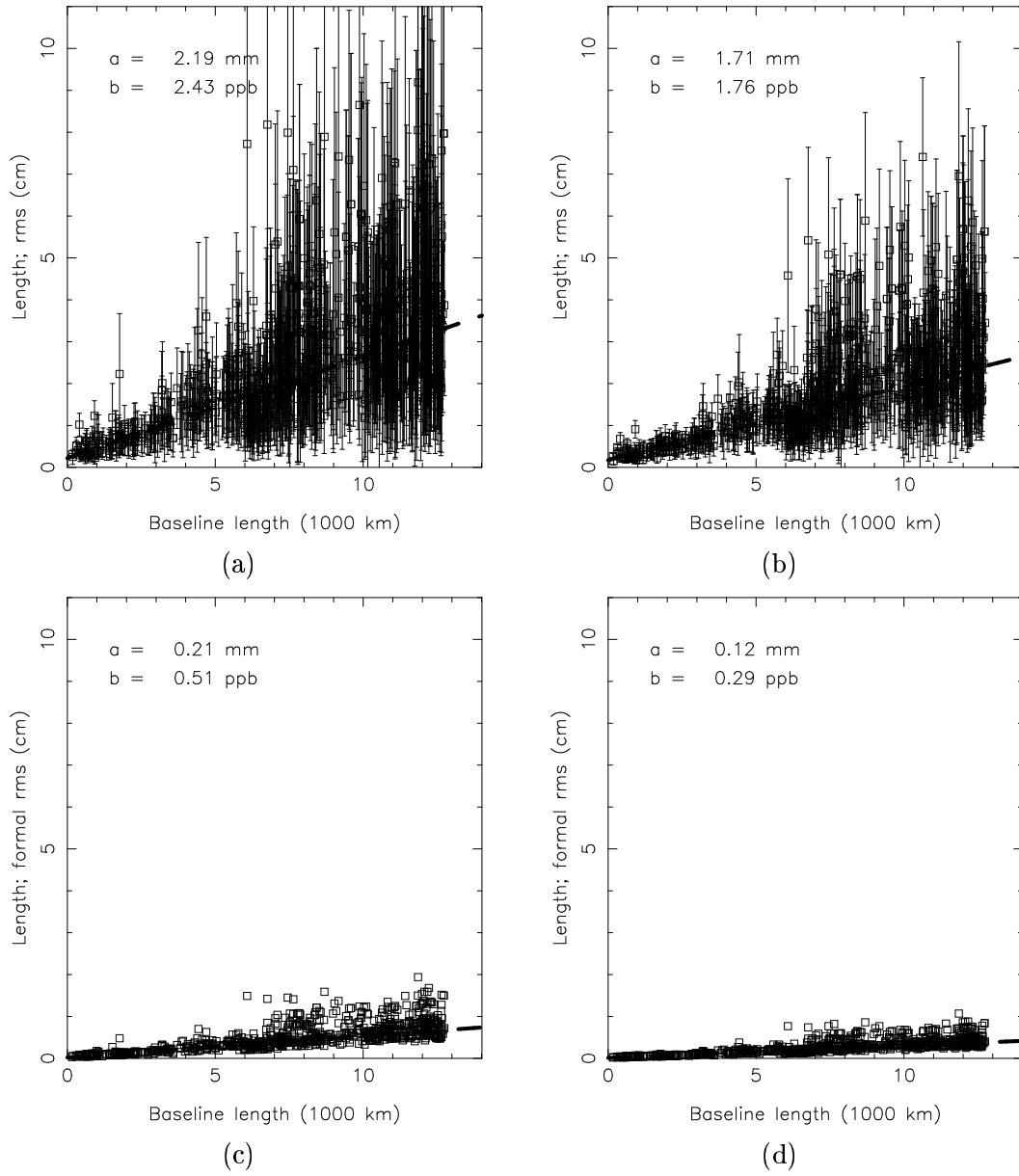


Figure 8.2: Baseline length repeatabilities of (a) 3-days-solutions and (b) weekly solutions. The repeatabilities in Figures (a) and (b) are derived from the unweighted residuals with respect to the mean. The mean estimated formal errors in Figures (c) (3-days) and (d) (weekly) are given in Figures (a) and (b) as $3\text{-}\sigma$ error bars.

The Figures 8.2a and 8.2b show the unweighted rms of a single 3-days baseline length estimation and a weekly baseline length estimation, respectively. The error bars are representing the mean $3\text{-}\sigma$ formal rms of a single baseline length estimation. In other words: We summarized the information of Figure 8.1a or 8.1b to a single data point with a corresponding error bar. The mean $1\text{-}\sigma$ formal rms values are plotted in the Figures 8.2c and 8.2d. We will focus on the relation between the mean formal rms estimation and the repeatability rms later on.

A site with many outliers or many data problems affects all baselines containing this site. Therefore the line fit was computed using also the information of the mean formal rms values of each baseline. Using an offset parameter a and a rate parameter b we may compute the mean quality σ_L of a baseline estimation of the length L [1000 km] to:

$$\sigma_L [mm] = a [mm] + b [ppb] \cdot L [1000 km]. \quad (8.2-1)$$

For the baseline WETT-ONSA in Figure 8.1 we found for example a repeatability of 2.3 mm for a weekly estimation. Using the determined coefficients a and b of Figure 8.2b we get a baseline length repeatability for a 920 km baseline of about $1.71 + 1.76 \cdot 0.92 = 3.3$ mm. This indicates that our example is optimistic. That is not true for the baseline KOKB-TIDB in Figure 8.1. The quality of a weekly estimation is of the order of 25 mm. This is considerably worse than the 15 mm we would expect for a 7770 km baseline according to eqn. (8.2-1).

Generally, we have to report larger residuals for the first 200 to 300 days (data of 1993) for the longer baselines. The increasing accuracy with time is mainly an effect of the *growing number of sites* and the densified global network. We should mention that three to four years ago (prior to the IGS activities) the achievable precisions were worse by a factor of more than 10 [BEUTLER ET AL. 1989].

Table 8.1 summarizes the quality of the baselines for the years 1993 up to 1995 for 3-days-solutions as well as for weekly solutions. The improvement from 1993 to 1995 is a factor of about 2.

A comparison between results of the 3-days-solutions and the weekly solutions (the values in row (3/7) vary between 1.4 and 1.8) proves the higher quality of the weekly solution. The values in row (3/7) vary between 1.4 and 1.8, a factor which agrees according to eqn. (6.3-5) quite well with $\sqrt{7/3} \approx 1.5$.

The fact that the formal rms is roughly proportional to the derived repeatability value was already demonstrated at the end of Section 2.8. In our case the proportionality factor is quite stable ($\approx 5.0 - 6.0$).

Table 8.1: Repeatability and mean formal rms of the baseline lengths for different time intervals.

years (interval)	# baselines (# Stat.)	solution type	Repeatab. rms		Mean formal rms		b/b'
			a [mm]	b [ppb]	a' [mm]	b' [ppb]	
1993 (0.75 yr)	383	3-days	0.00	4.63	0.28	0.79	5.9
	33	weekly	0.09	2.96	0.16	0.44	6.7
ratio 3-days / weekly: 3/7			1.8		1.8		
1994 (1.0 yr)	520	3-days	1.51	2.96	0.45	0.62	4.8
	44	weekly	1.07	2.00	0.22	0.35	5.7
ratio 3-days / weekly: 3/7			1.5		1.8		
1995 (1.0 yr)	765	3-days	2.24	1.93	0.14	0.44	4.4
	65	weekly	1.77	1.41	0.08	0.24	5.8
ratio 3-days / weekly: 3/7			1.4		1.8		
1993-1995 (2.75 yrs)	837	3-days	2.19	2.43	0.21	0.51	4.8
	71	weekly	1.71	1.76	0.12	0.29	6.1
ratio 3-days / weekly: 3/7			1.4		1.8		

Systematic Effects

Systematic effects may be detected relatively easily in the baseline lengths because of the high quality. The invariance of the baseline length with respect to translations and rotations allows furthermore an analysis of free global network solutions. We preferred to analyze the residuals of the 3-days-solutions rather than the weekly solutions because of the higher data density. In Figure 8.3 we selected 5 European baselines (always to the site WETT) of different baseline lengths ranging from 600 *km* to 3200 *km*.

An iterative approach [BROCKMANN 1990] was applied to determine significant frequencies, amplitudes and phase delays. In a first iteration step a spectral analysis detects the most significant frequencies. A least-squares adjustment solves for the unknown frequencies, amplitudes, phase delays, and also for an offset and a drift using the detected frequencies as a priori values. Because of the non-linearity of the problem we have to iterate the least-squares adjustment until no significant changes in the estimates are seen. The residual spectrum may serve as a new input for the spectral analysis for the detection of additional significant periods. The final frequencies and amplitudes are always the result of a least-squares adjustment.

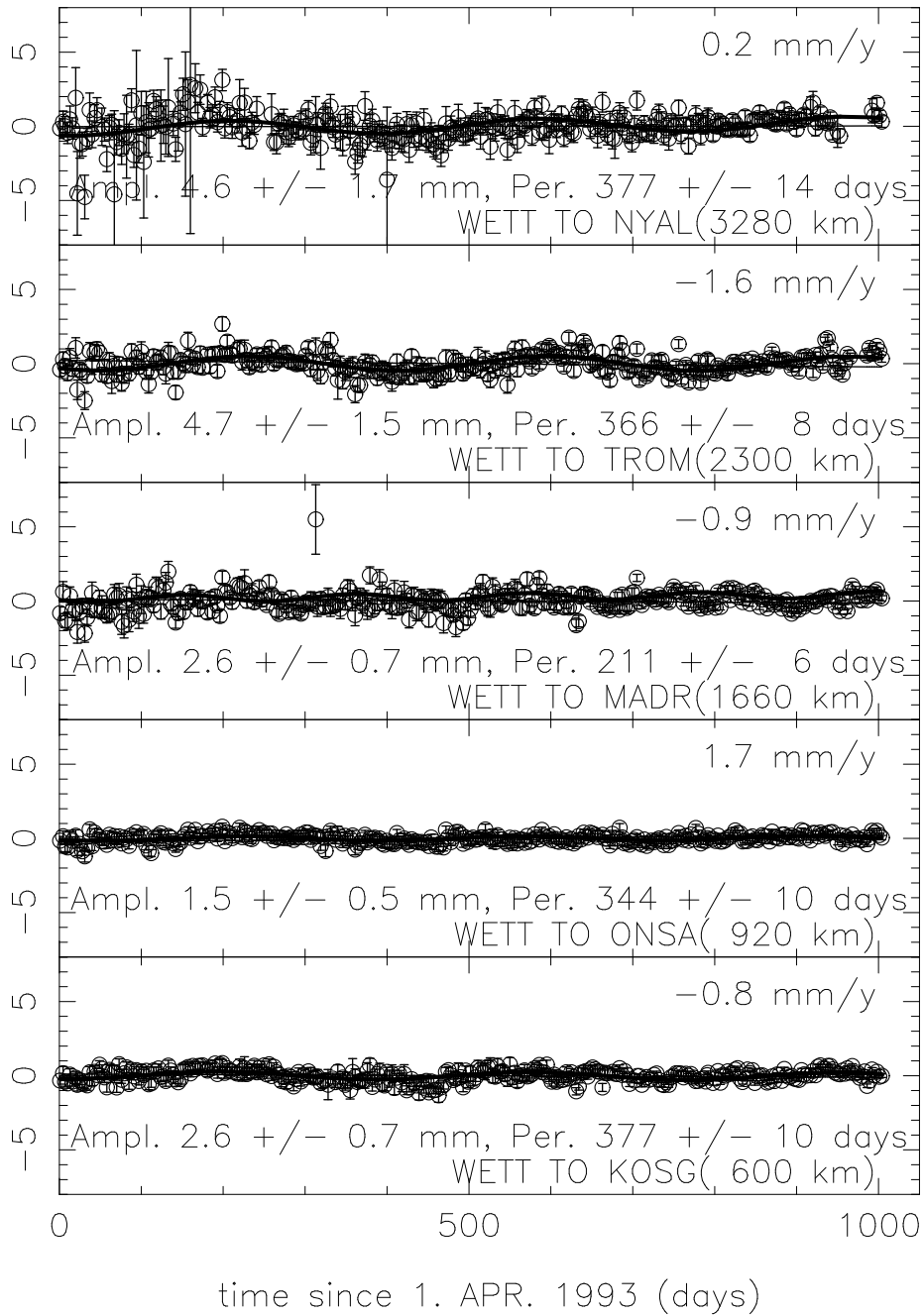


Figure 8.3: Systematic effects (in *cm*) in European baselines of different lengths.

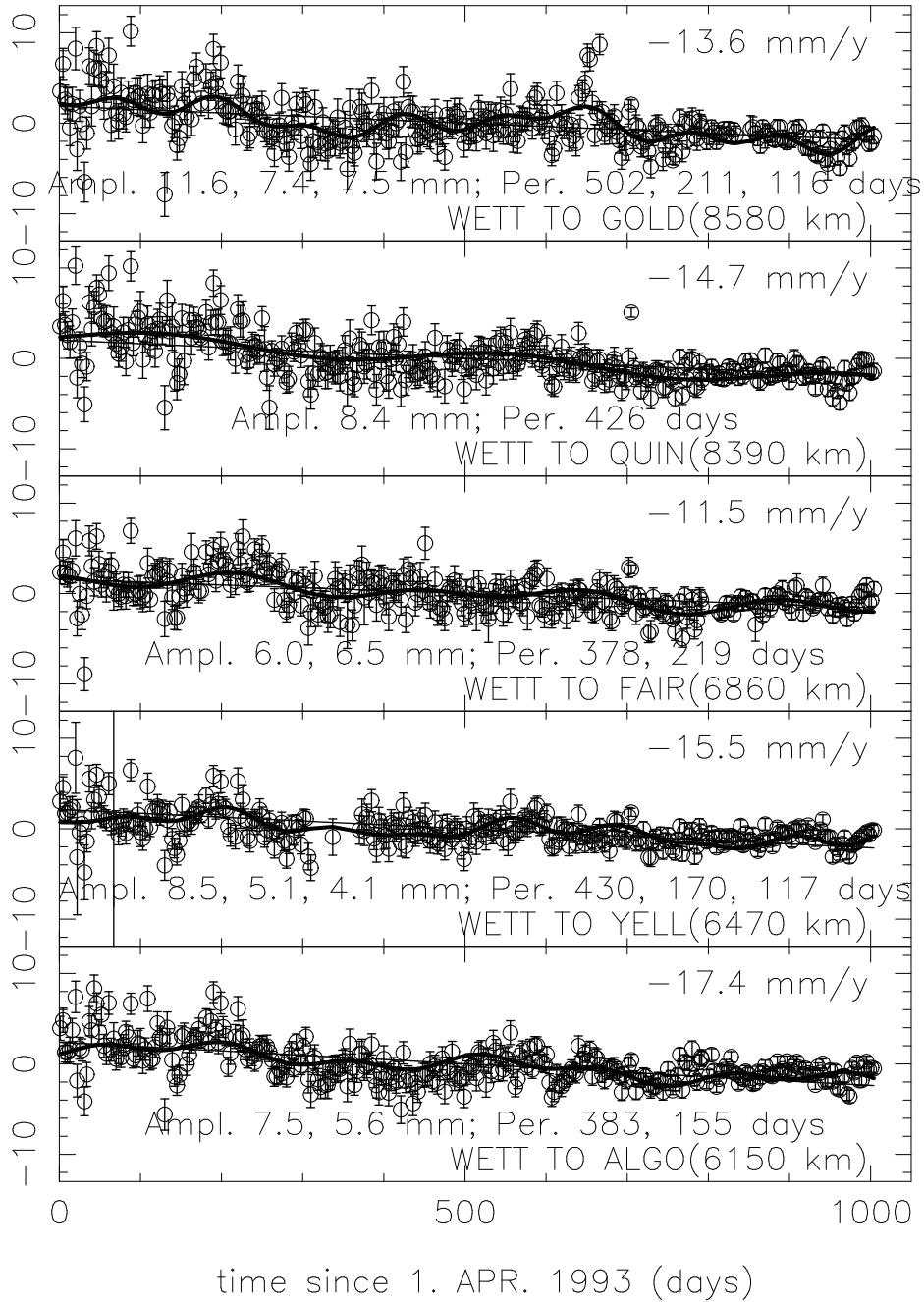


Figure 8.4: Systematic effects (in *cm*) in the baseline length for baselines between North America and Europe.

For most European baselines (Figure 8.3) we are able to detect a significant annual period. Only for the baseline WETT-MADR the semi-annual signal is larger than the annual signal. The estimated amplitudes are increasing with baseline length, which may indicate a deficit in the tidal model. For the coastal sites TROM and NYAL ocean loading effects may play an important role, too. We will come back to this point when focusing on variations in the north-, east- and up-components.

Examples for baselines between North America and Europe are given in Figure 8.4. The most significant frequency for most of the baselines is somewhat longer than an annual variation (about 380 - 430 days). The formal rms of the period is about 20 days.

The estimated amplitudes are ranging from about 6-7 *mm* for the 6000 *km* baselines to about 9-11 *mm* for the 8000 *km* baselines.

The second strongest signal has a period close to half of that of the strongest signal (170 days to 220 days, rms of 5 days). The amplitudes of 5 to 6 *mm* are estimated with an uncertainty of below 3 *mm*, which is quite near to the limits of significance.

Slightly below the significance level are periods around the well known 14 days tidal frequency and in some cases also periods of about 60 days (see also Figure 8.5).

The results are far from being conclusive. We interpret the systematic effects in the baseline length as a first clue for an imperfect tidal model. Our apriori model is identical with the step 1 correction of the recommended IERS [IERS 1992] tidal model. The correction of the step 2 (station heights are corrected for the frequency dependent K_1 tide) and the correction of the rotational deformation due to polar motion is not applied.

The "pole tide" correction cannot explain any variations in the baseline length. A constant offset of 3.8 *mm* for the baseline WETT-GOLD is the maximum value for the inter-continental baselines. The European baseline lengths are affected by ≤ 0.5 *mm*.

The step 2 corrections of the station heights are showing annual variations in the baseline lengths with amplitudes of up to 3.5 *mm* (WETT-NYAL or WETT-FAIR). An attempt to correlate the step 2 corrections with the estimated variations was not successful. Please note that the scale of each individual solution was not constrained. The variations of the global scale seem to have a more important influence on the baseline length.

8.2.1.2 Precision of Baseline Components

North-, East-, and Up-Components

The differences in quality of the north-, east-, and up-baseline components are due to satellite geometry. Table 8.2 shows the quality of the coordinate components for the 3-days-solutions and for the weekly solutions. As opposed to Table 8.1 we make no distinction between the quality for different years. Each individual free solution (3- or 7-days-solution) was compared with the combined coordinate set after a 7-parameter Helmert transformation. The transformation parameters were estimated using all sites of the individual solutions.

Table 8.2: Repeatability of the north-, east-, up-, and length- baseline components.

component	solution	Repeatab. rms	
		a [mm]	b [ppb]
North	3-days	2.57	1.24
	7-days	1.94	0.88
East	3-days	3.30	2.61
	7-days	2.51	1.80
Up	3-days	11.19	2.45
	7-days	8.16	1.74
Length	3-days	2.19	2.43
	7-days	1.71	1.76

The north component is the best determined. East components are of excellent accuracy for short baselines. The derived formal errors, displayed in Figure 6.5 as error ellipses, underline this statement. The error growth with baseline length is of the order of the error growth of the up-components. We also see the rule of thumb confirmed that the errors in the heights are about 2-3 times larger than those of the horizontal components.

An example may help to illustrate the listed quantities in Table 8.2: For a 1000 km baseline, as it would result from a typical weekly SINEX contribution of the CODE Analysis Center, we obtain using eqn. (8.2-1): 2.8 mm in north, 4.3 mm in east, 9.9 mm in up, and 3.5 mm in the baseline length.

Systematic Effects

We mentioned already that systematic effects from an unmodeled tidal signal or from ocean loading might remain in the time series of our baseline results. Tides affect mainly the height components. The results of a spectral analysis for periods between 6 and 80 days are given in Figure 8.5 for the baseline WETT-TROM. The amplitude of the 14 days period is estimated by the least-squares adjustment with

6.2 ± 2.6 mm slightly above the level of significance. Significant signals are found in Europe only for the baseline WETT-NYAL. The high noise of the height estimates (for 3-days-solutions we obtain from Table 8.2 for a 2300 km baseline a rms value of 17 mm) in comparison to the expected tide signals (e.g. 2-3 mm amplitudes from the (annual) step 2 correction) makes a verification of the tide model difficult.

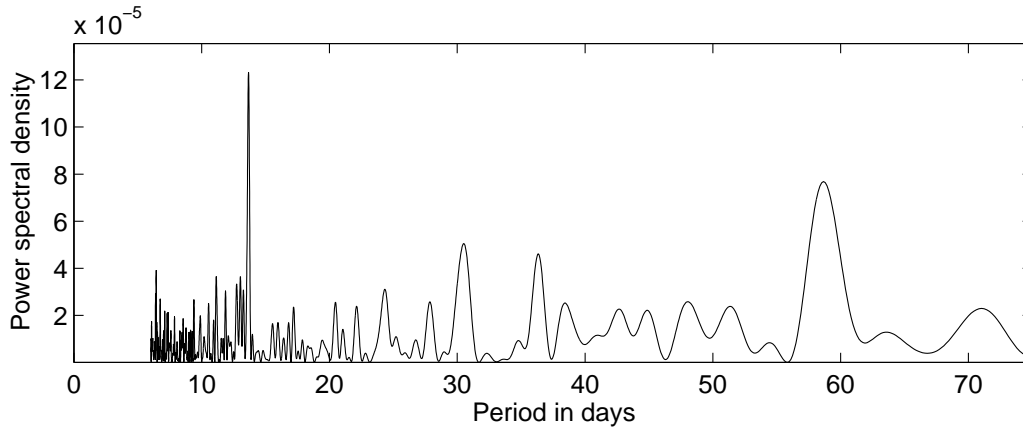


Figure 8.5: Power spectrum of the height components of the baseline WETT-TROM.

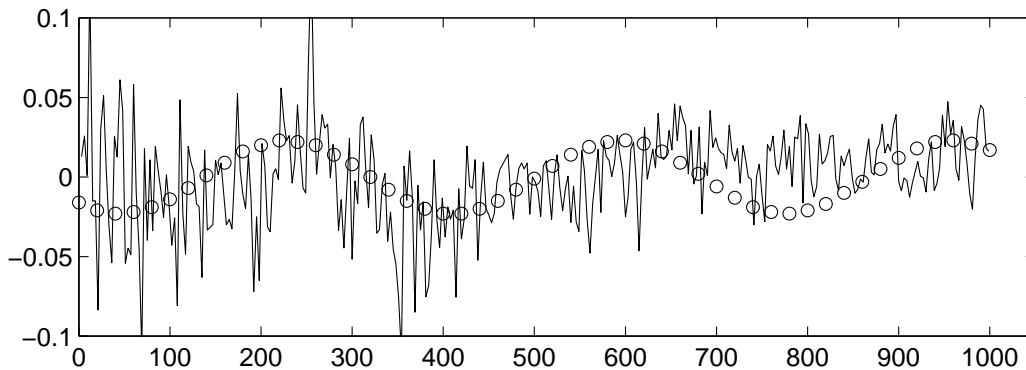


Figure 8.6: Height repeatability of the baseline WETT-QUIN in meter (solid line). For comparison we refer to the (not applied) step 2 corrections (circle) of the IERS tide model.

The situation for longer baselines is different, because the effects are higher. For the inter-continental baselines for example the step 2 corrections would reach amplitudes

of up to 25 mm. As opposed to the European baselines the step 2 corrections for the heights may explain the height residuals in the first 400 days quite well (see Figure 8.6). Nevertheless we cannot explain the full amount of the variations with the K_1 term correction. Signals for the mentioned 14 days period are also found, but with amplitudes of about 8.0 ± 5.0 below the level of significance. With longer time series and increasing accuracies it is only a question of time to be able to extract tidal corrections or ocean loading signals from the coordinate results.

A spectral analysis of the north- and east components also yields significant periods, but there is much less strength in the power spectrum and the estimated amplitudes are smaller, too. For the WETT-TROM baseline for example we found for the north-component a period of 363 ± 12 days and an amplitude of 3.3 ± 1.2 mm. We believe that the small signals in the horizontal components are a consequence of datum definition problems of the individual solution.

8.2.2 Accuracy of Global Site Coordinates

The comparison of the GPS coordinate estimates with results of other space techniques is the only way to assess the accuracy of the GPS technique. The ITRF93 coordinate and velocity set [BOUCHER AND ALTAMIMI 1994] as a "mixture" of results from VLBI, Laser, Doris, and GPS analyses is well suited for such a purpose. We have to keep in mind, however, that GPS results are contained in the ITRF (e.g. ITRF93).

8.2.2.1 IGS Core Sites

The coordinate quality between our GPS solutions and the ITRF93 values of those 13 IGS sites, which are fixed or tightly constrained by the IGS Analysis Centers for the determination of the orbits and the Earth rotation parameters, are of special interest. Figure 8.7 shows the estimated differences, separately for the north-, east-, and up-components, for the 2.5-years-solution and for 5 semi-annual solutions. The variations of the semi-annual solutions should give a first impression of the precision (internal reliability or consistency) of the combined solution.

All 6 solutions were performed as free network solutions according to Section 2.6.4. As mentioned already in the introduction of this section, we used the 6 sites, which we believe to be established best in the ITRF93, to define the geodetic datum of the combined solutions. We only solved for (horizontal) velocities in the 2.5-years-solution. These velocities are introduced in the semi-annual solutions as known and they are also used to compare the coordinates, without further Helmert parameters, at the common epoch 8.8.1994 (mean epoch of the data span).

Once more the high *consistency* of the north components and the larger noise in

the height components is confirmed. We also observe a moderate quality of isolated sites such as HART. The differences between the GPS solutions (2.5-years and semi-annual-solutions) and the ITRF93 values are significantly in many cases. If these differences are real, caused e.g. by errors in the local ties, has to be verified in the future. A considerable error in the height component of about 5 cm was found for example in the local tie of TIDB with the help of such comparisons.

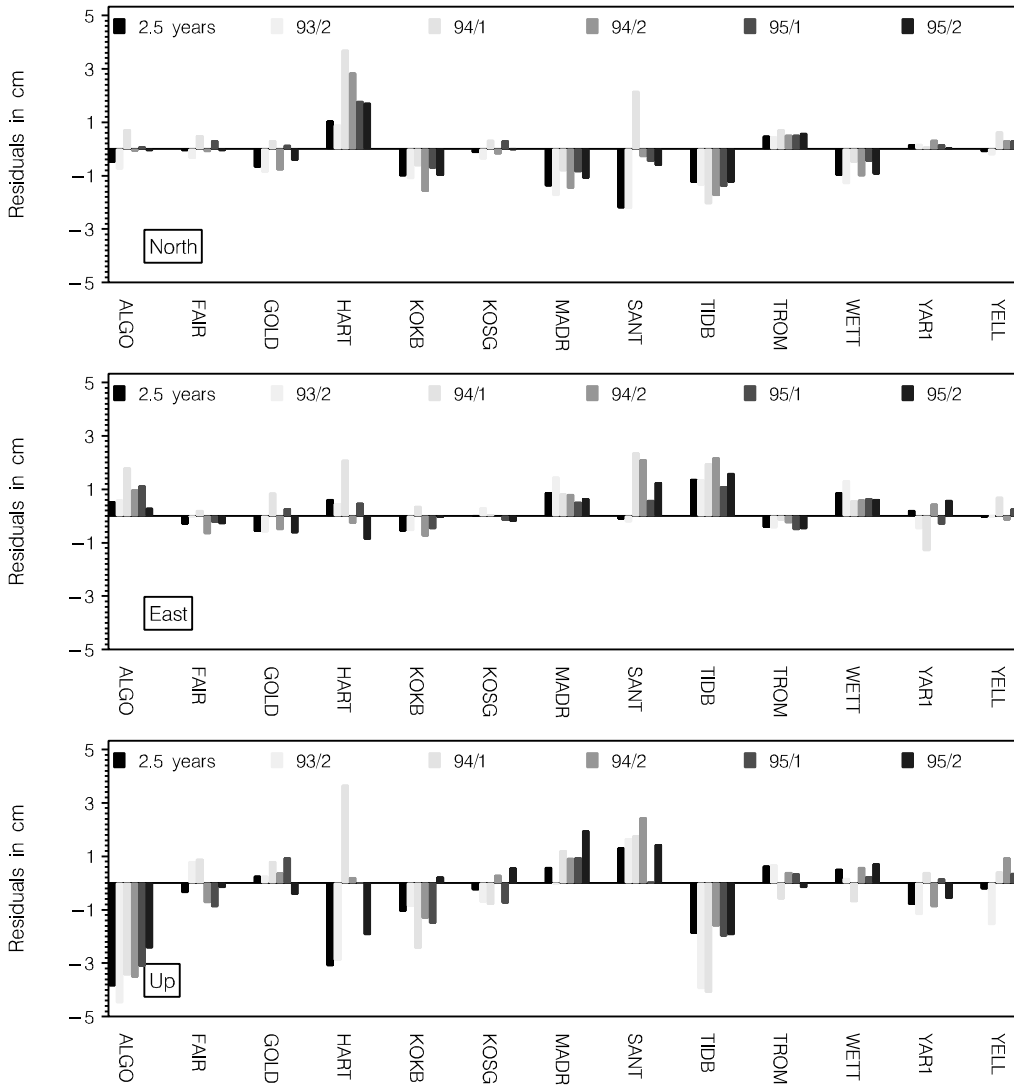


Figure 8.7: Coordinate differences of semi-annual solutions for the 13 IGS core sites with respect to ITRF93 for the components north, east, and up.

8.2.2.2 Europe

The same coordinate differences as above for the same 6 solution types are given in Figure 8.8 for 13 European sites. Most of them also collocated with other space techniques. The differences in the horizontal components are very similar from one semi-annual solution to the next.

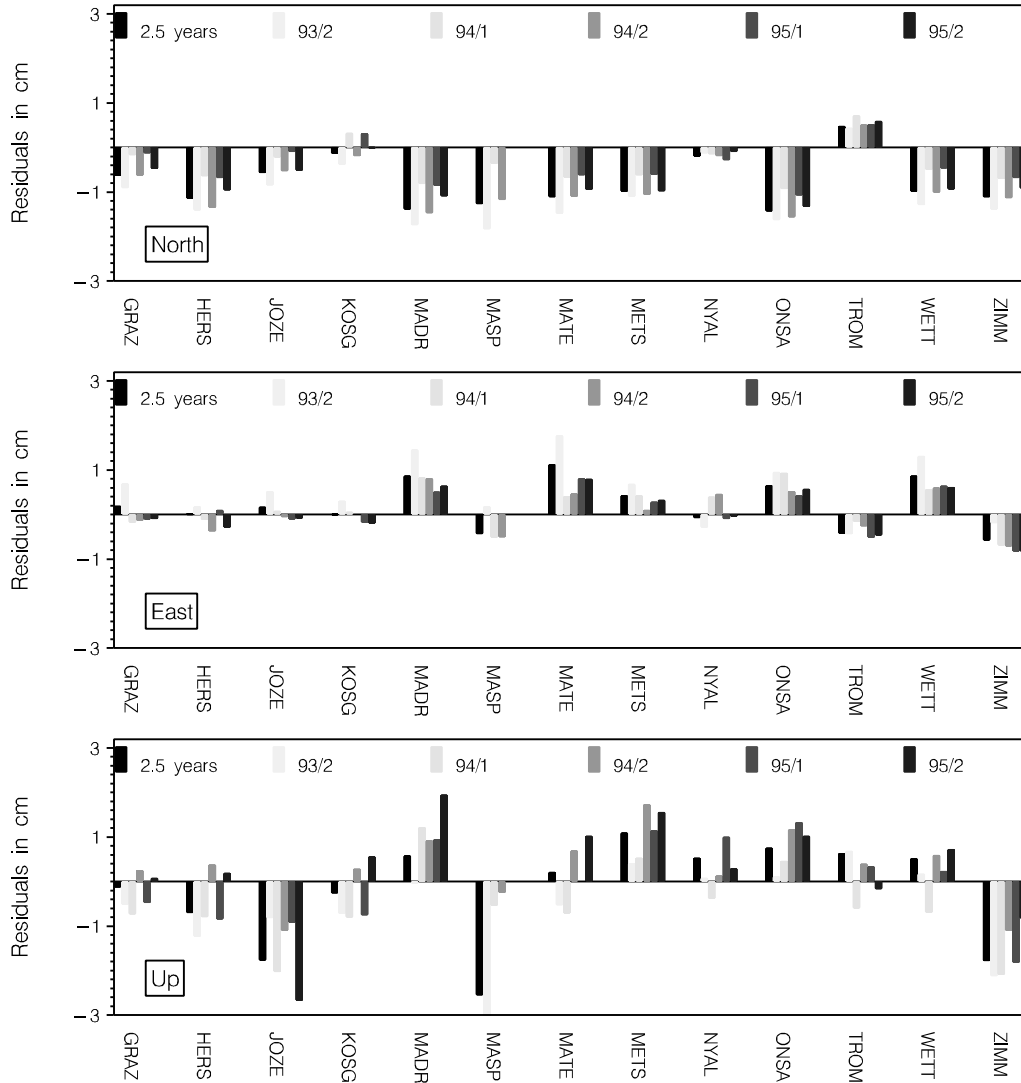


Figure 8.8: Coordinate differences of semi-annual solutions for 13 European sites with respect to ITRF93 for the components north, east and up.

This is also documented in an impressive way in Table 8.3. The consistency of a semi-annual solution is of the order of 1-2 *mm* for the horizontal components, of the order of 4 *mm* for the heights.

The systematic offsets, especially in the north components in Figure 8.8, are essentially removed by a Helmert transformation. Helmert transformations were applied in Table 8.3.

We should note, that the velocity model used is important for such comparisons. The GPS sets were propagated to the epoch of comparison (8.8.1994) using the GPS-derived velocities to achieve the best consistency. The velocity differences with respect to the ITRF93 are small, as we will see below, but nevertheless significant.

Table 8.3: Rms values of 7-parameter Helmert transformations of semi-annual solutions w.r.t. the 2.5-years-solution.

solution	Rms of Helmert transformation in [<i>mm</i>]					
	CORE			EURO		
	North	East	Up	North	East	Up
93/2	1.9	3.0	7.9	0.8	0.9	4.2
94/1	3.3	5.5	12.0	1.8	2.4	4.0
94/2	6.3	5.7	8.2	1.3	2.1	4.0
95/1	4.6	3.2	10.7	0.6	0.9	4.2
95/2	3.1	4.2	7.8	0.5	0.8	4.2

8.2.2.3 Comparisons with ITRF

The ITRF coordinates of the 13 IGS core sites are used by all IGS Analysis Centers to define the geodetic datum of the daily solutions and to ensure that the products (Earth rotation and orbits) are given in a well-defined reference frame. In 1993 the ITRF91 coordinate and velocity set was used, in 1994 the ITRF92, and in 1995 and 1996 the ITRF93.

Table 8.4 shows the improvement of the ITRF from the point of view of our GPS solutions. The recently published ITRF94 coordinates [BOUCHER AND ALTAMIMI 1996] are also included in this comparison. Without HART, ALGO, and SANT the agreement is better than 8 *mm* for all components with respect to ITRF93. The ITRF94 set shows no significant improvement for the core sites. That is caused by unexplained large ITRF94 residuals for TROM (10 *mm* East) and YAR1 (14.8 *mm* North) due to a velocity problem (from GPS point of view; same problem also discussed by [RAY 1996]).

We have to acknowledge that on a global scale the sub-*cm* agreement between different space techniques is not yet reached.

The steady improvement for both station groups in Table 8.4 is mainly a consequence of the GPS contributions to the ITRF system. The ITRF94 set is influenced by a "history" of nearly 3 years of IGS. The agreement between different IGS Analysis Centers was already shown in Section 7.2.

We have on the other hand to acknowledge that the earlier ITRF sets are combined at epoch 1988.0. The error propagation of the velocities (see also eqn. (6.4-2)) for a time of more than 6 years is also a reason for larger residuals of the ITRF91 and ITRF92 sets.

Table 8.4: Comparison of the GPS-derived coordinate set (2.5-years combined solution) with ITRF91, ITRF92, ITRF93 and ITRF94. Common epoch is 8.8.1994. A 7-parameter Helmert transformation was applied for the comparison with the 13 IGS core sites (CORE) and the 13 European sites of Figure 8.8 (EURO).

system	Rms of Helmert transformation in [mm]					
	CORE *			EURO**		
	North	East	Up	North	East	Up
ITRF91	16.6	14.9	34.6	10.5	13.7	26.2
ITRF92	12.1	12.0	23.9	9.2	7.4	17.7
ITRF93	4.7	4.3	11.7	3.7	3.4	9.7
ITRF94	5.2	4.2	11.9	2.1	1.6	5.0

* TIDB was excluded for ITRF91 (Up residual larger than 10 cm due to local tie problem).

** NYAL, MASP, and JOZE excluded for the ITRF91 and ITRF92 comparison (no ITRF values are available).

8.3 Velocities

8.3.1 GPS-Derived Horizontal Velocities for the IGS Network

8.3.1.1 Description of the Solution

The solution characteristics are identical to those of the computation of the coordinates (see Section 8.1). The only difference is that we use the ITRF94 coordinate- and velocity set as our reference for the multi-annual solution. A comparison with NNR-NUVEL1 [ARGUS AND GORDON 1991] is in this case possible more easily because the ITRF94 velocity field [BOUCHER AND ALTAMIMI 1996] is linked to the NNR-NUVEL1 set, whereas the ITRF93 velocity field was defined by the pole drift of the C04 IERS solution [BOUCHER AND ALTAMIMI 1994].

At present we only solve for horizontal velocities. The vertical components are tightly constrained to the ITRF94 values.

Half a year observation time, for some isolated sites even more, is a minimum requirement for significant velocity estimates.

Due to larger residuals for TROM and YAR1 (see previous section) we selected the ITRF94 coordinates of the five sites WETT, KOSG, FAIR, GOLD, and YELL as reference for the free network solution.

The geodetic datum of the velocity field is defined by asking for no-net-translations with respect to the ITRF94 velocity field for these five sites. In addition to these three conditions equations are asked that the velocity of WETT agrees with the ITRF94 velocity.

”Relative” velocity constraints (see Section 2.6.3) are introduced for those sites which had occupations on different monuments (WETT-WTZR, MASP-MAS1, RCM2-RCM4-RCM5, MCMU-MCMU-MCM4, etc.). That allows for the estimation of several coordinate sets but one common velocity.

8.3.1.2 Velocity Results

The results of the velocity estimation for 58 sites (using the information of 69 occupations) are given in Figure 8.9. For the other 33 out of totally 102 sites the velocity estimation had to be constrained to ITRF94/NNR-NUVEL1 (not enough data).

The agreement of our GPS-derived velocities with the ITRF94 set is excellent. According to Section 6.5 and Table 6.3 the quality of the GPS velocities is mainly a function of the covered time span and the quality of the coordinate estimation of a single day. This explains the larger errors for southern hemisphere sites.

Interesting are the discrepancies in Asia. The velocities for USUD, TSKB (North American plate NOAM), and SHAO, TAIW (both Eurasian plate EURA) are greater than predicted by ITRF94. On the other hand: GUAM moves probably not as fast as it is supposed to move being located on the Philippinian plate (PHIL). We have to acknowledge, however, that the connection of these sites to the European sites as well as to the Australian sites is rather weak. The densified IGS network using the already operational sites in LHAS (Lhasa, Tibet), IRKT (Irkutsk, Russia) IISC (Bangalore, India) and POL2 (Poligan, Kyrghyzstan, near KIT3) will help to better estimate the movements in this geotectonically active region. Permanent sites, filling the gap in the Indonesian region, are thus of great importance.

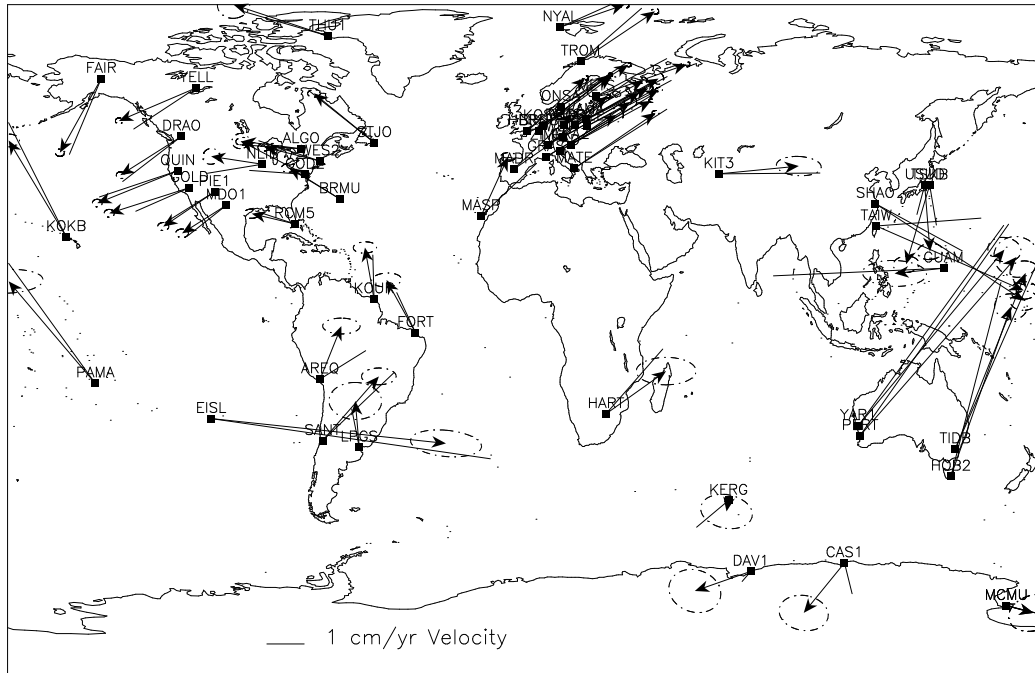
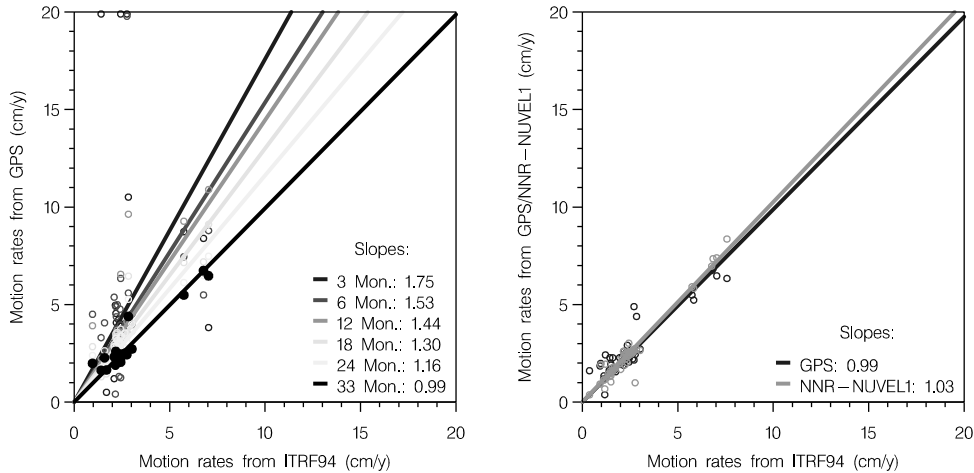


Figure 8.9: Velocity estimates (arrows) for 58 sites of the IGS network using 34 months of GPS data. The error ellipses are derived from the estimated formal rms, scaled with an empirical factor of 20. For comparison the ITRF94 velocities or, if not available, the NNR-NUVEL1 values are also given.

8.3.1.3 Comparisons with ITRF, VLBI and NNR-NUVEL1

To assess the accuracy of the GPS-derived velocities we study relative motions (*motion rates*) of the sites. The advantage is that possible mis-orientations between two velocity sets, due to a different datum definition, are irrelevant. A comparison of GPS with ITRF94 and VLBI is without further transformations only possible, if there are no translations between the velocity systems.

This is true, because the sets are all aligned with NNR-NUVEL1 (by constraining at least one site velocity or by applying no-net-rotation conditions). Comparisons of GPS-derived angular velocities may be found in [ARGUS AND HEFLIN 1995].



(a) Comparison of estimated motion rates derived from continuous observations of different time intervals. 24 sites are included, which were available for the entire time interval of 33 months.

(b) Comparison of estimated motion rates (33 month solution) for all 58 sites with ITRF94 and NNR-NUVEL1.

Figure 8.10: Correlation of motion rates derived from GPS with values of ITRF94 and NNR-NUVEL1.

Figure 8.10a compares the site motions for 24 GPS sites observed during the full time interval of 33 months with the ITRF94 motions. The slope of the line fit (forced through the origin) of all GPS-ITRF-pairs is an indicator of the agreement of both velocity sets. The length of the time series for the velocity estimation is of great importance. Not only the formal errors are smaller for longer time intervals (see Figure 6.4), the agreement with the results of other techniques (ITRF94) improves noticeably, too. The importance of a 2-3 years time interval for the velocities was already addressed in Table 6.3.

The good agreement of our estimates with NNR-NUVEL1 is illustrated by Figure 8.10b. Not only the slope of about 1.0 is remarkable, but in particular the small deviations from the line fit of below 1.0 cm/yr . Only for the Asian sites SHAO and TAIW (the two data points in Figure 8.10b at about $(3.0, 5.0) \text{ cm/yr}$) we find discrepancies larger than 1.0 cm/yr .

For 19 sites common to GPS and VLBI we performed the same kind of comparisons of motion rates (see Figure 8.11). A direct comparison GPS-VLBI leads to a slope of 1.06 and the largest residuum of 1.5 cm/yr for SHAO. The long VLBI history of 6 years for this site, which dominates the ITRF solution, also indicates problems in our GPS solutions for that region.

The question of the geomagnetic reversal time scale [DEMETS ET AL. 1994] is equivalent to the question of the scaling of the NNR-NUVEL1 velocity models (NNR-NUVEL1A is identical with NNR-NUVEL1, but scaled with 0.9562). We cannot answer this question with our studies because we do not have a unique site distribution on each of the 14 major tectonic plates. Too many well determined sites in Europe and North America are the contrast to a few mostly weak determined sites in the southern hemisphere.

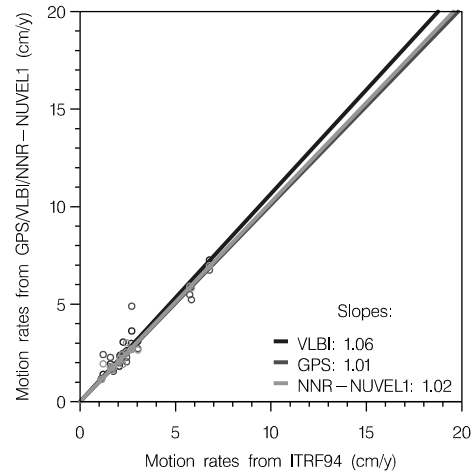


Figure 8.11: Correlation of motion rates derived from GPS with estimates of VLBI and NNR-NUVEL1. 19 sites common to VLBI are used.

8.3.2 Vertical Velocities

It was already mentioned that the determination of ellipsoidal heights is about three times weaker than the determination of the horizontal positions. A geometry effect and the large number of nuisance parameters (ambiguities and tropospheric zenith delays) are responsible for that fact. According to Table 6.3 we expect that the vertical velocities are determined with a similarly reduced quality.

8.3.2.1 Vertical Velocities of Europe

We modified the velocity solution presented in Section 8.3.1 by allowing for vertical velocities for all European sites with observations covering more than 2 years. The datum definition (all three components of WETT constrained) was changed, too: We force only the horizontal velocity of WETT to ITRF94.

Figure 8.12 shows the formal rms values of the horizontal and the vertical velocity estimations. A ratio of about 3 seems realistic.

We assume that realistic rms estimates differ from the formal rms values of the combined solution by a factor of about 20. From the comparisons of the horizontal estimates with other techniques like e.g. VLBI (last section) we know that the quality

of GPS velocities is at present below the $1\text{-}2\text{ mm/yr}$ level in Europe. The factor of 20 is derived from this simple comparison.

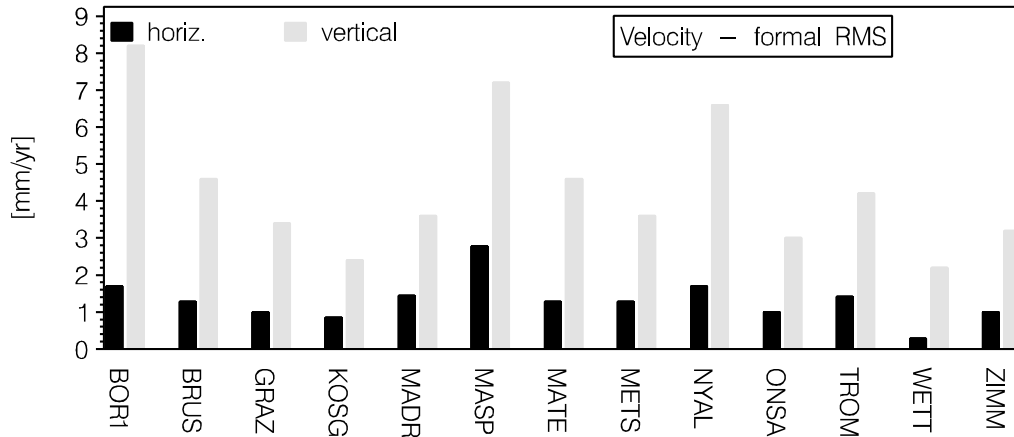


Figure 8.12: Formal rms from the combined solution (scaled with an empirical factor of 20) for horizontal and vertical velocity estimates in Europe. The small horizontal rms for WETT is a consequence of the constraints relative to the ITRF94.

The vertical velocity estimates are given in Figure 8.13. All values, with the exception of BOR1, which shows due to the shortest data span the largest formal rms, are positive. In view of the rms values (Figure 8.12) these results are not yet significant. The vertical velocity estimates show the same systematic behavior (all estimates with a positive sign), even if we constrain most of the European sites to zero movement for the heights and if we estimate vertical velocities only for a small number of sites. A general datum problem can therefore be excluded. We should also mention that the horizontal velocity estimates are not significantly changed by allowing vertical changes in time.

The results for METS are interesting because a land uplift due to postglacial rebound is expected [KAKKURI 1986]. From levelling about 3 mm/yr are detected [PAUNONEN 1996]. PELTIER [1995] came up with 3.1 mm/yr from an analysis of VLBI baselines. If we take into account only the difference of METS to the average movement of Europe (about 3 mm/yr), we end up with a value of about 6 mm/yr for the relative motion of METS in the vertical direction.

Due to the weaker estimation of the vertical velocities by all space techniques we believe that the ITRF94 values are consisting of a compromise between constraints

to zero velocity (which is the case for the NNR-NUVEL1 model) and signals from observations.

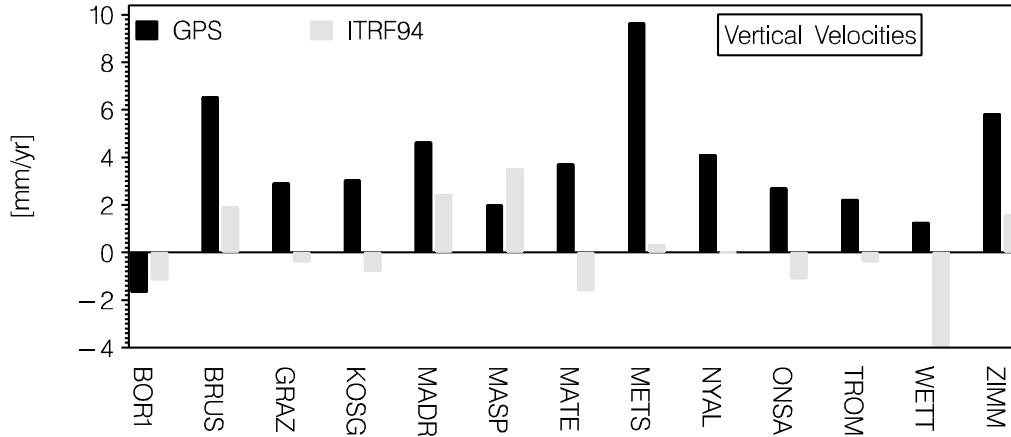


Figure 8.13: Vertical velocities of 13 European sites derived from GPS. For comparison the ITRF94 values are also given.

8.4 Earth Rotation

8.4.1 Quality of Different ERP Models

At CODE, each component of the Earth rotation is modeled as a polynomial of degree 1 for each subinterval. A subinterval usually has the length of 1 day. Today we set up ERPs in 2-hour time intervals allowing a sub-diurnal resolution. The principles of the estimation of sub-diurnal ERPs was already demonstrated in Figure 2.3. First results of sub-diurnal pole estimates and the corresponding corrections for the major pro- and retrograde tides were presented by WEBER ET AL. [1995B] and SPRINGER ET AL. [1995]. Our results, presented below, were obtained based on daily network solutions (normal equations) using an interval length of 24 hours.

When processing more than one day (n -days-solutions with corresponding n -days-arcs according to Chapter 4) it is reasonable to force continuity of the pole estimates at the day boundaries according to eqn. (2.6-12).

Figure 8.14 shows the x -pole estimates of overlapping 3-days-solutions with respect to the C04 pole solution. The C04 pole solution [FEISSEL 1995] is a combination of ERP estimates from different space techniques, in which VLBI plays the most important role.

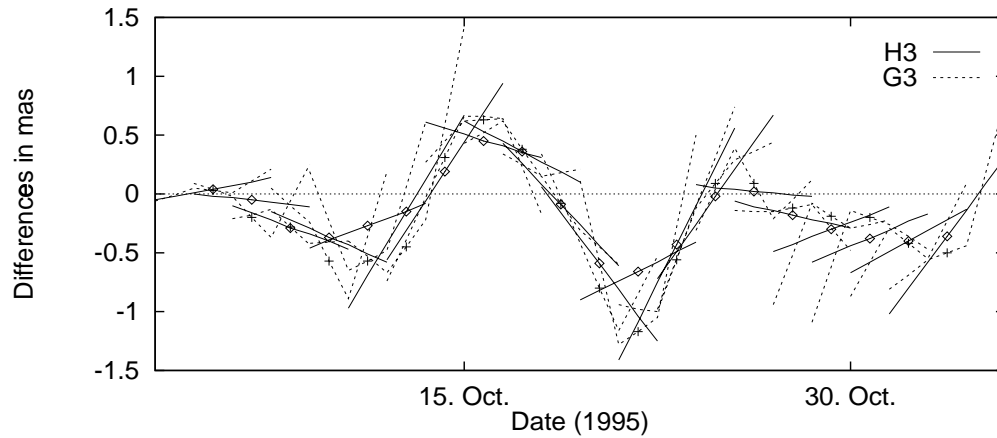


Figure 8.14: Earth rotation estimates (x -pole) from two different models with respect to the C04 IERS solution. H3 solutions are 3-days-solutions with a constant pole drift over all 3 days; G3 solutions are 3-days-solutions with polynomials of degree 1 for each day and continuity at the day boundaries.

The biases of the GPS-derived estimates with respect to the smooth C04 pole are very consistent for both pole models. This is true, even if the boundary days (of the G3 solution type) show large rates in some cases (due to the imperfect orbit model). We may conclude that periodical variations in these differences are a clear signal from the GPS observations.

We should mention that the differences with respect to the IERS rapid pole [Mc-CARTHY 1995B] do not show such a behavior. That indicates that the C04 pole series does not contain signals with frequencies below about 10 days, whereas the IERS rapid pole, mainly based on GPS, allows for such periods (since a change in the computation procedure in mid of 1995 [Mc-CARTHY 1995A]).

A different model is used for the solution type called H3: According to (2.6.3.3) we request a constant drift (for the absolute pole estimates) over all three days. The smaller degree of freedom of this model reduces the amplitudes of the periodical biases in Figure 8.14. The drift estimates approximate the tangent to the mean values quite well.

For combined solutions covering more than three days an application of a pole model of type H3 is therefore not appropriate if we expect pole periods of 5 to 10 days.

The result of overlapping 7-days-solutions (based on 7-days-arcs) is given in Figure 8.15 for the solution type G (polygon). The drift estimates of the boundary days (first

and last days of the 7-days-solution) were omitted because of the weak estimation accuracy. The estimates of the days -2 and +2 (with respect to the middle day) are quite consistent with the estimates of the corresponding values in the middle of the arc of other 7-days-solutions, from which we assume that they show the best accuracy (see also Figure 3.2).

The improvement of the ERP estimates when using longer arcs will be demonstrated in the next section.

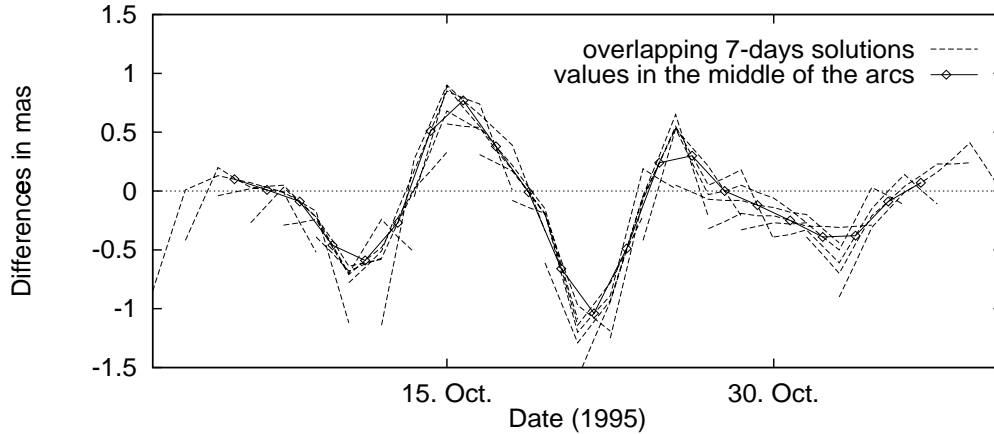


Figure 8.15: Earth rotation estimates (x -pole) from overlapping 7-days-arcs with respect to the C04 pole series. The pole model is of type G (polynomials of degree 1 with continuity conditions). The solid line connects the estimates of the middle days.

8.4.2 ERPs Derived from Long-Arcs

Figure 8.16 shows the difference of pole estimates stemming from 1-day- and 3-days-solutions with respect to the C04 pole for an interval of more than 2 years. The corrections of [IERS 1993] (Table II-3) were applied to be consistent with the realization of the terrestrial reference frame ITRF93. The geodetic datum of both solution types is defined by constraining the 13 IGS core sites to the ITRF93 coordinate values [BOUCHER AND ALTAMIMI 1994].

Table 8.5 shows the quality of both solution types. Whereas the x - and y -pole estimates are only slightly improved using the longer 3-days-arcs, we achieve a better agreement with C04 by a factor of more than 2.5 for the LOD estimates. The integrated LOD values (labeled as $d(UT1 - UTC)$ in Figure 8.16) are showing a quite consistent drift of about 5.5 msec/yr for the 3-days-solutions. In April 1995 the

drift increased (also visible from the jump in the LOD estimates). This change and also the annual period in the daily estimates of $UT1-UTC$ is still object of further investigations. Most of the drift may be explained by a rotation of the orbital planes due to the radiation pressure model [BEUTLER 1996]. The introduction of a (one) condition equation forcing the total rotation of the orbit system (with respect to the z -axis) to zero seems to result in a long-time stability of $UT1-UTC$ of better than 1 msec/year in comparison to the C04 series.

Condition equations with respect to the x - and y - axis would be necessary if we solve for nutation parameters to reduce drifts in the nutation rate estimates.

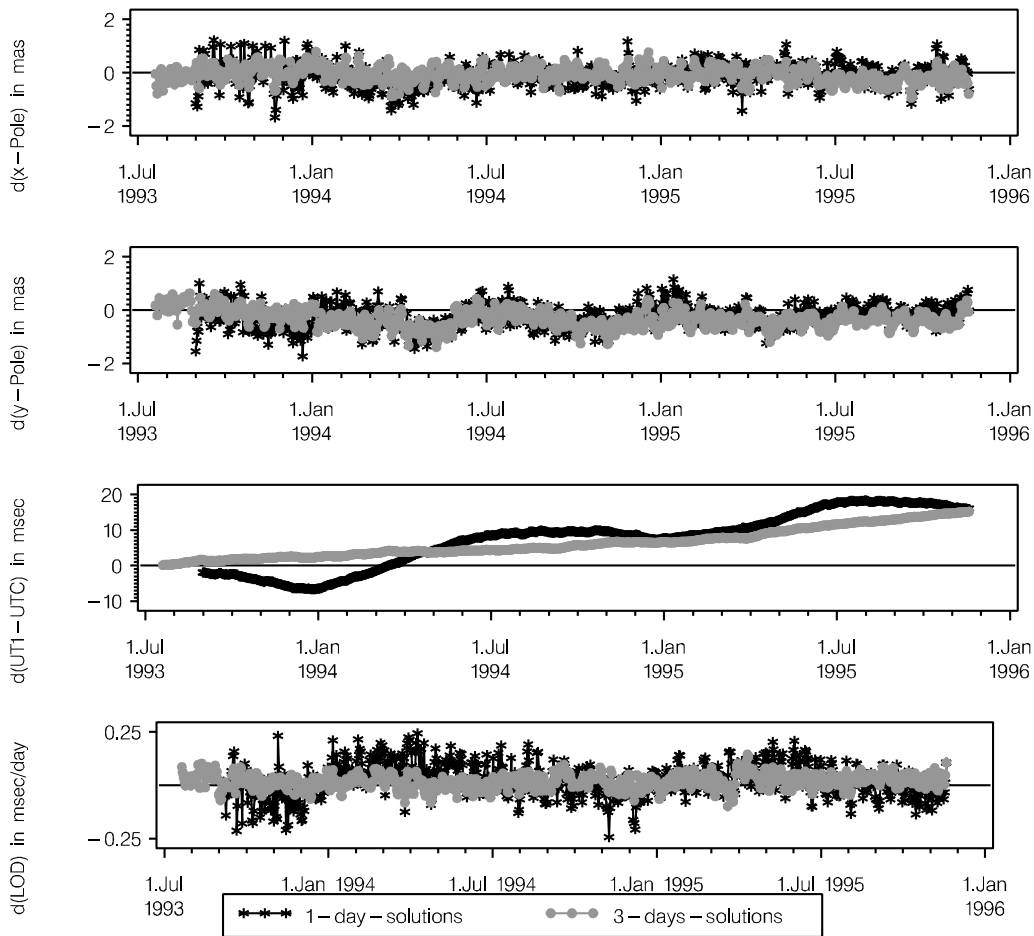


Figure 8.16: Earth rotation estimates for the x -pole, y -pole, and $UT1 - UTC$ (integrated from values of LOD) for 1-day- and 3-days-solutions with respect to the C04 pole series.

Table 8.5: Agreement of 1-day- and 3-days-solutions with the C04 pole. A common offset and drift is removed for the rms computation.

	Pole components		
	x [mas]	y [mas]	LOD [$msec/day$]
1-day	0.44	0.45	0.08
3-days	0.28	0.32	0.03

8.4.3 ERPs and the Definition of the Geodetic Datum

The Earth rotation describes the movement of the Earth's rotation axis with respect to the terrestrial reference frame adopted. The Earth rotation parameters x and y are therefore not separable from the realization of the terrestrial reference frame. A set of site coordinates and a corresponding velocity field is a realization of the terrestrial reference frame [BOUCHER AND ALTAMIMI 1994]. If this system is changed by a pure rotation of all its site coordinates, the pole coordinates of the new reference system can be directly derived by applying the same rotation to the pole parameters. A change of the velocity field leads to a drift in the Earth rotation parameters. That happened with the change from ITRF92 to ITRF93. The reference of the ITRF93 velocity field is given by the development of the C04 pole series in time, whereas the ITRF92 velocity field was aligned with the NNR-NUVEL1 velocity model.

The dependence of the GPS-derived UT1-UTC drift estimates on the selected geodetic datum is negligible. We can therefore forget about these parameters in this section.

The annual submission of site coordinates and velocities from different space techniques leads to an improved realization of the terrestrial reference frame every year. The corresponding change in the Earth rotation parameters can be derived from the resulting transformation parameters of a selected number of sites only in a first approximation.

A reprocessing of the originally GPS observations when the reference frame has to be changed is, according to Table 5.1, almost impossible. Based on the saved normal equations a system change may easily be accounted for. The definition of the geodetic datum may be changed using the constraining methods described in Section 2.6.3. Figure 8.17 shows the y -pole estimates based on three different reference frames: ITRF91, ITRF92, and ITRF93. We compare the pole parameters with the C04 pole series which was transformed according to [IERS 1993] (Table II-3) to the ITRF93 system. The change from ITRF92 to ITRF93 results in an offset for y of about $-0.85 \pm 0.08 mas$ at epoch 1993.0. The drift differences between both series (derived from the common time interval) of $-0.45 \pm 0.06 mas/yr$ can be attributed to the change of the velocity field as already mentioned before. The effect of the reference frame

change is much smaller for the x -pole: Offset (epoch 93.0): -0.15 ± 0.06 *mas* and drift difference between both series of -0.40 ± 0.05 *mas/yr*.

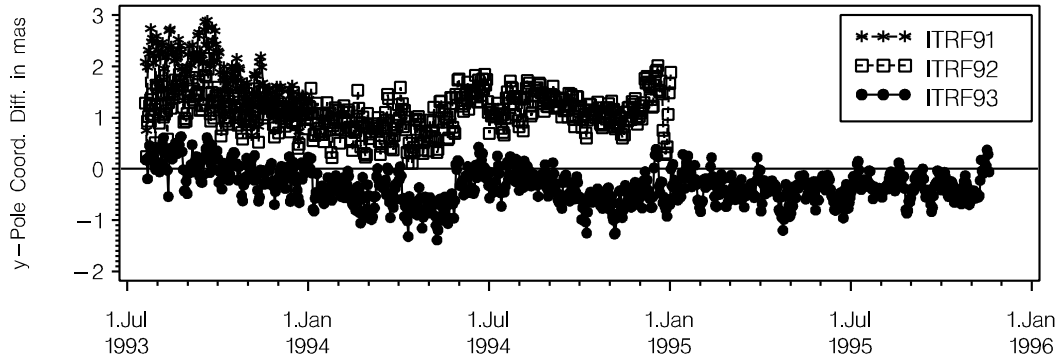


Figure 8.17: y -pole estimations based on three different reference frames with respect to C04. The geodetic datum was realized by constraining the coordinates of the 13 IGS core sites to the ITRF values.

In the following we analyze the impact of the number of constrained sites on the Earth rotation parameter estimates. One time series in Figure 8.18, called CODE93-40, shows of the y -pole for 1995 (shifted by $+1$ *mas*) derived from solutions, in which 40 sites are used to define the geodetic datum. The coordinate values were obtained from a free 2.6-years-solution including velocity estimation for all sites with an observing period longer than half a year. Observations are available for all 40 sites in the entire time interval.

The geodetic datum of the combined 2.6-years-solution was aligned with ITRF93 by defining that the GPS-derived geocenter is equal to the ITRF origin (given by the coordinate values of the 13 IGS core sites). The orientation of the free solution is given by three no-net-rotation conditions with respect to ITRF93. This procedure approximates the combined solution in which coordinates, velocities and ERPs are simultaneously solved for. Such a solution may be obtained by introducing the coordinate and velocity estimates of *all* sites as known in the sequential 3-days-solutions.

For comparison the solution used in Figure 8.16 (here labeled as ITRF93-13) is given. 13 IGS core sites are constrained to ITRF in this "reference" solution.

To demonstrate the impact of slightly inconsistent coordinate and velocity values we included a solution in Figure 8.18 (-1 *mas* shifted), called CODE93-13, in which we used the same 13 sites for the definition of the geodetic datum, but we constrained these sites to our GPS-derived coordinates instead to ITRF93.

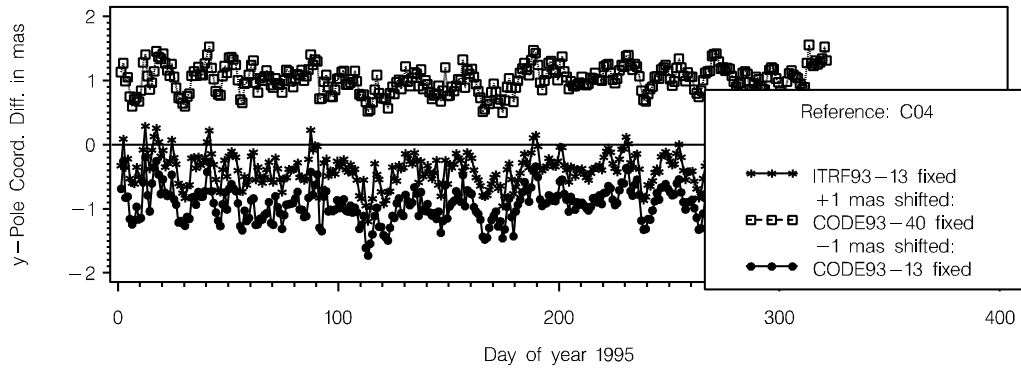


Figure 8.18: y -pole estimates based on ITRF and based on a GPS-derived coordinate and velocity set with a different number of fixed sites.

The rms values of a comparison of the three solution types with the C04 pole and with the rapid pole series are given in Table 8.6. The quality of all three solutions is almost the same which may lead to the conclusion that the quality of the Earth rotation parameters is almost independent of the number of fixed sites and of small inconsistencies in the coordinate/velocity set between GPS and ITRF.

Table 8.6: Quality of 3-days-solutions (Type H) based on different geodetic datum definitions. In the reference solution (ITRF93-13) the coordinates of 13 IGS core sites were constrained to ITRF93, in the second solution (CODE93-40, shifted by 1 *mas* in Figure 8.18) 40 coordinates were kept fixed on a GPS-derived free network solution, in the third solution (CODE93-13) the IGS core sites were kept fixed to the GPS-derived solution. A common offset was removed for the rms computation.

	C04		Rapid Pole	
	x [<i>mas</i>]	y [<i>mas</i>]	x [<i>mas</i>]	y [<i>mas</i>]
ITRF93 - 13	0.25	0.24	0.15	0.20
CODE93 - 40	0.27	0.21	0.19	0.17
CODE93 - 13	0.25	0.26	0.15	0.21

A "best" solution cannot be figured out from such comparisons. The C04 pole does not include pole frequencies below 10 days and the rapid pole is not an independent reference, too, because the ITRF93-13 fixed GPS solution contributes already with a considerable weight to this pole series.

That the constraining of as many sites as possible should improve the pole estimation is intuitively clear, because we condense the information of 2.6 years of GPS observations to a unique, consistent reference frame. Furthermore, such a procedure is almost equivalent to a combined solution, in which all parameters (coordinates, velocities and Earth rotation) are solved for simultaneously.

The dependence of the *pole estimation on the reference frame used and on the number of constrained sites* is demonstrated in Figure 8.19. Here we use the ITRF93-13 pole series instead of the C04 pole as reference (Figure 8.18).

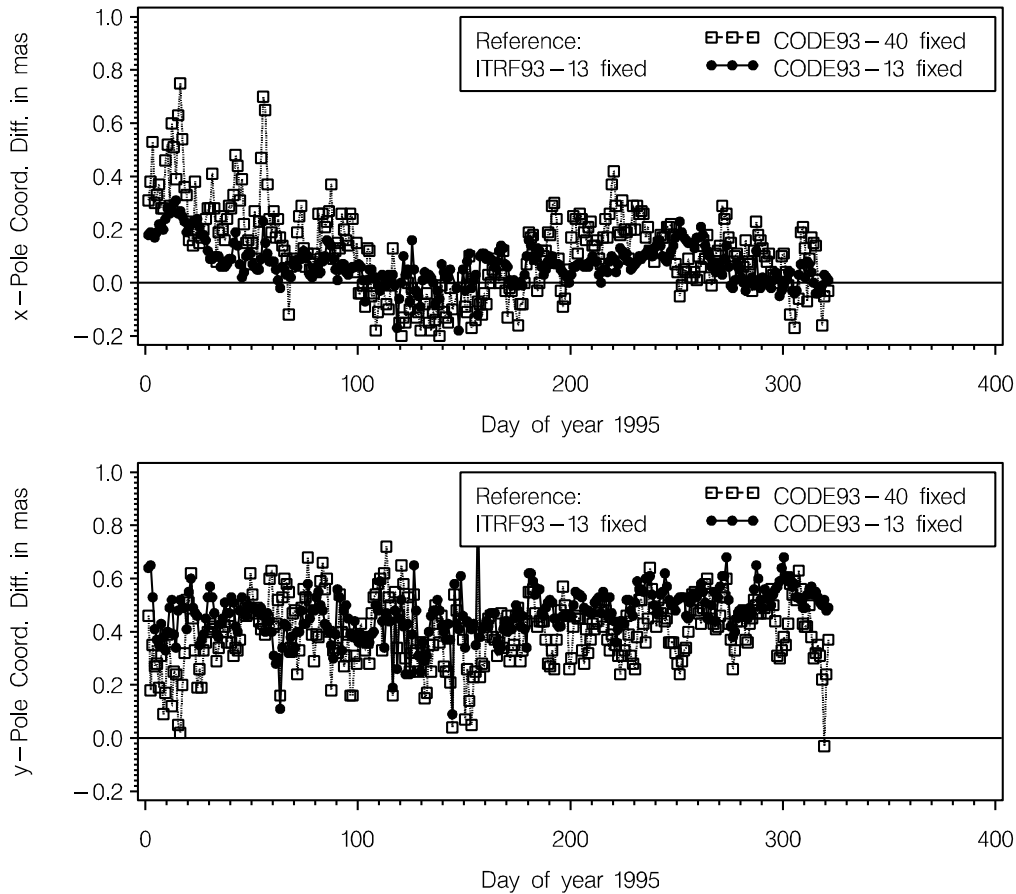


Figure 8.19: Impact of the number of sites used for the definition of the geodetic datum and of the reference frame on the Earth rotation parameters x and y .

A differently orientated reference system (and a different site velocity model) causes the offsets and drifts visible in Figure 8.19.

The variations with a period of about half a year in the x pole, visible in both series, is a consequence of the slightly different GPS coordinate system, which agree with ITRF93 on the 1-2 *cm* level according to Figure 8.7.

The derived amplitude of about 0.1 *mas* is negligible small, but not negligible in view of the scatter of the rapid pole.

The higher noise of the solution CODE93-40 in Figure 8.19 is artificial due to the selected reference solution. We are also free to interpret the noise as a consequence of fixing only a small number of sites. That all larger outliers of the CODE93-40 series can be correlated with one (or more) missing sites out of the 13 IGS core sites favors the interpretation, that this is a problem of the ITRF93-13 solution. We should point out that there is no one-to-one correlation between missing IGS core sites and ERP outliers. That means that missing sites may but do not have to lead to outliers in the pole estimation.

From a theoretical point of view it may be optimal to constrain only the minimum number of coordinate values necessary to define the reference system. That avoids the introduction of biases for those sites which show larger discrepancies to ITRF. Instead of constraining a number of sites the geodetic datum definition may also be realized by the six conditions we applied to the free 2.6-years-solution (origin constrained to zero and 3 no-net-rotation conditions with respect to ITRF). The disadvantage of this method is that the observations of each day define a slightly different geodetic datum. That causes the reference frame to change from day-to-day in particular if weak sites are included in the condition equations. Using more than 13 sites for the no-net-rotation conditions may reduce the problem of the day-to-day variations of the reference frame.

Figure 8.20 shows, in addition to the reference solution ITRF93-13, two other solution types: One solution based on an ambiguity-free solution, the second with fixed ambiguities. The QIF strategy was used for the ambiguity resolution step [MERVART 1995]. This algorithm resolves about 80 % of the ambiguities for baselines shorter than 2000 km using only the phase L1 and L2 measurements (no pseudorange observations necessary). Anti-spoofing (AS) may slightly degrade the quality of this strategy.

Both solutions (3 days, H Type) are free solutions as characterized above. The x -pole estimates of the "free" ambiguity-fixed solution show a comparable agreement with the C04 pole series as the reference solution ITRF93-13 ("fixed" ambiguity-free solution). We will see the strength of the ambiguity-fixed solution also in Section 8.5. That leads us to the conclusion that ambiguity fixing helps for the reference frame definition tasks especially on short (3-days) time intervals.

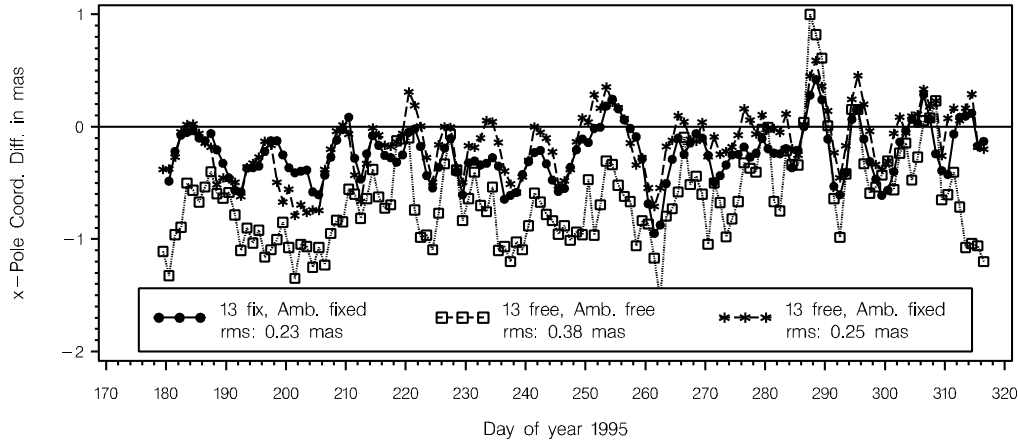


Figure 8.20: x -pole estimates based on free network solutions (with and without ambiguity fixing). Reference is the C04 pole series.

Table 8.7 completes this topic showing the rms values for the x - and y -pole coordinates derived from comparisons with the C04 and the rapid pole series. We may conclude that the free 3-days-solutions (both ambiguity-fixed and ambiguity-free) are not able to realize a stable geodetic datum definition for the determination of the Earth rotation.

Table 8.7: Quality of free 3-days-solutions (ambiguity-free and ambiguity-fixed) in comparison to a constrained solution (13 IGS core sites fixed). An offset between the series was removed for the rms computation.

	C04		Rapid Pole	
	x [mas]	y [mas]	x [mas]	y [mas]
13 fixed, Amb. fixed	0.23	0.12	0.24	0.18
13 free, Amb. free	0.38	0.31	0.34	0.39
13 free, Amb. fixed	0.25	0.16	0.30	0.30

8.5 Center of Mass

Geocenter coordinates with respect to the terrestrial reference frame can be estimated using GPS because the satellite orbits are sensitive to the Earth's gravity field.

Due to the high altitude of the GPS satellites the sensitivity is quite small compared to low orbiting satellites. We may assume that the Earth's potential parameters are already well determined by other space techniques. The estimation of Earth potential coefficients of low degree and order is possible with GPS. The three coefficients of first order can be interpreted according to Section 3.1.2.1 as a pure translation of the geocenter. The definition of the origin of the ITRF has to be realized by the coordinates of the observing sites. Three conditions (e.g. the no-net-translation conditions (2.6-29)) are necessary for that. We point out that these no-net-translation conditions are not necessary if we do not solve for the geocenter (assumption that the origin of the ITRF system is identical with the geocenter). An additional z -rotation condition is necessary to define the rotation of the reference frame (see also Figure 2.7).

A constraining of the coordinates of several sites to their ITRF values is also possible to define the geodetic datum.

Figure 8.22 shows the weekly geocenter estimates for two different series of GPS solutions. The Series H7 shows the estimates of ambiguity-free solutions (1994 and 1995), the series R7 the results of ambiguity-fixed solutions (1995 only). Ambiguity-fixed means in this case, that about 80-90 percent of the ambiguities of baselines below 2000 km or about 50 % of the total number of ambiguities have been resolved using the QIF strategy (see [MERVART 1995] and [SCHAER 1994]).

The X - and Y - components show an almost identical behavior for both series. This is the case for the repeatability, demonstrating a precision of the weekly geocenter estimation (for X and Y of about 2.4 cm), as well as for the results of the solution combined from 100 weekly solutions. The rms values given in Figure 8.22 are 3- σ formal rms errors of the combined solution. The rms of the mean of about 100 weekly



Figure 8.21: Connection between geocenter and terrestrial reference frame.

solutions, each with an rms of about 2.4 *cm*, is also of the same order of magnitude (factor $\sqrt{100} = 10$ smaller).

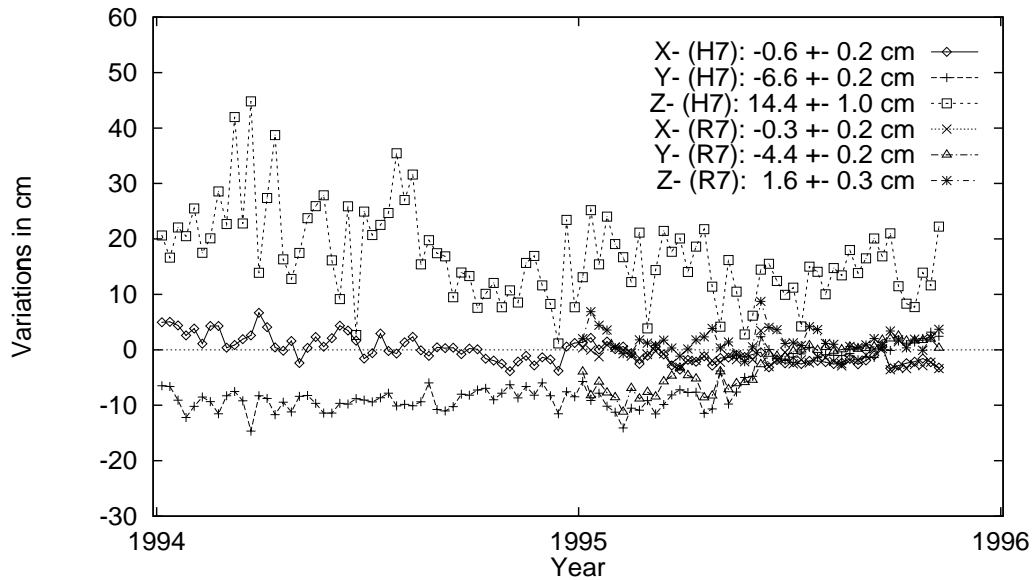


Figure 8.22: Weekly geocenter estimates from two different GPS solutions: series ambiguity-fixed and ambiguity-free.

The *Z*-component is better determined by a factor of about 3 for the ambiguity-fixed solutions, which underlines the advantage of a less redundant normal equation system.

Astonishing is the fact that the mean values of the *Z* component differ by about 13 *cm* for the 1995 data, which cannot be explained by the higher uncertainty in the estimation of the ambiguity-free solution.

Let us have a closer look at the results of the ambiguity-fixed solutions in Figure 8.23. Whereas we get an expectation value of almost zero for the *X*- and *Z*-components for the entire period we have to separate the time span into two periods for *Y*. In the first part (up to DOY 154, 1995) only the eclipsing satellites were modeled with pseudo-stochastic parameters (see Section 3.1.4 and 4.4). During this period we see a mean offset in the *Y*-geocenter component of -6.8 *cm*. In the second part *all* satellites were modeled using pseudo-stochastic parameters. The expectation value is not significantly different from zero, so that for this time period we have an excellent agreement between the definition of the ITRF93 origin and the geocenter estimates and therefore also with SLR as the main contributor to the definition of the origin of the ITRF.

That the geocenter estimates are strongly dependent on the used orbit models is not very surprising. We should point out that the extended radiation pressure model (see Section 3.1.2.4) has an equivalent (positive) effect on the geocenter estimates as it is the case for the pseudo-stochastic orbit modeling.

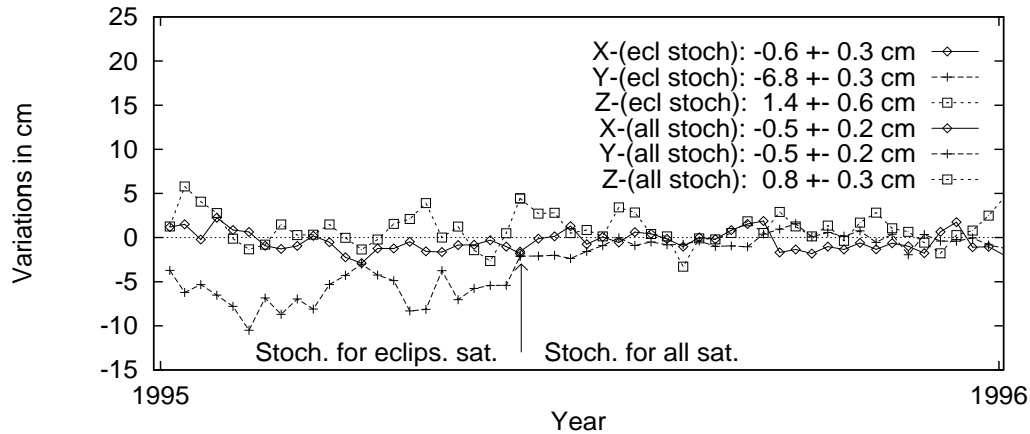


Figure 8.23: Weekly geocenter estimates of ambiguity-fixed solutions for 1995.

We pointed out already that the origin of the orbit system determines the geocenter. Comparisons of the transformation parameters between orbits of the different IGS Analysis Centers are suited to derive statements concerning the geocenter definition and, with the results presented above, concerning the used orbit model, too.

In Figure 8.24 we show the translation parameters X and Y between the orbit systems of the Analysis Centers and the combined IGS orbit. These values were extracted from the weekly reports of the IGS Analysis Center Coordinator [KOUBA 1995B].

For the X -translation we see, similar to the presented geocenter coordinate estimates in Figures 8.22 and 8.23, only very small variations from week to week and an expectation value of approximately zero (with the exception of GFZ).

The Y -shifts seem to be noisier, especially due to the fact that for some centers significant jumps can be detected. For COD the change when introducing pseudo-stochastic parameters for *all* satellites is clearly visible. For SIO the orbit comparisons attest an improvement of the orbit quality in the time range between GPS week 814 up to 826 (Aug. - Oct. 1995) which affects also considerably the Y -translation. The situation after Oct. 1995 is the following: 3 Analysis Centers using stochastic orbit modeling or using the extended radiation pressure model (SIO) produce an Y -shift of about 3 *cm*, 4 Analyses Centers without this modeling an offset of about -3 *cm*. About the same difference, -6.3 *cm*, was also mentioned above for the change

of the Y -geocenter coordinate due to the orbit model change.

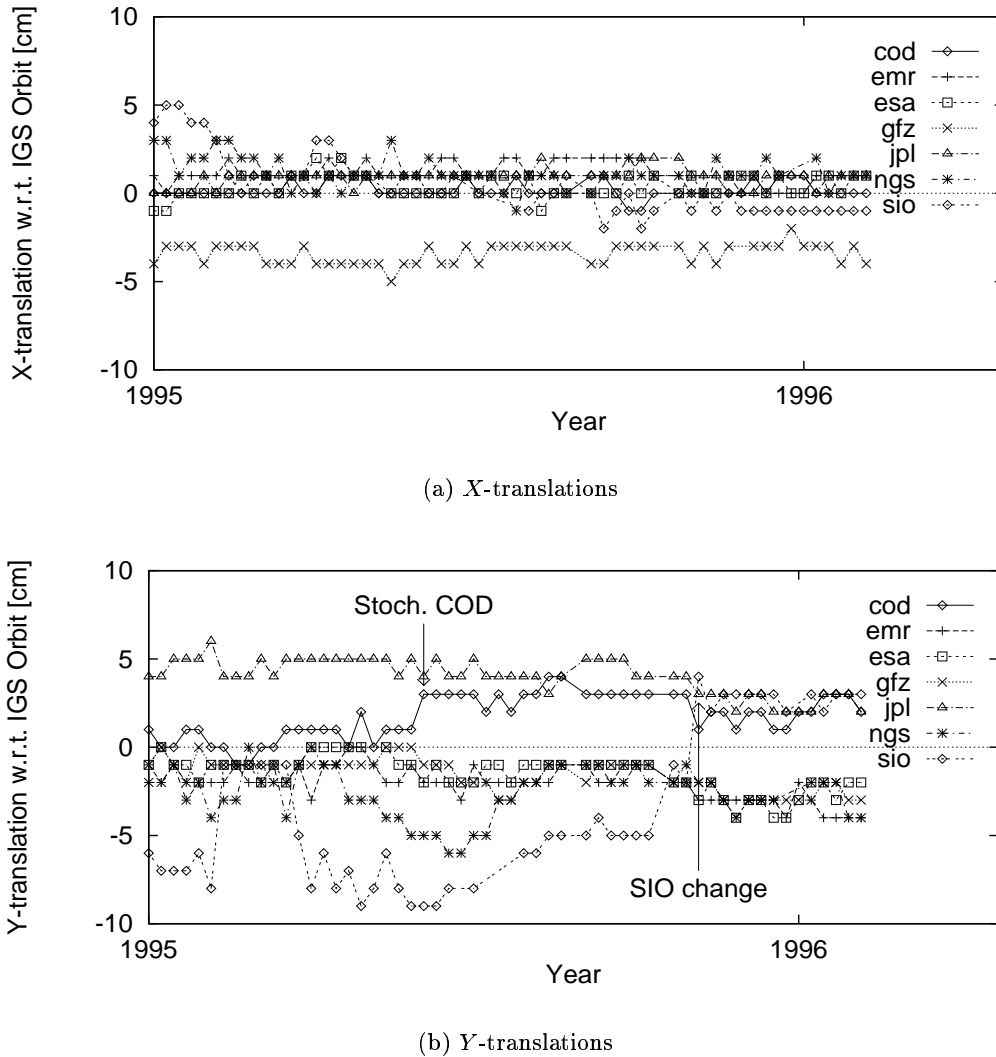


Figure 8.24: Translation parameters X and Y of the orbit systems of different IGS processing centers with respect to the combined IGS orbit. The values were extracted from the weekly IGS reports [KOUBA 1995B].

The study of the GPS-derived geocenter coordinates is certainly promising. Attempts to estimate other low order geopotential coefficients, especially S_{22} , C_{22} , S_{32} , C_{32} [BEUTLER ET AL. 1994] might be considered in the next future.

8.6 Satellite Antenna Offsets

At the end of 1993 we introduced the GPS satellite antenna offsets as unknown parameters into the global CODE solutions in order to verify the official IGS values [GOAD 1992].

Figure 8.25 shows the weekly estimates of the X -, Y - and Z -offsets in the satellite coordinate system for the GPS satellite groups Block I and Block II with respect to the official IGS values. The satellite coordinate system is defined by the direction of the antenna to the Earth (Z -axis) and by the direction of the solar panels (Y -axis). There is no distinction made between Block II and Block IIa satellites.

The estimates were obtained from ambiguity-free solutions up to the end of 1994 and then from ambiguity-fixed solutions. A difference in the quality, as it was demonstrated in the previous section for the geocenter Z -component, cannot be detected.

In Figure 8.25 we have to distinguish between two periods: In the first period (up to the gap in November 1994) we solved only for the parameters of the Block I satellites, whereas in the second part antenna offsets were estimated for both, Block I and Block II satellites.

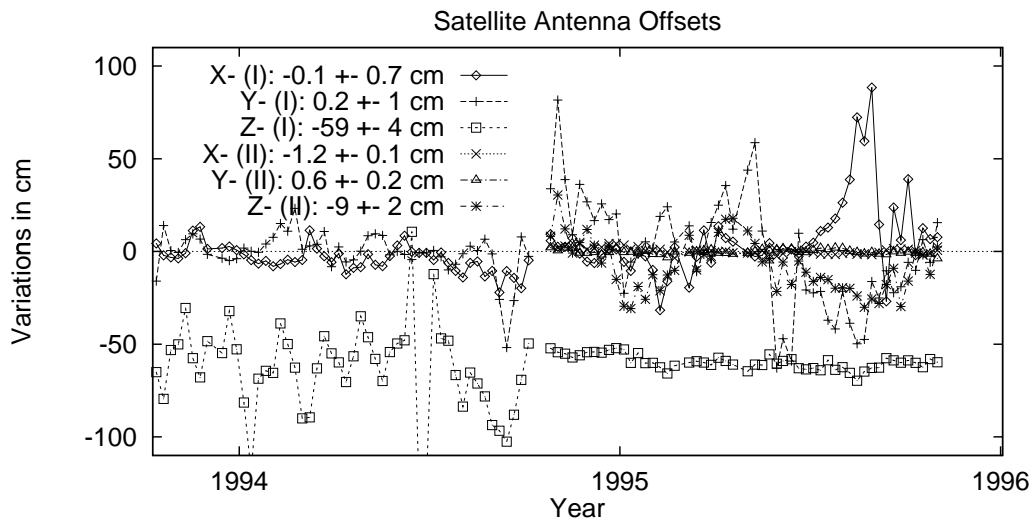


Figure 8.25: Weekly estimates of antenna offsets for the GPS Block I and Block II satellites (corrections with respect to the official IGS values). The given values were derived from the combined solution covering the entire time interval, the rms is the $3\text{-}\sigma$ formal rms error of the combined solution.

Due to the fact that the number of the active Block I satellites decreased steadily (PRN 11 switched off in Aug. 1993, PRN 3 and 13 in April 1994), the results for

this satellite group are based mainly on the observations of satellite PRN 12.

The consequences are the following: For the Block II satellites we find a good agreement with the values given in [FLIEGEL ET AL. 1992] $dx = .2794\ m$, $dy = .0\ m$, $dz = 1.0259\ m$. The Z -component of the Block I satellites shows about half a meter difference to the official values ($dx = .21\ m$, $dy = .0\ m$, $dz = .854$). This difference is interesting, but plays only a minor role for the determination of the high quality IGS orbits, because the orbital elements are determined in any case with respect to the satellite's center of mass. The orbit representation is therefore almost (below 2 cm) identical whether we solve for these parameters, or not. The effect is furthermore reduced by the double-differencing of the observations and due to the fact that satellite 12 is the only Block I satellite left for most of the time period.

We should mention, that the weekly estimates were derived from a solution in which the IGS core sites were constrained to the ITRF93 coordinate values. For free global solutions we have to add an additional condition concerning the scale of the network in order to avoid an increase of the scale and a bias in the Z -components for both satellite groups of about 2.3 m . The difference of half a meter between the Z -components of the two groups remains the same.

Bibliography

- ABUSALI, P., B. SCHUTZ, AND R. EANES (1994). Absolute Accuracy Evaluation of GPS Ephemerides using SLR Data. In *Abstracts to the 1994 AGU Fall Meeting, San Francisco, December 5-9, 1994*.
- ARGUS, D. AND R. GORDON (1991). No-net-rotation model of current plate velocities incorporating plate motion model NUVEL-1. *Geophys. Research Letters* 18, 2039–2042.
- ARGUS, D. AND M. HEFLIN (1995, August). Plate Motion and Crustal Deformation Estimated With Geodetic Data From the Global Positioning System. *Geophysical Research Letters* 22(15), 1973–1976.
- BAR-SEVER, Y. (1994). New GPS Attitude Model. IGS Mail No. 591, IGS Central Bureau Information System (igs_cb.jpl.nasa.gov).
- BAUERSIMA, I. (1983). NAVSTAR Global Positioning System (GPS) II, Radiointerferometrische Satellitenbeobachtungen. Mitteilungen Nr. 10 der Satelliten-Beobachtungsstation Zimmerwald, Bern.
- BEUTLER, G. (1982). Lösung von Parameterbestimmungsproblemen in Himmelsmechanik und Satellitengeodäsie mit modernen Hilfsmitteln. *Astronomisch-geodätische Arbeiten in der Schweiz*, Band 34.
- BEUTLER, G. (1990). Numerische Integration gewöhnlicher Differentialgleichungssysteme: Prinzipien und Algorithmen. Mitteilung Nr. 23 der Satelliten-Beobachtungsstation Zimmerwald, Druckerei der Universität Bern.
- BEUTLER, G. (1995). GPS satellite orbits. In *GPS for Geodesy*. Delft University. International School.
- BEUTLER, G. (1996). Block Rotation of the Orbital Nodes. *paper in preparation*.
- BEUTLER, G., I. BAUERSIMA, S. BOTTON, W. GURTNER, M. ROTHACHER, AND T. SCHILDKNECHT (1989). Accuracy and biases in the geodetic application of the Global Positioning System. *Manuscripta Geodaetica* 14, 28–35.
- BEUTLER, G., I. BAUERSIMA, W. GURTNER, AND M. ROTHACHER (1987). Correlations between simultaneous GPS double difference carrier phase observations in the multistation mode: Implementation considerations and first experiences. *Manuscripta Geodaetica* 12, 40–44.
- BEUTLER, G., E. BROCKMANN, W. GURTNER, U. HUGENTOBLE, L. MERVART, AND M. ROTHACHER (1994). Extended orbit modeling techniques at the CODE processing center of the international GPS service for geodynamics (IGS): theory and initial results. *Manuscripta Geodaetica* 19, 367–386.

- BEUTLER, G., E. BROCKMANN, U. HUGENTOBLE, L. MERVART, M. ROTHACHER, AND R. WEBER (1996). Combining n Consecutive One-Day-Arcs into one n -Days-Arc. *Journal of Geodesy* 70, 287–299.
- BEUTLER, G., W. GURTNER, I. BAUERSIMA, AND R. LANGLEY (1985, April 15-19). Modelling and Estimation of Orbits of GPS Satellites. *Proceedings of the first International Symposium on Precise Positioning with the Global Positioning System 1*, 99–111.
- BEUTLER, G., W. GURTNER, I. BAUERSIMA, AND M. ROTHACHER (1986). Efficient computation of the inverse of the covariance matrix of simultaneous GPS carrier phase difference observations. *Manuscripta Geodaetica* 11, 249–255.
- BEUTLER, G., J. KOUBA, AND T. SPRINGER (1995). Combining the Orbits of IGS Processing Centers. *BG* 69(4), 200–222.
- BEUTLER, G., I. MUELLER, R. NEILAN, AND R. WEBER (1994). The International GPS Service for Geodynamics (GPS). *Bulletin Géodésique* 68(1), 39–70.
- BLEWITT, G., Y. BOCK, AND J. KOUBA (1995). Position paper 2: Constructing the IGS Polyhedron by distributed processing. In J. F. Zumberge and R. Liu (Eds.), *Densification of the IERS Terrestrial Reference Frame Through Regional GPS Networks, Workshop Proceedings, November 30 - December 2, 1994*.
- BOCK, Y. (June 1991). Continuous monitoring of crustal deformations. *GPS World*, 40–47.
- BOUCHER, C. AND Z. ALTAMIMI (1994). IERS Technical Note 18, Results and Analysis of the ITRF93. International Earth Rotation Service (IERS), Central Bureau.
- BOUCHER, C. AND Z. ALTAMIMI (1996). IERS Technical Notes 20, Results and Analysis of the ITRF94. International Earth Rotation Service (IERS), Central Bureau.
- BROCKMANN, E. (1990). Untersuchungen zur Korrektur des IAU-Nutationsmodells durch VLBI-Beobachtungen. unpublished diploma thesis, Geodetic Institute, University of Bonn.
- BROCKMANN, E., G. BEUTLER, W. GURTNER, M. ROTHACHER, T. SPRINGER, AND L. MERVART (1993). Solutions Using European GPS Observations Produced at the "Center for Orbit Determination in Europe" (CODE) During the IGS Campaign. In *Proceedings of the 1993 IGS Workshop in Berne*.
- BROCKMANN, E. AND W. GURTNER (1996). Combination of GPS Solutions for Densification of the European Network: Concepts and Results Derived from 5 European Associated Analysis Centers of the IGS. In *EUREF workshop, Ankara, May 1996 (in press)*.
- BRONSTEIN AND SEMENDJAJEW (1985). *Taschenbuch der Mathematik*. Verlag Harri Deutsch, Thun und Frankfurt (Main).
- BRUYNINX, C. (1994). *Modeling and Methodology for high precision geodetic Positioning with the Global Positioning System (GPS) using carrier phase difference Observations*. Ph. D. thesis, Observatoire Royal de Belgique.
- CAPPELLARI, J., C. VELEZ, AND A. FUCHS (1976). Mathematical Theory of the Goddard Trajectory Determination System. Goddard Space Flight Center, X-582-76-77, Greenbelt, MD.

- COLOMBO, O. (1989). The Dynamics of the Global Positioning Orbits and the Determination of Precise Ephemerides. *Journal of Geophysical Research* 94(B7), 9167–9182.
- DAVIES, P. AND G. BLEWITT (1995). Type Two Associate Analysis Center at Newcastle-upon-Tyne. In *Proceedings of the IGS Workshop in Potsdam on Special Topics and New Directions, May 15-17, Potsdam*.
- DELIKARAGKOU, D., R. STEEVES, AND N. BECKER (1986). Development of an Active System using GPS. In *Proc. of the Fourth Inter. Geodetic Symposium on Satellite Positioning, Austin, Texas*, pp. 1189–1203.
- DEMETS, C., R. GORDON, D. ARGUS, AND S. STEIN (1990). Current plate motions. *Geophys. J. Int.* 101, 425–478.
- DEMETS, C., R. GORDON, D. ARGUS, AND S. STEIN (1994). Effect of recent revisions to the geomagnetic reversal time scale on estimates of current plate motions. *Geophys. Research Letters* 21, 2191–2194.
- DIERENDONCK, A. V., S. RUSSEL, E. KOPITZKE, AND M. BIRNBAUM (1978). The GPS Navigation Message. *Navigation: Journal of the Institute of Navigation* 25(2), 147–165.
- DILLINGER, W. AND D. ROBERTSON (1986). A Program for combined adjustment of VLBI observing sessions. *Manuscripta Geodaetica*, 278–281.
- DREWES, H., C. FÖRSTE, AND C. REIGBER (1992, April). Ein aktuelles plattentektonisches Modell aus Laser- un VLBI Auswertungen. *Zeitschrift für Vermessungswesen* 117(4), 205–214.
- EANES, R., B. SCHUTZ, AND B. TAPLEY (1983). Earth and Ocean Tide Effects on LAGEOS and Starlette. In *Proceedings of the Ninth International Symposium on Earth Tides*. E. Schweizerbartsche Verlag, Stuttgart.
- EISELE, V. (1991). *GPS und Integration von GPS in bestehende geodätische Netze*. DVW Landesverein Baden-Württemberg und das geodätische Institut der Universität Karlsruhe.
- FEISSEL, M. (1995). Monthly Bulletin B Publications. anonymous account at IERS.
- FIGURSKI, M., M. PIRASZEWSKI, J. ROGOWSKI, E. BROCKMANN, AND M. ROTHACHER (1995). Common Experiment of the Analysis Center CODE and the Institut of Geodesy and Geodetic Astronomy of Warsaw University of Technology (IGGA WUT) on the Combination of Regional and Global Solutions. In *Proceedings of the XXI. General Assembly of the International Union of Geodesy and Geophysics, Boulder, Colorado, July 2-14*.
- FLIEGEL, H., T. GALLINI, AND E. SWIFT (1992). Global Positioning System Radiation Force Model for Geodetic Application. *Journal of Geophysical Research* 97(B1), 559–568.
- GELB, A. (1974). Applied Optimal Estimation. pp. 374.
- GENDT, G. AND G. BEUTLER (1995). Consistency in the Troposphere Estimations Using the IGS network. In *Proceedings of the IGS Workshop in Potsdam on Special Topics and New Directions, May 15-17, Potsdam*.
- GOAD, C. (1992). IGS Standards.

- GURTNER, W. (1995). The Role of Permanent GPS Stations In IGS and Other Networks. In *Third International Seminar on GPS in Central Europe, 9-11 May 1995, Penc, Hungary*.
- GURTNER, W. AND R. LIU (1995). The Central Bureau Information System. In J. Zumberge, R. Liu, and R. Neilan (Eds.), *International GPS Service for Geodynamics 1994 Annual Report, IGS Central Bureau, JPL, Pasadena, September 1, 1995*.
- GURTNER, W. AND G. MADER (1990). Receiver Independent Exchange Format Version 2. *GPS Bulletin of the Commission VIII of the International Coordinates of Space Techniques for Geodesy and Geodynamics (CSTG) 3(3)*.
- Heck, B., M. I. (Ed.) (1995). *GPS-Leistungsbilanz '94*. Deutscher Verein für Vermessungswesen e.V., Schriftenreihe 18/1995: Konrad Wittwer Verlag, Stuttgart.
- HEDLING, G. AND B. JONSSON (1995). SWEPOS - a Swedish Network of Reference Stations for GPS. In *4th International Conference on Differential Satellite Navigation Systems (DSNS 95)*, Bergen.
- HEFTY, J. (1995). Combination of Polar Motion Series Determined by Individual IGS Analysis Centres using the Variance Component Estimation. Paper Presented at the 1995 IERS.
- HEISKANEN, W. AND H. MORITZ (1967). *Physical Geodesy*. W.H. Freeman, San Francisco, CA.
- HEITZ, S. (1980). *Mechanik fester Körper*, Volume 1. Dümmler Bonn.
- HEITZ, S. (1986). Grundlagen kinematischer und dynamischer Modelle der Geodäsie. Mitteilungen aus den Geodätischen Instituten der Rheinischen-Friedrich-Wilhelms-Universität Bonn.
- HELMERT, F. R. (1872). *Die Ausgleichsrechnung nach der Methode der kleinsten Quadrate*. Teubner, Leipzig.
- HERRING, T. AND D. DONG (1994). Measurement of diurnal and semidiurnal rotational variations and tidal parameters of the Earth. *JGR 99(B9)*, 18,051–18,071.
- HERRING, T. A. (1990). Geodesy by Radiointerferometry: The Application of Kalman Filtering to the Analysis of Very Long Baseline Interferometry Data. *Journal of Geophysical Research 95(B8)*, 12,561 – 12,581.
- HOFMANN-WELLENHOF, B., B. LICHTENEGGER, AND J. COLLINS (1994). *GPS Theory and Practice*. Third revised edition, Springer-Verlag Wien, New York.
- HUGENTOBLER, U. AND G. BEUTLER (1993). Resonance Phenomena in the Global Positioning System. In *Dynamics and Astrometry of Natural and Artificial Celestial Bodies*. Poznan, Poland.
- IERS (1992). IERS Technical notes, IERS Standards (1992). International Earth Rotation Service (IERS), Central Bureau.
- IERS (1993). 1993 IERS Annual Report. International Earth Rotation Service (IERS), Central Bureau.
- IERS (1994). 1994 IERS Annual Report. International Earth Rotation Service (IERS), Central Bureau.
- IERS (1995). draft of the IERS Standards (1995). International Earth Rotation Service (IERS), Central Bureau.

- KAKKURI, J. (1986). Newest results obtained in studying the Fennoscandian land uplift phenomenon. *Tectonophysics* 130, 327–331.
- KOCH, K. (1988). *Parameter estimation and hypothesis testing in linear models*. Springer, Berlin Heidelberg New York.
- KOCH, K. (1990). *Bayesian Inference with Geodetic Applications*. Springer, Berlin Heidelberg New York.
- KOUBA, J. (1995a). SINEX format version 0.05. e-mail send to all IGS Analysis Centers, 12. June 1995.
- KOUBA, J. (1995b). Weekly orbit comparisons for the IGS Analysis Center. IGSREPORTS, submitted weekly by e-mail.
- KOUBA, J. (1996). SINEX format description version 1.0. e-mail send to all IGS Analysis Centers, April 1996.
- KOUBA, J. AND J. POPELAR (1994). Modern Geodetic Reference Frames for Precise Positioning and Navigation. In *Proc. of the Inter. Symposium on Kinematic Systems in Geodesy, Geomatics and Navigation (KIS94), Banff, Canada*, pp. 79–86.
- LAMBECK, K. (1974). Study of the Earth as a Deformed Solid by Means of Space Methods. *La Géodynamique Spatiale - Space Geodynamics*, 537–654. Centre National d'Etudes Spatiales, Toulouse.
- LANDAU, H. (1988). *Zur Nutzung des Global Positioning Systems in Geodäsie und Geodynamik: Modellbildung, Software-Entwicklung und Analyse*. Ph. D. thesis, Universität der Bundeswehr München, Neubiberg. Schriftenreihe Studiengang Vermessungswesen, Heft 36.
- LEICK, A. (1995). *GPS Satellite Surveying*. John Wiley, Second edition.
- LERCH, F., R. S. NEREM, B. H. PUTNEY, B. V. T. L. FELSTENSTREGER, J. A. MARSHALL, S. M. KLOSKO, G. B. PATEL, R. G. WILLIAMSON, D. S. CHINN, J. C. CHAN, K. E. RACHLIN, N. L. CHANDLER, J. J. MCCARTHY, S. B. LUTHCKE, N. K. PAVLIS, D. E. PAVLIS, J. W. ROBBINS, S. KAPOOR, AND E. C. PAVLIS (1994). A Geopotential Model from Satellite Tracking, Altimeter, and Surface Gravity Data: GEM-T3. *Journal of Geophysical Research* 99, 2815–2839.
- LINDQWISTER, U., G. BLEWITT, J. ZUMBERGE, AND F. WEBB (1991). Millimeter-level baseline precision results from the California permanent GPS geodetic array. *GRS* 18, 1135–1138.
- MA, C., W. RYAN, AND D. GORDON (1995). Site Positions and Velocities, Source Positions, and Earth Orientation Parameters from the Space Geodesy Program-GSFC: Solution GLB979f. *Int. Earth Rotations Service (IERS), Annual submission 1995*.
- MCCARTHY, D. (1995a). Changes in the USNO GPS-only Combination Procedure. IG-SMAIL No. 1072, 28-SEP-95.
- MCCARTHY, D. (1995b). Weekly Rapid Earth Rotation Parameter Submissions. submitted weekly by e-mail.
- MELBOURNE, W. (1991). The first GPS IERS and Geodynamics experiment - 1991. In G. Mader (Ed.), *Permanent Satellite Tracking Networks for Geodesy and Geodynamics, IAG Symposium 109, Vienna*, pp. 65–80.

- MERVART, L. (1995). *Ambiguity Resolution Techniques in Geodetic and Geodynamic Applications of the Global Positioning System*. Ph. D. thesis, Astronomical Institute, University of Berne. published in: Geodätisch-geophysikalische Arbeiten in der Schweiz Vol. 53, Schweizerische Geodätische Kommission.
- MORITZ, H. AND I. MUELLER (1987). *Earth Rotation: Theory and Observation*. Ungar/Continuum, New York, NY.
- MUNK, W. AND G. MACDONALD (1960). *The Rotation of the Earth: A Geophysical Discussion*. The Johns Hopkins Press, Baltimore, MD.
- NEILAN, R. (1995). The Organization of the IGS. In J. Zumberge, R. Liu, and R. Neilan (Eds.), *1994 Annual Report of the International GPS Service for Geodynamics*. IGS Central Bureau.
- OSWALD, W. (1993). *Zur kombinierten Ausgleichung heterogener Beobachtungen in hybriden Netzen*. Ph. D. thesis, Universität der Bundeswehr München, Neubiberg. Schriftenreihe Studiengang Vermessungswesen, Heft 44.
- PAUNONEN, M. (1996). Expected land uplift of METS. personal e-mail.
- PELTIER, W. (1995). VLBI baseline variations from the ICE-4G model of postglacial rebound. *Geophys. Res. Letters* 22(4), 465–468.
- RAO, C. (1973). *Linear statistical inference and its applications*. J. Wiley, New York.
- RAY, J. (1996). Comments on ITRF94. e-mail to IGS users of ITRF94, March 1.
- REIGBER, C., C. FOERSTE, P. SCHWINTZER, F.-H. MASSMANN, W. ELLMER, AND H. MÜLLER (1991). Earth Orientation and Station Coordinates Computed from 10.3 Years of Lageos Observations. *Int. Earth Rotation Service (IERS)*.
- REMONDI, B. (1989). Extending the National Geodetic Survey Standard GPS Orbit Format. NOAA Technical Report NOS 133 NGS 46, Rockville, MD.
- ROCKEN, C., T. VANHOVEN, M. ROTHACHER, F. SOLHEIM, R. WARE, M. BEVIS, S. BUSINGER, AND R. CHADWICK (1994). Towards Near-Real-Time estimation of Atmospheric Water Vapor with GPS. In *Abstracts to the 1994 AGU Fall Meeting, San Francisco, December 5-9, 1994*.
- ROTHACHER, M. (1992). *Orbits of Satellite Systems in Space Geodesy*. Ph. D. thesis, Astronomical Institute, University of Berne. published in Geodätisch-geophysikalische Arbeiten in der Schweiz, Schweizerische Geodätische Kommission, Vol.46.
- ROTHACHER, M., G. BEUTLER, E. BROCKMANN, S. SCHAER, T. SPRINGER, U. WILD, A. WIGET, C. BOUCHER, S. BOTTON, AND H. SEEGER (1996). Annual Report 1995 of the CODE Processing Center of IGS. In I. C. Bureau (Ed.), *International GPS Service for Geodynamics 1995 Annual Report (in press)*.
- ROTHACHER, M., G. BEUTLER, W. GURTNER, E. BROCKMANN, AND L. MERVART (1993). Documentation of the Bernese GPS Software Version 3.4. Astronomical Institute, University of Berne.
- ROTHACHER, M., G. BEUTLER, W. GURTNER, U. WILD, D. SCHNEIDER, A. WIGET, A. GEIGER, AND H.-G. KAHLE (1990). The Role of the Atmosphere in Small GPS Networks. In *Proceedings of the Second International Symposium on Precise Positioning with the Global Positioning System, Ottawa, Canada, September 3-7, The Canadian Institute of Surveying and Mapping*, pp. 581–598.

- ROTHACHER, M., S. SCHAER, L. MERVART, AND G. BEUTLER (1995). Determination of Antenna Phase Center Variations Using GPS Data. In *Proceedings of the IGS Workshop in Potsdam on Special Topics and New Directions, May 15-17, Potsdam*.
- ROTHACHER, M., R. WEBER, E. BROCKMANN, G. BEUTLER, L. MERVART, U. WILD, A. WIGET, C. BOUCHER, S. BOTTON, AND H. SEEGER (1995). Annual Report 1994 of the CODE Processing Center of the IGS. In J. Zumberge, R. Liu, and R. Neilan (Eds.), *International GPS Service for Geodynamics 1994 Annual Report*.
- SALZMANN, M. (1993). *Least Squares Filtering and Testing for Geodetic Navigation Applications*. Ph. D. thesis, Netherlands Geodetic Commission. 37.
- SCHAER, S. (1994). Stochastische Ionosphaerenmodellierung beim "Rapid Static Positioning" mit GPS. unpublished diploma thesis, Astronomical Institute, University of Berne.
- SCHUPLER, B., R. ALLSHOUSE, AND T. CLARK (1994). Signal Characteristics of GPS User Antennas. Preprint accepted for publication in *Navigation* in late 1994.
- SCHWARZ, RUTISHAUSER, AND STIEFEL (1972). *Matrixnumerik*. Teubner Verlag.
- SEEBER, G. (1993). *Satellite Geodesy*. Walter de Gruyter, Berlin, New York.
- Seidelmann, P. (Ed.) (1992). *Explanatory Supplement to the Astronomical Almanac*. University Science Books, Mill Valley, CA.
- SEIDELMANN, P. AND T. FUKUSHIMA (1992). Why New Time Scales? *Astronomy and Astrophysics* 265, 833–838.
- SPRINGER, T., G. BEUTLER, E. BROCKMANN, AND M. ROTHACHER (1996). Towards a New Orbit Model. In *Proceedings of the IGS Analysis Center Workshop in Silver Spring, March 19-21 (in press)*.
- SPRINGER, T., G. BEUTLER, M. ROTHACHER, AND E. BROCKMANN (1995). The role of Orbit Models when Estimating Earth Rotation Parameters using the Global Positioning System. In *Abstracts to the 1995 AGU Fall Meeting*.
- STANDISH, E. (1995). JPL Planetary and Lunar Ephemerides, DE400/LE400. JPL IOM 314.10-108. to be submitted to *Astron. Astrophys.* for publication.
- STRANGE, W., N. WESTON, AND M. CHIN (1994, November). Positioning of the GPS Continuously Operating Reference Station (CORS) Network in the United States. *EOS Transactions* 75(44).
- TSUJI, H., Y. HATANAKA, T. SAGIYA, AND M. HASHIMOTO (1995, July). Coseismic crustal deformation from the 1994 Hokkaido-Toho-Oki earthquake monitored by a nationwide continuous GPS array in Japan. *GRL* 22(13), 1669–1672.
- WAHR, J. (1981). The Forced Nutations of an Elliptical, Rotating, Elastic, and Oceanless Earth. *Geophys. J. Roy. Astron. Soc.* 64, 705–727.
- WATKINS, M. (1996). GPS/SLR Orbit Comparisons. In *Proceedings of the IGS Analysis Center Workshop in Silver Spring, March 19-21 (in press)*.
- WEBER, R., G. BEUTLER, E. BROCKMANN, AND M. ROTHACHER (1995a). The contribution of GPS to the determination of the Celestial Pole Offsets. presented at the IERS workshop, May 1995.
- WEBER, R., G. BEUTLER, E. BROCKMANN, AND M. ROTHACHER (1995b). Monitoring Earth Orientation Variations at the Center for Orbit Determination in Europe

- (CODE). presented at the XXI. General Assembly of the International Union of Geodesy and Geophysics, Boulder, Colorado, July 2-14.
- WELLS, D., N. BECK, D. DELIKARAOGLOU, A. KLEUSBERG, E. KRAKIWSKY, G. LACHAPELLE, R. LANGLEY, M. NAKIBOGLU, K. SCHWARZ, J. TRANQUILLA, AND P. VANICEK (1987). *Guide to GPS positioning*. Canadian GPS Associates, Fredericton, New Brunswick, Canada.
- WILD, U. (1994). *Ionosphere and Geodetic Satellite Systems: Permanent GPS Tracking Data for modelling and Monitoring*. Ph. D. thesis, Astronomical Institute, University of Berne. published in: Geodätisch-geophysikalische Arbeiten in der Schweiz Vol. 48, Schweizerische Geodätische Kommission.
- WOLF, H. (1978). Das geodätische Gauss-Helmert-Modell und seine Eigenschaften. *Zeitschrift für Vermessungswesen* (103), 41–43.
- WÜBBENA, G. (1991). *Zur Modellierung von GPS-Beobachtungen für die hochgenaue Positionsbestimmung*. Ph. D. thesis, Fachrichtung Vermessungswesen der Universität Hannover No. 168. ISSN 0174-1454.
- ZURMÜHL (1964). *Matrizen*. Springer.

Part III

Appendix

A. Program Structure of ADDNEQ

A.1 Flowchart of Program ADDNEQ

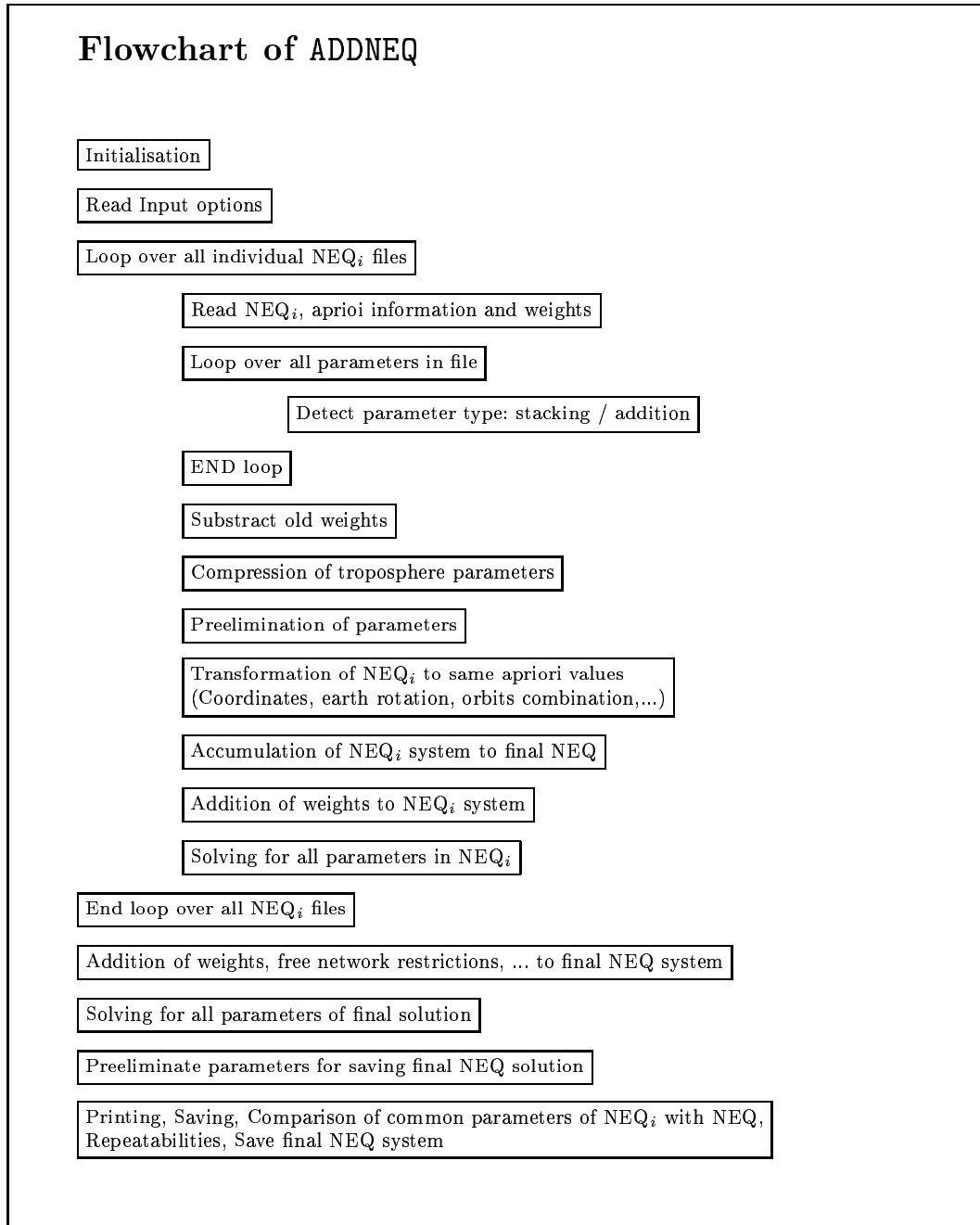


Figure A.1: Flowchart of the program ADDNEQ.

List of Figures

1.1	13 IGS core sites defining the reference frame of the satellite orbits.	4
2.1	Geometrical Interpretation of the least-squares estimation (LSE).	13
2.2	Tropospheric zenith delay for some European stations.	37
2.3	Sub-diurnal pole estimates of a 7-days-arc with and without blocking the retrograde diurnal frequency.	48
2.4	Discontinuous Polynomials.	55
2.5	Common Polynomials in subsequent time intervals.	56
2.6	"Absolute" estimation.	57
2.7	Error ellipses for coordinates and velocities of a 2-years free network solution (1993-1994) using different conditions.	61
2.8	Group rms of a Constraint.	67
3.1	Improvement of the estimated rms a posteriori of single difference L_1 observations using pseudo-stochastic parameters for longer arcs.	80
3.2	Quality of 7-days-arcs using different apriori weights for the pseudo-stochastic parameters.	81
4.1	Rms errors of a combined 3-days-orbit with respect to a conventional processed 3-days-orbit.	96
5.1	Solution statistics of a combined 2-years-solution.	100
5.2	Processing scheme for multi-session solutions.	101
5.3	Impact of additional observations on the coordinate estimates for KOSG.	102
5.4	Baseline selection of DOY 300 (1995) for the separately processed European Test Campaign.	103
5.5	Absolute values of the a posteriori derived correlation matrix of a daily solution containing 26 European sites.	104
5.6	Repeatability for the vertical components of the European sites: network solution versus baseline processing.	107
5.7	Processing scheme based on Baseline processing.	109
5.8	Subdivision of the global IGS network in subnetworks.	110
5.9	Orbit quality derived from subnetworks.	111

5.10	Computation of overlapping 3-days-solutions according to the old and the new processing scheme.	114
5.11	Combination of the normal equations of different processing steps.	115
6.1	Continuous observations of a coordinate component.	122
6.2	Continuous observation of coordinates versus epoch campaigns.	125
6.3	Error propagation for coordinates with estimated velocities.	127
6.4	Estimated rms errors for site velocities.	129
6.5	Estimated internal precision of coordinates and velocities using different time intervals.	130
7.1	Baseline configuration of the European subnetwork.	136
7.2	Rms of Helmert transformation between orbit systems achieved with the global solutions type I and type II.	137
7.3	Combination of the regional solution with the global solution type II for different processing strategies.	141
7.4	Comparison of the combination results with the global network solution type I.	142
7.5	Biases of multi-days combined solutions (of regional and global solutions type II) with respect to the corresponding correct solution (type I).	145
7.6	Residuals in vertical direction for site WETT.	154
7.7	Unweighted rms values for vertical components after a 7-parameter Helmert transformation comparing the weekly free Analysis Center results with the weekly combined COD-G solution (a) and with the MEAN solution (b).	154
7.8	Residuals in vertical direction for site JOZE.	156
8.1	Baseline length development for two different baselines.	159
8.2	Baseline length repeatabilities of (a) 3-days-solutions and (b) weekly solutions.	160
8.3	Systematic effects in European baselines of different lengths.	163
8.4	Systematic effects in the baseline length for baselines between North America and Europe.	164
8.5	Power spectrum of the height components of the baseline WETT-TROM.	167
8.6	Height repeatability of the baseline WETT-QUIN.	167
8.7	Coordinate differences of semi-annual solutions for the 13 IGS core sites with respect to ITRF93.	169
8.8	Coordinate differences of semi-annual solutions for 13 European sites with respect to ITRF93.	170

8.9	Velocity estimates for 58 sites of the IGS network using 33 months of GPS data.	174
8.10	Correlation of motion rates derived from GPS with values of ITRF94 and NNR-NUVEL1.	175
8.11	Correlation of motion rates derived from GPS with estimates of VLBI and NNR-NUVEL1.	176
8.12	Formal rms for horizontal and vertical velocity estimates in Europe.	177
8.13	Vertical velocities of 13 European sites derived from GPS.	178
8.14	Earth rotation estimates (x -pole) from two different models with respect to the C04 IERS solution.	179
8.15	Earth rotation estimates (x -pole) from overlapping 7-days-arcs with respect to the C04 pole series.	180
8.16	Earth rotation estimates for the x -pole, y -pole, and $UT1 - UTC$ (integrated from values of LOD) for 1-day- and 3-days-solutions with respect to the C04 pole series.	181
8.17	y -pole estimations based on three different reference frames with respect to C04.	183
8.18	y -pole estimates based on ITRF and based on a GPS-derived coordinate and velocity set with a different number of fixed sites.	184
8.19	Impact of the number of sites used for the definition of the geodetic datum and of the reference frame on the Earth rotation parameters x and y	185
8.20	x -pole estimates based on free network solutions (with and without ambiguity fixing).	187
8.21	Connection between geocenter and terrestrial reference frame.	188
8.22	Weekly geocenter estimates from two different GPS solutions: series ambiguity-fixed and ambiguity-free.	189
8.23	Weekly geocenter estimates of ambiguity-fixed solutions for 1995.	190
8.24	Translation parameters X and Y of the orbit systems of different IGS processing centers with respect to the combined IGS orbit.	191
8.25	Weekly estimates of antenna offsets for the GPS Block I and Block II satellites.	192
A.1	Flowchart of the program ADDNEQ.	206

List of Tables

1.1	The seven Analysis Centers of the IGS.	6
1.2	Workload of the daily 3-days CODE solutions.	6
2.1	Constraints and constraining options used in the program ADDNEQ. . .	54
2.2	Required information from each sequential solution for the production of a combined solution.	63
2.3	Estimated rms values from a monthly solution: January 1995.	71
3.1	Effect of perturbing forces on GPS satellites.	75
5.1	Rms values of the between-site correlations as an indicator of a correct stochastical model for the GPS phase observations.	106
5.2	Rms values of Helmert transformation between two combined solu- tions with and without processing the daily solutions using correct inter-baseline correlations.	108
5.3	Required CPU times and disk space for different processing schemes.	116
6.1	Quality increase of coordinates and velocities with a k times longer continuous observation interval.	124
6.2	Quality increase of coordinates and velocities with a k times longer time interval with an unchanged number of observations.	125
6.3	Resulting coordinate and velocity precision using different data qual- ity σ_0 and time intervals of continuous 3-days-solutions.	128
7.1	Rms error of the differences between the two global solutions (with and without additional European sites).	138
7.2	Repeatability of the comparisons of the combination results with the global network solutions type I.	142
7.3	Analyzed SINEX files: data used, number of sites, and repeatability for each Analysis Center.	152
7.4	Scaling factors $1/\sigma_i^2$ for normal equations used for the combination of the different weekly solutions.	153

7.5	Mean rms of coordinate components derived from the comparison (using 7-parameter Helmert transformations) of each Analysis Center with the combined COD-G solution.	155
8.1	Repeatability and mean formal rms of the baseline lengths for different time intervals.	162
8.2	Repeatability of the north-, east-, up-, and length- baseline components.	166
8.3	Rms values of 7-parameter Helmert transformations of semi-annual solutions w.r.t. the 2.5-years-solution.	171
8.4	Comparison of the GPS-derived coordinate set (2.5-years combined solution) with ITRF91, ITRF92, ITRF93 and ITRF94.	172
8.5	Agreement of 1-day- and 3-days-solutions with the C04 pole.	182
8.6	Quality of 3-days-solutions based on different geodetic datum definitions.	184
8.7	Quality of free 3-days-solutions.	187

Persönliche Daten

Name: Elmar Brockmann

Geburtsdatum/-ort: 21.12.1964, 59557 Lippstadt (NRW)

Familienstand: verheiratet, 2 Kinder (3 und 1.5 Jahre alt)

Staatsangehörigkeit: deutsch

Schulbildung: Abitur 1984

Grundwehrdienst: 15 Monate (Juli 1984 - Sept. 1985)

Studium: Dipl.-Ing. der Geodäsie im März 1991,
Univesität: Universität Bonn,
Dauer: 5 $\frac{1}{2}$ Jahre (Okt. 1995 - März 1991),
Schwerpunkte: Vermessungskunde (Prof. Witte),
Ausgleichsrechnung und Statistik
(Prof. Koch)

Diplomarbeit:
"Untersuchungen zur Korrektur des IAU-
Nutationsmodells aus VLBI-Beobachtungen"
(bei Prof. Campbell),

Tätigkeiten im Studium: 2 Jahre am Korrelator
des Max-Planck-Institutes für Radioastronomie: Kor-
relation der VLBI-Radioteleskop-Daten.
1 $\frac{1}{2}$ Jahre im Rechnerraum des geodätischen Institutes:
Datenauswertung und Rechnerbetreuung

Praktische Berufserfahrung: Anstellung als Ingenieur bei dem Vermessungsbüro
Paulus (ÖbVI) in Trier (Katastervermessung und In-
genieurvermessung), Apr.-Sep. 1991

Dissertation: bei Prof. Beutler, Astronomisches Institut der Uni-
versität Bern auf dem Gebiet der Satellitengeodäsie
(GPS), seit Nov. 1991

Not referenced in the Thesis:

- [ABUSALI ET AL. 1994]
- [BRUYNINX 1994]
- [COLOMBO 1989]
- [DILLINGER AND ROBERTSON 1986]
- [DREWES ET AL. 1992]
- [HECK 1995]
- [FIGURSKI ET AL. 1995]
- [GURTNER 1995]
- [GURTNER AND LIU 1995]
- [HEFTY 1995]
- [HEITZ 1980]
- [HERRING AND DONG 1994]
- [MORITZ AND MUELLER 1987]
- [MUNK AND MACDONALD 1960]
- [OSWALD 1993]
- [REIGBER ET AL. 1991]
- [WAHR 1981]
- [WATKINS 1996]
- [WILD 1994]
- [WÜBBENA 1991]

